UNIVERSITY OF LJUBLJANA
FACULTY OF MATHEMATICS AND PHYSICS
DEPARTMENT OF MATHEMATICS

María del Río Francos

FLAG GRAPHS AND SYMMETRY TYPE GRAPHS

Doctoral thesis

ADVISER: Prof. Dr. Tomaž Pisanski
COADVISER: Prof. Dr. Isabel Hubard

Ljubljana, 2014

UNIVERZA V LJUBLJANI
FAKULTETA ZA MATEMATIKO IN FIZIKO
ODDELEK ZA MATEMATIKO

María del Río Francos

PRAPORNI GRAFI IN GRAFI SIMETRIJSKIH TIPOV

Doktorska disertacija

MENTOR: prof. dr. Tomaž Pisanski
SOMENTOR: prof. dr. Isabel Hubard

Ljubljana, 2014

I would like to thank to my family for their immense support;
without them I could never reach my goals.

I would also thank to my friends from Mexico and Slovenia,
for their encouragement and company in this period of my life.

I dedicate this work to my adviser Tomaž Pisanski
and coadviser Isabel Hubard.
This work could not be finished without their help and support.

Abstract

A map, as a 2-cell embedding of a graph on a closed surface, is called a k-orbit map if the group of automorphisms (or symmetries) of the map partitions its set of flags into k orbits. In 2012, Steve Wilson introduced the concept of maniplex, aming to unify the notion of maps and abstract polytopes. In particular, maniplexes generalise maps on surfaces to higher ranks. The combinatorial structure of a maniplex of rank $(n-1)$ (or an $(n-1)$-maniplex) is completely determined by an edge-coloured n-valent graph with chromatic index n, with $n \geq 1$, often called the flag graph of the maniplex. Maps will be regarded as maniplexes of rank 2 (or 2-maniplexes), and defined as Lins and Vince studied the combinatorial maps since 1982-83. Thus, similarly to maps, a k-orbit maniplex is one that has k orbits of flags under the action of its automorphism group. In the first part of this thesis we introduce the notion of symmetry type graphs of maniplexes and make use of them to study k-orbit maniplexes, as well as fully-transitive 3-maniplexes. We classify all possible symmetry types of k-orbit 2-maniplexes for $k \leq 5$, as well as all self-dual, properly and improperly, k-orbit maps with $k \leq 7$. Moreover, we show that there are no fully-transitive k-orbit 3-maniplexes with $k > 1$ an odd number, we classify 3-orbit maniplexes and determine all face transitivities for 3- and 4-orbit maniplexes. Furthermore, we give generators of the automorphism group of a maniplex, given its symmetry type graph. The second part of this work is motivated by the classification for k-orbit, up to $k \leq 4$, that Orbanić, Pellicer and Weiss gave. Thus, motivated by their results, we use symmetry type graphs to extend such study and classify all the types of k-orbit maps with the same operations on maps, up to $k \leq 6$. Furthermore, we studied other operations on maps, such as the chamfering and leapfrog operations. In particular, we determine all possible symmetry types of maps that result from other maps after applying the chamfering operation and give the number of possible flag-orbits that has the chamfering map of a k-orbit map.

Mathematics Subject Classification (2010): 52B15, 05C25, 57M20, 52B10.

Keywords. Flag graph, symmetry type graph, k-orbit map, maniplex, medial, chamfering, truncation, leapfrog.

Povzetek

Zemljevid (t.j. celična vložitev grafa na sklenjeno ploskev) imenujemo k-orbitni zemljevid, če grupa avtomorfizmov (oz. simetrij) zemljevida razdeli njegovo množico praporov v k orbit. Pred kratkim (2012) je Steve Wilson, v želji da poenoti pojma zemljevidov in abstraktnih politopov, vpeljal t.i. maniplekse. Manipleksi predstavljajo posplošitev zemljevidov na objekte višjih dimenzij oziroma rangov. Kombinatorična struktura manipleksa ranga $(n-1)$ (ali $(n-1)$-manipleksa) je popolnoma določena s po povezavah pobarvanim n-valentnim grafom (s kromatičnim številom $n \geq 1$), t.i. prapornim grafom manipleksa. Zemljevide obravnavamo kot maniplekse ranga 2 (oz. 2-maniplekse) in jih definiramo v skladu z raziskavami kombinatoričnih zemljevidov Linsa in Vincea v letih 1982-83. Tako je, podobno kot pri zemljevidih, k-orbitni manipleks definiran kot manipleks, ki ima k prapornih orbit glede na delovanje njegove grupe avtomorfizmov. V prvem delu disertacije vpeljemo pojem simetrijskega grafa manipleksa in uporabimo simetrijske grafe pri obravnavi k-orbitnih manipleksov ter polno tranzitivnih 3-manipleksov. Klasificiramo vse možne simetrijske tipe k-orbitnih manipleksov za $k \leq 5$, pa tudi vseh pravih in nepravih samodualov k-orbitnih zemljevidov za $k \leq 7$. Pokažemo, da za nobeno liho število $k > 1$ ne obstaja polno tranzitiven k-orbitni 3-manipleks, klasificiramo 3-orbitne maniplekse in določimo vse tranzitivne avtomorfizme lic 3- in 4-orbitnih manipleksov. Predstavimo tudi generatorje grupe avtomorfizmov manipleksa, ki utreza danemu simetrijskemu grafu. Orbanić, Pellicer in Weiss so klasificirali k-orbitne zemljevide za vrednosti $k \leq 4$ s pomočjo operacij na zemljevidih, npr. z operacijama sredinjenja (angl. medial) in prisekanja (angl. truncation). V drugem delu disertacije na podlagi teh rezultatov uporabimo simetrijske grafe za razširitev takšnih raziskav in klasificiramo vse tipe k-orbitnih zemljevidov z istima operacijama na zemljevidih za vrednosti $k \leq 6$. Raziščemo tudi druge operacije na zemljevidih, kot sta npr. operaciji brušenja (angl. chamfering) in preskoka (angl. leapfrog). Določimo tudi vse možne simetrijske tipe zemljevidov, ki jih dobimo iz drugih zemljevidov z operacijama brušenja, in raziščemo, koliko prapornih orbit lahko ima brušeni zemljevid k-orbitnega zemljevida.

Math. Subject Classification (2010): 52B15, 05C25, 57M20, 52B10.

Ključne besede: graf praporov, simetrijski graf, k-orbitni zemljevid, manipleks, sredinjenje, brušenje, prisekanje, preskok.

Contents

Introduction

Throughout the years, the study of symmetric objects has been of interest to mathematicians, already in ancient times with the Platonic and Archimedean solids being a prime example. The idea of "the most symmetric" polyhedra, i.e. regular or Platonic polyhedra, was later an inspiration for several important generalizations: from regular maps to regular abstract polytopes.

We concentrate our study to objects known as maps and maniplexes of rank n, whose combinatorial structure is completely determined by an edge-coloured n-valent graph with chromatic index n, often called the flag graph. In particular, the flag graph of a map is a cubic graph. While abstract polytopes are a combinatorial generalisation of classical polyhedra and polytopes ([40]), maniplexes generalise maps on surfaces and (the flag graph of) abstract polytopes; maps shall be regarded as maniplexes of rank 2 (or 2-maniplexes). Some other interesting characteristics regarding the flag graph are described in [1].

A maniplex is called a k-orbit maniplex if its group of automorphisms, or symmetries, partitions the set of flags into exactly k orbits. The most symmetric maniplexes are known as regular, or reflexible, maniplexes, those for which its automorphism group acts transitively on their set of flags, i.e. they have exactly one flag-orbit. Other type of highly symmetric maniplexes is the chiral type, which does not allow reflections as symmetries (2-orbit maniplexes with maximum degree of symmetry by rotation). While these two types of maps and polytopes have been widely studied ([40, 57] and [28, 33, 46]), little is known about those that are neither regular nor chiral. Hence, a natural question is: how many possible types of maniplexes can we find that are neither regular nor chiral? There is only one type of 1-orbit maniplexes, it coincides with the notion of regular maniplexes. When we refer to 2-orbit maniplexes, chiral ones constitute just one type. There are $2^{n-1} - 2$ other 2-orbit types of n-maniplexes.

In [30] Hubard gives a complete characterisation of the automorphism groups of 2-orbit and fully-transitive polyhedra (i.e. polyhedra transitive on vertices, edges and faces) in terms of distinguished generators. Moreover, she finds generators of the automorphism group of a 2-orbit polytope of any given rank. Duarte and Hubard studied in [23] and [29], respectively, all seven types of 2-orbit maps, in different contexts.

Highly symmetric maniplexes can also be regarded to those with many face transitivities. In particular, edge-transitive maps were studied by Širan, Tucker and Watkins in [53]. Such maps have either 1, 2 or 4 orbits of flags under the action of the automorphism group.

The aim of this work is to give a classification on the possible different symmetry types of maniplexes. To fulfil our task we introduce a graph to which we refer as the symmetry type graph of the maniplex. With the symmetry type graph of a maniplex we can determine properties and information regarding the symmetries of the maniplex of rank $n-1$, such as its regularity, transitivity on vertices, edges, faces or any other face of higher rank $\leq n-1$. Then, we can formally define the symmetry type of the maniplex. That is, all those maniplexes that have isomorphic symmetry type graph belong to the same symmetry type of maniplexes, labelled by corresponding the symmetry type graph of the maniplex. A strategy of how to generate those graphs is shown in [4]. Dress and Huson (1987) refer to such graphs as the Delaney-Dress symbol, [21]. (The reader can also refer to [20, 34, 14] for more on the Delaney-Dress symbol.) Dress and Brinkmann (1996), as well as Balaban and Pisanski (2012), give an application to mathematical chemistry in [22] and [2], respectively. Symmetry type graphs of the Platonic and Archimedean solids were determined in [36]. In [44], Orbanić, Pellicer, Pisanski and Tucker (2011), show the edge-transitive maps fall into 14 types, each of them described by its symmetry type graph.

Orbanić, Pellicer and Weiss gave a classification for k-orbit maps, up to $k \leq 4$, using operations on maps, as the medial and truncation operation, [45]. Motivated on their results, in this thesis, we give an extension and complete the classification for k-orbit maps with the same operations on maps, up to $k \leq 6$. As it is shown in [45], the medial of a k-orbit map can have either k or $2k$ flag orbits under the action of its automorphism group, depending on whether the original map is or not self-dual. Also, concerning truncation of a k-orbit map, Orbanić, Pellicer and Weiss showed that the truncated map might have either k, $\frac{3k}{2}$ or $3k$ orbits on its flags under the action of its automorphism group, depending if the original map satisfies certain conditions. From applying the medial and truncation operations to maps, we present the possible symmetry types of k-orbit maps, for $k \leq 7$ and $k = 9$. We also enumerate in a compact way (Table 3.5) all possible symmetry types of maps up to $k \leq 10$. Furthermore, we studied other operations on maps, such as the chamfering and leapfrog operations, leading to another question: How many flag-orbits has a map that comes from a k-orbit map, after applying any operation on a map?

The content of this work is divided in two parts. In the first part we present basic notions concerning permutation groups and graph theory. As well as, in Chapters 2 and 3, we define and review some basic theory on maps, maniplexes and symmetry type graphs, and found all possible symmetry types of k-orbit maps up to $k \leq 5$. For maps, we use an equivalent definition to that proposed by Lins and Vince (1982-83) in [37] and [54],

respectively, and for maniplexes we use the definition given by Wilson (2012) in [56]. To conclude the first part of the thesis, in Chapter 4, we introduce the three well-known operators on maps and maniplexes: dual, Petrie dual and opposite. These were first described by Wilson in [57] (1979) for regular maps, later by Lins in [37] (1982) for all maps, and in [35] (1983) Jones and Thornton study these operators from an algebraic point of view. We use the symmetry type graph to show some properties of these three operators. Also, we analyse how the dualities of a map work on its symmetry type graph to define the extended symmetry type graph of a self-dual map.

In the second part we give the extension to the results in [45] for medial and truncation of k-orbit maps, and study the chamfering and leapfrog operations. All four operations can be described as subdivision of the triangles that correspond to the flags of the original map (see for example [32, 50]). Equivalently, we may describe these operations as rules transforming the flag graph of the original map to the flag graph of its medial, chamfering, truncation or leapfrog map and work with its symmetry type graph. We solve the second question regarding the number of flag-orbits that a map has after we apply the chamfering and leapfrog operations.

In Chapters 5 and 7, we review the results obtained in [45] for medial and truncation, and the complete list of possible symmetry type graphs with at most 6 vertices, as is given in [13] and [11]. In particular, in Chapter 5 we describe how to obtain the symmetry type graph of the medial of a map, by operations on the (extended) symmetry type graph of the map, we give for up to 7 vertices, the possible symmetry type graphs that a properly self-dual, an improperly self-dual and a medial map might have, and also show that every type of edge-transitive map is a medial type, Theorem 5.1.

In Chapter 6 we define and use the chamfering operation on k-orbit maps and determine, in terms of k, the number of possible flag-orbits that has the chamfering map of a k-orbit map. This operation divides each flag triangle of the original map into four different flags in the chamfering map. Thus, we find some conditions for the original map as for its chamfering map in manner to determine whether the chamfering map of a k-orbit map has $4k$ flag-orbits or not. Finally, we conclude with Theorems 6.1 and 6.2 where we obtain the number of flag-orbits that the chamfering map has if we repeat this operation t times on the same map. This operation is also used on the study of fullerenes (see [15]), for instance, which also leads to chemical applications as in [17]. Theorem 6.2 summarizes all the results presented in this chapter.

In Chapter 7 we determine the possible symmetry type graphs that a truncation of a map can have, and give an extension of the results for k-orbit maps for $k \leq 7$ and $k = 9$, given in a series of Propositions (7.5–7.11), which results are listed in Tables 7.1 and 7.2. Due to space, we leave on aside the truncation of 8-orbit maps. For this extension we use the same local arrangement of flags used in [45]. Later, in Section 7.2, are defined the

two-dimensional subdivision of a map and the leapfrog map, obtaining a classification of the possible symmetry type graphs for the leapfrog of k-orbit maps, with $k \leq 7$ and $k = 9$ (Table 7.3).

Finally, we present a summary of our results and remarks for further study.

Part I

Maps, Maniplexes and Symmetry type graphs

Chapter 1

Preliminaries

For the study of the structure of certain geometric objects as polyhedra or, in our case, maps on surfaces, it is common to look at its symmetries. In this chapter are presented basic definitions and results from permutation groups and graph theory that will be needed to follow the content of this thesis. For further information on these subjects the reader can refer to [5, 19], for permutation groups, and [3, 16], for graph theory.

1.1   Permutation groups

Let $\mathcal{F}$ be an arbitrary non-empty set. A bijection $\sigma : \mathcal{F} \to \mathcal{F}$ is a *permutation* of the set $\mathcal{F}$. The set of all permutations of $\mathcal{F}$ is a group called the *symmetric* (or *permutation*) *group* of $\mathcal{F}$, and is denoted as $Sym(\mathcal{F})$. A permutation whose inverse is itself is called an *involution*. If $\mathcal{F}$ and $\mathcal{F}'$ are two non-empty sets with the same cardinality, then the group $Sym(\mathcal{F})$ is isomorphic to the group $Sym(\mathcal{F}')$, and the isomorphism is given by $\sigma \mapsto \sigma'$, such that $\sigma' : \Phi' \mapsto \Psi'$ if and only if $\sigma : \Phi \mapsto \Psi$, where for each $\Phi \in \mathcal{F}$, Φ' denotes its images under the bijection between $\mathcal{F}$ and $\mathcal{F}'$.

The *action* (on the right) $(\mathcal{F}, G, \cdot)$ of a group G on a non-empty set $\mathcal{F}$ is a binary function $(\mathcal{F}, G) : \mathcal{F} \times G \to \mathcal{F}$ defined as $\Phi^x := \Phi \cdot x$, and is such that $\Phi^{id} = \Phi$, and $(\Phi^x)^y = \Phi^{xy}$, for every $\Phi \in \mathcal{F}$ and $x, y \in G$. Given two actions $(\mathcal{F}, G, \cdot)$ and $(\mathcal{F}', G', *)$, a pair (f, g) consisting of a surjective morphism $f : \mathcal{F} \to \mathcal{F}'$ and a group epimorphism $g : G \to G'$ is called an *action epimorphism* if for every $\Phi \in \mathcal{F}$ and every $x \in G$ it follows that

$$f(\Phi^x) := f(\Phi \cdot x) = f(\Phi) * g(x) := f(\Phi)^{g(x)}.$$

If both f and g are one-to-one we refer to (f, g) as an *action isomorphism*.

For any element $\Phi \in \mathcal{F}$, the set of all images of Φ under the action of all elements in

G is called the *orbit* of Φ under the action of G, and denoted by

$$\Phi^G := \{\Phi^x | x \in G\}.$$

The set of all elements in G that fix a element $\Phi \in \mathcal{F}$ forms a group, known as the *stabilizer* of Φ under the action of G, and we denote this groups as

$$\mathrm{Stab}_G(\Phi) := \{x \in G | \Phi^x = \Phi\}.$$

The following are well known properties of both sets, Φ^G and $\mathrm{Stab}_G(\Phi)$, with $\Phi \in \mathcal{F}$, [19].

(i) Two orbits Φ^G and Ψ^G are either equal (as sets) or disjoint, so the set of all orbits is a partition of $\mathcal{F}$ into mutually disjoint subsets.

(ii) For $x, y \in G$ and $\Phi, \Psi \in \mathcal{F}$, the stabilizer $\mathrm{Stab}_G(\Phi)$ is a subgroup of G and $\mathrm{Stab}_G(\Psi) = x^{-1}\mathrm{Stab}_G(\Phi)x$ (is the *conjugate class* of other stabilizer) whenever $\Psi = \Phi^x$. Moreover, $\Phi^x = \Phi^y$ if and only if $\mathrm{Stab}_G(\Phi)x = \mathrm{Stab}_G(\Phi)y$.

(iii) (The orbit-stabilizer property) $\Phi^G \cong G/\mathrm{Stab}_G(\Phi)$. If G is finite, then $|\Phi^G| = [G : \mathrm{Stab}_G(\Phi)]$ for all $\Phi \in \mathcal{F}$.

The set of all elements in a group G that conjugate a subgroup $H \leq G$ is called the *normalizer* of H under the action of G, and we denote it as

$$\mathrm{Norm}_G(H) := \{x \in G | x^{-1}Hx = H\}.$$

If for any two elements $\Phi, \Psi \in \mathcal{F}$ there is an element $x \in G$ such that $\Phi^x = \Phi$, then it is said that G acts *transitively* on $\mathcal{F}$. Say this in other way, the action of G is transitive on $\mathcal{F}$ whenever $\Phi^G = \mathcal{F}$, for any $\Phi \in \mathcal{F}$. If the stabilizer of every $\Phi \in \mathcal{F}$ under the action of the group G is such that $\mathrm{Stab}_G(\Phi) = id$, then the action of G on $\mathcal{F}$ is called *semi-regular*. Moreover, a transitive and semi-regular action of a group on a set is called a *regular* action. Then we have the following properties supposing that G that acts transitively on a set $\mathcal{F}$.

(i) For any $\Phi, \Psi \in \mathcal{F}$ there exist $x \in G$ such that $\mathrm{Stab}_G(\Phi) = x^{-1}\mathrm{Stab}_G(\Psi)x$ (all stabilizers are conjugated in G).

(ii) If G is finite, then $[G : \mathrm{Stab}_G(\Phi)] = |\mathcal{F}|$, for each $\Phi \in \mathcal{F}$.

(iii) If G is finite, then the action of G is regular if and only if $|G| = |\mathcal{F}|$.

The action of a group G on a set $\mathcal{F}$ can be extended to subsets of $\mathcal{F}$. That is, for any non-empty subset $\mathcal{B} \subseteq \mathcal{F}$ the elements $x \in G$ acting on $\mathcal{B}$ define the set $\mathcal{B}^x := \{\Psi^x | \Psi \in \mathcal{B}\}$. If the action of G is transitive on $\mathcal{F}$, then the subset $\mathcal{B} \subseteq \mathcal{F}$ is called a *block* for G if for each $x \in G$ either $\mathcal{B}^x = \mathcal{B}$ or $\mathcal{B}^x \cap \mathcal{B} = \emptyset$. Furthermore, the set of all blocks $\Sigma := \{\mathcal{B}^x | x \in G\}$, for a group G that acts transitively on the set $\mathcal{F}$, form a partition of $\mathcal{F}$ and every element in Σ is a block for G. The group G acts on the set Σ on a natural way.

1.2   Graphs

A *graph* $\mathcal{G} := (V, E)$ is defined by a pair of sets V and E, also sometimes denoted by $V(G)$ and $E(G)$. The elements in V are called *vertices* and those in E are pairs of vertices, called *edges*. We shall say that two vertices $u, v \in V$ are *adjacent* in $\mathcal{G}$ if the pair $\{u, v\} =: e$ is a element in E, where u and v are called the endpoints of e. The vertices $u, v \in V$ are said to be *incident* to the edge $e := \{u, v\} \in E$. We refer as the *valency* of a vertex $v \in V$ to the number of edges to which v is incident in $\mathcal{G}$. If all vertices in a graph $\mathcal{G}$ have the same valency, say n, then we shall say that $\mathcal{G}$ is an *n-valent* graph. In particular, a 3-valent graph is named as a *cubic graph*.

There are different type of edges that one can find in a graph: *parallel edges* (or *multiple edges*), that are two or more edges with the same endpoints, and *loops*, edges whose both endpoints correspond to the same vertex. If a graph $\mathcal{G}$ have neither parallel edges nor loops is called as a *simple* graph, otherwise $\mathcal{G}$ is known as *general graph* or a *multi-graph*. There is another type of edge that can be used in graphs as those defined in Section 1.3, these are *semi-edges* (or pending edges), edges with a single endpoint. We refer to those graphs with semi-edges but no loops in them as *pre-graphs*, see for instance [48]. An example of a simple graph is depicted in the left of Figure 1.1, and in the right is a general graph with parallel edges in red, loops in colour blue and semi-edges in green.
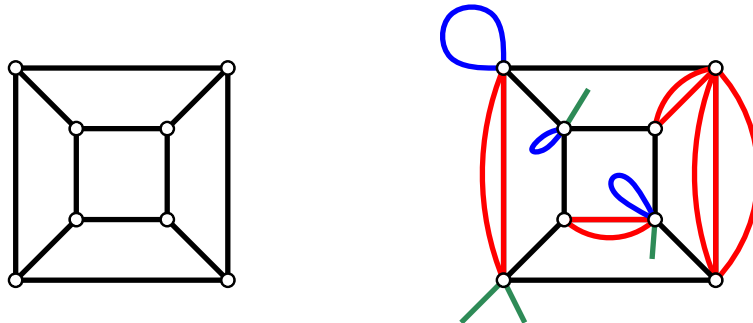
Figure 1.1: Simple cube graph Q_3 (left), and Q_3 with loops, semi-edges and parallel edges (right).

Let $\mathcal{H}$ and $\mathcal{G}$ be two graphs such that $V(\mathcal{H}) \subseteq V(\mathcal{G})$ and $E(\mathcal{H}) \subseteq E(\mathcal{G})$, then $\mathcal{H}$ is a *subgraph* of $\mathcal{G}$. In case that $V(\mathcal{H}) = V(\mathcal{G})$ and $E(\mathcal{H}) \subseteq E(\mathcal{G})$, then $\mathcal{H}$ is a *spanning subgraph* of $\mathcal{G}$. An *independent* set of edges in a graph $\mathcal{G}$ is a set of edges such that no two edges in the set have a vertex in common; similarly for vertices. A set of independent edges in a graph $\mathcal{G}$ is also known as a *matching* of the graph. Moreover, an independent set of edges in $\mathcal{G}$ such that each vertex of $\mathcal{G}$ is incident to an edge of the matching is a *perfect matching* of $\mathcal{G}$.

A *walk* in a graph is an alternating sequence of vertices and edges, but more commonly

denoted as a sequence of vertices $(v_0, v_1, \ldots, v_q)$ where the pairs $\{v_{i-1}, v_i\}$ correspond to elements in E, with $0 \leq i \leq q$. The length of the walk corresponds to the value of q. Whenever $v_0 = v_q$, the walk is then called a *closed walk*. The graph $\mathcal{G}$ is said to be a *connected* graph if there is a walk connecting any pair of vertices in the graph.

A matching is a disconnected subgraph of a graph, a perfect matching is also known as a *1-factor* of the graph. Moreover, a 2-factor is a collection of cycles that spans all vertices of the graph.

Whenever we can give a partition of two disjoint vertex sets in a connected graph $\mathcal{G}$, such that no vertex from a part is adjacent to any other of the same part, (i.e., all the edges of $\mathcal{G}$ connect only vertices from both parts of the partition) then $\mathcal{G}$ is called a *bipartite* graph. If the vertex set of $\mathcal{G}$ can be partitioned into more than two sets, with the same property as before, then $\mathcal{G}$ is called *multi-partite* or *n-partite* graph.

Two graphs $\mathcal{H}$ and $\mathcal{G}$ are said to be *isomorphic* if there is an isomorphism $\varphi : V(\mathcal{G}) \to V(\mathcal{H})$, such that $\{\varphi(u), \varphi(v)\} \in E(\mathcal{H})$ if and only if $\{u, v\} \in E(\mathcal{G})$. An isomorphism from a graph to itself is an *automorphism* of the graph. The set of all automorphisms of a graph $\mathcal{G}$ forms a group, the *automorphism group* of $\mathcal{G}$, denoted as $\mathrm{Aut}(\mathcal{G})$. A graph is *vertex-transitive* (resp. *edge-transitive*) if acts transitively on $V(\mathcal{G})$ (respectively $E(\mathcal{G})$).

1.2.1 Graph colourings

To define properties from a graph, it is helpful to either label the vertices or edges of the graph that we are studying. Similarly, we can assign colours to the vertices and the edges, in particular, we work with edge-coloured graphs. An *edge-colouring* of a graph $\mathcal{G}$ is a function $c : E \to S$, where S is a set of colours. Such edge-colouring is called *proper* if $c(e) \neq c(f)$ for any two adjacent edges $e, f \in E$ (edges with at least one incident vertex in common).

Note that if $\mathcal{G}$ can be partitioned into disjoint matchings, we can colour every matching in $\mathcal{G}$ with a different colour, and define a proper edge-colouring of $\mathcal{G}$. Hence, the union of two disjoint matchings determine a 2-factor of $\mathcal{G}$ composed by even cycles with alternating coloured edges.

There are two interesting subgroups of the automorphism group of a graph associated with the edge-coloured graph $\hat{\mathcal{G}}$: the *colour respecting automorphism group* $\mathrm{Aut}_r(\hat{\mathcal{G}})$, consisting of all automorphisms of $\mathcal{G}$ that induce a permutation of the colours of the edges, and the *colour preserving automorphism group* $\mathrm{Aut}_c(\hat{\mathcal{G}})$, consisting of all automorphisms of $\mathcal{G}$ that send two adjacent vertices by colour i into other two adjacent by the same colour i. Clearly $\mathrm{Aut}_c(\hat{\mathcal{G}}) \leq \mathrm{Aut}_r(\hat{\mathcal{G}}) \leq \mathrm{Aut}(\mathcal{G})$. When the edge-colouring c of a graph is clear from the context, we abuse notation and denote by $\mathcal{G}$ both the graph and the edge-coloured graph, with this notation, $\mathrm{Aut}_c(\mathcal{G}) \leq \mathrm{Aut}_r(\mathcal{G}) \leq \mathrm{Aut}(\mathcal{G})$.

1.3 Action graphs and Schreier coset graphs

Considering the group $Sym(\mathcal{F})$, of permutations of a set $\mathcal{F} \neq \emptyset$, we can define a graph as a combinatorial representation of a subgroup $H \leq Sym(\mathcal{F})$ acting on the set $\mathcal{F}$. Such graph is know as an *action graph* ([38]) (see [38]).

1.3.1 Cayley graphs

Consider a non-trivial group G acting on a set $\mathcal{F} \neq \emptyset$. Let $S \subset G$ be a subset of G such that $S^{-1} = S \neq \emptyset$. Define the *Cayley graph* $\mathcal{G}(\mathcal{F}, S)$, as a graph with vertex set $\mathcal{F}$ such that two vertices $\Phi, \Psi \in \mathcal{F}$ are adjacent by and edge represented by an element $s \in S$, whenever $\Phi = \Psi^s$ (similarly, $\Phi^{s^{-1}} = \Psi$).

Example 1.1. *Consider the set with four elements $\{a, b, c, d\}$ and G its symmetric group. Let $S := \{id, (ab)(cd)\} \subset G$. Then, we can build the Cayley graph with four vertices, and semi-edges represented by $id \in S$ and edges represented by $(ab)(cd) \in S$ as is depicted in Figure 1.2.*
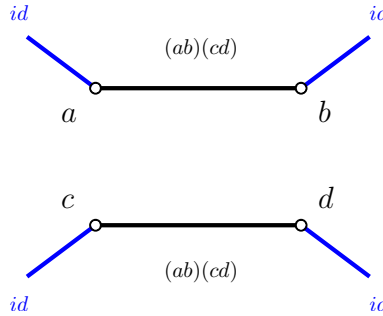
Figure 1.2: Cayley graph with four vertices a, b, c, d joined by blue semi-edges and black edges representing the action of the elements $id, (ab)(cd) \in S$.

A walk W in the Cayley graph $\mathcal{G}(\mathcal{F}, S)$ defines a word $w := s_{i_0} s_{i_1} \cdots s_{i_n}$ with $s_{i_0}, s_{i_1}, \ldots, s_{i_n} \in S$. Conversely, any word $w := s_{i_0} s_{i_1} \cdots s_{i_n}$, in the group generated by the elements of S, induces a walk $W(\Phi, w)$ starting at a vertex $\Phi \in \mathcal{F}$ and ending at the vertex Φ^w. Moreover, the Cayley graph $\mathcal{G}(\mathcal{F}, S)$ is connected if and only if S generates a transitive subgroup of G.

Another concept that will help us to understand the construction of the graphs in Chapter 3 is the concept of covering projection.

Covering projection

Given a graph $\mathcal{G}$, and a partition $\mathcal{X}$ of its vertex set V, the *quotient $\mathcal{G}_{\mathcal{X}}$, with respect to $\mathcal{X}$*, is defined as the pre-graph with vertex set $\mathcal{X}$, such that for any two vertices $A, B \in \mathcal{X}$, there is an edge from A to B if and only if there exists $u \in A$ and $v \in B$ such that there is an edge from u to v. Edges between vertices in the same part of the partition $\mathcal{X}$ quotient into semi-edges.

Let $\mathcal{G}$ and $\hat{\mathcal{G}}$ be two graphs, suppose there exists a surjective function

$$\psi : V(\mathcal{G}) \to V(\hat{\mathcal{G}})$$

assigning to each vertex $u \in V(\mathcal{G})$ a vertex in $V(\hat{\mathcal{G}})$ in such way that the set of edges with incident vertex $u \in V(\mathcal{G})$, is bijectively sent onto the set of edges with incident vertex $\psi(u) \in V(\hat{\mathcal{G}})$, that is, ψ induces a bijection between $\{e \in E(\mathcal{G})|u \in e\}$ and $\{\hat{e} \in E(\hat{\mathcal{G}})|\Psi(u) \in \hat{e}\}$. Then, Ψ is called a *covering projection*. The graph $\hat{\mathcal{G}}$ is called *base graph* and $\mathcal{G}$ is called *covering graph*.

Furthermore, supposing that $\mathcal{G}$ is a connected graph and that there is a group G whose action is semi-regular on the vertices of $\mathcal{G}$, then $\psi : V(\mathcal{G}) \to V(\hat{\mathcal{G}})$ is a *regular covering projection*. Equivalently, ψ induces a *quotient* of $\mathcal{G}$ in the following sense: Let $\mathcal{G}/G := \{\Phi^G \mid \Phi \in V(\mathcal{G})\}$ be the set of all the orbits of the vertex-set of $\mathcal{G}$. If there exist an isomorphism $\varphi : \mathcal{G}/G \to \hat{\mathcal{G}}$, which projects each orbit Φ^G into a vertex in $\hat{\mathcal{G}}$, such that the projection $\psi = \varphi \circ \phi_G$ is well defined, where $\phi_G : \mathcal{G} \to \mathcal{G}/G$. And $\mathcal{G}$ is called a *regular covering*, and the image $\hat{\mathcal{G}}$ is also called a base graph, [27].

In Figures 1.3 and 1.4 are depicted two different covering graphs with base graph the well-known Petersen graph.
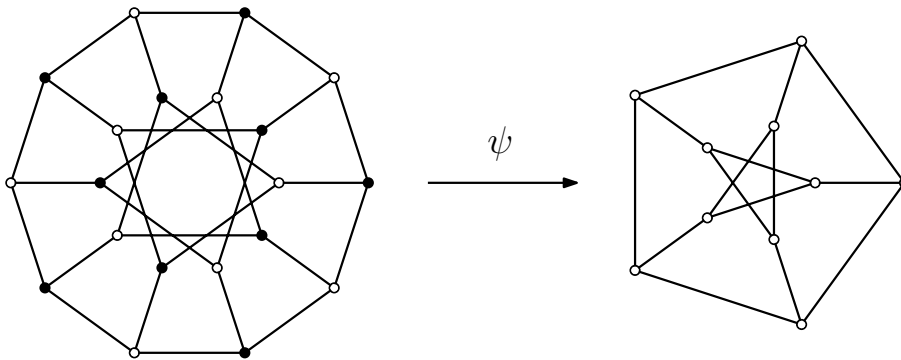

Figure 1.3: Desargue graph $G(10,3)$ (left), as the covering graph of Petersen graph $G(5,2)$, corresponding to a Kronecker cover or canonical double cover.

In Chapters 2 and 3, we define two different graphs: the *flag graph* and the *symmetry type graph* of a map. Both graphs are used to understand the whole structure of our object
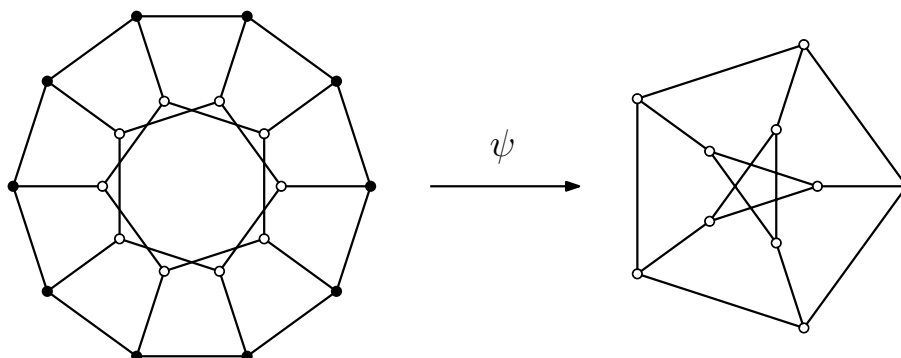
Figure 1.4: Dodecahedron graph $G(10, 2)$ (left), as the covering graph of Petersen graph $G(5, 2)$, with Z_2 as the group acting on the vertices of $G(10, 2)$.

of study: the *maniplexes*. These graphs are examples of connected action graphs. The first one corresponds to a Schreier coset graph, while the second one is the base graph of the flag graph as a covering graph.

1.3.2   Schreier coset graphs

According to [9], in [51], Schreier consider a graph whose vertices represent the cosets of any given subgroup H of a given group G. That is, given a set $S = \{x_1, \ldots, x_n\}$ such that its elements generate the group G, the right cosets Hx represent the vertices of the "(right) Schreier colour graph", and two vertices representing the cosets Hx and Hy are joined by a coloured-edge represented by the element $z \in S$ whenever $Hy = Hxz$. In case that $Hx = Hxz$, then the vertex Hx is joined to itself with a loop of colour representing $z \in S$. Ignoring the colours and adding direction to the edges, by ordering the pairs (Hx, Hxz), we obtain a Schreier coset graph. In Figure 1.5 are depicted the Schreier graphs of the permutation group on three elements S_3, and of the alternating group A_4.

$$S_3 = \langle (12), (123) \rangle \qquad\qquad A_4 = \langle (12)(34), (123) \rangle$$

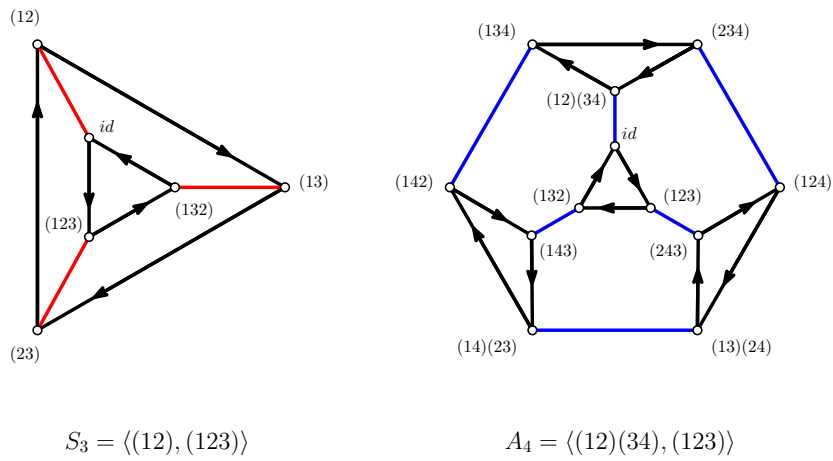Figure 1.5: Schreier graphs of the group $S_3 := \langle (12), (123) \rangle$ (left) and of the alternating group $A_4 := \langle (12)(34), (123) \rangle$).

Chapter 2

Maps and Maniplexes

The aim of this work is to give a classification on the symmetry types of maps and maniplexes. Both, maps and maniplexes, can be defined by a set of flags $\mathcal{F}$ and a sequence of relations connecting pairwise the elements in $\mathcal{F}$. In this chapter, we first review the basic theory regarding maps ([25, 27]), according to their flag structure, and later we define maniplexes as a generalization of maps, given by Wilson in [56].

2.1 Maps

Topologically, a *map* is a 2-cellular embedding of a connected graph on a closed surface, with no boundary, in the sense that the graph divides the surface into simply connected regions. We shall say that the vertices and edges of the map correspond to those of its underlying graph, and the faces of $\mathcal{M}$ are described by some *distinguished closed walks* of the graph, homeomorphic to discs, in such way that each edge of the map is in either exactly two distinguished cycles, or twice on the same one. (Note that the distinguished cycles of the graph can be identified with the simply connected regions obtained by removing the graph from the surface.)

We shall say that a map $\mathcal{M}$ is *non-degenerated* whenever each edge of $\mathcal{M}$ has exactly two vertices, and every edge is incident to exactly two faces of $\mathcal{M}$. Otherwise, $\mathcal{M}$ is is said to be a *degenerated* map. In the second part of this thesis we work only with non-degenerated maps, since the operations that we study, in such part, are well-defined only for non-degenerated maps. In Figure 2.1 are depicted three different embeddings of the cube graph Q_3 on different surfaces, one in sphere and other two in the torus. In Figure 2.2 are depicted two examples of degenerated maps. We denote the set of vertices, edges and faces of the map $\mathcal{M}$ as $V(\mathcal{M})$, $E(\mathcal{M})$ and $F(\mathcal{M})$, respectively, and frequently refer to them as the 0-, 1- and 2-faces of $\mathcal{M}$, respectively.
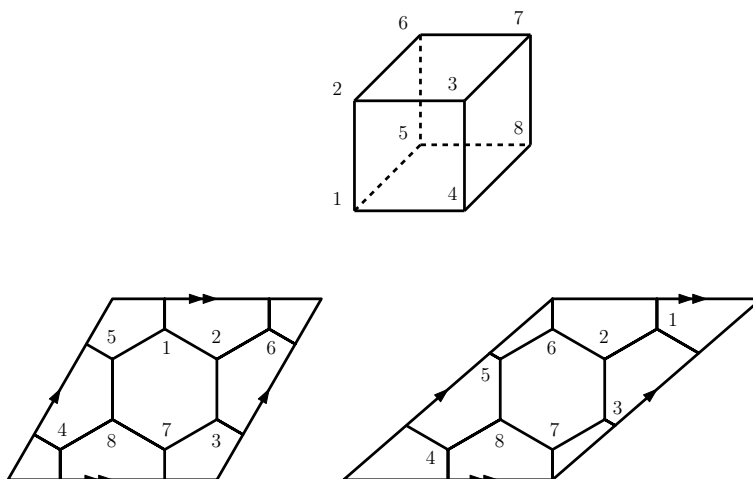
Figure 2.1: Three different embeddings of the cube graph Q_3 on different surfaces, one in sphere and other two in the torus.
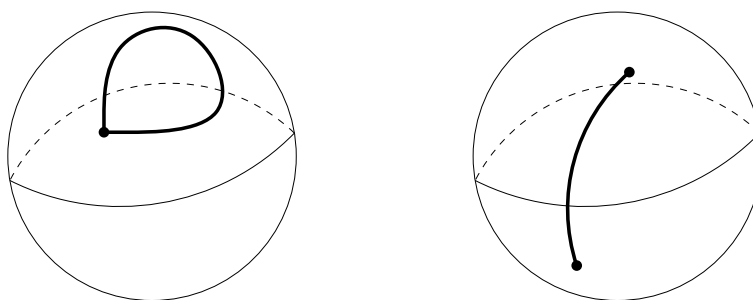

Figure 2.2: Degenerated maps.

In 1982-83, Lins and Vince studied the concept of combinatorial maps in [37] and [54], respectively. For this work, we follow such combinatorial definition of a map. This is, we understand a map $\mathcal{M}$ as an edge coloured cubic graph $\mathcal{G}_{\mathcal{M}}$, to which we refer as the *flag graph* of the map $\mathcal{M}$; this is defined in the following subsection.

2.1.1   Flag graph

Let $\mathcal{BS}(\mathcal{M})$ be the barycentric subdivision of a map $\mathcal{M}$, where each face of $\mathcal{M}$ is decomposed into triangles with a vertex in common (see Figure 2.3). In fact, $\mathcal{BS}(\mathcal{M})$ is a map with triangular faces in the same surface as $\mathcal{M}$. For each triangle Φ in $\mathcal{BS}(\mathcal{M})$ we label its vertices by Φ_0, Φ_1 and Φ_2 according to whether they represent a vertex, an edge or a face (mutually incident) in the map $\mathcal{M}$. Note that each triangle of $\mathcal{BS}(\mathcal{M})$ is adjacent to other three triangles. If two triangles Φ and Ψ of $\mathcal{BS}$ are adjacent by the edge with vertices Φ_j and Φ_k, with $j, k \in \{0, 1, 2\}$ and $j \neq k$, then we say that Φ and Ψ are i-adjacent, for $i \in \{0, 1, 2\}$ and $i \neq j, k$. In this case we shall denote Ψ by Φ^i (likewise Φ by Ψ^i) and note that for every triangle Φ and $i \in \{0, 1, 2\}$, $(\Phi^i)^i = \Phi$.

Hence, a (non-degenerated) map $\mathcal{M}$ can be seen as a set $\mathcal{F}(\mathcal{M})$ of *flags*, and the relation between pairs of elements in $\mathcal{F}(\mathcal{M})$ in the following way. A flag of $\mathcal{M}$ is an ordered triple of a vertex, an edge and a face mutually incident in $\mathcal{M}$. One can identify a flag (Φ_0, Φ_1, Φ_2) of the map $\mathcal{M}$ with the triangle Φ in $\mathcal{BS}(\mathcal{M})$, where the flag assigned to the triangle Φ^i shares the elements Φ_j and Φ_k in the triple (Φ_0, Φ_1, Φ_2), but differs in the third element Φ_i, with $j, k \in \{0, 1, 2\}$ and $j \neq k$, for $i \in \{0, 1, 2\}$ and $i \neq j, k$. In other words, the set of flags of a map $\mathcal{M}$ is in direct correspondence with the set of triangular faces of the barycentric subdivision $\mathcal{BS}(\mathcal{M})$. Moreover, denote by Φ^0, Φ^1 and
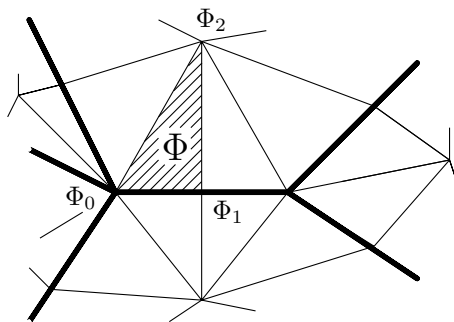

Figure 2.3: Barycentric subdivision of $\mathcal{M}$ and the flag $\Phi = (\Phi_0, \Phi_1, \Phi_2) \in \mathcal{F}(\mathcal{M})$.

Φ^2 the corresponding adjacent flags of Φ in $\mathcal{M}$, and extend this notation by induction in the following way

$$(\Phi^{i_0, i_1, \ldots, i_{k-1}})^{i_k} = \Phi^{i_0, i_1, \ldots, i_{k-1}, i_k}.$$

Note that $\Phi^{i,i} = \Phi$ for $i = 0, 1, 2$ and that $\Phi^{0,2} = \Phi^{2,0}$, for every flag Φ in $\mathcal{F}(\mathcal{M})$. Moreover, the connectivity of the underlying graph of $\mathcal{M}$ implies that given any two flags Φ and Ψ of $\mathcal{M}$, there exist integers $i_0, i_1, \ldots, i_k \in \{0, 1, 2\}$ such that $\Psi = \Phi^{i_0, i_1, \ldots, i_k}$.

For each flag of $\mathcal{M}$ (face of $\mathcal{BS}(\mathcal{M})$) we assign a vertex, and define an edge between two of them whenever the corresponding flags are adjacent (see Figure 2.4). We can
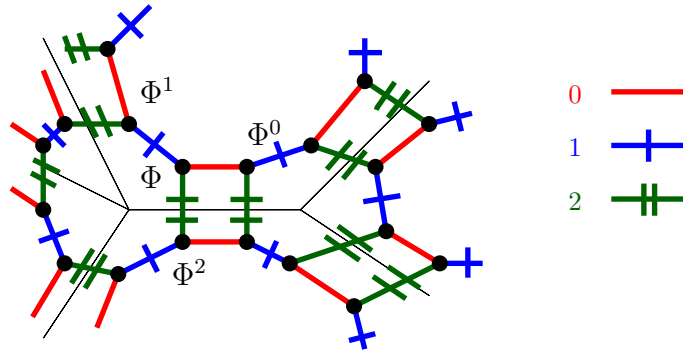

Figure 2.4: Local representation of the flag graph $\mathcal{G}_{\mathcal{M}}$ of a map $\mathcal{M}$.

naturally colour the edges of this new graph with colours $0, 1, 2$ in such a way that the edge between any two i-adjacent flags has colour i. The obtained 3-edge-coloured graph is called the *flag graph* $\mathcal{G}_{\mathcal{M}}$ of $\mathcal{M}$. (Note that this cubic graph with the vertex set $\mathcal{F}(\mathcal{M})$ defines the dual of the barycentric subdivision $\mathcal{BS}(\mathcal{M})$, in the sense of Section 4.1.)

Observe that the edges of a given colour form a perfect matching (an independent set of edges containing all the vertices of the graph) in $\mathcal{G}_{\mathcal{M}}$. Hence the union of two sets of edges of different colours is a subgraph whose connected components are even cycles. Such subgraph is called a *2-factor* of $\mathcal{G}_{\mathcal{M}}$. Since $\Phi^{0,2} = \Phi^{2,0}$, we note that the 2-factor of $\mathcal{G}_{\mathcal{M}}$ with edges of colours 0 and 2 consists of 4-cycles.

A map $\mathcal{M}$ is said to be *orientable* if its underlying surface is orientable. It is not difficult to see that $\mathcal{M}$ is orientable if and only if its flag graph $\mathcal{G}_{\mathcal{M}}$ is bipartite, [25].

An *automorphism* of $\mathcal{G}_{\mathcal{M}}$ is a bijection of the vertices of $\mathcal{G}_{\mathcal{M}}$ that preserves the incidences of the graph; the set of all automorphisms of $\mathcal{G}_{\mathcal{M}}$ is the *automorphism group* $\mathrm{Aut}(\mathcal{G}_{\mathcal{M}})$ of $\mathcal{G}_{\mathcal{M}}$. There are two interesting subgroups of $\mathrm{Aut}(\mathcal{G}_{\mathcal{M}})$ associated with the graph $\mathcal{G}_{\mathcal{M}}$: the *colour respecting automorphism group* $\mathrm{Aut}_r(\mathcal{G}_{\mathcal{M}})$, consisting of all automorphisms of $\mathcal{G}_{\mathcal{M}}$ that induce a permutation of the colours of the edges, and the *colour preserving automorphism group* $\mathrm{Aut}_p(\mathcal{G}_{\mathcal{M}})$, consisting of all automorphisms of $\mathcal{G}_{\mathcal{M}}$ that send two adjacent vertices by colour i into other two adjacent by the same colour i. Clearly $\mathrm{Aut}_p(\mathcal{G}_{\mathcal{M}}) \leq \mathrm{Aut}_r(\mathcal{G}_{\mathcal{M}}) \leq \mathrm{Aut}(\mathcal{G}_{\mathcal{M}})$.

2.1.2   Monodromy group

To each map $\mathcal{M}$ we can associate a subgroup of the permutation group of the flags of $\mathcal{M}$ in the following way. Let s_0, s_1, s_2 be permutations in the symmetric group $Sym(\mathcal{F}(\mathcal{M}))$, acting on the right, such that for any flag $\Phi \in \mathcal{F}(\mathcal{M})$,

$$\Phi^{s_i} := \Phi \cdot s_i = \Phi^i;$$

with $i = 0, 1, 2$. These permutations generate a group $\mathrm{Mon}(\mathcal{M})$, called the *monodromy (or connection) group* of the map $\mathcal{M}$ ([32]). Observe that if $\Psi \in \mathcal{F}(\mathcal{M})$ is such that $\Psi = \Phi^{i_0, i_1, \ldots, i_k}$, then

$$\Psi^{s_{i_{k+1}}} = (\Phi^{i_0, i_1, \ldots, i_k})^{s_{i_{k+1}}} = \Phi^{i_0, i_1, \ldots, i_k, i_{k+1}},$$

with $i_0, i_1, \ldots, i_k, i_{k+1} \in \{0, 1, 2\}$. Recall that for every flag $\Phi \in \mathcal{F}(\mathcal{M})$, $\Phi^{i,i} = \Phi$ and that $\Phi^{0,2} = \Phi^{2,0}$. Given a non-degenerated map, a triangle Φ of the barycentric subdivision is different to its adjacent triangles , then the *distinguished generators* s_0, s_1, s_2 of $\mathrm{Mon}(\mathcal{M})$ are fix-point free involutions. Moreover, the product $s_0 s_2 = s_2 s_0$ is also fix-point free as each edge of a map is always contained in four different flags and $s_0 s_2$ always sends the flag $\Phi := (\Phi_0, \Phi_1, \Phi_2)$ to the unique flag Ψ that shares with Φ the element Φ_1, but differs in the other two elements. Furthermore, the connectivity of the map implies that the action of the group $\mathrm{Mon}(\mathcal{M})$ is transitive on $\mathcal{F}(\mathcal{M})$.

Observe that the distinguished generators s_0, s_1, s_2 of $\mathrm{Mon}(\mathcal{M})$ label the coloured edges of the flag graph $\mathcal{G}_{\mathcal{M}}$ in a natural way. That is, each edge of colour i is labelled with the generator s_i. In this way, one can think of the walks among the edges of $\mathcal{G}_{\mathcal{M}}$ as words in $\mathrm{Mon}(\mathcal{M})$. In fact, if $\Phi, \Psi \in \mathcal{F}(\mathcal{M})$ are two flags such that $\Psi = \Phi^w$, for some $w = s_{i_0} s_{i_1} \ldots s_{i_k} \in \mathrm{Mon}(\mathcal{M})$, then the walk of $\mathcal{G}_{\mathcal{M}}$ starting at the vertex Φ and travelling in order among the edges $i_0, i_1, \ldots, i_k$ will finish at the vertex Ψ. And vice versa, every walk among the coloured edges of $\mathcal{G}_{\mathcal{M}}$ starting at Φ and finishing at Ψ induces a word $w \in \mathrm{Mon}(\mathcal{M})$ that satisfies that $\Phi^w = \Psi$. Note however that in general the action of $\mathrm{Mon}(\mathcal{M})$ is not semi-regular on $\mathcal{F}(\mathcal{M})$, implying that one can have differently "coloured" walks in $\mathcal{G}_{\mathcal{M}}$ going from Φ to Ψ that induce different words of $\mathrm{Mon}(\mathcal{M})$ (but act on the flag Φ in the same way).

Since $s_0 s_2 = s_2 s_0$ is fixed-point free, the 4-cycles with edges of alternating colours 0 and 2 in $\mathcal{G}_{\mathcal{M}}$ define the set of edges on the map. In other words, the edges of $\mathcal{M}$ can be identified with the orbits of $\mathcal{F}(\mathcal{M})$ under the action of the subgroup generated by the involutions s_0 and s_2; that is,

$$E(\mathcal{M}) = \{\Phi^{\langle s_0, s_2 \rangle} \mid \Phi \in \mathcal{F}(\mathcal{M})\}.$$

Similarly, we find that the vertices and faces of $\mathcal{M}$ are identified with the respective orbits of the subgroups $\langle s_1, s_2 \rangle$ and $\langle s_0, s_1 \rangle$ on $\mathcal{F}(\mathcal{M})$. That is,

$$V(\mathcal{M}) = \{\Phi^{\langle s_1, s_2 \rangle} \mid \Phi \in \mathcal{F}(\mathcal{M})\} \quad \text{and} \quad F(\mathcal{M}) = \{\Phi^{\langle s_0, s_1 \rangle} \mid \Phi \in \mathcal{F}(\mathcal{M})\}.$$

Thus, the group $\langle s_0, s_1, s_2 \rangle$ acts transitively on sets of vertices, edges and faces of $\mathcal{M}$.

In particular, for each flag $\Phi \in \mathcal{F}(\mathcal{M})$, the set $(\Phi)_0 := \{\Phi^w \mid w \in \langle s_1, s_2 \rangle\}$ is the orbit of the flag Φ around a vertex of $\mathcal{M}$. Similarly, $(\Phi)_1 := \{\Phi^w \mid w \in \langle s_0, s_2 \rangle\}$ and $(\Phi)_2 := \{\Phi^w \mid w \in \langle s_0, s_1 \rangle\}$ are the orbits of the flag Φ around an edge and a face of the map $\mathcal{M}$. The following lemma states that in fact, for each k, $(\Phi)_k$ is precisely the set of flags contained in the k-face of Φ, and hence we can identify the k-face of Φ with the set $(\Phi)_k$.

Lemma 2.1. *Let $\mathcal{M}$ be a map, $\mathcal{F}(\mathcal{M})$ its set of all flags and $\mathrm{Mon}(\mathcal{M})$ its monodromy group. For each $\Phi \in \mathcal{F}(\mathcal{M})$ and $k \in \{0, 1, 2\}$, let $(\Phi)_k := \{\Phi^w \mid w \in \langle s_i, s_j \rangle, i \neq j \neq k\}$. If $\Phi, \Psi \in \mathcal{F}(\mathcal{M})$ and $k \in \{0, 1, 2\}$ are such that $(\Phi)_k \cap (\Psi)_k \neq \emptyset$, then $(\Phi)_k = (\Psi)_k$.*

Proof. If $(\Phi)_k \cap (\Psi)_k \neq \emptyset$, then there exist $w_0, w_1 \in \langle s_i, s_j \rangle$ such that $\Phi^{w_0} = \Psi^{w_1}$. But for any $w \in \langle s_i, s_j \rangle$ we have that $\Phi^w = \Phi^{w_0 w_0^{-1} w} = \Psi^{w_1 w_0^{-1} w}$, and since $w_1 w_0^{-1} w \in \langle s_i, s_j \rangle$, then $\Phi^w \in (\Psi)_k$, implying that $(\Phi)_k \subseteq (\Psi)_k$. A similar argument shows the other contention. ∎

A map is called *equivelar* if each of its faces has the same number p of edges and if each of its vertices belongs to the same number q of edges, [41].

2.1.3   Automorphism group, and k-orbit maps

We shall say that a symmetry, or an *automorphism*, of a map $\mathcal{M}$ is an automorphism of its underlying graph that preserves the set of faces of the map. The set of all automorphisms of $\mathcal{M}$ forms a group, the automorphism group of $\mathcal{M}$, we denote this group as $\mathrm{Aut}(\mathcal{M})$.

An automorphism $\alpha \in \mathrm{Aut}(\mathcal{M})$ of the map $\mathcal{M}$ induces a permutation of the flags in $\mathcal{F}(\mathcal{M})$ such that $\Phi \alpha := (\Phi_0 \alpha, \Phi_1 \alpha, \Phi_2 \alpha)$, with $\Phi \in \mathcal{F}(\mathcal{M})$. Moreover, $\alpha \in \mathrm{Aut}(\mathcal{M})$ preserves the adjacencies between flags; that is, $(\Phi \alpha)^i = \Phi^i \alpha$, with $\Phi \in \mathcal{F}(\mathcal{M})$. From here it follows that

$$\Phi^{s_i} \alpha = (\Phi \alpha)^{s_i},$$

for every flag $\Phi \in \mathcal{F}(\mathcal{M})$ and $i \in \{0, 1, 2\}$ [32]. Therefore, an automorphism of $\mathcal{M}$ is a bijection of $\mathcal{F}(\mathcal{M})$ whose action commutes with the elements of $\mathrm{Mon}(\mathcal{M})$. Thus, $\mathrm{Aut}(\mathcal{M})$ can be seen as a subgroup of $Sym(\mathcal{F}(\mathcal{M}))$ that preserves the coloured adjacencies; that is, $\mathrm{Aut}(\mathcal{M}) \cong H \leq \mathrm{Aut}_p(\mathcal{G}_{\mathcal{M}})$. Conversely, for every $\gamma \in \mathrm{Aut}_p(\mathcal{G}_{\mathcal{M}})$, we have that two vertices $\Phi \gamma$ and $\Psi \gamma$ of $\mathcal{G}_{\mathcal{M}}$ are adjacent by an edge coloured $i = 0, 1, 2$ if and only if $\Psi = \Phi^i$, then it follows that $\Phi^i \gamma = \Psi \gamma = (\Phi \gamma)^i$, hence γ induces an automorphism of $\mathcal{M}$. Then, an automorphism of a map $\mathcal{M}$ can be seen as an edge-colour preserving automorphism of the flag graph $\mathcal{G}_{\mathcal{M}}$. Therefore, $\mathrm{Aut}(\mathcal{M}) \cong \mathrm{Aut}_p(\mathcal{G}_{\mathcal{M}})$.

Let $\alpha \in \mathrm{Aut}_p(\mathcal{G}_\mathcal{M})$ be such that $\Phi\alpha = \Phi$ for some vertex Φ of $\mathcal{G}_\mathcal{M}$. Since α preserves the colours of the edges of $\mathcal{G}_\mathcal{M}$, it must fix all the edges incident to Φ and hence all neighbours of Φ. It is not difficult to see that, by the connectivity of the map, α fixes all the vertices of $\mathcal{G}_\mathcal{M}$, as well as all its edges and hence is the identity of $\mathrm{Aut}_p(\mathcal{G}_\mathcal{M})$. That is, the action of the automorphism group $\mathrm{Aut}_p(\mathcal{G}_\mathcal{M})$ on the vertices of $\mathcal{G}_\mathcal{M}$ is semi-regular and therefore the action of $\mathrm{Aut}(\mathcal{M})$ is semi-regular on the flags of $\mathcal{M}$.

Denote by $\mathrm{Orb}(\mathcal{M}) := \{\mathcal{O}_\Phi | \Phi \in \mathcal{F}(\mathcal{M})\}$, the set of flag-orbits of $\mathcal{M}$ under the action of $\mathrm{Aut}(\mathcal{M})$. Given two orbits $\mathcal{O}_1, \mathcal{O}_2 \in \mathrm{Orb}(\mathcal{M})$ and a flag $\Phi \in \mathcal{O}_1$, let $\Phi, \Psi \in \mathcal{O}_1$ such that $\Phi^v \in \mathcal{O}_2$ for some $v \in \mathrm{Mon}(\mathcal{M})$. Then, there exists $\alpha \in \mathrm{Aut}(\mathcal{M})$ such that $\Psi = \Phi\alpha$. Hence, $\Psi^v = (\Phi\alpha)^v = \Phi^v\alpha$. Thus, $\Phi^v, \Psi^v \in \mathcal{O}_2$, and we obtain the following lemma.

Lemma 2.2. *Let $\Phi \in \mathcal{F}(\mathcal{M})$, $\mathcal{O}_1, \mathcal{O}_2 \in \mathrm{Orb}(\mathcal{M})$, and $v \in \mathrm{Mon}(\mathcal{M})$. If $\Phi \in \mathcal{O}_1$ and $\Phi^v \in \mathcal{O}_2$, then $\Psi \in \mathcal{O}_1$ if and only if $\Psi^v \in \mathcal{O}_2$.*

Let $\Phi \in \mathcal{F}(\mathcal{M})$ be a base flag of $\mathcal{M}$, and choose a word $w = s_{i_0}s_{i_1}\cdots s_{i_n}$ in $\mathrm{Mon}(\mathcal{M})$ such that the flag Φ^w is in the same flag orbit as Φ. Then, there is an automorphism, denoted by α_w, in $\mathrm{Aut}(\mathcal{M})$ such that $\Phi^w = \Phi\alpha_w$, we also denote α_w as $\alpha_{i_0,i_1,\dots,i_n}$. Since the action of $\mathrm{Aut}(\mathcal{M})$ is semi-regular on the set $\mathcal{F}(\mathcal{M})$, for $u, w \in \mathrm{Mon}(\mathcal{M})$ such that there are automorphisms $\alpha_u, \alpha_w \in \mathrm{Aut}(\mathcal{M})$ of $\mathcal{M}$, it follows that $\alpha_u = \alpha_w$ if and only if $\Phi^u = \Phi^w$, and hence wu^{-1} stabilizes the flag $\Phi \in \mathcal{F}(\mathcal{M})$. Observe that for any $x \in N := \mathrm{Stab}_{\mathrm{Mon}(\mathcal{M})}(\Phi)$, and $w \in \mathrm{Mon}(\mathcal{M})$ such that the automorphism α_w exists, then

$$(\Phi^w)^{xw^{-1}} = (\Phi\alpha_w)^{xw^{-1}} = (\Phi^x\alpha_w)^{w^{-1}} = (\Phi\alpha_w)^{w^{-1}} = (\Phi^w)^{w^{-1}} = \Phi.$$

Therefore, w is an element in $\mathcal{N}$, the normalizer of N under the action of $\mathrm{Mon}(\mathcal{M})$.

For $w \in \mathrm{Mon}(\mathcal{M})$, such that the automorphism α_w exists, we can define a function $\varphi : \mathrm{Aut}(\mathcal{M}) \to \mathcal{N}/N$, such that $\varphi : \alpha_w \mapsto Nw$. Since $N \triangleleft \mathcal{N}$, it follows that $\varphi(\alpha_{uw}) = Nuw = NuNw = \varphi(\alpha_u)\varphi(\alpha_w)$, with $u, w \in \mathcal{N}$. Recall that $\alpha_u = \alpha_w$ if and only if $wu^{-1} \in N$, implying that φ is a well-defined injective morphism. Furthermore, note that for $w, v \in \mathcal{N}$ such that $Nw \neq Nv$, it follows that $\Phi^w \neq \Phi^v$, then the corresponding automorphisms to w and v are different, i.e. $\alpha_w \neq \alpha_v$. Therefore, φ is also surjective. Hence, the existence of the isomorphism φ implies that the automorphism group of $\mathcal{M}$ can be seen as the set $\{\alpha_w | w \in \mathcal{N}\}$.

For every $v \in \mathrm{Mon}(\mathcal{M})$ and $\Phi \in \mathcal{F}(\mathcal{M})$ the action of $\mathrm{Mon}(\mathcal{M})$ on the set $\mathrm{Orb}(\mathcal{M})$ is defined as $\mathcal{O}_\Phi \cdot v = \mathcal{O}_{\Phi^v}$, where $\mathcal{O}_\Phi := \{\Phi\alpha | \alpha \in \mathrm{Aut}(\mathcal{M})\}$. This action is transitive, as is the action of $\mathrm{Mon}(\mathcal{M})$ on $\mathcal{F}(\mathcal{M})$. Moreover, for $w \in \mathcal{N}$ it follows that $\mathcal{O}_\Phi \cdot w = \mathcal{O}_{\Phi^w} = \mathcal{O}_\Phi$. Since the action of $\mathrm{Aut}(\mathcal{M})$ is semi-regular, the isomorphism φ induces a bijection $\bar{\varphi} : \mathrm{Aut}(\mathcal{M}) \to \mathcal{O}_\Phi$, such that $\bar{\varphi} : \alpha_w \mapsto \Phi^w$. This latter implies that there exist a bijection between every two flag-orbits, i.e. all orbits have the same size. In fact, for some $w, u \in \mathrm{Mon}(\mathcal{M})$, if $\mathcal{N}w = \mathcal{N}u$ then $wu^{-1} \in \mathcal{N}$ and therefore $\alpha_{wu^{-1}} \in \mathrm{Aut}(\mathcal{M})$.

Consequently we can see that $|\mathrm{Orb}(\mathcal{M})| = [\mathrm{Mon}(\mathcal{M}) : \mathcal{N}]$. In particular, if the map is finite, the size of each orbit equals $|\mathrm{Aut}(\mathcal{M})|$ and

$$|\mathrm{Orb}(\mathcal{M})| = \frac{|\mathcal{F}(\mathcal{M})|}{|\mathrm{Aut}(\mathcal{M})|}$$

(see Proposition 3.6 of [32]).

We say that the map $\mathcal{M}$ is a *k-orbit map* whenever the automorphism group $\mathrm{Aut}(\mathcal{M})$ has exactly k orbits on $\mathcal{F}(\mathcal{M})$. Furthermore, if $k = 1$ (i.e. the action of $\mathrm{Aut}(\mathcal{M})$ is transitive on the flags), then we say that $\mathcal{M}$ is a *regular* map. The 2-orbit maps were widely studied and classified (in different contexts) in [23] and [29]. From [30] we can deduce a complete characterization of the automorphism groups of 2-orbit and fully-transitive maps (i.e. transitive on vertices, edges and faces) in terms of distinguished generators. The most studied and understood type of 2-orbit maps is the chiral one. A *chiral* map is a 2-orbit map with the property that every flag of the map and its adjacent flags are in different orbits.

In 1997 , Graver and Watkins, [26], first studied edge-transitive maps, and showed that there are 14 types of edge-transitive maps: regulars, six 2-orbit and seven 4-orbit types of maps. In 2001, Tucker, Watkins, and Širáň, found that there exists a map for each type, [53]. Orbanić, in his PhD thesis, [43], study edge-transitive maps through the theory of F-maps and from a computational point of view. More recently, Orbanić, Pellicer, and Weiss extended the study of k-orbit maps and classified them up to $k \le 4$, [45].

2.2 Maniplexes

In 2012, Wilson introduced the concept of maniplex, [56], aiming to unify the notion of maps and abstract polytopes, we refer the reader to [40] for the basic theory of abstract polytopes. Even though in this work we do not define abstract polytopes, it is not hard to verify that everything that we show for maniplexes can be applied for (the flag graph of) abstract polytopes, as is shown in [10]. The combinatorial structure of $(n-1)$-maniplexes is completely determined by an edge-coloured n-valent graph with chromatic index n, often called the flag graph. In particular, non-degenerate maps correspond to 2-maniplexes.

Given a set of *flags* $\mathcal{F}$ and a sequence of matchings $(s_0, s_1, \ldots, s_{n-1})$, such that each s_i partitions the set $\mathcal{F}$ into sets of size 2 and the partitions defined by s_i and s_j are disjoint when $i \ne j$, we can define an $(n-1)$-*complex* $\mathcal{M}$, as Wilson does in [56]: a connected graph $\mathcal{G}_{\mathcal{M}}$, whose vertex set is $\mathcal{F}$, and with edges of colour i corresponding to the matching induced by s_i. Note that each s_i can be thought as a permutation of $\mathcal{F}$, sending each $\Phi \in \mathcal{F}$ to the unique element $\Phi^i \in \mathcal{F}$ such that $\{\Phi, \Phi^i\}$ is an edge of colour i. Hence as permutations, all the s_i are involutions. Furthermore, by definition $\Phi \ne \Phi^i$ implying that

the s_i are point free. Thus, we say that two flags Φ and Ψ are i-adjacent if $\Phi^{s_i} = \Psi$ (note that s_i is an involution, and $\Phi^{s_i} = \Psi$ implies that $\Psi^{s_i} = \Phi$, so the concept is symmetric). In fact, an $(n-1)$-complex is defined similarly as to what Vince calls a *combinatorial map* in [54].

An $(n-1)$-*maniplex* $\mathcal{M}$ is an $(n-1)$-complex such that for any two permutations s_i and s_j such that $|i - j| \geq 2$, it follows that $s_i s_j = s_j s_i$. given a flag Φ of $\mathcal{M}$ and $i, j \in \{0, \ldots, n\}$ such that $|i - j| \geq 2$, we have that the action of $s_i, s_j \in \text{Mon}(\mathcal{M})$ on the set $\mathcal{F}(\mathcal{M})$ implies that

$$\Phi^{i,j} = \Phi^{s_i s_j} = \Phi^{s_j s_i} = \Phi^{j,i}.$$

Similarly as we saw with maps, we can verify that $s_i s_j$ does not have fix points, as $s_i s_j$ always sends any flag Φ to the unique flag $\Phi^{i,j} = \Phi^{j,i}$ that shares with Φ all its elements but Φ_i and Φ_j.

By definition, the edges of $\mathcal{G}_\mathcal{M}$ of one given colour form a perfect matching. The *2-factors* of the graph $\mathcal{G}_\mathcal{M}$ are the subgraphs spanned by the edges of two different colours of edges. In particular, the connected components in $\mathcal{G}_\mathcal{M}$ of the induced subgraph with edges of colours i and j, with $|i - j| \geq 2$, are disjoint 4-cyles. The set of *i-faces* of an $(n-1)$-maniplex $\mathcal{M}$ is defined by the connected components of the induced subgraph with edges of colours $j \in \{0, 1, \ldots, n-1\} \setminus \{i\}$ in $\mathcal{G}_\mathcal{M}$. A 0-face is a *vertex*, a 1-face is an *edge* and an $(n-1)$-face is a *facet*. We shall refer to $(n-1)$ as the *rank* of the maniplex.

A 0-complex is a 0-maniplex, whose graph has exactly one edge of colour 0 connecting exactly two vertices (flags), as it is depicted in the left of Figure 2.5. Each of its flags is both vertex and facet. A 1-maniplex corresponds to an l-gon, whose graph has $2l$ vertices
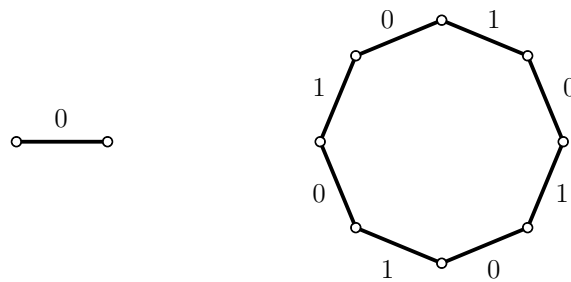
Figure 2.5: The 0-maniplex (left) and the 1-maniplex regarded geometrically as a 4-gon (right).

and two matchings of l edges each coloured by 0 and 1, respectively. The 0- and 1-faces of a 1-maniplex are edges of the graph. Hence, the 1-maniplex has l vertices and l edges. For instance, in the right of Figure 2.5 is depicted the 1-maniplex of a 4-gon.

In the graph $\mathcal{G}_\mathcal{M}$ of a 2-maniplex $\mathcal{M}$, the faces, edges and vertices of $\mathcal{M}$ are represented by the $(0,1)$, $(0,2)$ and $(1,2)$ 2-factors, respectively; where only the $(0,2)$ 2-factor is composed of 4-cycles, since $s_0 s_2 = s_2 s_0$. In fact, a 2-maniplex can be considered as a map

and vice versa. In particular, a map that has no faces with a single edge nor a vertex of degree one is a 2-maniplex, so that maniplexes generalize the notion of maps to higher rank.

Given an $(n-1)$-maniplex $\mathcal{M}$, to each i-face F of $\mathcal{M}$, we can associate an $(i-1)$-maniplex $\mathcal{M}_F$ by identifying two flags of F whenever there is a path between them consisting of edges with colours in $\{i+1, \ldots, n\}$, where multiple edges with the same colour must be identified. Equivalently, we can remove from $\mathcal{G}_{\mathcal{M}}$ all edges of colours $\{i+1, \ldots, n-1\}$, and then take one of the connected components.

Abusing of the notation, we say that the *monodromy group* $\mathrm{Mon}(\mathcal{M})$ is the group generated by $s_0, \ldots, s_{n-1}$, seen as permutations of $\mathcal{F}$. In this way, the action of $\mathrm{Mon}(\mathcal{M})$ on $\mathcal{F}$ is faithful and transitive.

The set of i-faces of an $(n-1)$-maniplex corresponds to the orbit of the flags in $\mathcal{F}$ under the action of the group generated by the set $S_i := \{s_j | i \neq j\}$, with $i \in \{0, 1, \ldots, n-1\}$. Given an i-face F, if $\Phi \in F$ we shall denote F by $(\Phi)_i$. Hence, $(\Phi)_i := \{\Phi^w | w \in \langle S_i \rangle\}$. It is then straightforward to see that $(\Phi)_i \cap (\Psi)_i \neq \emptyset$ if and only if $(\Phi)_i = (\Psi)_i$. Furthermore, an i-face F of $\mathcal{M}$ is an $(i-1)$-maniplex $\mathcal{M}_F$ whose monodromy group corresponds to $\langle s_0, \ldots, s_{i-1} \rangle$. Given that $s_i s_j = s_j s_i$ in $\mathrm{Mon}(\mathcal{M})$, whenever $|i - j| \geq 2$. Then, $\langle s_0, \ldots, s_{i-1} \rangle$ commutes with $\langle s_{i+1}, \ldots, s_n \rangle$.

2.2.1   Automorphism group

An *automorphism* α of an $(n-1)$-maniplex $\mathcal{M}$ is a colour-preserving automorphism of the graph $\mathcal{G}_{\mathcal{M}}$. Hence, α can be seen as a permutation of the flags in $\mathcal{F}$ that commutes with each of the permutations in the monodromy group. In a similar way as it happens for maps, the connectivity of the graph $\mathcal{G}_{\mathcal{M}}$ implies that the action of the automorphism group $\mathrm{Aut}(\mathcal{M})$ of $\mathcal{M}$ is semi-regular on the vertices of $\mathcal{G}_{\mathcal{M}}$.

Note that Lemma 2.2, for maps, also holds for maniplexes. Then we have the following lemma.

Lemma 2.3. *For any two flags* $\Phi, \Psi \in \mathcal{F}(\mathcal{M})$ *that are in the same flag-orbit* $\mathcal{O}_1$*, if the flag* Φ^v *is in a flag-orbit* $\mathcal{O}_2$*, then* $\Psi^v \in \mathcal{O}_2$*, with* $v \in \mathrm{Mon}(\mathcal{M})$.

A flag Φ of $\mathcal{M}$ contained in an i-face F naturally induces a flag $\overline{\Phi}$ in $\mathcal{M}_F$. Similarly, if $\gamma \in \mathrm{Aut}(\mathcal{M})$ fixes F, then γ induces an automorphism $\overline{\gamma} \in \mathrm{Aut}(\mathcal{M}_F)$, defined by $\overline{\Phi}\overline{\gamma} := \overline{\Phi\gamma}$. To check that this is well-defined, suppose that $\overline{\Phi} = \overline{\Psi}$; we want to show that $\overline{\Phi\gamma} = \overline{\Psi\gamma}$. Since $\overline{\Phi} = \overline{\Psi}$, it follows that $\Psi = \Phi^w$ for some $w \in \langle s_{i+1}, \ldots, s_n \rangle$. Then $\Psi\gamma = (\Phi^w)\gamma = (\Phi\gamma)^w$, so that $\overline{\Psi\gamma} = \overline{\Phi\gamma}$.

We say that a maniplex $\mathcal{M}$ is *i-face-transitive* if $\mathrm{Aut}(\mathcal{M})$ is transitive on the faces of rank i. We say that $\mathcal{M}$ is *fully-transitive* if it is i-face-transitive for every $i = 0, \ldots, n-1$.

If $\text{Aut}(\mathcal{M})$ has k orbits on the flags of $\mathcal{M}$, we say that $\mathcal{M}$ is a k-orbit maniplex. A 1-orbit maniplex is also called a *reflexible* maniplex. A 2-orbit maniplex with adjacent flags belonging to different orbits is a *chiral* maniplex. If a maniplex has at most 2 orbits of flags and $\mathcal{G}_{\mathcal{M}}$ is a bipartite graph, such that each part is contained in an orbit, then the maniplex is said to be *rotary*.

As it was pointed out in Chapter 1, the graph $\mathcal{G}_{\mathcal{M}}$ of an $(n-1)$-maniplex $\mathcal{M}$ can be seen as a Schreier coset graph. That is, considering a base flag $\Phi \in \mathcal{F}$ and its stabilizer, $N :=$ $\text{Stab}_{\text{Mon}(\mathcal{M})}(\Phi)$, under the action of the monodromy group, $\text{Mon}(\mathcal{M}) := \langle s_0, \ldots, s_{n-1} \rangle$, of $\mathcal{M}$. The right cosets Nu represent the vertices of $\mathcal{G}_{\mathcal{M}}$ and two vertices Nu and Nv are joined by a coloured edge $i = 0, \ldots, n-1$ whenever $Nu = Nvs_i$ for any $u, v \in \text{Mon}(\mathcal{M})$.

Chapter 3

Symmetry type graph

As we pointed out in Chapter 2, the aim of this work is to give a classification on the symmetry types of maps and maniplexes. In this chapter we define and give properties of an n-valent edge-coloured graph, that we call the symmetry type graph of an $(n-1)$-maniplex, $n \leq 3$. Given a map (or maniplex) $\mathcal{M}$, we use the symmetry type graph as a tool to determine properties and information regarding the symmetries of $\mathcal{M}$. Such graph is basically the quotient graph of the flag graph $\mathcal{G}_{\mathcal{M}}$ of $\mathcal{M}$, obtained from the action of the group of automorphisms of $\mathcal{M}$ on the flags. Therefore, we consider pre-graphs; that is, graphs that allow multiple edges and semi-edges. The notion of symmetry type graph is equivalent to the Delaney-Dress symbol described in [21].

Given a graph $\mathcal{G}$, and a partition $\mathcal{B}$ of its vertex set V, the *quotient with respect to* $\mathcal{B}$, $\mathcal{G}_{\mathcal{B}}$, is defined as a pre-graph with vertex set $\mathcal{B}$, such that for any two vertices $B, C \in \mathcal{B}$, there is an edge from B to C if and only if there exists $u \in B$ and $v \in C$ such that there is an edge from u to v. Edges between vertices in the same part of the partition $\mathcal{B}$ quotient into semi-edges (edges with exactly one end point). Note that a quotient of an edge-coloured graph need not be an edge coloured graph.

3.1 Symmetry type graphs of maps and maniplexes

In this section, maps will be regarded as 2-maniplexes. Let $\mathcal{G}_{\mathcal{M}}$ be the (n-edge-coloured) flag graph of a k-orbit $(n-1)$-maniplex $\mathcal{M}$, and $\mathrm{Orb}(\mathcal{M}) := \{\mathcal{O}_{\Phi} \mid \Phi \in \mathcal{F}(\mathcal{M})\}$ the set of all the orbits of $\mathcal{F}(\mathcal{M})$ under the action of the automorphism group $\mathrm{Aut}(\mathcal{M})$ of $\mathcal{M}$.

We define the *symmetry type graph* $T(\mathcal{M})$ of the maniplex $\mathcal{M}$ to be the coloured factor pre-graph of $\mathcal{G}_{\mathcal{M}}$ with respect to $\mathrm{Orb}(\mathcal{M})$. That is, the vertex set of $T(\mathcal{M})$ is the set of orbits $\mathrm{Orb}(\mathcal{M})$ of the flags of $\mathcal{M}$ under the action of $\mathrm{Aut}(\mathcal{M})$, and given two flag orbits $\mathcal{O}_{\Phi}$ and $\mathcal{O}_{\Psi}$, there is an edge of colour i between them if and only if there exists

flags $\Phi' \in \mathcal{O}_\Phi$ and $\Psi' \in \mathcal{O}_\Psi$ such that Φ' and Ψ' are i-adjacent in $\mathcal{M}$. Edges between vertices in the same orbit shall factor into semi-edges. Because of Lemma 2.3 the colours of the edges of $\mathcal{G}_\mathcal{M}$ induce colours on the edges of $T(\mathcal{M})$, implying that $T(\mathcal{M})$ is an edge-coloured graph.

The simplest symmetry type graph arises from regular maps. In fact, the symmetry type graph of a reflexible $(n-1)$-maniplex has only one vertex and n semi-edges, one of each colour $0, 1, \ldots, n-1$. Recall that the edges of $\mathcal{M}$ are represented by 4-cycles of alternating colours i and j in $\mathcal{G}_\mathcal{M}$, for $|i-j| \geq 2$. Each of these 4-cycles should then factor into one of the five pre-graphs in Figure 3.1.
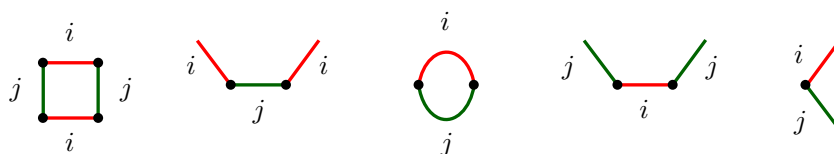

Figure 3.1: Possible quotients of (i, j) coloured 4-cycles, $|i-j| \geq 2$.

Clearly, if $\mathcal{M}$ is a k-orbit maniplex, then $T(\mathcal{M})$ has exactly k vertices. Thus, the number of types of k-orbit maniplexes depends on the number of n-valent pre-graphs on k vertices that can be properly edge coloured with n colours and that the connected components of the 2-factor with colours i and j, with $|i-j| \geq 2$ are always as in Figure 3.1. Given vertices u, v of $T(\mathcal{M})$, if there is an i-edge joining them, with $i \in \{0, 1, \ldots, n-1\}$, we shall denote such edge as $(u, v)_i$. Similarly, $(v, v)_i$ shall denote the semi-edge of colour i incident to the vertex v. In light of the above observations we state the following lemma.

Lemma 3.1. *Let $T(\mathcal{M})$ be the symmetry type graph of a maniplex. If there are three vertices $u, v, w \in V(T(\mathcal{M}))$ such that $(u, v)_i, (v, w)_j \in E(T(\mathcal{M}))$ with $|i-j| \geq 2$, then the connected component of the (i, j) 2-factor that contains v has four vertices.*

It is then straightforward to see that there are exactly seven types of 2-orbit 2-maniplexes, shown in Figure 3.2. (The relations between some of these types, as shown in the figures, will be discuss in Subsections 4.1.1 and 4.2.1.) These seven types of 2-orbit 2-maniplexes have been widely studied in different contexts, see for example [23] and [29]; we follow [29] for the notation of the types of the symmetry type 2-maniplexes with two flag orbits. It is likewise straightforward to see that there are only three types of 3-orbit 2-maniplexes, and these are shown in Figure 3.3.

In [45], Orbanić, Pellicer, and Weiss studied all the types of k-orbit 2-maniplexes, in the context of maps, for $k \leq 4$. For symmetry type graphs of 2-maniplexes of three and four orbits, we follow the notation of [45].

Recall that the action of $\mathrm{Mon}(\mathcal{M})$ on the set $\mathrm{Orb}(\mathcal{M})$ is defined as $\mathcal{O}_\Phi \cdot v = \mathcal{O}_{\Phi v}$, and it is a transitive action, as the one of $\mathrm{Mon}(\mathcal{M})$ on $\mathcal{F}(\mathcal{M})$ is transitive. The action
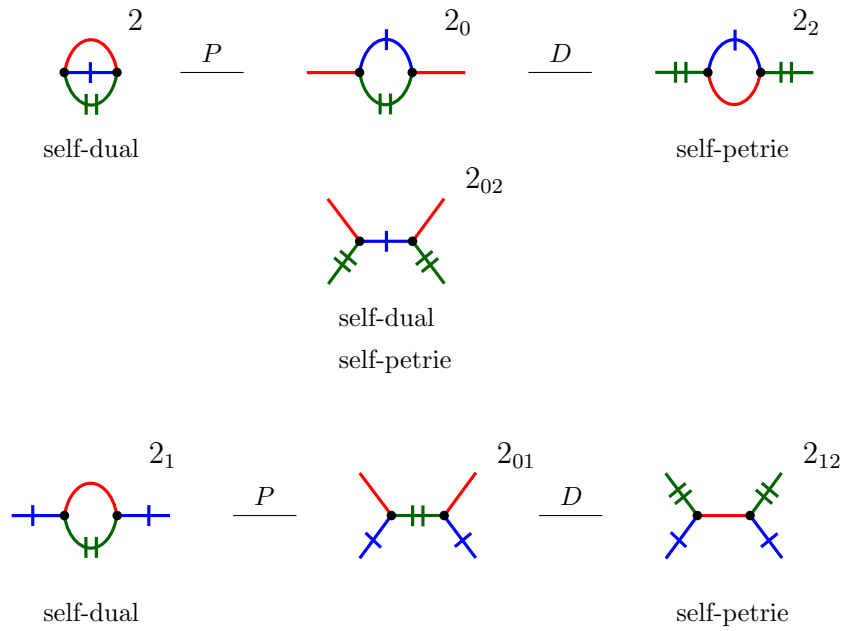
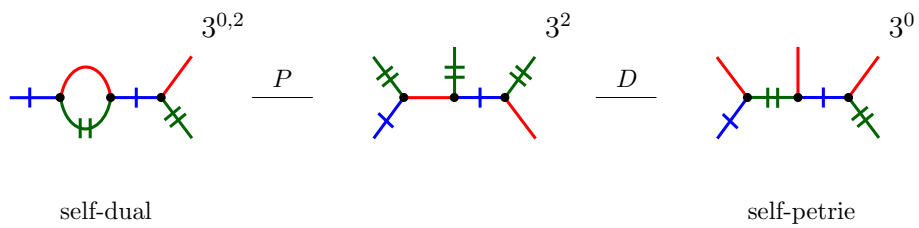Figure 3.2: The seven symmetry type graphs of 2-orbit maps.

Figure 3.3: The three symmetry type graphs of 3-orbit maps.

of $\mathrm{Mon}(\mathcal{M})$ on $\mathrm{Orb}(\mathcal{M})$ can be easily seen on the symmetry type graph $T(\mathcal{M})$. In fact, in the same way as the words of $\mathrm{Mon}(\mathcal{M})$ can be seen as walks among the edges of $\mathcal{G}_{\mathcal{M}}$, they can be seen as walks among the edges of $T(\mathcal{M})$. This immediately implies that, as $\mathrm{Mon}(\mathcal{M})$ acts transitively on $\mathrm{Orb}(\mathcal{M})$, the symmetry type graph $T(\mathcal{M})$ is connected. A walk on $T(\mathcal{M})$ that starts at a vertex $\mathcal{O}_\Phi$ and finishes at a vertex $\mathcal{O}_\Psi$ corresponds to an element of $\mathrm{Mon}(\mathcal{M})$ that sends all the flags in the orbit $\mathcal{O}_\Phi$ to flags in the orbit $\mathcal{O}_\Psi$. We can further see that a closed walk among the edges of $T(\mathcal{M})$ that starts and finishes at a vertex $\mathcal{O}_\Phi$ corresponds to an element of $\mathrm{Mon}(\mathcal{M})$ that permutes the flags of the orbit $\mathcal{O}_\Phi$.

Given $I \subset \{0, 1, \ldots, n\}$, we say that an I-walk in $T(\mathcal{M})$ (or in $\mathcal{G}_{\mathcal{M}}$) is a walk along edges of $T(\mathcal{M})$ (resp. $\mathcal{G}_{\mathcal{M}}$) of colours in I. The following lemma shall help us to understand the orbits of the k-faces of a map $\mathcal{M}$, in terms of the symmetry type graph of $\mathcal{M}$.

Lemma 3.2. *Let $\mathcal{M}$ be a map with symmetry type graph $T(\mathcal{M})$. For any two flags Φ and Ψ of $\mathcal{M}$, there is a $\{0, 1, \ldots, n\} \setminus \{i\}$-walk in $T(\mathcal{M})$ between the vertices $\mathcal{O}_\Phi$ and $\mathcal{O}_\Psi$ of $T(\mathcal{M})$ if and only if $(\Phi)_i$ and $(\Psi)_i$ are in the same orbit of i-faces under the action of $\mathrm{Aut}(\mathcal{M})$.*

Proof. Let $I := \{0, 1, \ldots, n\} \setminus \{i\}$. Suppose there is an I-walk in $T(\mathcal{M})$ between the vertices $\mathcal{O}_\Phi$ and $\mathcal{O}_\Psi$, and let $w \in \langle s_j | j \neq i \rangle$ be the associated element of $\mathrm{Mon}(\mathcal{M})$ corresponding to such walk. Then $\Phi^w \in \mathcal{O}_\Psi$; that is, there exists $\alpha \in \mathrm{Aut}(\mathcal{M})$ such that $\Phi^w \alpha = \Psi$. Now, by definition, $(\Phi\alpha)^w \in (\Phi\alpha)_i$. On the other hand, as the action of $\mathrm{Mon}(\mathcal{M})$ commutes with the action of $\mathrm{Aut}(\mathcal{M})$, then $(\Phi\alpha)^w = (\Phi^w)\alpha \in (\Phi^w\alpha)_i = (\Phi^w)_i\alpha$. That is, $\Psi \in (\Phi\alpha)_i \cap (\Phi^w\alpha)_i$. By Lemma 2.1 we then have that $(\Phi\alpha)_i = (\Phi^w\alpha)_i = (\Phi^w)_i\alpha$. Hence, $(\Phi\alpha)_i$ and $(\Phi^w)_i$ are in the same orbit of i-faces under $\mathrm{Aut}(\mathcal{M})$. Moreover, $(\Phi\alpha)_i = (\Phi)_i\alpha$ implies that $(\Phi\alpha)_i$ and $(\Phi)_i$ belong to the same orbit under $\mathrm{Aut}(\mathcal{M})$. We therefore can conclude that $(\Phi)_i$ and $(\Psi)_i = (\Phi^w\alpha)_i$ are in the same orbit of i-faces under the action of $\mathrm{Aut}(\mathcal{M})$.

For the converse, let $\alpha \in \mathrm{Aut}(\mathcal{M})$ be such that $(\Phi)_i\alpha = (\Psi)_i$. That is, $\{\Phi^w \mid w \in \langle s_j | j \neq i \rangle\}\alpha = \{\Psi^u \mid u \in \langle s_j | j \neq i \rangle\}$. Hence, there exists $w \in \langle s_j | j \neq i \rangle$ such that $\Phi^w\alpha = \Psi$. Now,

$$\mathcal{O}_\Phi \cdot w = \mathcal{O}_{\Phi^w} = \mathcal{O}_{\Phi^w\alpha} = \mathcal{O}_\Psi.$$

Therefore $w \in \langle s_j | j \neq i \rangle$ induces an I-walk in $T(\mathcal{M})$ starting at $\mathcal{O}_\Phi$ and finishing at $\mathcal{O}_\Psi$. ∎

The following theorem is an immediate consequence of the above Lemma.

Theorem 3.1. *Let $\mathcal{M}$ be an $(n-1)$-maniplex with symmetry type graph $T(\mathcal{M})$. Then, the number of connected components in the $(n-1)$-factor of $T(\mathcal{M})$ of colours $\{0, 1, \ldots, n-1\} \setminus \{i\}$, determine the number of orbits of i-faces of $\mathcal{M}$, where $i \in \{0, 1, \ldots, n-1\}$.*

3.1.1 Symmetry type graphs of highly symmetric maniplexes

One can classify maniplexes with small number of flag orbits (under the action of the automorphism group of the maniplex) in terms of their symmetry type graphs. The number of distinct possible symmetry types of a k-orbit $(n-1)$-maniplex is the number of connected n-valent pre-graphs on k vertices, that can be edge-coloured with exactly n colours and that the connected components of the 2-factors with colours i and j are always as in Figure 3.1, with $|i-j| \geq 2$. Furthermore, given a symmetry type graph, one can read from the appropriate coloured subgraphs the different types of face transitivities that the maniplex has.

As pointed out before, the symmetry type graph of a reflexible $(n-1)$-maniplex consists of one vertex and n semi-edges. The classification of two-orbit maniplexes in terms of the local configuration of their flags follows immediately from the possible symmetry type graphs. In fact, for each n, there are $2^n - 1$ possible symmetry type graphs with 2 vertices and n (semi-)edges, since given any proper subset I of the colours $\{0, 1, \ldots, n-1\}$, there is a symmetry type graph with two vertices, $|I|$ semi-edges corresponding to the colours of I incident to each vertex, and where all the edges between the two vertices use the colours not in I (see Figure 3.4). From [29], and thinking of an n-polytope as an $(n-1)$-maniplex ([56]), we can deduce that this symmetry type graph corresponds precisely to maniplexes in class 2_I.

$$I \subset \{0, 1, \ldots, n-1\}, \qquad J = \{0, 1, \ldots, n-1\} \setminus I$$
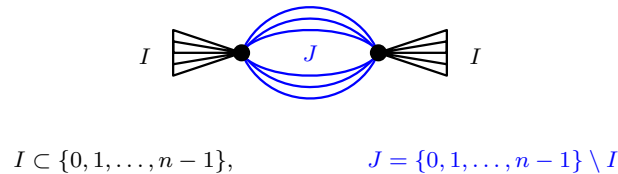
Figure 3.4: The symmetry type graph of a maniplex in class 2_I.

Highly symmetric maniplexes can be regarded as those with few flag orbits or those with many face transitivities. In particular, it follows from Theorem 3.1, that an edge-transitive 2-maniplex $\mathcal{M}$ has a symmetry type graph $T(\mathcal{M})$ with only one connected component of the 2-factor of colours 0 and 2, as those in Figure 3.1, with $i, j \in \{0, 2\}$. Then $T(\mathcal{M})$ has either 1, 2, or 4 vertices. It is immediate to see that an edge transitive 2-maniplex is a 1-, 2-, or 4-orbit 2-maniplex (see [26]).

The classification of symmetry type graphs of 3-orbit 2-maniplexes (see Figure 3.3), together with Theorem 3.1 imply the following result.

Corollary 3.1. *Every 3-orbit map has exactly two orbits of edges.*

As pointed out in [45], there are 22 types of 4-orbit 2-maniplexes. The 7 edge-transitive ones are shown in Figure 3.5, while the 15 that are not edge-transitive are depicted in
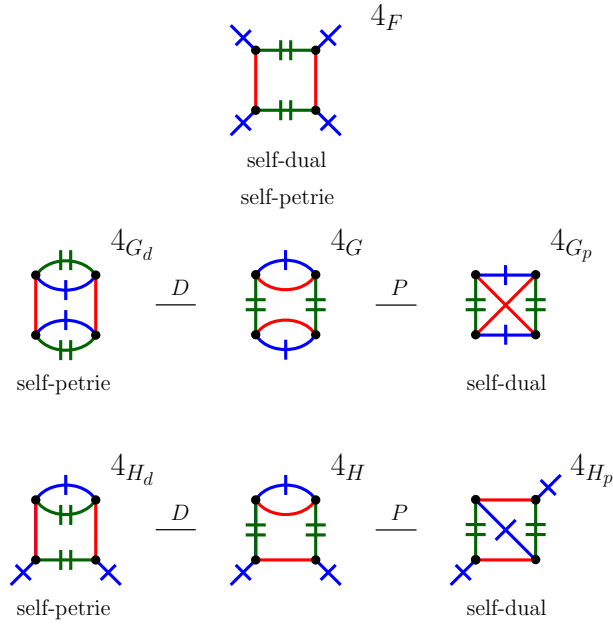
Figure 3.5: The seven symmetry type graphs of edge-transitive 4-orbit maps.

Figure 3.6.

Using the twenty two symmetry type graphs of 4-orbit 2-maniplexes, and the structure of the 2-factors of colours 0 and 2, one can see that there are thirteen different types of 5-orbit 2-maniplexes. Their symmetry type graphs are shown in Figure 3.7.

In this section we classify the possible symmetry type graphs with 3 vertices and study some properties of symmetry type graphs of 4-orbit maniplexes and fully-transitive 3-maniplexes.
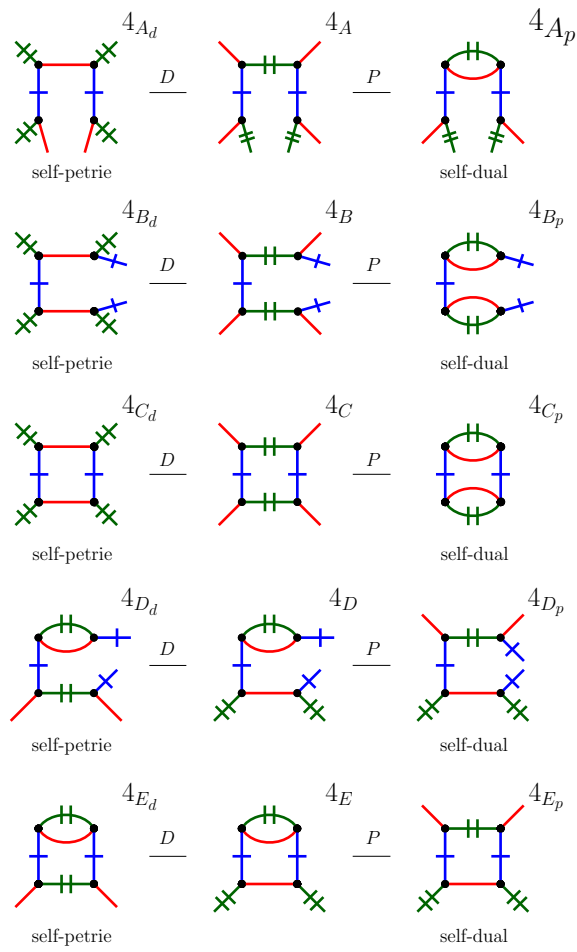
Figure 3.6: The fifteen symmetry type graphs of 4-orbit maps that are not edge-transitive.
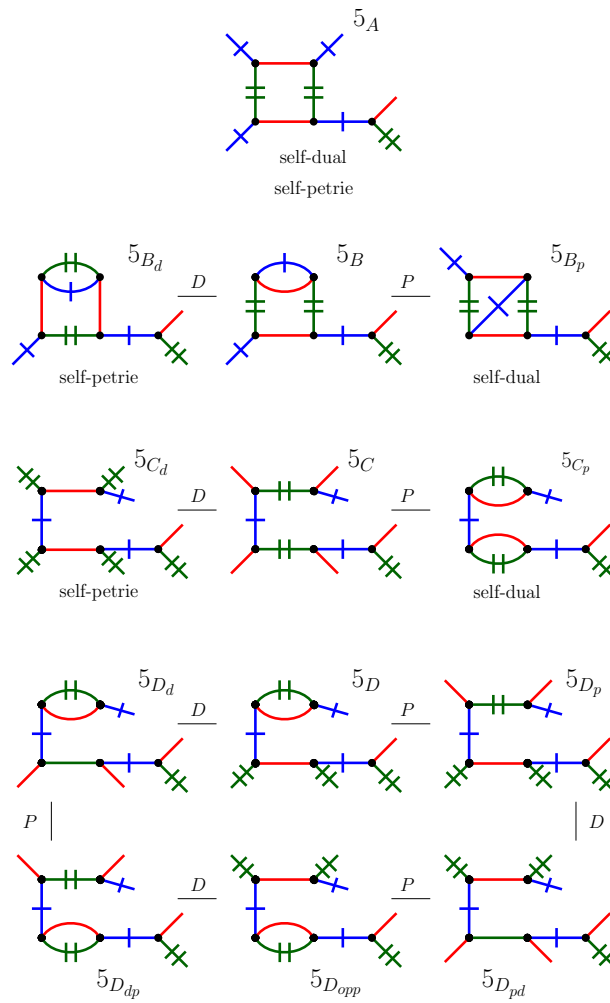
Figure 3.7: The thirteen symmetry type graphs of 5-orbit maps.

On symmetry type graphs of 3-orbit maniplexes

In this subsection, we count all possible symmetry type graphs of 3-orbit maniplexes and enunciate results regarding the transitivity on their j-faces.

Proposition 3.1. *There are exactly $2n - 3$ different possible symmetry type graphs of 3-orbit maniplexes of rank $n - 1$.*

Proof. Let $\mathcal{M}$ be a 3-orbit $(n-1)$-maniplex and $T(\mathcal{M})$ its symmetry type graph. Then, $T(\mathcal{M})$ is an n-valent well edge-coloured graph with vertices v_1, v_2 and v_3. Recall that the set of colours $\{0, 1, \ldots, n-1\}$ correspond to the distinguished generators $s_0, s_1, \ldots, s_{n-1}$ of the monodromy group of $\mathcal{M}$, and that by $(u, v)_i$ we mean the edge between vertices u and v of colour i.

Since $T(\mathcal{M})$ is a connected graph, without loss of generality, we can suppose that there is at least one edge joining v_1 and v_2 and another joining v_2 and v_3. Let $j, k \in \{0, 1, \ldots, n-1\}$ be the colours of these edges, respectively. That is, without loss of generality we may assume that $(v_1, v_2)_j$ and $(v_2, v_3)_k$ are edges of $T(\mathcal{M})$. By Lemma 3.1, we must have that $k = j \pm 1$, as otherwise $T(\mathcal{M})$ would have to have at least 4 vertices. This implies that, up to graph isomorphism, the only edges of $T(\mathcal{M})$ are either $(v_1, v_2)_j$ and $(v_2, v_3)_{j+1}$, $(v_1, v_2)_j$ and $(v_2, v_3)_{j-1}$ or $(v_1, v_2)_j$, $(v_2, v_3)_{j+1}$ and $(v_2, v_3)_{j-1}$, with $j \in \{1, 2, \ldots, n-2\}$. (See Figure 3.8).

$$J = \{0, 1, \ldots, n-1\} \setminus \{j-1, j, j+1\}$$
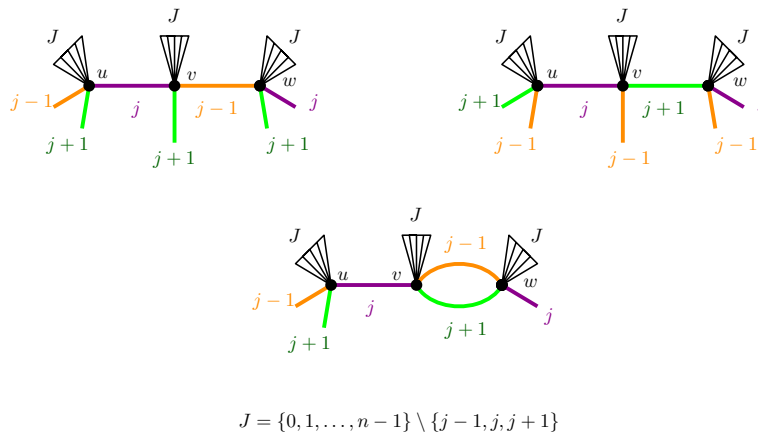
Figure 3.8: Possible symmetry type graphs of 3-orbit $(n-1)$-maniplexes with edges of colours $j-1$, j, and $j+1$, with $j \in \{1, 2, \ldots, n-2\}$.

Here there are $n - 1$ such graphs with exactly two edges and $n - 2$ such graphs with three edges. Therefore, there are $2n - 3$ possible different symmetry type graphs of 3-orbit maniplexes of rank $n - 1$. ■

Given a 3-orbit $(n - 1)$-maniplex $\mathcal{M}$ with symmetry type graph having exactly two

edges e and e' of colours j and $j+1$, respectively, for some $j \in \{0, \ldots, n-2\}$, we shall say that $\mathcal{M}$ is in class $3^{j,j+1}$. If, on the other hand, the symmetry type graph of $\mathcal{M}$ has one edge of colour j and parallel edges of colours $j-1$ and $j+1$, for some $j \in \{1, \ldots, n-2\}$, then we say that $\mathcal{M}$ is in class 3^j. From Figure 3.8 we observe that a maniplex in class $3^{j,j+1}$ is i-face-transitive whenever $i \neq j, j+1$, while a maniplex in class 3^j if i-face-transitive for every $i \neq j$. (Note that this notation holds for $n \leq 3$, in case of 2-maniplexes we follow the notation in [45].) From here, we have the following result.

Proposition 3.2. *A 3-orbit maniplex is j-face-transitive if and only if it does not belong to any of the classes 3^j, $3^{j,j+1}$ or $3^{j-1,j}$.*

Theorem 3.2. *There are no fully-transitive 3-orbit maniplexes.*

On symmetry type graph of 4-orbit maniplexes

It does not take long to realise that counting the number of possible symmetry type graphs with $k \geq 4$ vertices, and perhaps classifying them in a similar fashion as was done for 2 and 3 vertices, becomes considerably more difficult. In this section, we shall analyse symmetry type graphs with 4 vertices and determine how far a 4-orbit maniplex can be from being fully-transitive. The proof of Lemma 3.3 is straight-froward from the fact that by taking away the i-edges of a symmetry type graph $T(\mathcal{M})$, the resulting $T^i(\mathcal{M})$ cannot have too many components.

Lemma 3.3. *Let $\mathcal{M}$ be a 4-orbit $(n-1)$-maniplex and let $i \in \{0, \ldots, n-1\}$. Then $\mathcal{M}$ has one, two or three orbits of i-faces.*

If an $(n-1)$-maniplex $\mathcal{M}$ is not fully-transitive, there exists at least one $i \in \{0, \ldots, n-1\}$ such that $T^i(\mathcal{M})$ is disconnected. We shall divide the analysis of the types in three parts: when $T^i(\mathcal{M})$ has three connected components (two of them of one vertex and one with two vertices), when $T^i(\mathcal{M})$ has a connected component with one vertex and another connected component with three vertices, and finally when $T^i(\mathcal{M})$ has two connected components with two vertices each. Let v_1, v_2, v_3, v_4 be the vertices of $T(\mathcal{M})$.

Suppose that $T^i(\mathcal{M})$ has three connected components with v_2 and v_3 in the same component. Without loss of generality we may assume that $T(\mathcal{M})$ has edges $(v_1, v_2)_i$ and $(v_3, v_4)_i$. Let $k \in \{0, 1, \ldots, n-1\} \setminus \{i\}$ be the colour of an edge between v_2 and v_3. Since there is no edge of $T(\mathcal{M})$ between v_1 and v_4, Lemma 3.1 implies that there are at most two such possible k, namely $k = i-1$ and $k = i+1$. If $i \notin \{0, n-1\}$, $T(\mathcal{M})$ can have either both edges or exactly one of them, while if $i \in \{0, n-1\}$ there is one possible edge (see Figure 3.9).

Let us now assume that $T^i(\mathcal{M})$ has two connected components, one consisting of the vertex v_1 and the other one containing vertices v_2, v_3 and v_4. This means that the i-edge
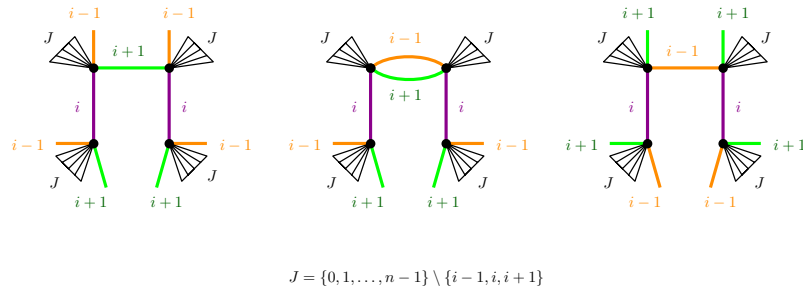
$$J = \{0, 1, \ldots, n-1\} \setminus \{i-1, i, i+1\}$$

Figure 3.9: Symmetry type graphs of an $(n-1)$-maniplex $\mathcal{M}$ with four orbits on its flags, and three orbits on its i-faces.

incident to v_1 is the unique edge that connects this vertex with the rest of the graph and, without loss of generality, $T(\mathcal{M})$ has the edge $(v_1, v_2)_i$. As with the previous case, Lemma 3.1 implies that an edge between v_2 and v_3 has colour either $i-1$ or $i+1$.

First observe that having either $(v_2, v_3)_{i-1}$ or $(v_2, v_3)_{i+1}$ in $T(\mathcal{M})$ immediately implies (by Lemma 3.1) that there is no edge between v_2 and v_4. Now, if both edges $(v_2, v_3)_{i-1}$ and $(v_2, v_3)_{i+1}$ are in $T(\mathcal{M})$, then the only edge between v_3 and v_4 would have to have colour i, contradicting the fact that $T^i(\mathcal{M})$ has two connected components. Hence, there is exactly one edge between v_2 and v_3. It is now straightforward to see that $T(\mathcal{M})$ should be one of the graphs in Figure 3.10, implying that there are four possible symmetry type graphs with these conditions for each $i \neq 0, 1, n-2, n-1$, but only two symmetry type graph of this kind when $i = 0, 1, n-2$, or $n-1$.

$$J = \{0, 1, \ldots, n-1\} \setminus \{i-2, i-1, i\} \qquad J = \{0, 1, \ldots, n-1\} \setminus \{i, i+1, i+2\}$$

Figure 3.10: Symmetry type graphs of $(n-1)$-maniplexes with four orbits on its flags, and two orbits on its i-faces such that one contains three flag orbits and the other contains a single flag orbit.

It is straightforward to see from Figure 3.10 that the next lemma follows.

Lemma 3.4. *Let $\mathcal{M}$ be a 4-orbit $(n-1)$-maniplex with two orbits of i-faces such that $T^i(\mathcal{M})$ has a connected component consisting of one vertex, and another one consisting of three vertices. Then either $T^{i-1}(\mathcal{M})$ or $T^{i+1}(\mathcal{M})$ has two connected components, each with two vertices.*

Finally, we turn our attention to the case where $T^i(\mathcal{M})$ has two connected components, with two vertices each. Suppose that v_1 and v_2 belong to one component, while v_3 and v_4 belong to the other. As the two components must be connected by edges of colour i, we may assume that $(v_1, v_3)_i$ is an edge of $T(\mathcal{M})$. If the vertices v_2 and v_4 have semi-edges of colour i, Lemma 3.1 implies that $T(\mathcal{M})$ is one of the graphs shown in Figure 3.11. Note that if $i \in \{0, n-1\}$ there is one possible symmetry type graph for this particular case.

$$J = \{0, 1, \ldots, n-1\} \setminus \{i-1, i, 1+1\},$$

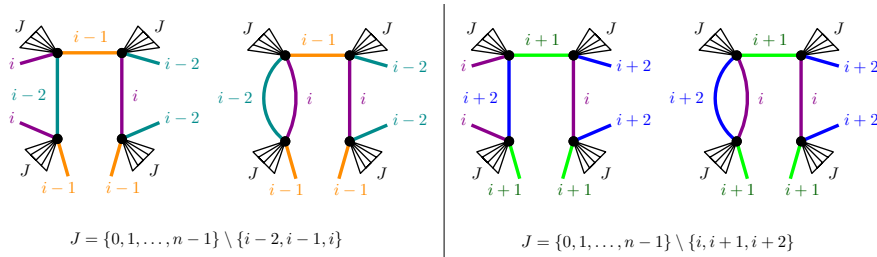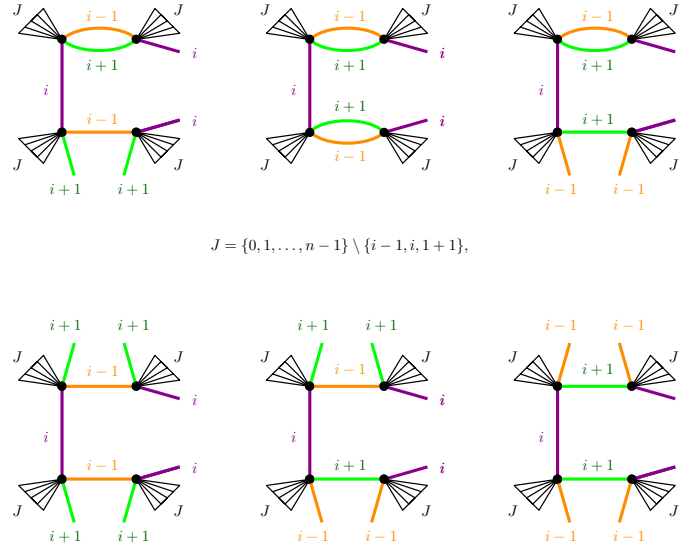Figure 3.11: Six of the symmetry type graphs of $(n-1)$-maniplexs with four orbits on its flags, and two orbits on its i-faces such that each contains two flag orbits.

On the other hand, if $(v_1, v_3)_i$ and $(v_2, v_4)_i$ are both edges of $T(\mathcal{M})$, given $j \in \{0, 1, \ldots, n-1\} \setminus \{i-1, i, i+1\}$, we use again Lemma 3.1 to see that $(v_1, v_2)_j$ is an edge of $T(\mathcal{M})$ if and only if $(v_3, v_4)_j$ is also an edge of $T(\mathcal{M})$. By contrast, $T(\mathcal{M})$ can have either four semi-edges, an edge and two semi-edges, or two edges of colour $i \pm 1$ (each joining the vertices of each connected component of $T^i(\mathcal{M})$). Hence, if $i \neq 0, n-1$, for each $J \subset \{0, 1, \ldots, n-1\} \setminus \{i-1, i, i+1\}$ there are ten possible symmetry type graphs with four semi-edges of each of the colours in J and edges of colours not in J, as shown in Figures 3.12 and 3.13, while for $J = \{0, 1, \ldots, n-1\} \setminus \{i-1, i, i+1\}$ there are six such graphs (shown in Figure 3.13). On the other hand if $i \in \{0, n-1\}$, for each $J \subset \{0, 1, \ldots, n-1\} \setminus \{i-1, i, i+1\}$ there are two graphs as in Figure 3.12 and one as in Figure 3.13, while for $J = \{0, 1, \ldots, n-1\} \setminus \{i-1, i, i+1\}$, there is only one of the graphs in Figure 3.13.

Theorem 3.3 summarizes our analysis of the transitivity of 4-orbit maniplexes. In particular, case one holds if and only if $T(\mathcal{M})$ does not belong to any of the Figures 3.9 to 3.13. Moreover, case two holds if and only if $T(\mathcal{M})$ is as any of the possible symmetry type graphs in Figures 3.12 and 3.13, whenever $J \subset \{0, 1, \ldots, n-1\} \setminus \{i-1, i, i+1\}$.

$$\emptyset \neq J \subset \{0,1,\dots,n-1\} \setminus \{i-1,i,1+1\},$$

Figure 3.12: Four families of possible symmetry type graphs of $(n-1)$-maniplexes with four orbits on its flags, and two orbits on its i-faces such that each contains two flag orbits.

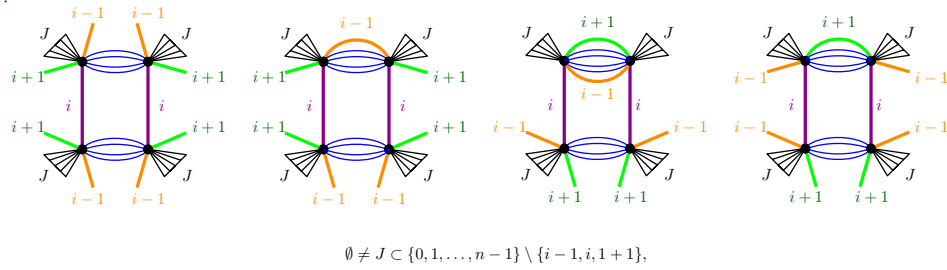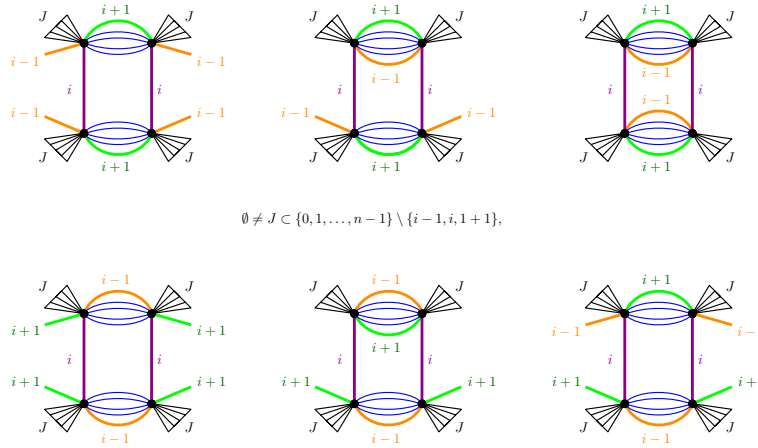$$\emptyset \neq J \subset \{0,1,\dots,n-1\} \setminus \{i-1,i,1+1\},$$

Figure 3.13: The remaining six families of possible symmetry type graphs of $(n-1)$-maniplexes with four orbits on its flags, and two orbits on its i-faces such that each contains two flag orbits.

Similarly, case three holds if and only if $T(\mathcal{M})$ is as those possible symmetry type graphs in Figure 3.10 with parallel edges coloured by i and $i \pm 2$. Finally, case four holds if and only if $T(\mathcal{M})$ is as any of the possible symmetry type graphs in Figures 3.9, 3.11 and Figure 3.13, even for $J = \{0, 1, \ldots, n-1\} \setminus \{i-1, i, i+1\}$.

Theorem 3.3. *Let $\mathcal{M}$ be a 4-orbit maniplex. Then, one of the following holds.*

1. *$\mathcal{M}$ is fully-transitive.*

2. *There exists $i \in \{0, \ldots, n-1\}$ such that $\mathcal{M}$ is j-face-transitive for all $j \neq i$.*

3. *There exist $i, k \in \{0, \ldots, n-1\}$, $i \neq k$, such that $\mathcal{M}$ is j-face-transitive for all $j \neq i, k$.*

4. *There exists $i \in \{0, \ldots, n-1\}$ such that $\mathcal{M}$ is j-face-transitive for all $j \neq i, i \pm 1$.*

3.1.2   On fully-transitive n-maniplexes for small n.

Every 1-maniplex is reflexible and hence fully-transitive. Fully-transitive 2-maniplexes correspond to fully-transitive maps. From the symmetry type graph is easy to see that if a map is edge-transitive, then it should have one, two or four orbits of flags. Moreover, a fully-transitive map should be regular, a two-orbit map in class 2, 2_0, 2_1 or 2_2, or a four-orbit map in class 4_{Gp} or 4_{Hp}.

When considering fully-transitive n-maniplexes, $n \geq 3$, the analysis becomes considerably more complicated. In [29] Hubard shows that there are $2^{n+1} - n - 2$ classes of fully-transitive two-orbit n-maniplexes. By Theorem 3.2, there are no 3-orbit fully-transitive n-maniplexes. Extending the twenty-two possible symmetry type graphs of 4-orbit 2-maniplexes by adding (semi-) edges of colour 3 in such way that the $(0, 3)$ and $(1, 3)$ 2-factors are as in Figure 3.1. There are twenty possible symmetry type graphs of 4-orbit 3-maniplexes that are fully transitive, these graphs are depicted in Figure 3.14.

Theorem 3.4. *Let $\mathcal{M}$ be a fully-transitive 3-maniplex and let $T(\mathcal{M})$ be its symmetry type graph. Then either $\mathcal{M}$ is reflexible or $T(\mathcal{M})$ has an even number of vertices.*

Proof. On the contrary suppose that $T(\mathcal{M})$ has an odd number of vertices, different than 1. Whenever $|i - j| > 1$, the connected components of the (i, j) 2-factor of a symmetry type graph are as in Figure 3.1. Hence, there is a connected component of the $(0, 2)$ 2-factor of $T(\mathcal{M})$ with exactly one vertex v (and, hence, semi-edges of colours 0 and 2). The connectivity of $T(\mathcal{M})$ implies that there is a vertex v_1 adjacent to v in $T(\mathcal{M})$.

If v_1 is the only neighbour of v, then $T(\mathcal{M})$ has the edges $(v, v_1)_1$ and $(v, v_1)_3$ as otherwise $\mathcal{M}$ is not fully-transitive. Since the connected components of the $(0, 3)$ 2-factor
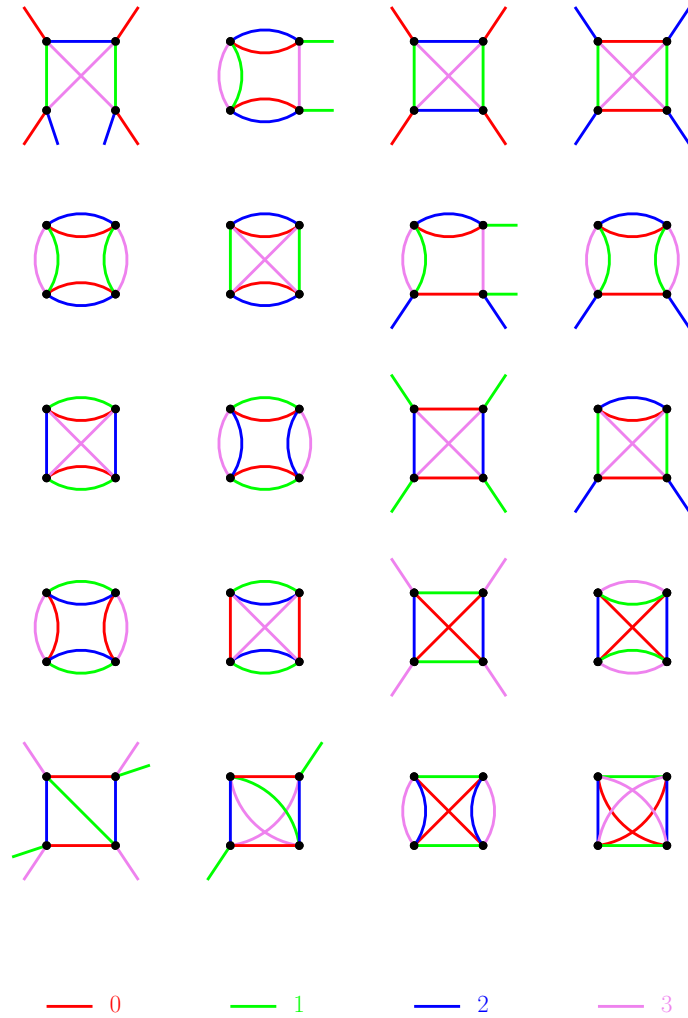
Figure 3.14: Symmetry type graphs of 4-orbit fully-transitive 3-maniplexes

of $T(\mathcal{M})$ are as in Figure 3.1, v_1 has a 0 coloured semi-edge. Because $T(\mathcal{M})$ has more than two vertices, the edge of v_1 of colour 2 joins v_1 to another vertex, say u. But removing the edge $(v_1, u)_2$ disconnects the graph, contradicting the fact that $\mathcal{M}$ is 2-face-transitive.

On the other hand, if v has more than one neighbour it has exactly two, say v_1 and u, and $T(\mathcal{M})$ has the two edges $(v, v_1)_1$ and $(v, u)_3$. This implies that the connected component of the $(1, 3)$ 2-factor containing v has four vertices: v, v_1, u and v_2. (Therefore $(v_1, v_2)_3$ and $(u, v_2)_1$ are edges of $T(\mathcal{M})$.) Using the $(0, 3)$ 2-factor one sees that u has a semi-edge of colour 0.

Now, if $(v_1, v_2)_0$ is an edge of $T(\mathcal{M})$ or there are semi-edges coloured 0 at v_1 and v_2, then the vertices v, v_1, v_2 and u are joined to the rest of $T(\mathcal{M})$ only by the edges of colour 2, implying that removing them disconnects $T(\mathcal{M})$ (there exists at least another vertex in $T(\mathcal{M})$ since it has an odd number of vertices), which is again a contradiction. On the other hand, if v_1 (or v_2) has an edge of colour 0 to a vertex v_3 then, by Lemma 3.1 v_2 (or v_1) has a 0-edge to a vertex v_4. Again, if $(v_3, v_4)_1$ is an edge of $T(\mathcal{M})$ or there are semi-edges coloured 1 at v_3 and v_4, since the number of vertices of the graph is odd, removing the edges of colour 2 will leave only the vertices $u, v, v_1, \ldots, v_4$ in one component, which is a contradiction. Proceeding now by induction on the number of vertices one can conclude that $T(\mathcal{M})$ cannot have an odd number of vertices ■

3.2 Generators of the automorphism group of a k-orbit maniplex

It is well-known among polytopists that the automorphism group of a regular n-polytope can be generated by n involutions. In fact, given a base flag $\Phi \in \mathcal{F}(\mathcal{M})$, the distinguished generators of $\mathrm{Aut}(\mathcal{M})$ with respect to Φ are involutions $\rho_0, \rho_1, \ldots, \rho_{n-1}$ such that $\Phi \rho_i = \Phi^i$.

Generators for the automorphism group of a two-orbit n-polytope can also be given in terms of a base flag (see [29]). In this section we give a set of distinguished generators (with respect to some base flag) for the automorphism group of a k-orbit $(n-1)$-maniplex in terms of the symmetry type graph $T(\mathcal{M})$, provided that $T(\mathcal{M})$.

Given two walks W_1 and W_2 along the edges and semi-edges of $T(\mathcal{M})$ such that the final vertex of W_1 is the starting vertex of W_2, we define the sequence $W_1 W_2$ as the walk that traces all the edges of W_1 and then all the edges of W_2 in the same order; the inverse of W_1, denoted by W_1^{-1}, is the walk which has the final vertex of W_1 as its starting vertex, and traces all the edges of W_1 in reversed order. Since each of the elements of $\mathrm{Mon}(\mathcal{M})$ associated to the edges of $T(\mathcal{M})$ is its own inverse, we shall forbid walks that trace the

same edge two times consecutively (or just remove the edge from such walk, shortening its length by two). Given a set of walks in $T(\mathcal{M})$, we say that a subset $\mathcal{W}' \subseteq \mathcal{W}$ is *a generating set of $\mathcal{W}$* if each $W \in \mathcal{W}$ can be expressed as a sequence of elements of $\mathcal{W}'$ and their inverses. Now, let $\mathcal{W}$ be the set of closed walks along the edges and semi-edges of $T(\mathcal{M})$ starting at a distinguished vertex v_0. Recall that the walks along the edges and semi-edges of $T(\mathcal{M})$ correspond to permutations of the flags of $\mathcal{M}$; moreover, each closed walk of $\mathcal{W}$ corresponds to an automorphism of $\mathcal{M}$. Thus, by finding a generating set of $\mathcal{W}$, we will find a set of automorphisms of $\mathcal{M}$ that generates $\mathrm{Aut}(\mathcal{M})$. (However, the converse is not true, as an automorphism of $\mathcal{M}$ may be described in more than one way as a closed walk of $T(\mathcal{M})$.) Given $T(\mathcal{M})$, we may easily find such generating set. The construction goes as follows:

Let $\mathcal{M}$ be a k-orbit maniplex of rank $n-1$ such that $\mathcal{C} = (v_0, v_1, v_2, ..., v_q)$ is a walk of minimal length that visits all the vertices of $T(\mathcal{M})$. The sets of vertices and edges (and semi-edges) of $T(\mathcal{M})$ will be denoted by V and E, respectively. The set of edges visited by $\mathcal{C}$ will be denoted by $E_{\mathcal{C}}$. In this section, the edges joining two vertices v_i and v_j will be denoted by $(v_i, v_j)_1, (v_i, v_j)_2, (v_i, v_j)_3,...,(v_i, v_j)_h$; if $j = i+1$ then $(v_i, v_j)_1 \in E_{\mathcal{C}}$. (Note that in order to not start carrying many subindices, we modify the notation of the edges of $T(\mathcal{M})$ that we had used throughout the previous section. If one wants to be consistent with the notation of the edges used previously, one would have to say that the edges between v_i and v_j are $(v_i, v_j)_{a_1}, (v_i, v_j)_{a_2}, \ldots (v_i, v_j)_{a_h}$). Similarly, we denote all semi-edges incident to a vertex v_i by $(v_i, v_i)_1, (v_i, v_i)_2, (v_i, v_i)_3,...,(v_i, v_i)_l$. For the sake of simplicity, $(v_i, v_j)_1$ will be just called (v_i, v_j). Let $\mathcal{W}$ be the set of all closed walks in $T(\mathcal{M})$ with v_0 as its starting vertex. We shall now construct $G(\mathcal{W}) \subseteq \mathcal{W}$, a generating set of $\mathcal{W}$.

For each edge $(v_i, v_j)_m \in E \setminus E_{\mathcal{C}}$ we shall define the walk $w_{i,j,m} = ((v_0, v_1), (v_1, v_2), ..., (v_{i-1}, v_i), (v_i, v_j)_m$ That is, we walk from v_0 to v_i in $E_{\mathcal{C}}$, and then we take the edge $(v_i, v_j)_m$, and then we walk back from v_j to v_0 in $E_{\mathcal{C}}$. Let $\mathcal{W}_e \subseteq \mathcal{W}$ be the set of all such walks.

For each semi-edge $(v_i, v_i)_l \in E \setminus E_{\mathcal{C}}$ we shall define the walk $w_{i,i,l} = ((v_0, v_1), (v_1, v_2), ..., (v_{i-1}, v_i), (v_i, v_i)_l$ That is, we walk from v_0 to v_i in $E_{\mathcal{C}}$, and then we take the semi-edge $(v_i, v_i)_l$, and then we walk back from v_i to v_0 in $E_{\mathcal{C}}$. Let $\mathcal{W}_s \subseteq \mathcal{W}$ be the set of all such walks.

We define $G(\mathcal{W}) = \mathcal{W}_e \cup \mathcal{W}_s$.

Lemma 3.5. *With the notation from above, $G(\mathcal{W})$ is a generating set for $\mathcal{W}$.*

Proof. We shall prove that any $W \in \mathcal{W}$ can be expressed as a sequence of elements of $G(\mathcal{W})$ and their inverses. Let $W \in \mathcal{W}$ be a closed walk among the edges and semi-edges of $T(\mathcal{M})$ starting at v_0. From now on, semi-edges will be referred to simply as "edges".

We shall proceed by induction over n, the number of edges in $E \setminus E_{\mathcal{C}}$ visited by W. If W visits only one edge in $E \setminus E_{\mathcal{C}}$, then $W \in G(\mathcal{W})$ or $W^{-1} \in G(\mathcal{W})$. Let us suppose

that, if a closed walk among the edges of $T(\mathcal{M})$ visits m different edges in $E \setminus E_{\mathcal{C}}$, with $m < n$, then it can be expressed as a sequence of elements of $G(\mathcal{W})$ and their inverses.

Let $W \in \mathcal{W}$ be a walk that visits exactly n edges in $E \setminus E_{\mathcal{C}}$. Let $(v_a, v_b)_l \in E \setminus E_{\mathcal{C}}$ be the last edge of $E \setminus E_{\mathcal{C}}$ visited by W. Without loss of generality we may assume that the vertex v_b was visited after v_a, so let $(v_c, v_a)_m$ be the edge that W visits just before $(v_a, v_b)_l$ (note that $(v_c, v_a)_m$ may or may not be in $E_{\mathcal{C}}$). Let $W_1 \in \mathcal{W}$ be the closed walk that traces the same edges (in the same order) as W until reaching $(v_c, v_a)_m$ and then traces the edges (v_a, v_{a-1}), (v_{a-1}, v_{a-2}), ...,(v_1, v_0), and let $W_2 \in \mathcal{W}$ be the closed walk that traces the edges $(v_0, v_1), (v_1, v_2), ..., (v_{a-1}, v_a)$ and then traces $(v_a, v_b)_l$ and continues the way W does to return to v_0. It is clear that W_1 visits exactly $n-1$ edges in $E \setminus E_{\mathcal{C}}$ and that W_2 visits only one. By inductive hypothesis both W_1 and W_2 can be expressed as a sequence of elements of $G(\mathcal{W})$, and therefore so does W since $W = W_1 W_2$. ∎

Let Φ be a base flag of $\mathcal{M}$ that projects to the initial vertex of a walk that contains all vertices of $T(\mathcal{M})$ of a symmetry type graph. Following the notation of [32], given $w \in \mathrm{Mon}(\mathcal{M})$ such that Φ^w is in the same orbit as Φ (that is, $w \in \mathrm{Norm}_{\mathrm{Mon}(\mathcal{M})}(\mathrm{Stab}_{\mathrm{Mon}(\mathcal{M})}(\Phi)))$, we denote by α_w the automorphism taking Φ to Φ^w. Moreover, if $w = s_{i_1} s_{i_2} \ldots s_{i_k}$ for some $i_1, \ldots i_k \in \{0, \ldots, n-1\}$, then we may also denote α_w by $\alpha_{i_1, i_2, \ldots i_k}$.

The following theorem gives distinguished generators (with respect to some base flag) of the automorphism group of a maniplex $\mathcal{M}$ in terms of a distinguished walk of $T(\mathcal{M})$, that travels through all the vertices of $T(\mathcal{M})$. Its proof is a consequence of the previous lemma.

Theorem 3.5. *Let $\mathcal{M}$ be a k-orbit n-maniplex and let $T(\mathcal{M})$ its symmetry type graph. Suppose that $v_1, e_1, v_2, e_2 \ldots, e_{q-1}, v_q$ is a distinguished walk that visits every vertex of $T(\mathcal{M})$, with the edge e_i having colour a_i, for each $i = 1, \ldots q-1$. Let $S_i \subset \{0, \ldots, n-1\}$ be such that v_i has a semi-edge of colour s if and only if $s \in S_i$. Let $B_{i,j} \subset \{0, \ldots, n-1\}$ be the set of colours of the edges between the vertices v_i and v_j (with $i < j$) that are not in the distinguished walk and let $\Phi \in \mathcal{F}(\mathcal{M})$ be a base flag of $\mathcal{M}$ such that Φ projects to v_1 in $T(\mathcal{M})$. Then, the automorphism group of $\mathcal{M}$ is generated by the union of the sets*

$$\{\alpha_{a_1, a_2, \ldots, a_i, s, a_i, a_{i-1}, \ldots, a_1} \mid i = 1, \ldots, k-1, s \in S_i\},$$

and

$$\{\alpha_{a_1, a_2, \ldots, a_i, b, a_j, a_{j-1}, \ldots, a_1} \mid i, j \in \{1, \ldots, k-1\}, i < j, b \in B_{i,j}\}.$$

We note that, in general, a set of generators of $\mathrm{Aut}(\mathcal{M})$ obtained from Theorem 3.5 can be reduced since there might be more than one element of $G(\mathcal{W})$ representing the same automorphism. For example, the closed walk W through an edge of colour 2, then a 0-semi-edge and finally a 2-edge corresponds to the element $s_2 s_0 s_2 = s_0$ of $\mathrm{Mon}(\mathcal{M})$.

Hence, the group generator induced by the walk W is the same as that induced by the closed walk consisting only of the semi-edge of colour 0.

The following two corollaries give a set of generators for 2- and 3-orbit polytopes, respectively, in a given class. The notation follows that of Theorem 3.5, where if the indices of some α do not fit into the parameters of the set, we understand that such automorphism is the identity.

Corollary 3.2. *[30] Let $\mathcal{M}$ be a 2-orbit $(n-1)$-maniplex in class 2_I, for some $I \subset \{0, \ldots, n-1\}$ and let $j_0 \notin I$. Then*

$$\left\{\alpha_i, \alpha_{j_0,i,j_0}, \alpha_{k,j_0} \mid i \in I,\ k \notin I\right\}$$

is a generating set for $\mathrm{Aut}(\mathcal{M})$.

Corollary 3.3. *Let $\mathcal{M}$ be a 3-orbit $(n-1)$-maniplex.*

1. *If $\mathcal{M}$ is in class 3^i, for some $i \in \{1, \ldots, n-2\}$, then*

$$\left\{\alpha_j, \alpha_{i,i-1,i+1,i}, \alpha_{i,i+1,i+2,i+1,i}, \alpha_{i,i+1,i,i+1,i} \mid j \in \{0, \ldots, n-1\} \setminus \{i\}\right\}$$

is a generating set for $\mathrm{Aut}(\mathcal{M})$.

2. *If $\mathcal{M}$ is in class $3^{i,i+1}$, for some $i \in \{0, \ldots, n-2\}$, then*

$$\left\{\alpha_j, \alpha_{i,i-1,i}, \alpha_{i,i+1,i+2,i+1,i}, \alpha_{i,i+1,i,i+1,i} \mid j \in \{0, \ldots, n-1\} \setminus \{i\}\right\}$$

is a generating set for $\mathrm{Aut}(\mathcal{M})$.

Chapter 4

Operators on maps and maniplexes

In 1979, Wilson puts together three different operators on maps: *dual, Petrie* and *opposite*; in order to transform a regular map into another regular map, [57]. Later, in 1982, Lins showed properties of these operators on the flag graph of the map, to which he considered as dualities of the map and named them *dual, phial* and *skew*, respectively, [37]. Both, Wilson and Lins, showed that the dual and Petrie operators generate a copy of S_3, with the opposite operator as the third involution of the group.

In 2009, Hubard, Orbanić and Weiss, generalized the concept of duality and extend the concept of Petrie-dual to higher ranks, regarding abstract polytopes, [32]. Later, in 2012, Wilson described the dual, Petrie and opposite operators for maniplexes. In this chapter, we define and show some properties of these three operators on maps and maniplexes.

4.1   Dual and self-dual maps and maniplexes

Given two n-maniplexes $\mathcal{M}$ and $\mathcal{M}^*$, an *anti-isomorphism* $\delta : \mathcal{M} \to \mathcal{M}^*$ is a bijection on the flags of $\mathcal{M}$ to the flags of $\mathcal{M}^*$ that for each flag $\Phi \in \mathcal{F}(\mathcal{M})$ and each $i \in \{0, 1, \ldots, n\}$, $\Phi^i \delta = (\Phi \delta)^{n-i} \in \mathcal{F}(\mathcal{M}^*)$. If there exists an anti-isomorphism from $\mathcal{M}$ to $\mathcal{M}^*$, then $\mathcal{M}$ and $\mathcal{M}^*$ are said to be *duals* of each other. In terms of the flag graphs, δ can be regarded as a bijection between the vertices of $\mathcal{G}_\mathcal{M}$ and the vertices of $\mathcal{G}_{\mathcal{M}^*}$ that sends edges of colour i of $\mathcal{G}_\mathcal{M}$ to edges of colour $n - i$ of $\mathcal{G}_{\mathcal{M}^*}$, for each $i \in \{0, 1, \ldots, n\}$. In Figure 4.1 is depicted an example of the flag graphs of two dual maps: the cube and the octahedron.

If there exists a duality from a n-maniplex $\mathcal{M}$ to itself, we shall say that $\mathcal{M}$ is a *self-dual maniplex*, and δ is called a *duality* of $\mathcal{M}$. Given δ, ω two dualities of a self-dual maniplex $\mathcal{M}$, and $\Phi \in \mathcal{F}(\mathcal{M})$, we have that $\Phi^i \delta \omega = (\Phi \delta)^{2-i} \omega = (\Phi \delta \omega)^i$, implying that $\delta \omega$ is an automorphism of $\mathcal{M}$. Thus, the product of two dualities of a self-dual maniplex is no longer a duality, but an automorphism of the map. In particular, the square of any
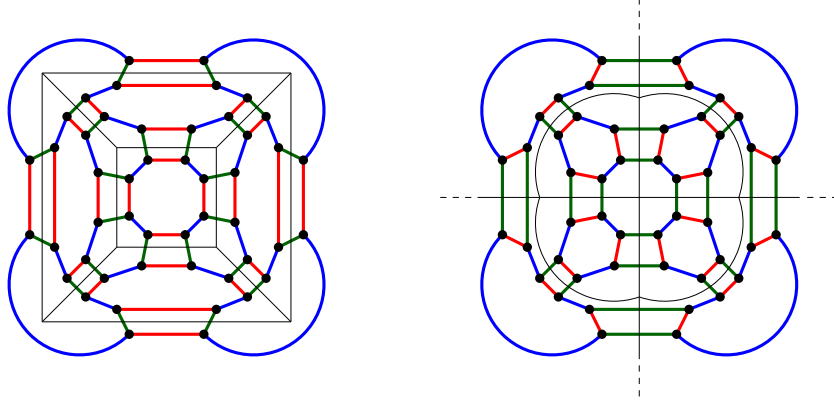
Figure 4.1: Flag graphs of the cube (left) and its dual, the octahedron (right).

duality is an automorphism. The set of all dualities and automorphisms of a map $\mathcal{M}$ is called the *extended group* $\mathcal{D}(\mathcal{M})$ of the map $\mathcal{M}$. The automorphism group $\mathrm{Aut}(\mathcal{M})$ is then a subgroup of index at most two in $\mathcal{D}(\mathcal{M})$. In fact, the index is two if and only if the maniplex is self-dual.

Recall that for each flag $\Phi \in \mathcal{F}(\mathcal{M})$ the set $\mathcal{O}_\Phi$ denotes the orbit of Φ under the action of $\mathrm{Aut}(\mathcal{M})$, and $\mathrm{Orb}(\mathcal{M}) := \{\mathcal{O}_\Phi \mid \Phi \in \mathcal{F}(\mathcal{M})\}$ denotes the set of all the orbits of $\mathcal{F}(\mathcal{M})$ under $\mathrm{Aut}(\mathcal{M})$. Hubard and Weiss showed the following very useful lemma in [33], regarding the action of the dualities of a self-dual maiplex on its set of flag-orbits.

Lemma 4.1. *Let $\mathcal{M}$ be a self-dual maniplex, δ a duality of $\mathcal{M}$ and $\mathcal{O}_1, \mathcal{O}_2 \in \mathrm{Orb}(\mathcal{M})$. If δ sends a flag from $\mathcal{O}_1$ to a flag in $\mathcal{O}_2$, then all the dualities send flags of $\mathcal{O}_1$ to flags in $\mathcal{O}_2$.*

Proof. Let δ be a duality of a self-dual maniplex $\mathcal{M}$. Given two orbits $\mathcal{O}_1, \mathcal{O}_2 \in \mathrm{Orb}(\mathcal{M})$ and a flag $\Phi \in \mathcal{O}_1$, suppose that $\Phi\delta \in \mathcal{O}_2$. For any $\Psi \in \mathcal{O}_1$, we know that there exists $\alpha \in \mathrm{Aut}(\mathcal{M})$ such that $\Psi = \Phi\alpha$, Then

$$\Psi\delta = (\Phi\alpha)\delta = (\Phi\delta\delta^{-1}\alpha)\delta = \Phi\delta(\delta^{-1}\alpha\delta),$$

since $\delta^{-1}\alpha\delta \in \mathrm{Aut}(\mathcal{M})$, it follows that $\Psi\delta \in \mathcal{O}_2$. Moreover, if there is δ', any other duality of $\mathcal{M}$, then $\Phi\delta' = \Phi\delta\delta^{-1}\delta'$ where $\delta^{-1}\delta' \in \mathrm{Aut}(\mathcal{M})$, that implies that $\Phi\delta' \in \mathcal{O}_2$.   ■

This lemma allows us to divide the self-dual n-maniplex into two different classes. Given $\mathcal{M}$ a self-dual maniplex, we say that $\mathcal{M}$ is *properly self-dual* if its dualities preserve all flag-orbits of $\mathcal{M}$. Otherwise, we say that $\mathcal{M}$ is *improperly self-dual*.

One can take a more algebraic approach in dealing with dual maniplex and dualities. In fact, if $\mathcal{M}$ is an n-maniplex with monodromy group $\mathrm{Mon}(\mathcal{M})$ generated by the sequence

$(s_0, s_1, \ldots, s_n)$, the monodromy group of the dual n-maniplex $\mathcal{M}^*$ is generated by the sequence $(s_n, s_{n-1}, \ldots, s_0)$. Moreover, in [32] was proved that a map $\mathcal{M}$ is self-dual if and only if $d : \text{Mon}(\mathcal{M}) \to \text{Mon}(\mathcal{M})$ sending s_i to s_{n-i} is a group automorphism such that $d(N)$ and N are conjugated, where $N = Stab_{\text{Mon}(\mathcal{M})}(\Phi)$ and $\Phi \in \mathcal{F}(\mathcal{M})$. In other words, this latter implies that $s_i = d^{-1}s_{n-i}d$.

4.1.1 Symmetry type graph of dual and self-dual maniplexes

The *dual type* of a symmetry type graph $T(\mathcal{M})$ is simply a symmetry type graph with the same vertices and edges as $T(\mathcal{M})$, but with a permutation of the colours of its edges and semi-edges in such a way that each colour $i \in \{0, 1, \ldots, n\}$ is replaced by the colour $n - i$. The following proposition is hence straightforward.

Proposition 4.1. *If a maniplex $\mathcal{M}$ has symmetry type graph $T(\mathcal{M})$ then its dual $\mathcal{M}^*$ has the dual of $T(\mathcal{M})$ as a symmetry type graph.*

A symmetry type graph is said to be *self-dual* if it is isomorphic to its dual type. Therefore, the symmetry type graph of a self-dual maniplex is a *self-dual symmetry type graph*. However, the converse is not true. Not every maniplex with a self-dual type is a self-dual maniplex, for example, the cube and the octahedron are duals to each other (hence, they are not self-dual) and have the same symmetry type graph (as they are regular maps).

Recall that each duality δ of a self-dual maniplex $\mathcal{M}$ induces a bijection between the vertices of $\mathcal{G}_{\mathcal{M}}$ and the vertices of $\mathcal{G}_{\mathcal{M}^*}$ that sends edges of colour i of $\mathcal{G}_{\mathcal{M}}$ to edges of colour $n - i$ in $\mathcal{G}_{\mathcal{M}^*}$, for each $i \in \{0, 1, \ldots, n\}$. Then, Lemma 4.1, implies that δ induces a permutation d of the vertices of $T(\mathcal{M})$, such that the edge colours i and $n - i$ are interchanged, with $i = 0, 1, \ldots, n$. We will refer to such permutation d as a duality of the symmetry type graph $T(\mathcal{M})$ of a self-dual maniplex $\mathcal{M}$. In particular, the symmetry type graph of a properly self-dual maniplex has a duality that fixes each of its vertices, while the symmetry type graph of an improperly self-dual maniplex has a duality that moves at least two of its vertices. Even more, since δ^2 is an automorphism of $\mathcal{M}$, then δ^2 fixes each orbit of $\mathcal{M}$. Hence d^2 acts as the identity on the vertices of $T(\mathcal{M})$. Therefore, for any duality δ of a self-dual maniplex $\mathcal{M}$ the corresponding duality d of its symmetry type graph $T(\mathcal{M})$ is a polarity; i.e. a duality of order two. However, in a similar way as before, the symmetry type graph does not posses all the information of the maniplex. That is, given a self-dual maniplex $\mathcal{M}$, its symmetry type graph $T(\mathcal{M})$ might not give us enough information on whether $\mathcal{M}$ is properly or improperly self-dual. An example of this is that chiral maniplexes can be either properly or improperly self-dual (see [33]), and hence the symmetry type graph of a chiral maniplexes accepts dualities that fix both vertices as well as dualities that interchange them.

Given a self-dual symmetry type graph $T(\mathcal{M})$ of a self-dual maniplex $\mathcal{M}$, the above paragraph incite us to add one edge (or semi-edge) of colour D to each vertex of $T(\mathcal{M})$, representing the action of the dualities of $\mathcal{M}$ on the flag orbits. The new pre-graph shall be called the *extended symmetry type graph* of the self-dual maniplex $\mathcal{M}$ and denoted by $\overline{T(\mathcal{M})}$. Since a self-dual reflexible maniplex is always properly self-dual, then the extended symmetry type graph of a self-dual reflexible maniplex consists of a vertex and $n+1$ semi-edges, of colours $0, 1, \ldots, n$ and D, respectively. Hence, as the distinguished generators $s_0, s_1, \ldots, s_n$ of $\mathrm{Mon}(\mathcal{M})$ label the edges of $T(\mathcal{M})$, the edges of $\overline{T(\mathcal{M})}$ are labeled by $s_0, s_1, \ldots s_n$ and d.

In what follows we will restrict our study only to what concerns respect the self-dual symmetry type graph of a map (2-maniplex), since it will be helpful for the study in Chapter 5.

Self-dual symmetry type graphs of maps

Since for every flag Φ of a self-dual map $\mathcal{M}$ and any duality δ of $\mathcal{M}$ we have that $\Phi^1 \delta = (\Phi \delta)^1$, the two factors of colours 1 and D of $\overline{T(\mathcal{M})}$ are a quotient of a 4-cycle. Furthermore, since $(\Phi \delta)^0 \delta = (\Phi \delta^2)^2$, and $\delta^2 \in \mathrm{Aut}(\mathcal{M})$, then the path of $\overline{T(\mathcal{M})}$ coloured $D, 0, D$ starting at a given vertex $\mathcal{O}_\Phi$, ends at $\mathcal{O}_{\Phi^2}$; that is, any path of colours $D, 2, D, 0$ finishes at the same vertex of $\overline{T(\mathcal{M})}$ that started.

We make here the remark that not every self-dual symmetry type accepts proper dualities, and that some symmetry types might accept more than one, essentially different, duality. Every 2-orbit self-dual symmetry type admits both, a proper self-duality and an improperly self-duality. However, this is not always the case, for example, the only self-dual type of 3-orbit maps only admits a proper self-duality. Whenever an extended symmetry type graph has a properly self-duality, the colour D of the graph consists of one semi-edge per vertex. In fact, we have the following proposition.

Proposition 4.2. *Let $\mathcal{M}$ be a self-dual map and let $T(\mathcal{M})$ be its symmetry type graph.*

a) *If $T(\mathcal{M})$ has a connected component in its 2-factor of colours 0 and 2 that has exactly 4 vertices, then $\mathcal{M}$ is improperly self-dual.*

b) *If $T(\mathcal{M})$ has a connected component in its 2-factor of colours 0 and 2 that has exactly 2 vertices, one edge and 2 semi-edges, then $\mathcal{M}$ is improperly self-dual.*

Proof. For $a)$, let $v_1, \ldots, v_4$ the four vertices of a connected component in the 2-factor of $T(\mathcal{M})$ of colours 0 and 2. Without loss of generality let us assume that $\{v_1, v_2\}$ and $\{v_3, v_4\}$ are 0-edges of $T(\mathcal{M})$, while $\{v_1, v_4\}$ and $\{v_2, v_3\}$ are 2-edges of $T(\mathcal{M})$. If $\mathcal{M}$ is a properly self-dual map, then the colour D of the extended graph $\overline{T(\mathcal{M})}$ consists of

one semi-edge per vertex. Hence, the path $D, 2, D, 0$ takes the vertex v_1 to the vertex v_3, contradicting the fact that every $D, 2, D, 0$ starts and finishes at the same vertex. Therefore $\mathcal{M}$ is improperly self-dual. Part b) follows in a similar way.   ∎

The above proposition implies that if a map $\mathcal{M}$ is properly self-dual, then the connected components in the 2-factor of $T(\mathcal{M})$ of colours 0 and 2 either have one vertex or have two vertices and a double edge between them. Hence, up to five orbits, the types that admit properly self-dualities are types 1, 2, 2_1, 2_{02}, 3^{02}, 4_{Ap}, 4_{Bp}, 4_{C_p} and 5_{C_p} (see Figures 3.2, 3.3, 3.6 and 3.7). Figure 4.2 shows all self-dual symmetry type graphs with six and seven vertices that admit properly self-dualities.
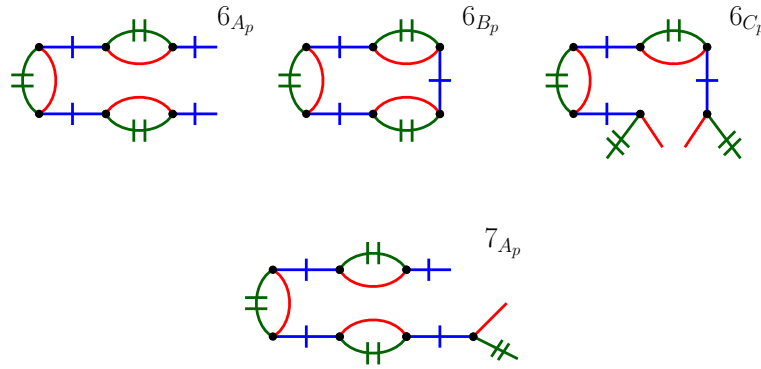
Figure 4.2: Symmetry type graphs with 6 and 7 orbits that admit proper self-dualitites.

It should be now straightforward to see that the following corollary holds.

Corollary 4.1. *If k is even, there are exactly three extended symmetry type graphs with k vertices admitting a proper self-duality. If k is odd, there is exactly one extended symmetry type graph with k vertices admitting a proper self-duality.*

The number of extended symmetry type graphs having improper self-dualities is more convoluted. Figures 4.3, 4.4 and 4.5 shows the possible extended symmetry type graphs with at most seven orbits, having improperly self-dualitites.

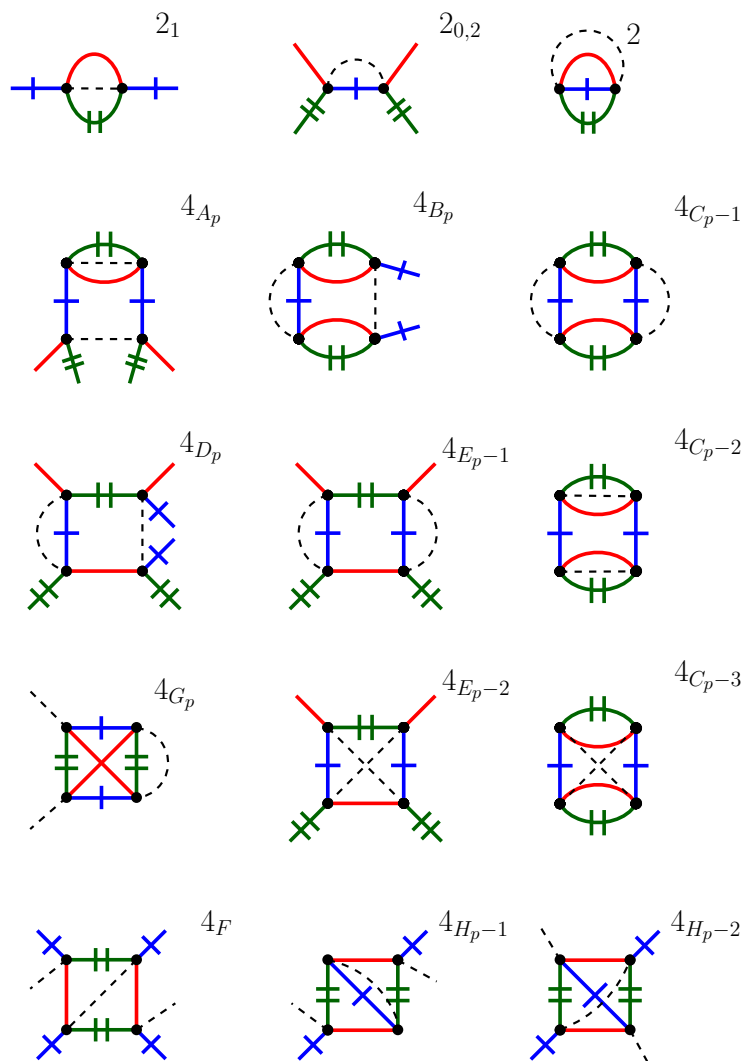Figure 4.3: Extended symmetry type graphs with at most 4 orbits, having improper self-dualitites.
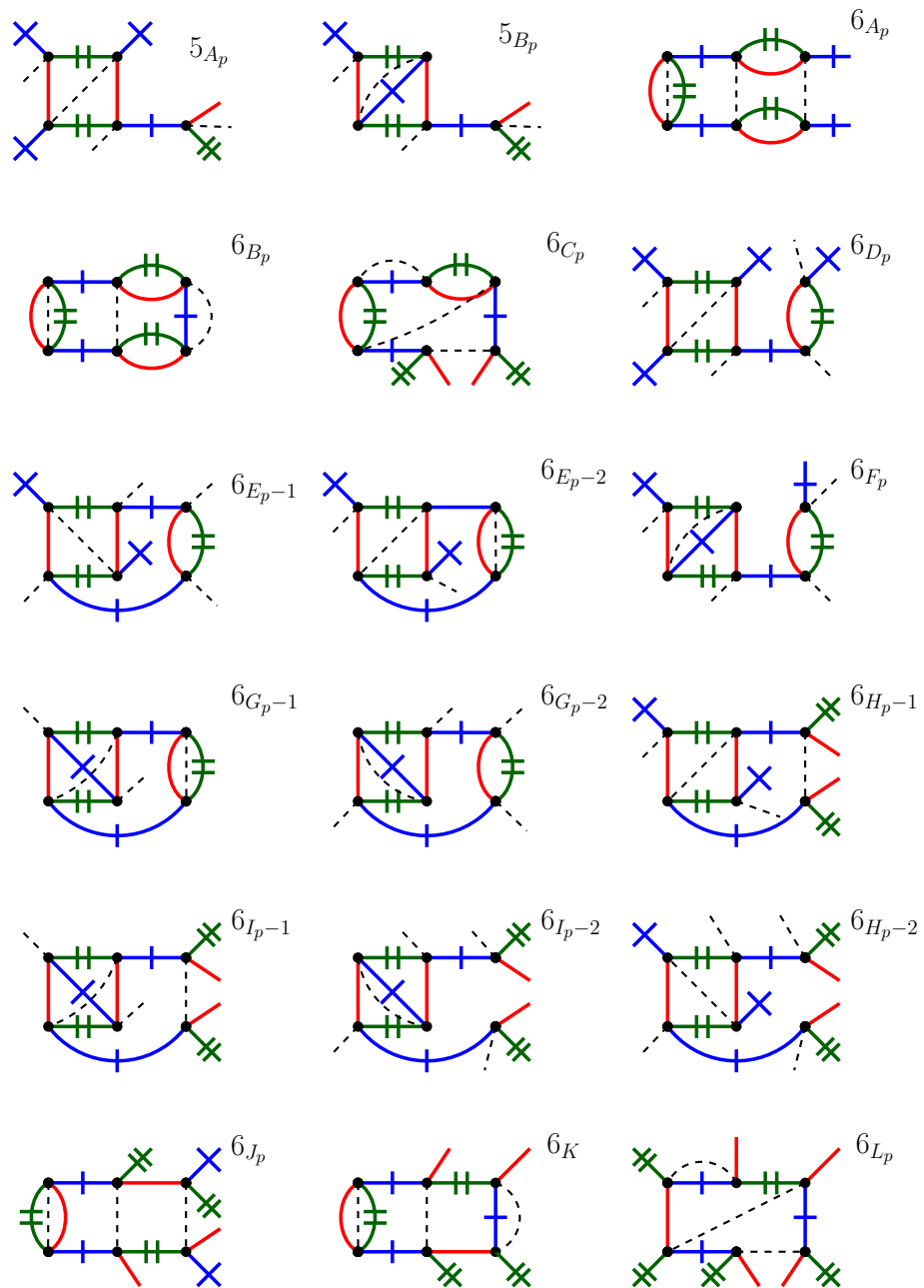
Figure 4.4: Extended symmetry type graphs with 5 and 6 orbits, having improper self-dualitites.
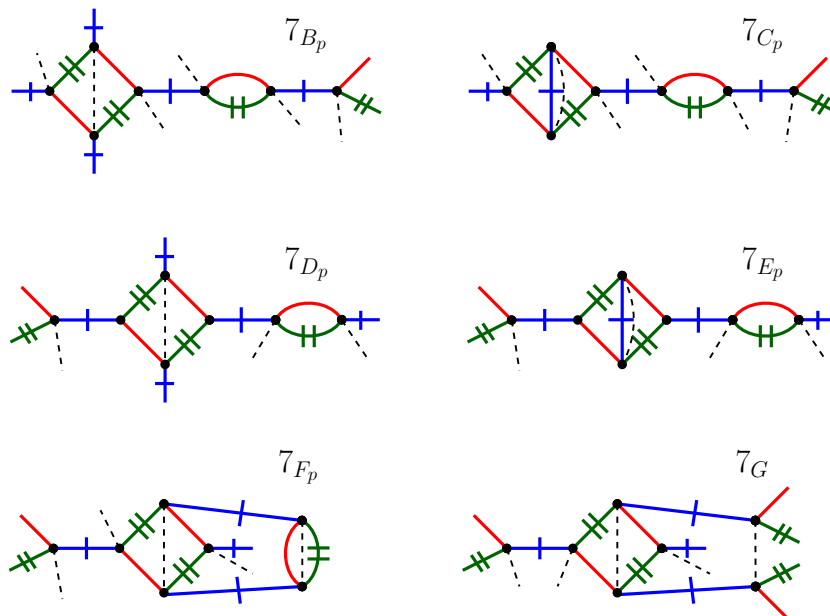
Figure 4.5: Extended symmetry type graphs with 7 orbits, having improper self-dualitites.

4.2 Petrie and self-petrie maps and maniplexes

In [6], Coxeter introduced the Petrie-polygons and extended this concept to any dimension. According to Coxeter, it was John Flinders Petrie who proposed the use of the "zig-zag" polygons, in manner to find more regular polyhedra (with an infinite number of faces). A *Petri polygon* is a "zig-zag" path among the edges of a map $\mathcal{M}$ in which every two consecutive edges, but not three, belong to the same face. Note that each edge of a Petrie polygon appears either just once in exactly two different Petrie polygons of $\mathcal{M}$, or twice in the same Petrie polygon of $\mathcal{M}$. Hence we can define a map with the same set of vertices and edges of $\mathcal{M}$, but with the Petrie polygons as faces. This map is known as the *Petrie-dual* (or *Petrial*) map of $\mathcal{M}$, and we denote it by $\mathcal{M}^P$. If a map $\mathcal{M}$ and its Petrie-dual $\mathcal{M}^P$ are isomorphic maps, then $\mathcal{M}$ is said to be *self-Petrie*.

Let s_0, s_1, s_2 be the distinguished generators of $\mathrm{Mon}(\mathcal{M})$. Since the set of vertices and edges in $\mathcal{M}^P$ coincide with those of $\mathcal{M}$, then the set of flags of $\mathcal{M}^P$ coincide with $\mathcal{F}(\mathcal{M})$. Even more, two flags in the flag graph $\mathcal{G}_{\mathcal{M}^P}$ are 1-adjacent if and only if they are adjacent in the flag graph $\mathcal{G}_{\mathcal{M}}$ by s_1 (by the definition of the Petrie polygon). However, recall that a walk along the s_0 and s_1 edges of $\mathcal{G}_{\mathcal{M}}$ define a face of $\mathcal{M}$, but a face in $\mathcal{M}^P$ corresponds to a "zig-zag" path in $\mathcal{M}$. Hence, two flags $\Phi, \Psi \in \mathcal{F}(\mathcal{M}^P)$ are 0-adjacent in $\mathcal{G}_{\mathcal{M}^P}$ if and only if $\Phi^{s_0 s_2} = \Psi$ (in $\mathcal{G}_{\mathcal{M}}$). Thus, the set of faces of $\mathcal{M}^P$ is defined as $\{\Phi^{\langle s_0 s_2, s_1 \rangle} \mid \Phi \in \mathcal{F}(\mathcal{M})\}$. The 4-cycles that represent the edges of $\mathcal{M}$ are no longer cycles of the flag-graph $\mathcal{G}_{\mathcal{M}^P}$. However, since a flag and its 2-adjacent flag in $\mathcal{M}^P$ differ only

on the face, and the vertices and edges of $\mathcal{M}^P$ are the same as those of $\mathcal{M}$, Φ and Ψ are 2-adjacent in $\mathcal{M}^P$ if and only if they are 2-adjacent in $\mathcal{M}$. In Figure 4.6 are presented the flag graph of a cube in the left, and the flag graph of its Petrial in the right.
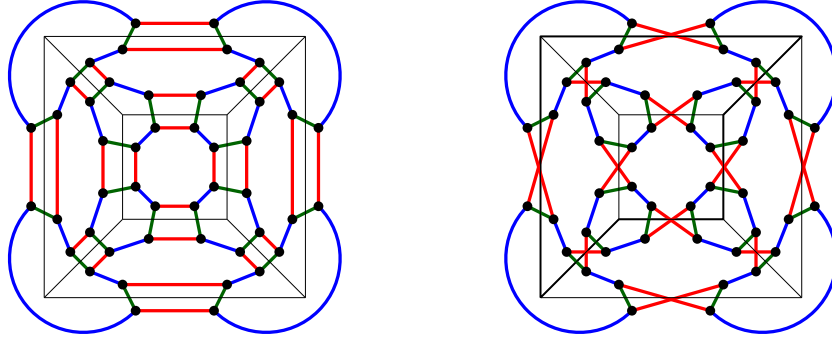

Figure 4.6: Flag graph of a cube (left) and its Petrial (right).

Therefore, there is a bijection, π say, between the vertices of $\mathcal{G}_\mathcal{M}$ and the vertices of $\mathcal{G}_{\mathcal{M}^P}$ that preserves the colours 1 and 2, and interchanges each (0,2)-path of length two by an edge of colour 0. The monodromy group of the Petrie dual map of $\mathcal{M}$ is generated by the triple $(s_0 s_2, s_1, s_2)$ (where s_0, s_1, s_2 are the generators of $\mathrm{Mon}(\mathcal{M})$).

For $n > 2$, the Petrie maniplex $\mathcal{M}^P$ of an n-maniplex $\mathcal{M}$ has the same set of flags than $\mathcal{M}$, and the bijection between the vertices of $\mathcal{G}_\mathcal{M}$ and the vertices of $\mathcal{G}_{\mathcal{M}^P}$ is defined in the following way. If the monodromy group of $\mathcal{M}$ is generated by the elements of the sequence $(s_0, s_1, \ldots, s_n)$, then $\bar\pi : \mathrm{Mon}(\mathcal{M}) \to \mathrm{Mon}(\mathcal{M}^P)$ is such that

$$\bar\pi : (s_0, s_1, \ldots, s_{n-3}, s_{n-2}, s_{n-1}, s_n) \mapsto (s_0, s_1, \ldots, s_{n-3}, , s_n s_{n-2}, s_{n-1}, s_n);$$

where the elements of the sequence $(s_0, s_1, \ldots, s_{n-3}, , s_n s_{n-2}, s_{n-1}, s_n)$ generate the monodromy group $\mathrm{Mon}(\mathcal{M}^P)$ of the Petrie dual maniplex of $\mathcal{M}$.

A *Petrie-polygon* on an $(n-1)$-maniplex $\mathcal{M}$ is a path along the edges of $\mathcal{M}$ such that any $n-1$ consecutive edges but no n belong to a Petie-polygon of a face of rank $n-1$ ([40]). Moreover, one can see that there is a bijection between all faces in $\mathcal{M}^P$ of ranks $n-2$ and $n-1$ and those of the same rank in $\mathcal{M}$.

4.2.1   Symmetry type graphs of Petrie maps and maniplexes

Similarly to the dual type, the *Petrie type* of a symmetry type graph $T(\mathcal{M})$ is a symmetry type graph with the same number of vertices of $T(\mathcal{M})$, which edges coloured 1 and 2 are preserved from $T(\mathcal{M})$, but any (0,2)-path in $T(\mathcal{M})$ is interchanged by an edge coloured by 0.

If $\mathcal{M}$ is an n-maniplex, π is a bijection between the set of flags $\mathcal{F}(\mathcal{M})$ and the set of flags $\mathcal{F}(\mathcal{M}^P)$ that preserves all edge-colours $0, 1, \ldots, n-3, n-1, n$ and interchanges each $(n-2, n)$-path by colour $n-2$ on the edges of $\mathcal{M}^P$. Hence, the *Petrie type* of a symmetry type graph $T(\mathcal{M})$ is a symmetry type graph with the same number of vertices of $T(\mathcal{M})$, which edges coloured $0, 1, \ldots, n-3, n-1, n$ are preserved from $T(\mathcal{M})$, but any $(n-2, n)$-path in $T(\mathcal{M})$ is interchanged by an edge coloured by $n-2$.

A symmetry type graph it is said to be *self-Petrie* if it is isomorphic to its Petrie type. The symmetry type graph of a self-Petrie maniplex is a *self-Petrie symmetry type graph*.

Then, similarly to Proposition 4.1 we have the following propsition for the Petrie symmetry type graphs of a maniplex.

Proposition 4.3. *If a maniplex $\mathcal{M}$ has symmetry type graph $T(\mathcal{M})$ then its Petrie-dual $\mathcal{M}^P$ has the petrie-dual of $T(\mathcal{M})$ as symmetry type graph.*

4.3 Opposite and self-opposite maps and maniplexes

Lins and Wilson, in [37] and [57], respectively, showed that for a map $\mathcal{M}$, it can be seen that the bijection π and the duality δ are operators on $\mathcal{M}$ that generate a subgroup of $Sym(\mathcal{F}(\mathcal{M}))$ isomorphic to S_3; where $\delta \circ \pi \circ \delta = \pi \circ \delta \circ \pi$ is the third element of order two in it, which defines a bijection between the set of flags of $\mathcal{M}$ and the set of flags of a map $\mathcal{M}'$ known as the *opposite* map of $\mathcal{M}$. As the dual $\mathcal{M}^*$ is obtained by exchanging vertices and faces of the map, and the Petrie $\mathcal{M}^P$ is obtained by exchanging faces with Petrie paths, fixing the vertices and edges, the opposite map $\mathcal{M}^{opp}$ is obtained by exchanging vertices with Petrie paths leaving the faces of $\mathcal{M}$ as faces of $\mathcal{M}^{opp}$ but with a different orientation than that in the faces in $\mathcal{M}$.

Therefore, $opp := \delta \circ \pi \circ \delta = \pi \circ \delta \circ \pi$ defines a bijection between the vertices of $\mathcal{G}_{\mathcal{M}}$ and $\mathcal{G}_{\mathcal{M}^{opp}}$ that preserves the edge colours 0 and 1, and interchanges each (0,2)-path of length two by an edge of colour 2. The monodromy group of the opposite map of $\mathcal{M}$ is generated by the triple $(s_0, s_1, s_0 s_2)$ (where s_0, s_1, s_2 are the generators of $\mathrm{Mon}(\mathcal{M})$).

Then, we can define the opposite maniplex $\mathcal{M}^{opp}$ of a maniplex $\mathcal{M}$ as that one with the same set of flags as $\mathcal{F}(\mathcal{M})$ and with sequence $(s_0, s_1, s_0 s_2, s_3, \ldots, s_n)$. It is not hard to see that for $n \geq 3$, the bijections δ and $\bar{\pi}$ generate a subgroup of $Sym(\mathcal{F}(\mathcal{M}))$ isomorphic to the dihedral group $D_4 = \langle \delta, \pi | \delta^2, \pi^2, (\delta\pi)^4 \rangle$. For $n \geq 5$, both operations induced by $\delta \circ \pi \circ \delta$ and $(\delta \circ \pi)^2 = (\pi \circ \delta)^2$, restricted to a face of rank 3, yield the same operation, namely the opposite operation.
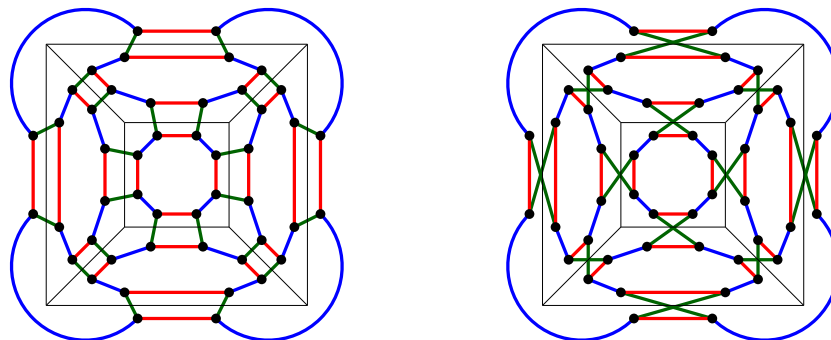
Figure 4.7: Flag graph of a cube (left) and its opposite (right).

4.3.1   Symmetry type graphs of opposite maps and maniplexes

The *opposite type* of a symmetry type graph $T(\mathcal{M})$ is a symmetry type graph with the same number of vertices of $T(\mathcal{M})$, which edges coloured $0, 1, 3, \ldots, n$ are preserved from $T(\mathcal{M})$, but any $(0, 2)$-path in $T(\mathcal{M})$ is interchanged by an edge coloured by 2.

A symmetry type graph it is said to be *self-opposite* if it is isomorphic to its opposite type. The symmetry type graph of a self-opposite maniplex is a *self-opposite symmetry type graph*.

Then, similarly to Propositions 4.1 and 4.3, we have the following propsition for the opposite symmetry type graphs of a maniplex.

Proposition 4.4. *If a maniplex $\mathcal{M}$ has symmetry type graph $T(\mathcal{M})$ then its opposite $\mathcal{M}^{opp}$ has the opposite of $T(\mathcal{M})$ as symmetry type graph.*

Part II

Map operations

Introduction to map operations

In the previous chapter we defined three operators on maps and maniplexes: *dual*, *Petrie dual* and *opposite*. Given the flag graph $\mathcal{G}_{\mathcal{M}}$ associated to the map or maniplex $\mathcal{M}$, the feature of these operators on $\mathcal{M}$ is that all three graphs $\mathcal{G}_{\mathcal{M}^*}$, $\mathcal{G}_{\mathcal{M}^P}$ and $\mathcal{G}_{\mathcal{M}^{opp}}$, corresponding to the dual $\mathcal{M}^*$, the Petrie dual $\mathcal{M}^P$ and the opposite $\mathcal{M}^{opp}$ maps or maniplexes, have the same vertex set $\mathcal{F}(\mathcal{M})$ as $\mathcal{G}_{\mathcal{M}}$. Also, each bijection δ, π and opp, between the generators of the monodromy group $\mathrm{Mon}(\mathcal{M})$ and the generators of the respective monodromy groups $\mathrm{Mon}(\mathcal{M}^*)$, $\mathrm{Mon}(\mathcal{M}^P)$ or $\mathrm{Mon}(\mathcal{M}^{opp})$, induces a permutation on the edges of $\mathcal{G}_{\mathcal{M}}$, describing the graphs $\mathcal{G}_{\mathcal{M}^*}$, $\mathcal{G}_{\mathcal{M}^P}$ and $\mathcal{G}_{\mathcal{M}^{opp}}$ of the dual, the Petrie dual and the opposite map or maniplex of $\mathcal{M}$, respectively. Later, using the same permutation on the edges of $\mathcal{G}_{\mathcal{M}}$ (in manner to obtain the graphs $\mathcal{G}_{\mathcal{M}^*}$, $\mathcal{G}_{\mathcal{M}^P}$ and $\mathcal{G}_{\mathcal{M}^{opp}}$ from $\mathcal{G}_{\mathcal{M}}$), we showed that we can obtain the possible symmetry type graphs $T(\mathcal{M}^*)$, $T(\mathcal{M}^P)$ and $T(\mathcal{M}^{opp})$ from $T(\mathcal{M})$.

In [45], Orbanić, Pellicer and Weiss, found all possible symmetry types of k-orbit maps resulting from other (non-degenerated) maps, or 2-maniplexes, after applying operations such as medial and truncation operations, for $k \leq 4$. Motivated by the results in [45], in the second part of the thesis, we look for a similar answer for maps obtained as a result after applying other operations as leapfrog and chamfering. Also, we will obtain an extension of the study in [45] and classify all possible symmetry types of maps up to 6-orbit maps.

In the following chapters, we define geometrically and combinatorially the operations of medial, chamfering, truncation and leapfrog. In particular, we study the possible symmetry type of maps that are obtained from these operations.

Unlike in the case of the dual, Petrie dual and opposite operators, where the flag graphs $\mathcal{G}_{\mathcal{M}}$, $\mathcal{G}_{\mathcal{M}^*}$, $\mathcal{G}_{\mathcal{M}^P}$ and $\mathcal{G}_{\mathcal{M}^{opp}}$ have the same number of vertices, we shall notice that when we apply either the medial, chamfering, truncation or leapfrog operations to a map $\mathcal{M}$, the set of flags of the new map $\widetilde{\mathcal{M}}$ is an integer multiple of $|\mathcal{F}(\mathcal{M})|$. This latter is a clear consequence of the transformations made on the map $\mathcal{M}$ after applying any of the operations. In fact, each operation can be described by a division of the fundamental triangles (of the barycentric subdivision $\mathcal{BS}(\mathcal{M})$) that induces an algorithm to obtain $\mathcal{G}_{\widetilde{\mathcal{M}}}$ out of $\mathcal{G}_{\mathcal{M}}$. Such an algorithm will enable us to give an appropriate partition $(\mathcal{A}_0, \ldots, \mathcal{A}_r)$

on the vertices of the flag graph $\mathcal{G}_{\widetilde{\mathcal{M}}}$, of the medial, chamfering, truncated or leapfrog map $\widetilde{\mathcal{M}}$, in such way that $\mathcal{F}(\widetilde{\mathcal{M}}) = \mathcal{A}_0 \cup \cdots \cup \mathcal{A}_r$ where each $\mathcal{A}_j$ is a block for the monodromy group $\mathrm{Mon}(\widetilde{\mathcal{M}})$, with $j = 0, \ldots, r$.

It is not hard to see that the automorphism group $\mathrm{Aut}(\mathcal{M})$ of $\mathcal{M}$ induces a subgroup $H \leq \mathrm{Aut}(\widetilde{\mathcal{M}})$ of the automorphism group of $\widetilde{\mathcal{M}}$. Intuitively, since the automorphism group of the map $\mathcal{M}$ partitions its set of flags in k orbits, we might think that if $|\mathcal{F}(\widetilde{\mathcal{M}})| = r|\mathcal{F}(\mathcal{M})|$, then the map $\widetilde{\mathcal{M}}$ is a rk-orbit map. However, it is possible that $\widetilde{\mathcal{M}}$ has less than rk flag-orbits. We will discuss this phenomenon in the following chapters.

In Chapter 5, we study the medial operation on maps and enumerate all medial symmetry type graphs with at most 7 vertices. In particular we show that every type of edge-transitive map is a medial type. In Chapter 6, we study the chamfering operation on maps. Finally, in Chapter 7, we study the truncation and leapfrog operations, based on the results obtained in [45] for truncation, and give an extension to such results up to $k \leq 7$ and $k = 9$.

Chapter 5

Medial operation on maps

There is an interesting operation on maps called *the medial* of a map (see [8, 45, 49]). It is well-known that the medial of a tetrahedron is an octahedron and its medial is a cube-octahedron (see Figure 5.1). While the former polyhedra are regular, the latter is only a 2-orbit edge-transitive as a map. For any map $\mathcal{M}$, we define the medial of $\mathcal{M}$,
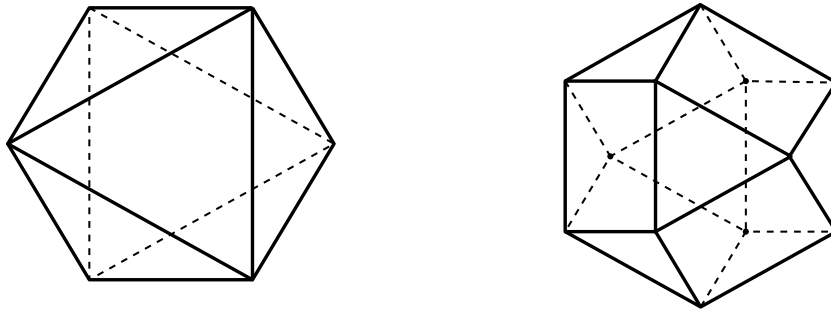
Figure 5.1: Octahedron (left) and its medial map, the cube-octahedron (right).

$\mathrm{Me}(\mathcal{M})$, in the following way. The vertex set of $\mathrm{Me}(\mathcal{M})$ is the edge set of $\mathcal{M}$, $E(\mathcal{M})$. Two vertices of $\mathrm{Me}(\mathcal{M})$ have an edge joining them if the corresponding edges of $\mathcal{M}$ share a vertex and belong to the same face. This is,

$$E(\mathrm{Me}(\mathcal{M})) := \{\{\Phi_0, \Phi_2\} | \Phi \in \mathcal{F}(\mathcal{M})\}.$$

This gives raise to a graph embedded on the same surface as $\mathcal{M}$. Hence, the faces of $\mathrm{Me}(\mathcal{M})$ are simply the connected regions of the complement of the graph on the surface. It is then not difficult to see that the face set of $\mathrm{Me}(\mathcal{M})$ is in one to one correspondence with the set containing all faces and vertices of $\mathcal{M}$, i.e.

$$F(\mathrm{Me}(\mathcal{M})) := F(\mathcal{M}) \cup V(\mathcal{M}).$$

In fact, it is straightforward to see that the medial of a map $\mathcal{M}$ and the medial of its dual $\mathcal{M}^*$ are isomorphic.

We note that every flag of the original map $\mathcal{M}$ is divided into two flags of the medial map $\mathrm{Me}(\mathcal{M})$, as is depicted in Figure 5.2. In fact, given a flag $\Phi = (\Phi_0, \Phi_1, \Phi_2)$ of $\mathcal{M}$,
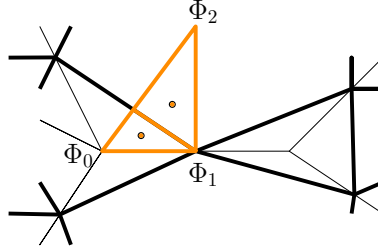

Figure 5.2: The two flags of $\mathcal{F}(\mathrm{Me}(\mathcal{M}))$ corresponding to the flag $\Phi = (\Phi_0, \Phi_1, \Phi_2) \in \mathcal{F}(\mathcal{M})$.

one can write the two flags of $\mathrm{Me}(\mathcal{M})$ corresponding to Φ as

$$(\Phi, 0) := (\Phi_1, \{\Phi_0, \Phi_2\}, \Phi_0) \quad \text{and} \quad (\Phi, 2) := (\Phi_1, \{\Phi_0, \Phi_2\}, \Phi_2).$$

It is then straightforward to see that the adjacencies of the flags of $\mathrm{Me}(\mathcal{M})$ are closely related to those of the flags of $\mathcal{M}$, in the following way.

$$(\Phi, 0)^0 = (\Phi^{s_1}, 0), \quad (\Phi, 0)^1 = (\Phi^{s_2}, 0), \quad (\Phi, 0)^2 = (\Phi, 2),$$
$$(\Phi, 2)^0 = (\Phi^{s_1}, 2), \quad (\Phi, 2)^1 = (\Phi^{s_0}, 2), \quad (\Phi, 2)^2 = (\Phi, 0),$$

where s_0, s_1 and s_2 are the generators of $\mathrm{Mon}(\mathcal{M})$. Let m_0, m_1 and m_2 be the distinguished generators of $\mathrm{Mon}(\mathrm{Me}(\mathcal{M}))$. Then m_0, m_1 and m_2 are fixed-point free involutions, where $m_0 m_2 = m_2 m_0$ and, $(m_1 m_2)^4 = id$. The latter relation implied by the fact that every vertex of a medial map $\mathrm{Me}(\mathcal{M})$ has valency 4.

It is now easy to obtain the flag graph of $\mathrm{Me}(\mathcal{M})$ from the flag graph of $\mathcal{M}$. An algorithm showing how to do this is indicated in Figure 5.3. Such algorithm induces a bipartition $(\mathcal{A}_0, \mathcal{A}_2)$ on the vertices of $\mathcal{G}_{\mathrm{Me}(\mathcal{M})}$, where $\mathcal{A}_0 := \{(\Phi, 0) | \Phi \in \mathcal{F}(\mathcal{M})\}$ and $\mathcal{A}_2 := \{(\Phi, 2) | \Phi \in \mathcal{F}(\mathcal{M})\}$, and consequently we have the following proposition.

Proposition 5.1. *The flag graph $\mathcal{G}_{\mathrm{Me}(\mathcal{M})}$, of the medial map $\mathrm{Me}(\mathcal{M})$ of a map $\mathcal{M}$, can be quotient into a graph isomorphic to the symmetry type graph 2_{01}.*

Proof. Let $\mathcal{A}_0 = \{(\Phi, 0) | \Phi \in \mathcal{F}(\mathcal{M})\}$ and $\mathcal{A}_2 = \{(\Phi, 2) | \Phi \in \mathcal{F}(\mathcal{M})\}$. Then, $\mathcal{F}(\mathrm{Me}(\mathcal{M})) = \mathcal{A}_0 \cup \mathcal{A}_2$ and $\mathcal{A}_0 \cap \mathcal{A}_2 = \emptyset$. Hence, $(\mathcal{A}_0, \mathcal{A}_2)$ is a bi-partition of the set of flags $\mathcal{F}(\mathrm{Me}(\mathcal{M}))$. Based on Figure 5.3, it is straightforward to see that the quotient of $\mathcal{G}_{\mathrm{Me}(\mathcal{M})}$ over such bi-partition, is isomorphic to the symmetry type graph of a map with symmetry type 2_{01} (see Figure 3.2). ∎
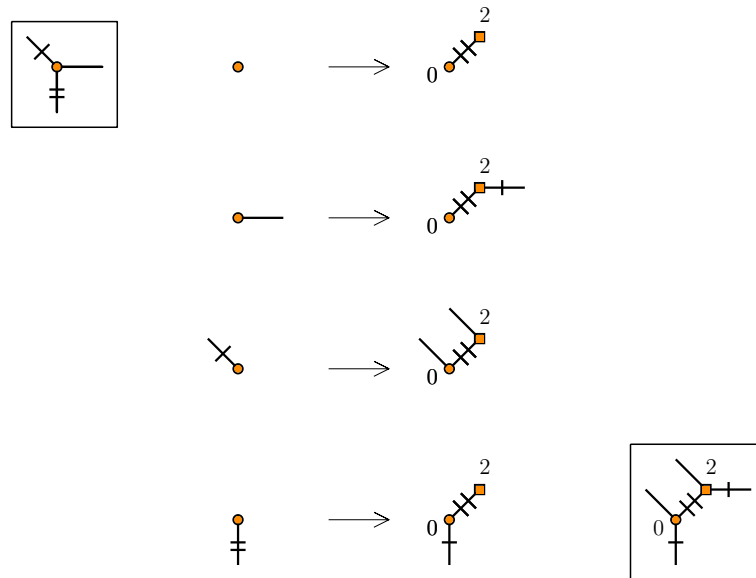
Figure 5.3: Any local representation of a flag, in the left. The result under the medial operation, locally obtained, in the right.

In the past several authors have observed that the medial of any regular map must be edge-transitive; in fact, in [32] Hubard, Orbanić and Weiss showed that the medial of a regular map is either regular (if the original map is self-dual) or of type 2_{01} (otherwise).

The nature of edge-transitive tessellations have been studied by Graver and Watkins, [26]. They were the first to determine all 14 different symmetry types of edge-transitive maps. Later, Širan, Tucker and Watkins [53] have provided examples of maps from each of the 14 types. Several authors have been trying to determine the nature of edge-transitive maps that are medial maps, i.e. maps that are medials of other maps. For instance, Lemma 2.2 in [53] lists six symmetry types that can be edge-transitive medials of edge-transitive maps. In [32] it is shown that there are, in fact, seven such symmetry types. In [45, Table 2] the authors give 10 symmetry types of edge-transitive maps that may be medials of other, not necessarily edge-transitive maps. Unfortunately, they miss the fact that four other edge-transitive types may also be medials.

5.1   Medial of k-orbit maps

In [32], Hubard, Orbanić and Weiss showed that the automorphism group of the medial map $\mathrm{Me}(\mathcal{M})$ of a map $\mathcal{M}$ is isomorphic to the extended group $\mathcal{D}(\mathcal{M})$ of $\mathcal{M}$, and used proper and improper self-dualities of the maps to characterize regular and 2-orbit medial maps, in terms of their symmetry type. In particular they showed that a medial map $\mathrm{Me}(\mathcal{M})$ is regular if and only if $\mathcal{M}$ is regular and self-dual. In [32, Table 4] we further

observe that every 2-orbit symmetry type can be the medial map of a regular or a 2-orbit map. In [45], Orbanić, Pellicer and Weiss extended this to characterize the symmetry types of all medial maps of 2-orbit maps. They further proved that if $\mathcal{M}$ is a k-orbit map, then $\mathrm{Me}(\mathcal{M})$ is a k-orbit or a $2k$-orbit map, depending on whether or not $\mathcal{M}$ is a self-dual map. Here we show that every symmetry type of edge-transitive map is a medial symmetry type.

In the following subsections, we make use of symmetry type graphs and extended symmetry type graphs (see Section 4.1.1), and an operation on them to obtain medial symmetry type graphs. We further enumerate all the medial types with at most 7 vertices and show that indeed every type of edge-transitive map is a medial type.

5.1.1   Medial symmetry type graphs

We shall say that a *medial symmetry type graph* is the symmetry type graph of a medial map, denoted by $T(\mathrm{Me}(\mathcal{M}))$. In what follows we classify all possible medial symmetry type graphs with at most 7 vertices. To this end, we develop basic operations on the symmetry type graphs as well as on the extended symmetry type graphs, based on the flag graphs of a map and its medial.

If a map $\mathcal{M}$ is not a self-dual map, we may think of the vertices of the medial symmetry type graph $T(\mathrm{Me}(\mathcal{M}))$, as those obtained by two copies of the vertices of the symmetry type graph $T(\mathcal{M})$. As with the flag graph, given a vertex $\mathcal{O}_\Phi$ of $T(\mathcal{M})$ we can write its corresponding two copies in $T(\mathrm{Me}(\mathcal{M}))$ as $(\mathcal{O}_\Phi, 0)$ and $(\mathcal{O}_\Phi, 2)$. Note that the edges between these copies of the vertices of $T(\mathcal{M})$ must respect the colour adjacency of the flags in the flag graph of $\mathrm{Me}(\mathcal{M})$. Then, we can follow the same algorithm shown in the Figure 5.3 to determine the adjacencies between the vertices of $T(\mathrm{Me}(\mathcal{M}))$. In other words, the vertices $(\mathcal{O}_\Phi, 0)$ and $(\mathcal{O}_\Phi, 2)$ are adjacent by an edge of colour 2; for $i = 0, 2$ there is an edge of colour 0 between $(\mathcal{O}_\Phi, i)$ and $(\mathcal{O}_\Psi, i)$ if and only if $\mathcal{O}_\Phi$ and $\mathcal{O}_\Psi$ are adjacent by the colour 1. Finally, there is an edge of colour 1 between $(\mathcal{O}_\Phi, i)$ and $(\mathcal{O}_\Psi, i)$ if and only if $\mathcal{O}_\Phi$ and $\mathcal{O}_\Psi$ are adjacent by the colour 0 or 2.

Hence, if a k-orbit map $\mathcal{M}$ is not a self-dual map, the medial symmetry type graph $T(\mathrm{Me}(\mathcal{M}))$ of $\mathrm{Me}(\mathcal{M})$ (obtained as it was described in the paragraph above) has $2k$ vertices. On the other hand, when $\mathcal{M}$ is a self-dual k-orbit map, to obtain its medial symmetry type graph with k vertices, we take into consideration the extended symmetry type graph $\overline{T(\mathcal{M})}$. In this case we shall identify each vertex of the form $(\mathcal{O}_\Phi, 0)$ with a vertex of the form $(\mathcal{O}_\Psi, 2)$ by an edge of colour 2, whenever $\mathcal{O}_\Phi$ and $\mathcal{O}_\Psi$ are adjacent by the colour D in $\overline{T(\mathcal{M})}$, and permute colours 0 and 1. Hence, the colours of the edges of

$T(\mathrm{Me}(\mathcal{M}))$ can be defined by the following involutions:

$$
\begin{aligned}
m_0 &= s_1, \\
m_1 &= s_0 \quad (\text{or } s_2), \\
m_2 &= d.
\end{aligned}
$$

Note that if $\mathrm{Me}(\mathcal{M})$ is a k-orbit map, with k odd, then $\mathcal{M}$ is a self-dual k-orbit map. However, if k is even, then $\mathcal{M}$ is either a k- or a $k/2$-orbit map. Hence, to obtain all medial symmetry type graphs with at most 7 vertices, one has to apply the above operations to all symmetry type graphs with at least 3 vertices, as well as to all extended symmetry type graphs with at most 7 vertices.

In [45, Table 2] are given the symmetry types of medials coming from 1- and 2-orbit maps. Following the algorithm described above, in the left table of Table 5.1 we repeat the information contained in [45, Table 2] and give the symmetry type of medials coming from 3-orbit maps. In the right table of Table 5.1 and in both tables of Table 5.2 are given the symmetry type of medials coming from k-orbit self-dual maps, for $4 \leq k \leq 7$. In the second row, of all tables in Tables 5.1 and 5.2, "P" stands for properly self-dual, "I" for improperly self-dual and "N" for not self-dual, the number after the I, in the cases it exists, stands for the type of improperly duality that the map possesses. All medial types with at most 5 vertices are already given in Figures 3.2–3.7; medial types with 6 and 7 vertices are given in Figures 5.4 and 5.5, respectively.

Sym type of $\mathcal{M}$	Sym type of $\mathrm{Me}(\mathcal{M})$		
Duality	P	I	N
1	1	—	2_{01}
2	2_2	2	4_G
2_0	—	—	4_H
2_1	2_{02}	2_0	4_C
2_2	—	—	4_H
2_{01}	—	—	4_A
2_{02}	2_{12}	2_1	4_F
2_{12}	—	—	4_A
3^0	—	—	6_D
3^2	—	—	6_D
3^{02}	3^0	—	6_M

Sym type of $\mathcal{M}$	Sym type of $\mathrm{Me}(\mathcal{M})$			
Duality	P	I-1	I-2	I-3
4_{A_p}	4_{B_d}	4_{H_d}	—	—
4_{B_p}	4_{A_d}	4_{E_d}	—	—
4_{C_p}	4_{C_d}	4_{C_p}	4_{G_d}	4_{G_p}
4_{D_p}	—	4_{D_d}	—	—
4_{E_p}	—	4_{B_p}	4_{H_p}	—
4_F	—	4_A	—	—
4_{G_p}	—	4_E	—	—
4_{H_p}	—	4_{A_p}	4_{E_p}	—
5_A	—	$5_{D_{pd}}$	—	—
5_{B_p}	—	$5_{D_{op}}$	—	—
5_{C_p}	5_{C_d}	—	—	—

Table 5.1: Medial symmetry types from 1-, 2-, 3-orbit maps (in the left), and from 4-, and 5-orbit self-dual maps (in the right).
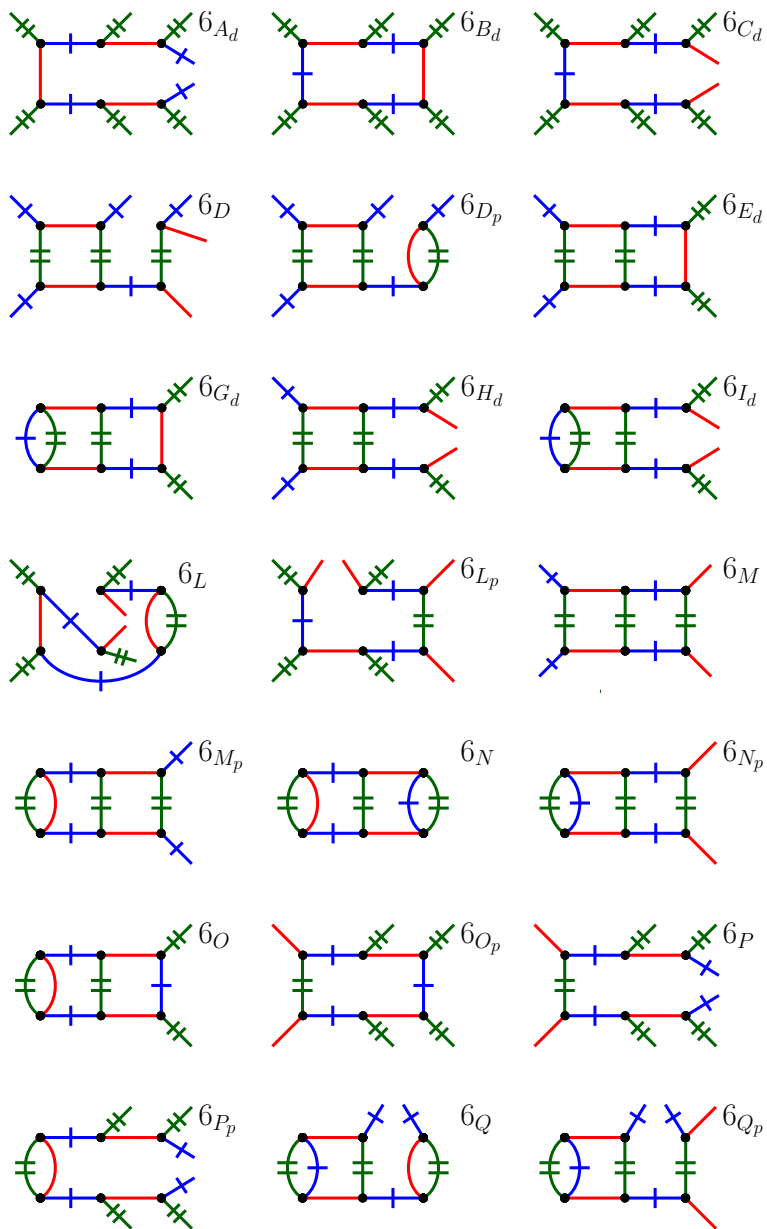
Figure 5.4: Medial symmetry types with 6 vertices.

Sym type of $\mathcal{M}$	Sym type of Me($\mathcal{M}$)		
Duality	P	I-1	I-2
6_{A_p}	6_{C_d}	6_{N_p}	—
6_{B_p}	6_{B_d}	6_N	—
6_{C_p}	6_{A_d}	6_{M_p}	—
6_{D_p}	—	6_{L_p}	—
6_{E_p}	—	6_{O_p}	6_{I_d}
6_{F_p}	—	6_L	—
6_{G_p}	—	6_{G_d}	6_O
6_{H_p}	—	6_{H_d}	6_P
6_{I_p}	—	6_{E_d}	6_{P_p}
6_{J_p}	—	6_{Q_p}	—

Sym type of $\mathcal{M}$	Sym type of Me($\mathcal{M}$)	
Duality	P	I
6_K	—	6_Q
6_{L_p}	—	6_{D_p}
7_{A_p}	7_{A_d}	—
7_{B_p}	—	7_H
7_{C_p}	—	7_{H_p}
7_{D_p}	—	7_I
7_{E_p}	—	7_{I_p}
7_{F_p}	—	7_{E_d}
7_G	—	7_J

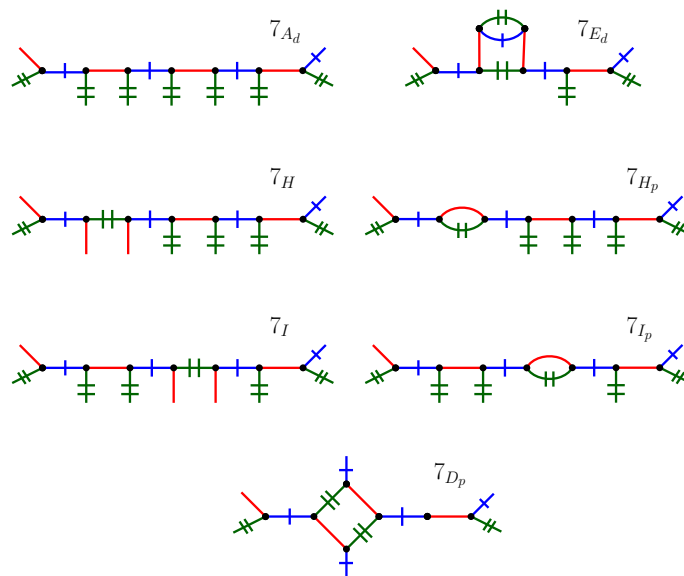Table 5.2: Medial symmetry types from 6- and 7-orbit self-dual maps.

Figure 5.5: Medial symmetry types with 7 vertices.

5.1.2   Symmetry types of edge-transitive maps that are medial of other edge-transitive maps

To show that each of the 14 edge-transitive symmetry type graphs is the symmetry type graph of a medial map we shall, for each type, give an example.

Orbanić, in [42] generated a data base of small non-degenerated edge transitive maps. His data base contains small non-degenerated edge transitive maps of types 1, 2_{12}, 2_2, 4_F, 4_{H_d} and 4_{G_d}; the remaining types can be obtained from these one by making use of the Petrie and dual operations (see Figures 3.2 and 3.5).

Using the tables in Table 5.1, we obtain Table 5.3. The first column of Table 5.3 lists all the candidate types for maps that could, by applying medial operation, yield the maps with edge-transitive types. The second column indicates which type of duality the map in the first column should have to obtain the medial type in the third column. In the second column the number after the Improper, in the cases it exists, stands for the type of improperly duality that the map possesses, see right table of Table 5.1.

$T(\mathcal{M})$	Duality	$T(Me(\mathcal{M}))$
1	Proper	1
	None	2_{01}
2_{02}	Proper	2_{12}
	Improper	2_1
	None	4_F
2_1	Improper	2_0
2	Proper	2_2
	Improper	2
	None	4_G
4_{C_p}	Improper-2	4_{G_d}
	Improper-3	4_{G_p}
$2_0, 2_2$	None	4_H
4_{A_p}	Improper	4_{H_d}
4_{E_p}	Improper-2	4_{H_p}

Table 5.3: Edge-transitive medial symmetry types

Theorem 5.1. *Each of the 14 edge-transitive symmetry type graphs is the symmetry type graph of a medial map.*

Proof. Recall that the monodromy group of the medial map $Me(\mathcal{M})$ of a map $\mathcal{M}$ is the group $Mon(Me(\mathcal{M})) := \langle m_0, m_1, m_2 \rangle$, generated by three involutions where $(m_0 m_2)^2 = (m_1 m_2)^4 = id$. Let $N := \mathrm{Stab}_{Mon(Me(\mathcal{M}))}((\Phi, 2))$ be the stabilizer of the base flag $(\Phi, 2) \in$

$\mathcal{F}(\mathrm{Me}(\mathcal{M}))$ under the action of the monodromy group of $\mathrm{Me}(\mathcal{M})$. Observe that

$$(\Phi, 2)^{m_1} = (\Phi^{s_0}, 2), \quad (\Phi, 2)^{m_0} = (\Phi^{s_1}, 2) \quad \text{and} \quad (\Phi, 2)^{m_2 m_1 m_2} = (\Phi^{s_2}, 2).$$

Then, the subgroup $H := \langle m_1, m_0, m_2 m_1 m_2 \rangle \leq \mathrm{Mon}(\mathrm{Me}(\mathcal{M}))$ stabilizes the subset $\mathcal{A}_2 := \{(\Phi, 2) | \Phi \in \mathcal{F}(\mathcal{M})\}$ of the flag-set $\mathcal{F}(\mathrm{Me}(\mathcal{M}))$. According to [45, Sec. 4.1], we have that H has index 2 in $\mathrm{Mon}(\mathrm{Me}(\mathcal{M}))$.

Then the de-medialized map is defined by taking the action of H on the cosets of $N \leq H$ and relabeling generators of H in the respective order by m_0, m_1 and m_2. Note that the dual of the result (yielding the same medial map) could be obtained by taking the conjugate stabilizer $m_2 N m_2$ instead of N.

Using this method, the software package MAGMA and the database of small non-degenerate edge-transitive maps [42], all the examples supporting options in Table 5.3 are calculated and summarized in Table 5.4. It is not claimed that they are minimal examples, though we tried to choose minimal such cases where both an original map and its medial are non-degenerate and both with edge multiplicity 1. ∎

Edge-transitive Med($\mathcal{M}$)						Example map $\mathcal{M}$					
InitType	ID	Tran	MType	Genus	Symbol	Type	$\lvert V\rvert$	$\lvert E\rvert$	$\lvert F\rvert$	$\lvert P\rvert$	Map symbol
1	41	P	1	1	$\langle 4;4;8\rangle$	1	8	16	8	8	$\langle 4;4;4\rangle$
2	113	D	2_{01}	0	$\langle 4;3;4;8\rangle$	1	6	12	8	4	$\langle 4;3;6\rangle$
2	8335		2_{12}	25	$\langle 4;4;10;10\rangle$	2_{02}	16	80	16	40	$\langle 10;10;4\rangle$
2	504	DP	2_{1}	1	$\langle 4;4;6,8\rangle$	2_{02}	12	24	12	2	$\langle 4;4;24\rangle$
3	180	P	4_{F}	-8	$\langle 4,4;12,4;6,12\rangle$	2_{02}	9	18	3	3	$\langle 4;12;12\rangle$
2ex	456	D	2_{0}	37	$\langle 4;8;8\rangle$	2_{1}	36	144	36	24	$\langle 8;8;12,12\rangle$
2ex	21		2_{2}	7	$\langle 4;7;14\rangle$	2	8	28	8	14	$\langle 7;7;4\rangle$
2ex	2	DP	2	1	$\langle 4;4;10\rangle$	2	5	10	5	2	$\langle 4;4;10\rangle$
5	13	D	4_{G}	1	$\langle 4;6;3;12\rangle$	2	14	21	7	3	$\langle 3;6;14\rangle$
5	301		4_{Gd}	19	$\langle 4,4;8;8\rangle$	4_{Cp}	18	72	18	12	$\langle 8;8;12,12\rangle$
5	275	DP	4_{Gp}	18	$\langle 4;8;8;8\rangle$	4_{Cp}	17	68	17	4	$\langle 8;8;34,34\rangle$
4	450	D	4_{H}	-8	$\langle 4;7,4;8\rangle$	2_{2}	14	28	8	8	$\langle 4;7;7\rangle$
4	17200		4_{Hd}	26	$\langle 4,4;8;8\rangle$	4_{Ap}	25	100	25	20	$\langle 8;8;10,10\rangle$
4	7496	DP	4_{Hp}	19	$\langle 4;8;8;8\rangle$	4_{Ep}	18	72	18	36	$\langle 8;8;4\rangle$

Table 5.4: Examples of edge-transitive maps of all 14 types that are medials.

The table is divided into two halves and each line represents one example. The first half contains data needed to retrieve a map Me($\mathcal{M}$) from the database [42]. Three parameters are needed: a type (**MType**, one of the types 1, 2, 2ex, 3, 4 or 5 according to [26]), an identifier within a subdatabase for the type (column **ID**) and a sequence of operations (column **Tran**, where D stands for dual and P for Petrie-dual; note: operations compose like functions). The retrieved map (denoted by Me($\mathcal{M}$)) is the medial of the map $\mathcal{M}$ whose type, number of vertices, edges, faces, Petrie-polygons and symbol are in the seventh to twelfth columns of the table (second half). In a symbol of the form $\langle a_1,\ldots,a_i; b_1,\ldots,b_j; c_1,\ldots,c_k\rangle$, the numbers i, j, and k are the numbers of orbits of vertices, faces and Petrie-polygons in each particular orbit. We further note that the edge-multiplicity of all the maps in the table is 1 and all the maps are non-degenerate (i.e. all parameters in map symbol are greater or equal to 3). Column **MType** denotes the type of Me($\mathcal{M}$), while the column **Type** denotes the type of $\mathcal{M}$. In **Genus** column we use special notation, namely non-negative numbers denote orientable genus while negative numbers denote non-orientable genus of both maps.

5.2 $\mathrm{Me}(\mathrm{Me}(\mathcal{M}))$, maps of type $\{4,4\}$

Note that if the map $\mathcal{M}$ is equivelar of Schläfli type $\{p,q\}$, the faces of $\mathrm{Me}(\mathcal{M})$ are p-gons and q-gons. Therefore, $\mathrm{Me}(\mathcal{M})$ is equivelar if and only if $p = q$; in such case $\mathrm{Me}(\mathcal{M})$ has Schläfli type $\{p,4\}$.

Proposition 5.2. *Let $\mathcal{M}$ be a k-orbit map. If $\mathrm{Me}(\mathrm{Me}(\mathcal{M}))$ is also a k-orbit map, then $\mathcal{M}$ has Schläfli type $\{4,4\}$.*

Proof. $\mathrm{Me}(\mathrm{Me}(\mathcal{M}))$ is a k-orbit map if and only if both $\mathrm{Me}(\mathcal{M})$ and $\mathcal{M}$ are self-dual maps. Since $\mathrm{Me}(\mathcal{M})$ is a medial map, then each of its vertices has valency 4; the fact that is self-dual implies that $\mathrm{Me}(\mathcal{M})$ has Schläfly type $\{4,4\}$. On the other hand the faces of $\mathrm{Me}(\mathcal{M})$ correspond to the vertices and faces of $\mathcal{M}$. Because each face of $\mathrm{Me}(\mathcal{M})$ is a 4-gon, each face of $\mathcal{M}$ is also a 4-gon and each vertex of $\mathcal{M}$ has valency 4, implying the proposition.   ∎

The maps of type $\{4,4\}$ are maps on the torus or on the Klein Bottle. In [31], Hubard, Orbanić, Pellicer and Weiss study the symmetry types of equivelar maps on the torus. The maps of type $\{4,4\}$ on the torus have symmetry type 1, 2, 2_1, 2_{02} or 4_{C_p} and are all self-dual. The medial of a map $\{4,4\}$ on the torus of type 1, 2 or 4_{C_p} is of the same type as the original, while for types 2_1 and 2_{02} the medial is precisely of the other type. Therefore $\mathrm{Me}(\mathrm{Me}(\mathcal{M}))$ has the same symmetry type graph, whenever $\mathcal{M}$ is a map on the torus of Schläfli type $\{4,4\}$. In Figures 5.6–5.9 examples of equivelar toroids of type $\{4,4\}$ and their corresponding medial maps are depicted.
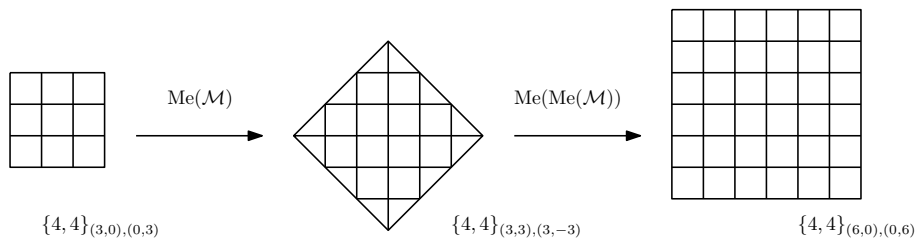

$$\{4,4\}_{(3,0),(0,3)} \qquad \{4,4\}_{(3,3),(3,-3)} \qquad \{4,4\}_{(6,0),(0,6)}$$

Figure 5.6: Medial of regular toroids of type $\{4,4\}$.

In [58] Wilson shows that there are two kinds of map of type $\{4,4\}$ in the Klein bottle, and denotes them by $\{4,4\}_{\setminus m,n \setminus}$ and $\{4,4\}_{|m,n|}$, respectively. The map in the Klein bottle, described as $\{4,4\}_{|m,n|}$, results by using two glide reflections of length m on parallel axes to the lines of the square grid $\{4,4\}$, that are $\frac{n}{2}$ apart, lying along a line or midway between two lines. And, the map in the Klein bottle, described as $\{4,4\}_{\setminus m,n \setminus}$, results by using two glide reflections of length $n\frac{\sqrt{2}}{2}$ on axes at 45° angle to the lines of the square grid $\{4,4\}$ that are $m\frac{\sqrt{2}}{2}$ apart, passing through vertices and face-centres or through midpoints
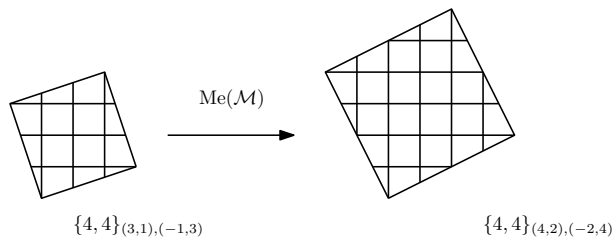
Figure 5.7: Medial of chiral toroids of type {4, 4}.
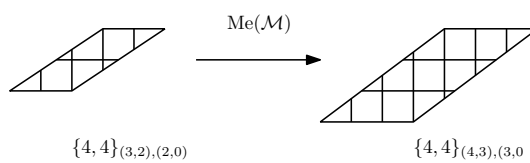
Figure 5.8: Medial of 4-orbit toroids of type {4, 4}, with symmetry type 4_{C_p}.
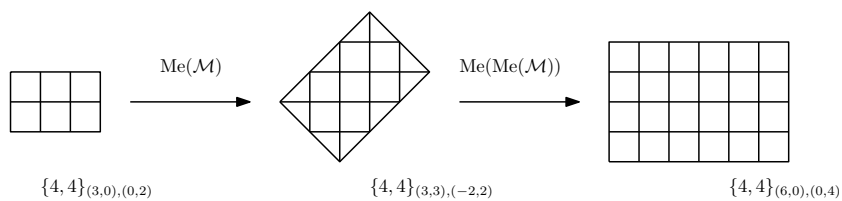
Figure 5.9: Medial of 2-orbit toroids of type {4, 4}, with symmetry types 2_{02} and 2_1.

of edges. In both cases, the generating glide reflections preserve the square grid $\{4,4\}$. From [58] we can see that these maps have $2mn$ edges, and thereby $8mn$ flags. Moreover, the automorphism group of $\{4,4\}_{\backslash m,n \backslash}$ it has $4m$ elements, while for $\{4,4\}_{|m,n|}$ has $8m$ elements if n is even and $4m$ otherwise. Thus, $\{4,4\}_{\backslash m,n \backslash}$ is a $2n$-orbit map and $\{4,4\}_{|m,n|}$ has n flag orbits if n is even and $2n$ otherwise. In Figure 5.10 examples of equivelar maps of type $\{4,4\}$ in the Klein bottle are depicted.
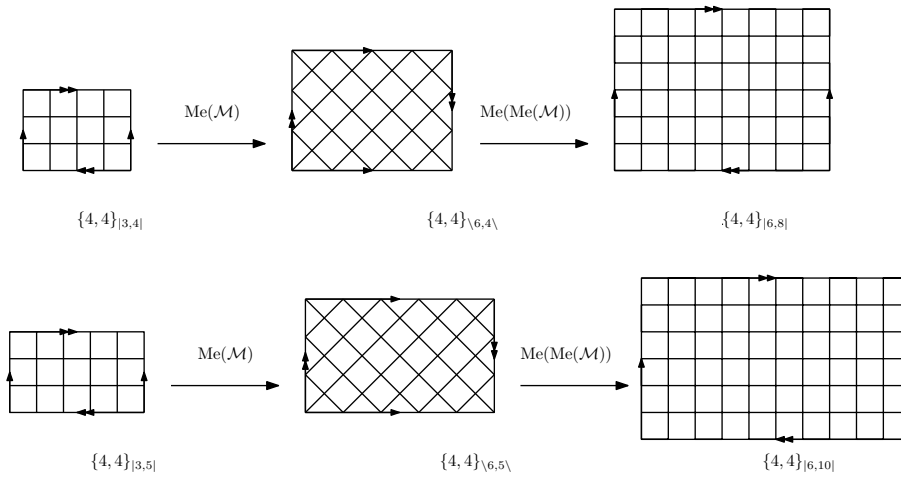

$$\{4,4\}_{|3,4|} \qquad \{4,4\}_{\backslash 6,4 \backslash} \qquad \{4,4\}_{|6,8|}$$

$$\{4,4\}_{|3,5|} \qquad \{4,4\}_{\backslash 6,5 \backslash} \qquad \{4,4\}_{|6,10|}$$

Figure 5.10: Medial of maps of type $\{4,4\}_{|m,n|}$ in the Klein bottle.

Based on [58, Table I], we have that for a map of type $\{4,4\}_{\backslash m,n \backslash}$, it can be seen that $\mathrm{Me}(\mathrm{Me}(\{4,4\}_{\backslash m,n \backslash})) = \{4,4\}_{\backslash 2m,2n \backslash}$; which has $32mn$ flags and its automorphism group has $8m$ elements. Hence, the map $\mathrm{Me}(\mathrm{Me}(\{4,4\}_{\backslash m,n \backslash}))$ is a $4n$-orbit map (i.e. has two times the number of orbits than the map $\{4,4\}_{\backslash m,n \backslash}$). On the other hand, if the map $\mathcal{M}$ is of type $\{4,4\}_{|m,n|}$, the map $\mathrm{Me}(\mathrm{Me}(\mathcal{M}))$ is the dual map of $\{4,4\}_{|2m,2n|}$. Since for any map and its dual have the same number of flag orbits, and the edges on both maps are in one-to-one correspondence, we can compute that $\mathrm{Me}(\mathrm{Me}(\mathcal{M}))$ has $32mn$ flags and its automorphism group has $16m$ elements. Hence the map $\mathrm{Me}(\mathrm{Me}(\{4,4\}_{|m,n|}))$ is a $2n$-orbit map. We therefore have the following proposition.

Proposition 5.3. *Let $\mathcal{M}$ be a k-orbit map. Then $\mathrm{Me}(\mathrm{Me}(\mathcal{M}))$ is a k-orbit map if $\mathcal{M}$ is a map on the torus of type $\{4,4\}$, or is a map on the Klein Bottle of type $\{4,4\}_{|m,n|}$, where n is odd.*

In Table 5.5 are enumerated all symmetry types of self-dual and medial types of k-orbit maps, with $1 \leq k \leq 10$.

We shall note that for $k = 8$ there is a self-dual symmetry type with no polarities, its symmetry type graph is depicted in Figure 5.11.

k	1	2	3	4	5	6	7	8	9	10	
No. of types	1	7	3	22	13	70	67	315	393	1577	(a)
No. of self dual types	1	3	1	8	3	12	7	45	25	91	(b)
No. of self polar types	1	3	1	8	3	12	7	44	25	91	(c)
No. of self dualities	1	6	1	21	3	23	7	101	25	128	(d)
No. of self polarities	1	6	1	17	3	21	7	83	25	124	(e)
No. of medial types from k-orb maps	1	6	1	15	3	19	7	73	25	120	(f)
No. of total medial types	1	7	1	20	3	21	7	88	25	128	(g)

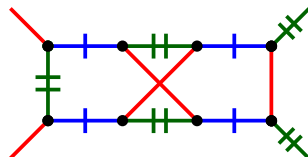Table 5.5: Number of symmetry type graphs, self-dual types and medials types

Figure 5.11: A self-dual symmetry type graph with 8 vertices and no polarities

5.3   Dual of medial map

To conclude with this chapter, we describe the dual map of $\mathrm{Me}(\mathcal{M})$. It is straightforward to see that the faces of the map $(\mathrm{Me}(\mathcal{M}))^*$ are 4-gons (squares). Moreover, the valency of the vertices of the map $(\mathrm{Me}(\mathcal{M}))^*$ correspond to the length of the faces and the valency of the vertices of $\mathcal{M}$. In Figure 5.12 is depicted the dual of the cuboctahedron (dual of the medial of the octahedron).
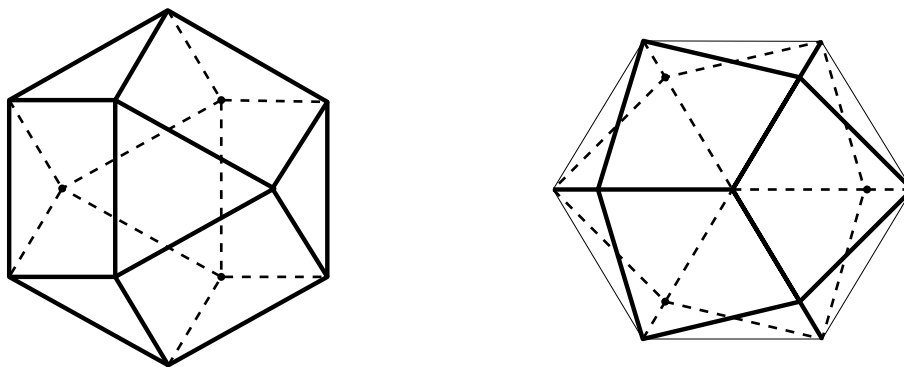

Figure 5.12: Cuboctahedron (left) and its dual (right).

Recall that the bijection $\delta : \mathrm{Mon}(\mathcal{M}) \to \mathrm{Mon}(\mathcal{M}^*)$ induces a permutation on the edges of $\mathcal{G}_\mathcal{M}$ sending edges of colour $i = 0, 1, 2$ to edges of colour $2 - i$. Then, the following proposition is a consequence from Proposition 5.1.

Proposition 5.4. *The flag graph $\mathcal{G}_{(\mathrm{Me}(\mathcal{M}))^*}$, of the dual of the medial map $(\mathrm{Me}(\mathcal{M}))^*$ of a map $\mathcal{M}$, can be quotient into a graph isoorphic to the symmetry type graph 2_{12}.*

Chapter 6

Chamfering operation on maps

The chamfering map $\mathrm{Cham}(\mathcal{M})$ of any map $\mathcal{M}$ is produced, as its name says: by chamfer the edges in $\mathcal{M}$. More precisely, the edges of a map $\mathcal{M}$ are replaced by hexagonal faces, surrounding the faces of $\mathcal{M}$, in $\mathrm{Cham}(\mathcal{M})$ (see Figure 6.1). Hence, the set of faces
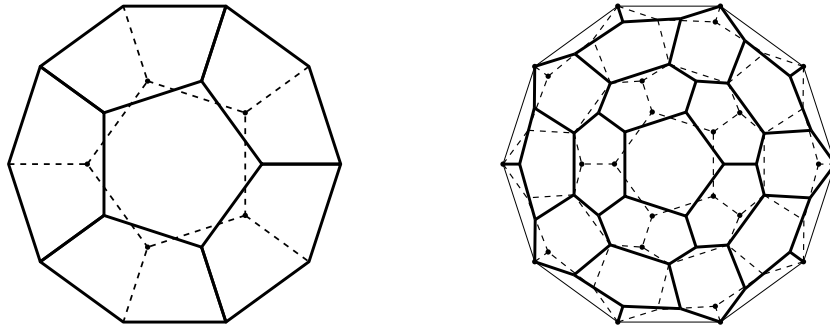

Figure 6.1: Dodecahedron (left) and the chamfering of the dodecahedron (right).

of $\mathrm{Cham}(\mathcal{M})$ is in correspondence with the set of faces $F(\mathcal{M})$ and the set of edges $E(\mathcal{M})$ of $\mathcal{M}$. That is, the set of faces of $\mathrm{Cham}(\mathcal{M})$ is

$$F(\mathrm{Cham}(\mathcal{M})) = F(\mathcal{M}) \cup E(\mathcal{M}).$$

The map $\mathrm{Cham}(\mathcal{M})$ has two types of edges: those between hexagonal faces and those between a face Φ_2 in $F(\mathcal{M})$ and its adjacent hexagonal faces (corresponding to the incident edges on the face Φ_2 in $\mathcal{M}$). This is, the set of edges of $\mathrm{Cham}(\mathcal{M})$ is

$$E(\mathrm{Cham}(\mathcal{M})) = \{\{\Phi_0, \{\Phi_0, \Phi_2\}\}|\Phi \in \mathcal{F}(\mathcal{M})\} \cup \{\{\Phi_1, \Phi_2\}|\Phi \in \mathcal{F}(\mathcal{M})\}.$$

In fact, $\mathrm{Cham}(\mathcal{M})$ has exactly $4|E(\mathcal{M})|$ edges. Finally, the set of vertices of $\mathcal{M}$ is a proper subset of the vertices of $\mathrm{Cham}(\mathcal{M})$, and the remaining $2|E(\mathcal{M})|$ vertices in $V(\mathrm{Cham}(\mathcal{M}))\backslash$

$V(\mathcal{M})$ (each of these vertices are adjacent to exactly one vertex in $V(\mathcal{M})$), all have degree 3. Thus, the set of vertices of $\mathrm{Cham}(\mathcal{M})$ is

$$V(\mathrm{Cham}(\mathcal{M})) = V(\mathcal{M}) \cup \{\{\Phi_0, \Phi_2\} | \Phi \in \mathcal{F}(\mathcal{M})\}.$$

For an alternative definition of chamfering we refer the reader to [15].

Observe that the map on the left (dodecahedron) in Figure 6.1 is regular, while the map on the right is a 4-orbit map with symmetry type 4_{D_p} (Figure 6.2). There is a single
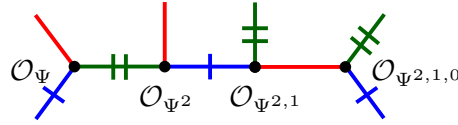

Figure 6.2: Symmetry type graph 4_{D_p}.

orbit of flags, $\mathcal{O}_\Psi$, on a pentagon and three different flags on a hexagon. Note that by chamfering a non-degenerated map $\mathcal{M}$, every flag $\Phi := (\Phi_0, \Phi_1, \Phi_2)$ in $\mathcal{F}(\mathcal{M})$ is divided into four flags of $\mathrm{Cham}(\mathcal{M})$, as is depicted in Figure 6.3, and the corresponding four flags
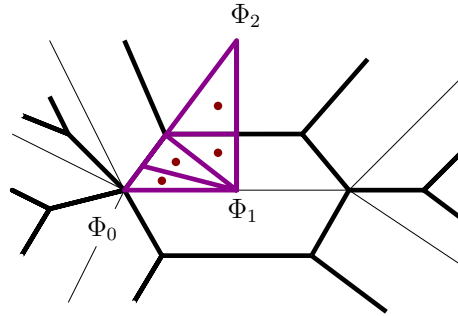

Figure 6.3: The four respective flags of $\mathcal{F}(Cham(\mathcal{M}))$ to the flag $\Phi = \{\Phi_0, \Phi_1, \Phi_2\} \in \mathcal{F}(\mathcal{M})$.

to $\Phi \in \mathcal{F}(\mathcal{M})$ in $\mathrm{Cham}(\mathcal{M})$ can be written as

$$(\Phi, 0) := (\Phi_0, \{\Phi_0, \{\Phi_0, \Phi_2\}\}, \Phi_1), \qquad (\Phi, 1) := (\{\Phi_0, \Phi_2\}, \{\Phi_0, \{\Phi_0, \Phi_2\}\}, \Phi_1),$$
$$(\Phi, 2) := (\{\Phi_0, \Phi_2\}, \{\Phi_1, \Phi_2\}, \Phi_1), \qquad (\Phi, 3) := (\{\Phi_0, \Phi_2\}, \{\Phi_1, \Phi_2\}, \Phi_2).$$

It is then straightforward to see that the adjacencies of the flags of $\mathrm{Cham}(\mathcal{M})$ are closely related to those of the flags of $\mathcal{M}$. In fact, we have that,

$$
\begin{array}{lll}
(\Phi, 0)^0 = (\Phi, 1), & (\Phi, 0)^1 = (\Phi^{s_2}, 0), & (\Phi, 0)^2 = (\Phi^{s_1}, 0), \\
(\Phi, 1)^0 = (\Phi, 0), & (\Phi, 1)^1 = (\Phi, 2), & (\Phi, 1)^2 = (\Phi^{s_1}, 1), \\
(\Phi, 2)^0 = (\Phi^{s_0}, 2), & (\Phi, 2)^1 = (\Phi, 1), & (\Phi, 2)^2 = (\Phi, 3), \\
(\Phi, 3)^0 = (\Phi^{s_0}, 3), & (\Phi, 3)^1 = (\Phi^{s_1}, 3), & (\Phi, 3)^2 = (\Phi, 2).
\end{array}
$$

Thus, we define the algorithm in Figure 6.4 to construct the flag graph of $\mathrm{Cham}(\mathcal{M})$ out of $\mathcal{G}_{\mathcal{M}}$, and consequently the following proposition.
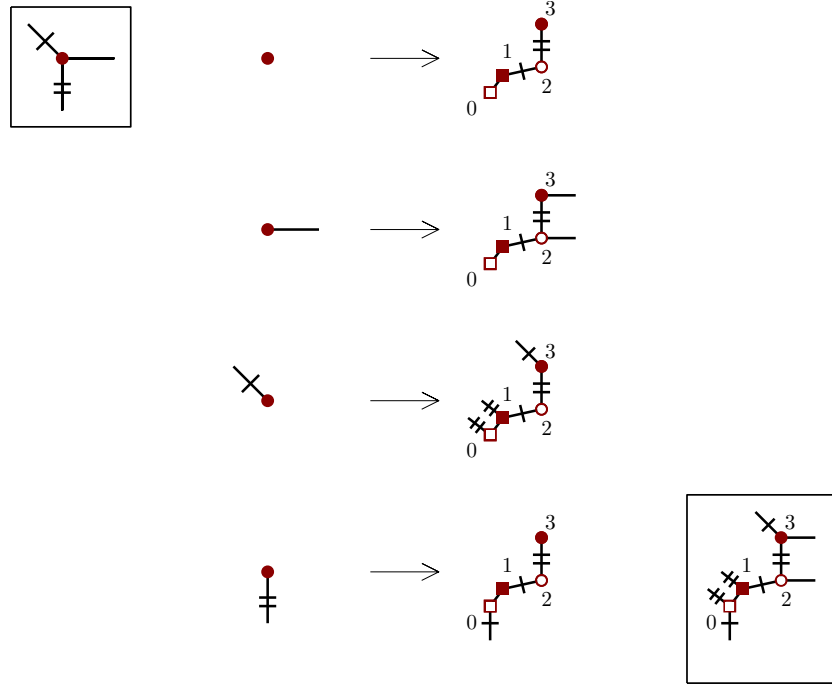

Figure 6.4: Local representation of a flag in $\mathcal{G}_{\mathcal{M}}$, in the left. The image under the chamfering operation, locally obtained, in the right.

Proposition 6.1. *The flag graph* $\mathcal{G}_{\mathrm{Cham}(\mathcal{M})}$, *of the chamfering map* $\mathrm{Cham}(\mathcal{M})$ *of a map* $\mathcal{M}$, *can be quotient into a graph isomorphic to the symmetry type graph* 4_{D_p}.

Proof. Let $\mathcal{A}_i = \{(\Phi, i) | \Phi \in \mathcal{F}(\mathcal{M})\}$ Then, $\mathcal{F}(\mathrm{Cham}(\mathcal{M})) = \mathcal{A}_0 \cup \mathcal{A}_1 \cup \mathcal{A}_2 \cup \mathcal{A}_3$ and $\mathcal{A}_i \cap \mathcal{A}_j = \emptyset$ whenever $i \neq j$. Hence, $(\mathcal{A}_0, \mathcal{A}_1, \mathcal{A}_2, \mathcal{A}_3)$ is a partition of the set of flags $\mathcal{F}(\mathrm{Cham}(\mathcal{M}))$. Based on Figure 6.4, it is straightforward to see that the quotient of $\mathcal{G}_{\mathrm{Cham}(\mathcal{M})}$ over such partition, is isomorphic to the symmetry type graph of a map with symmetry type 4_{D_p} (see Figure 6.2).   ∎

Note that for any flags $\Upsilon \in \mathcal{A}_3$, $\Upsilon^2 \in \mathcal{A}_2$, $\Upsilon^{2,1} \in \mathcal{A}_1$ and $\Upsilon^{2,1,0} \in \mathcal{A}_0$, we can define a flag $\Phi_\Upsilon \in \mathcal{F}(\mathcal{M})$, by assembling these four flags in $\mathrm{Cham}(\mathcal{M})$. Observe that an automorphism $\bar{\alpha} \in \mathrm{Aut}(\mathrm{Cham}(\mathcal{M}))$ that sends a flag $\Upsilon' \in \mathcal{A}_i$ to another flag also contained in $\mathcal{A}_i$, with $i = 0, 1, 2, 3$, is induced by an automorphism $\alpha \in \mathrm{Aut}(\mathcal{M})$ that sends $\Phi_{\Upsilon'}$ to the assembled flag $\Phi_{\Upsilon'\bar{\alpha}}$ in $\mathcal{M}$. Say this in other way, for each automorphism $\alpha \in \mathrm{Aut}(\mathcal{M})$, there is an automorphism $\bar{\alpha} \in \mathrm{Aut}(\mathrm{Cham}(\mathcal{M}))$ such that $(\Phi, i)\bar{\alpha} = (\Phi\alpha, i)$, with $\Phi \in \mathcal{F}(\mathcal{M})$ and $i = 0, 1, 2, 3$. Then, it follows that

$$|\mathrm{Orb}(\mathrm{Cham}(\mathcal{M}))| \leq 4|\mathrm{Orb}(\mathcal{M})|.$$

Motivated by [45], we are interested on study the number of possible flag-orbits that the chamfering map $\mathrm{Cham}(\mathcal{M})$ of a k-orbit map $\mathcal{M}$ might have.

Certainly, the chamfering map $\mathrm{Cham}(\mathcal{M})$, of a k-orbit map $\mathcal{M}$, has $4k$ orbits on the set of flags $\mathcal{F}(\mathrm{Cham}(\mathcal{M}))$, if for any $\Phi, \Psi \in \mathcal{F}(\mathcal{M})$ there is no flag of the form (Φ, i) in the same orbit as a flag of the form (Ψ, j), with $i, j \in \{0, 1, 2, 3\}$ and $i \neq j$. In fact, if the chamfering map $\mathrm{Cham}(\mathcal{M})$ of a k-orbit map $\mathcal{M}$ is a $4k$-orbit map then, the algorithm presented in Figure 6.4 works as an algorithm on the vertices of $T(\mathcal{M})$ to obtain the symmetry type graph $T(\mathrm{Cham}(\mathcal{M}))$ with $4k$ vertices, of the chamfering map of $\mathcal{M}$, we shall call such graph as the *chamfering symmetry type graph* of $T(\mathcal{M})$.

We denote by r_0, r_1 and r_2 the distinguished generators of $\mathrm{Mon}(\mathrm{Cham}(\mathcal{M}))$. Observe that, in particular, $(\Phi^{s_0}, 3) = (\Phi, 3)^{r_0}$, $(\Phi^{s_1}, 3) = (\Phi, 3)^{r_1}$, and $(\Phi^{s_2}, 3) = (\Phi, 3)^{r_2 r_1 r_0 r_1 r_0 r_1 r_2}$, for any $\Phi \in \mathcal{F}(\mathcal{M})$. This is, the action of the subgroup

$$M = \langle r_0, r_1, r_2 r_1 r_0 r_1 r_0 r_1 r_2 \rangle \leq \mathrm{Mon}(\mathrm{Cham}(\mathcal{M}))$$

over the subset of flags $\mathcal{A}_3 = \{(\Phi, 3) | \Phi \in \mathcal{F}(\mathcal{M})\}$ in $\mathrm{Cham}(\mathcal{M})$ is isomorphic to the action of the monodromy group $\mathrm{Mon}(\mathcal{M})$ over the set $\mathcal{F}(\mathcal{M})$, inducing the following action isomorphism.

$$(f, g) : (\mathcal{F}(\mathcal{M}), \langle s_0, s_1, s_2 \rangle) \to (\mathcal{A}_3, \langle r_0, r_1, r_2 r_1 r_0 r_1 r_0 r_1 r_2 \rangle),$$

where $f : \Phi \mapsto (\Phi, 3)$ is a bijective function, and $g : (s_0, s_1, s_2) \mapsto (r_0, r_1, r_2 r_1 r_0 r_1 r_0 r_1 r_2)$ is a group isomorphism, [32]. Then, the action of M is transitive on the set of flags $\mathcal{A}_3$. In fact the action of M on $\mathcal{F}(\mathrm{Cham}(\mathcal{M}))$ fixes the set $\mathcal{A}_3$ and permutes the sets $\mathcal{A}_0$, $\mathcal{A}_1$ and $\mathcal{A}_2$. Furthermore, because

$$(\Phi, 3)^{r_2} = (\Phi, 2), \ (\Phi, 3)^{r_2 r_1} = (\Phi, 1) \ \text{ and } \ (\Phi, 3)^{r_2 r_1 r_0} = (\Phi, 0),$$

conjugating M by the elements r_2, $r_2 r_1$ and $r_2 r_1 r_0$ in $\mathrm{Mon}(\mathrm{Cham}(\mathcal{M}))$, we obtain three different subgroups of $\mathrm{Mon}(\mathrm{Cham}(\mathcal{M}))$, that act transitively on the set of flags $\mathcal{A}_2$, $\mathcal{A}_1$ and $\mathcal{A}_0$, respectively. Therefore, by letting $a_0 = r_2 r_1 r_0$, $a_1 = r_2 r_1$, $a_2 = r_2$, and $a_3 = id$, the conjugate subgroup $a_i^{-1} M a_i \leq \mathrm{Mon}(\mathrm{Cham}(\mathcal{M}))$ fixes the set $\mathcal{A}_i$, for each $i = 0, 1, 2, 3$, and permutes the sets $\mathcal{A}_{j_1}$, $\mathcal{A}_{j_2}$ and $\mathcal{A}_{j_3}$, with $j_1, j_2, j_3 \in \{0, 1, 2, 3\} \setminus \{i\}$.

With the following lemma we see that the chamfering map of a k-orbit map $\mathcal{M}$, not necessarily has $4k$ flag-orbits. Recall that an *equivelar* map with Schläfli type $\{6, 3\}$ is a map that all its faces are 6-gons, and all its vertices have degree 3.

Lemma 6.1. *Let* $\mathrm{Cham}(\mathcal{M})$ *be the chamfering map of a map* $\mathcal{M}$. *If there is an automorphism* $\alpha \in \mathrm{Aut}(\mathrm{Cham}(\mathcal{M}))$ *such that* $(\Phi, i)\alpha = (\Psi, j)$ *for some* $\Phi, \Psi \in \mathcal{F}(\mathcal{M})$ *and* $i \neq j$, *with* $i, j \in \{0, 1, 2, 3\}$. *Then,* $\mathcal{M}$ *is an equivelar map with Schläfli type* $\{6, 3\}$.

Proof. Consider the partition $(\mathcal{A}_0, \mathcal{A}_1, \mathcal{A}_2, \mathcal{A}_3)$ of the set $\mathcal{F}(\mathrm{Cham}(\mathcal{M}))$, where $\mathcal{A}_i = \{(\Phi, i)|\Phi \in \mathcal{F}(\mathcal{M})\}$, $i = 0, 1, 2, 3$, and recall that if we assemble the flags $\Upsilon \in \mathcal{A}_3$, $\Upsilon^2 \in \mathcal{A}_2$, $\Upsilon^{2,1} \in \mathcal{A}_1$ and $\Upsilon^{2,1,0} \in \mathcal{A}_0$, we can define a flag $\Phi_\Upsilon \in \mathcal{F}(\mathcal{M})$.

Suppose that there is an automorphism $\alpha \in \mathrm{Aut}(\mathrm{Cham}(\mathcal{M}))$ such that $(\Phi, i)\alpha = (\Psi, j)$ for some $\Phi, \Psi \in \mathcal{F}(\mathcal{M})$ and $i \neq j$, with $i, j \in \{0, 1, 2, 3\}$. We shall verify the image, under α, of the assembled flags $(\Phi, 0), (\Phi, 1), (\Phi, 2), (\Phi, 3)$, corresponding to $\Phi \in \mathcal{F}(\mathcal{M})$, in terms of the adjacent flags of (Ψ, j). Note that $\Phi_0 \in (\Phi, 0)$ and $\Phi_2 \in (\Phi, 3)$, but they are neither in $(\Phi, 1)$ nor in $(\Phi, 2)$. Then, we have the following cases.

0) For $i = 0$.

   - If $(\Phi, 0)\alpha = (\Psi, 1)$, then $\Phi_0\alpha = \{\Psi_0, \Psi_2\}$ and $\Phi_2\alpha = (\Psi^{2,1})_1$, since $(\Phi, 0)\alpha = (\Psi, 1) := (\{\Psi_0, \Psi_2\}, \{\Psi_0\{\Psi_0, \Psi_2\}\}, \Psi_1)$ and
     $(\Phi, 3)\alpha = (\Phi, 0)^{0,1,2}\alpha = ((\Phi, 0)\alpha)^{0,1,2} = (\Psi, 1)^{0,1,2} = (\Psi^{2,1}, 0) := (\Psi_0, \{\Psi_0, \{\Psi_0, (\Psi^2)_2\}\}, (\Psi^{2,1})$

   - If $(\Phi, 0)\alpha = (\Psi, 2)$, then $\Phi_0\alpha = \{\Psi_0, \Psi_2\}$ and $\Phi_2\alpha = (\Psi^{0,1})_1$, since $(\Phi, 0)\alpha = (\Psi, 2) := (\{\Psi_0, \Psi_2\}, \{\Psi_1, \Psi_2\}, \Psi_1)$ and
     $(\Phi, 3)\alpha = (\Phi, 0)^{0,1,2}\alpha = ((\Phi, 0)\alpha)^{0,1,2} = (\Psi, 2)^{0,1,2} = (\Psi^{0,1}, 1) := (\{(\Psi^0)_0, \Psi_2\}, \{(\Psi^0)_0, \{(\Psi^0)_0,$

   - If $(\Phi, 0)\alpha = (\Psi, 3)$, then $\Phi_0\alpha = \{\Psi_0, \Psi_2\}$ and $\Phi_2\alpha = (\Psi^{0,1})_1$, since $(\Phi, 0)\alpha = (\Psi, 3) := (\{\Psi_0, \Psi_2\}, \{\Psi_1, \Psi_2\}, \Psi_2)$ and
     $(\Phi, 3)\alpha = (\Phi, 0)^{0,1,2}\alpha = ((\Phi, 0)\alpha)^{0,1,2} = (\Psi, 3)^{0,1,2} = (\Psi^{0,1}, 2) := (\{(\Psi^0)_0, \Psi_2\}, \{(\Psi^{0,1})_1, \Psi_2\}, (\Psi$

Similarly, we follow the same analysis in the next cases.

1) For $i = 1$.

   - If $(\Phi, 1)\alpha = (\Psi, 0)$, then $\Phi_0\alpha = \{\Psi_0, \Psi_2\}$ and $\Phi_2\alpha = (\Psi^{2,1})_1$.
   - If $(\Phi, 1)\alpha = (\Psi, 2)$, then $\Phi_0\alpha = \{(\Psi^0)_0, \Psi_2\}$ and $\Phi_2\alpha = (\Psi^1)_1$.
   - If $(\Phi, 1)\alpha = (\Psi, 3)$, then $\Phi_0\alpha = \{(\Psi^0)_0, \Psi_2\}$ and $\Phi_2\alpha = (\Psi^1)_1$.

2) For $i = 2$.

   - If $(\Phi, 2)\alpha = (\Psi, 0)$, then $\Phi_0\alpha = \{\Psi_0, (\Psi^2)_2\}$ and $\Phi_2\alpha = (\Psi^1)_1$.
   - If $(\Phi, 2)\alpha = (\Psi, 1)$, then $\Phi_0\alpha = \{(\Psi^0)_0, \Psi_2\}$ and $\Phi_2\alpha = (\Psi^1)_1$.
   - If $(\Phi, 2)\alpha = (\Psi, 3)$, then $\Phi_0\alpha = \{(\Psi^{1,0})_0, \Psi_2\}$ and $\Phi_2\alpha = \Psi_1$.

3) For $i = 3$.

   - If $(\Phi, 3)\alpha = (\Psi, 0)$, then $\Phi_0\alpha = \{\Psi_0, (\Psi^{1,2})_2\}$ and $\Phi_2\alpha = \Psi_1$.
   - If $(\Phi, 3)\alpha = (\Psi, 1)$, then $\Phi_0\alpha = \{(\Psi^{1,2})_0, (\Psi^{1,2})_2\}$ and $\Phi_2\alpha = \Psi_1$.
   - If $(\Phi, 3)\alpha = (\Psi, 2)$, then $\Phi_0\alpha = \{(\Psi^{1,2})_0, \Psi_2\}$ and $\Phi_2\alpha = (\Psi^{0,1})_1$.

Observe from the cases above, that all the vertices $\{\Psi_0, \Psi_2\}$, $\{(\Psi^0)_0, \Psi_2\}$, $\{\Psi_0, (\Psi^2)_2\}$, $\{(\Psi^{1,0})_0, \Psi_2\}$, $\{\Psi_0, (\Psi^{1,2})_2\}$, $\{(\Psi^{1,2})_0, (\Psi^{1,2})_2\}$ and $\{(\Psi^{1,2})_0, \Psi_2\}$ are vertices with degree 3 in $\mathrm{Cham}(\mathcal{M})$. So as all the faces $(\Psi^{2,1})_1$, $(\Psi^{0,1})_1$, $(\Psi^1)_1$ and Ψ_1, correspond to 6-gons in $\mathrm{Cham}(\mathcal{M})$. Thus, the vertex Φ_0 has degree 3 and the face Φ_2 is a 6-gon in $\mathcal{M}$, with $\Phi \in \mathcal{F}(\mathcal{M})$. Furthermore, let $\Phi^w = \Delta \in \mathcal{F}(\mathcal{M})$, with $w \in \mathrm{Mon}(\mathcal{M})$. Then we have that

$$(\Delta, i)\alpha = (\Phi^w, i)\alpha = (\Phi, i)^{\bar{w}}\alpha = ((\Phi, i)\alpha)^{\bar{w}} = (\Psi, j)^{\bar{w}},$$

with $\bar{w} \in \mathrm{Mon}(\mathrm{Cham}(\mathcal{M}))$. Recall that the conjugated subgroup M^{a_i} of $\mathrm{Mon}(\mathrm{Cham}(\mathcal{M}))$ fixes the set $\mathcal{A}_i$ and permutes the sets $\mathcal{A}_{j_1}$, $\mathcal{A}_{j_2}$ and $\mathcal{A}_{j_3}$, with $j_1, j_2, j_3 \in \{0, 1, 2, 3\} \setminus \{i\}$, where $a_0 = r_2 r_1 r_0$, $a_1 = r_2 r_1$, $a_2 = r_2$, and $a_3 = id$. Since $(\Delta, i) = (\Phi, i)^{\bar{w}}$, it follows that $\bar{w} \in M^{a_i}$, and henceforth $(\Delta, i)\alpha = (\Psi, j)^{\bar{w}} \in \mathcal{A}_{j_k}$, with $j, j_k \in \{0, 1, 2, 3\} \setminus \{i\}$.

Thus, we follow with a similar analysis as the previous one for $(\Delta, i)\alpha = (\Psi, j)^{\bar{w}}$, and we conclude that the vertex Δ_0 has degree 3 and the face Δ_2 is a 6-gon in $\mathcal{M}$. This latter was for arbitrary $\Delta \in \mathcal{F}(\mathcal{M})$ and $w \in \mathrm{Mon}(\mathcal{M})$. Therefore, we have that each vertex in $V(\mathcal{M})$ has degree 3 and every face $F(\mathcal{M})$ is a 6-gon. Consequently, the map $\mathcal{M}$ is an equivelar map with Schäfli type $\{6, 3\}$. ■

By the Euler characteristic of a map, the surface of an equivelar map with Schläfli type $\{6, 3\}$ is either the torus or Klein bottle. In the following subsection we find the number of flag-orbits of the chamfering of an equivelar map of type $\{6, 3\}$.

6.1   Chamfering of equivelar maps of type $\{6,3\}$.

The maps of type $\{6, 3\}$ are maps on the torus or on the Klein bottle. In [31] Hubard, Orbanić, Pellicer and Weiss studied the symmetry types of equivelar maps in the torus. In [58] Wilson shows that there are two kinds of maps of type $\{6, 3\}$ in the Klein bottle, and denotes them by $\{6, 3\}_{|m,n|}$ and $\{6, 3\}_{\backslash m,n \backslash}$ respectively, where the two glide reflections of these maps are on axes that are at distance a multiple of n and have length a multiple of m.

An equivelar toroidal map of type $\{6, 3\}$ is described as $\{6, 3\}_{v_1, v_2}$, where the linearly independent vectors v_1 and v_2 are a linear combination of the basis $\{\sqrt{3}e_1, \frac{\sqrt{3}}{2}e_1 + \frac{3}{2}e_2\}$, with the origin in the centre of an hexagon in the $\{6, 3\}$-tessellation of the plane. Equivelar toroids with Schläfli type $\{6, 3\}$ are either regular, chiral, or have symmetry type 3^{02} or 6_{H_p}. In Figures 6.5–6.8 examples of equivelar toroids and their corresponding chamfering maps are depicted.

Note that by chamfering a toroidal map $\mathcal{M} := \{6, 3\}_{v_1, v_2}$ we replace the edges of $\mathcal{M}$ by the corresponding hexagonal faces in $\mathrm{Cham}(\mathcal{M})$. Thus, the centres of adjacent faces of $\mathrm{Cham}(\mathcal{M})$ are at half distance than in the centres of adjacent hexagons of $\mathcal{M}$. This
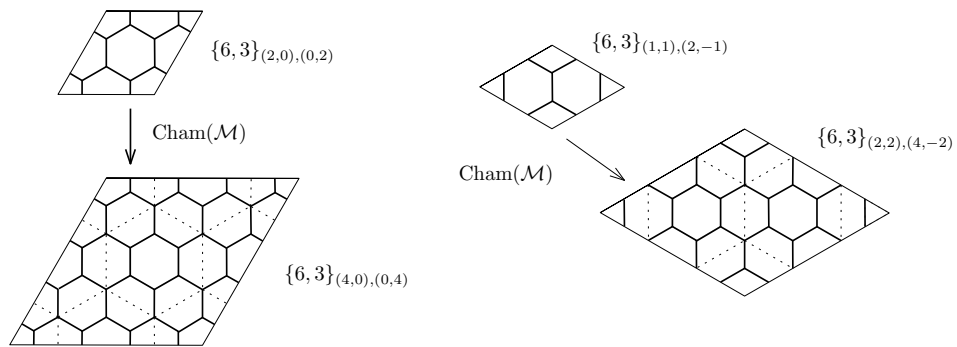
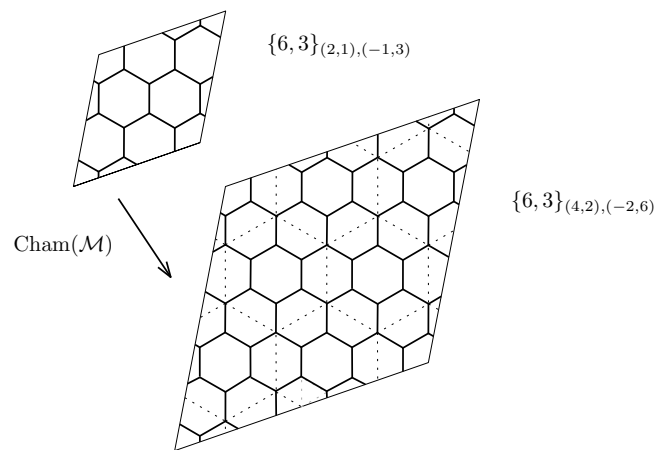Figure 6.5: Chamfering of regular toroids of type $\{6, 3\}$.

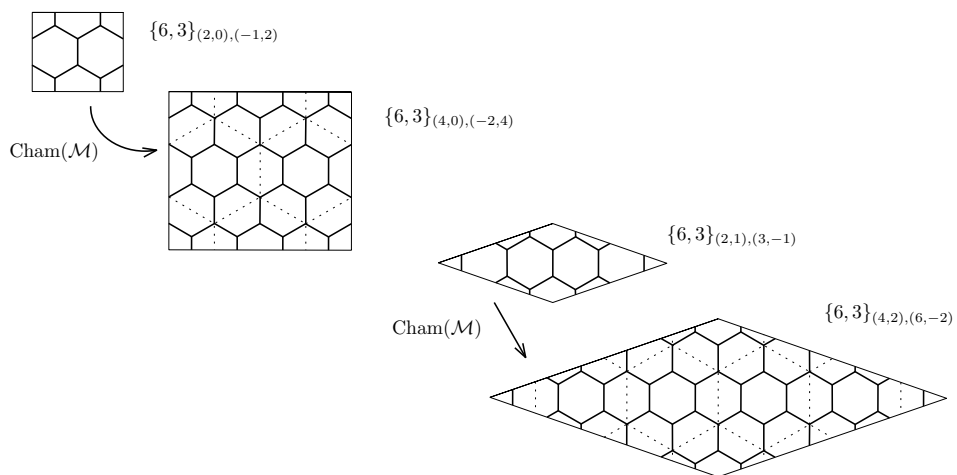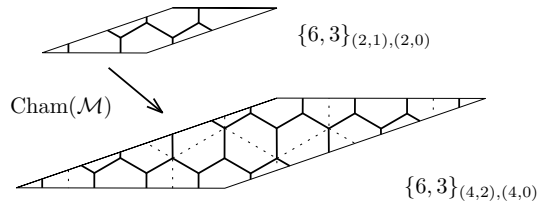Figure 6.6: Chamfering of chiral toroids of type $\{6, 3\}$.

Figure 6.7: Chamfering of 3-orbit toroids of type $\{6, 3\}$.

Figure 6.8: Chamfering of 3-orbit toroids of type $\{6,3\}$.

implies that the chamfering map $\mathrm{Cham}(\mathcal{M})$ is the equivelar toroidal map $\{6,3\}_{2v_1,2v_2}$. Thus, we have the following lemma.

Lemma 6.2. *Let $\mathcal{M}$ be an equivelar toroidal map of type $\{6,3\}$. Then the symmetry type graph $T(\mathrm{Cham}(\mathcal{M}))$ is isomorphic to $T(\mathcal{M})$.*

As what it concerns to equivelar maps of type $\{6,3\}$ in the Klein bottle. Following [58], the two kinds of maps of type $\{6,3\}$ in the Klein bottle are denoted by $\{6,3\}_{|m,n|}$ and $\{6,3\}_{\backslash m,n\backslash}$ respectively, where m and n are measured respect to the centres of the hexagons. The map in the Klein bottle, described as $\{6,3\}_{|m,n|}$, results by using two glide reflections of length $\frac{m}{2}$ on axes of type (a) or (b), as in Figure 6.9, that are $n\frac{\sqrt{3}}{2}$ apart. And, the map in the Klein bottle, described as $\{6,3\}_{\backslash m,n\backslash}$, results by using two glide reflections of length $m\frac{\sqrt{3}}{2}$ on axes of type (c) or (d) as in Figure 6.9, that are $\frac{n}{2}$ apart. In both cases, the generating glide reflections are symmetries of the regular hexagonal tessellation of the plane. Since the glide reflection axes (a), (b), (c) and (d) are either parallel to the
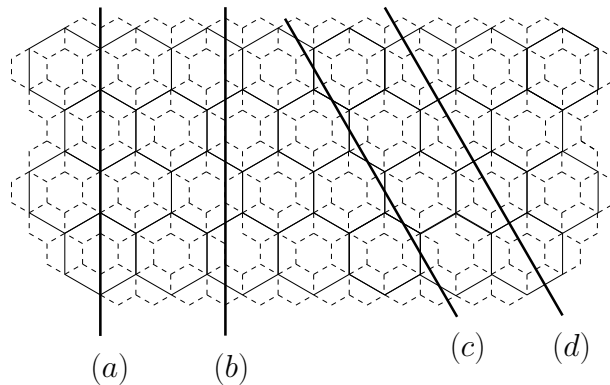
Figure 6.9: Possible glide reflection axes in $\{6,3\}$.

edges of the hexagons or cross the edges in their midpoint, by chamfering an equivelar map $\mathcal{M}$ in the Klein bottle, of type either $\{6,3\}_{|m,n|}$ or $\{6,3\}_{\backslash m,n\backslash}$, the distance between both glide reflection axes and their length are the half than for those in $\mathcal{M}$. This is, in $\mathrm{Cham}(\mathcal{M})$, the values of m and n are the half as those for $\mathcal{M}$. Therefore, the chamfering

map Cham($\mathcal{M}$) is an equivelar map in the Klein bottle described as $\{6,3\}_{|2m,2n|}$, or as $\{6,3\}_{\backslash 2m,2n\backslash}$, with glide reflection axes of type (a) or (d), respectively.

Hence, we obtain the following lemma.

Lemma 6.3. *If $\mathcal{M}$ is the toroidal map $\{6,3\}_{v_1,v_2}$ or a map in the Klein bottle of type either $\{6,3\}_{|m,n|}$, or $\{6,3\}_{\backslash m,n\backslash}$, then Cham($\mathcal{M}$) is a map on the same surface of type $\{6,3\}_{2v_1,2v_2}$, $\{6,3\}_{|2m,2n|}$, or $\{6,3\}_{\backslash 2m,2n\backslash}$, respectively.*

Following [58] we can see that maps $\{6,3\}_{|m,n|}$ and $\{6,3\}_{\backslash m,n\backslash}$ have $3mn$ edges and thereby $12mn$ flags. Moreover, the automorphism group of these maps have $4m$ elements. Thus, the maps $\{6,3\}_{|m,n|}$ and $\{6,3\}_{\backslash m,n\backslash}$ are $3n$-orbit maps. Hence, Cham($\{6,3\}_{|m,n|}$) = $\{6,3\}_{|2m,2n|}$ and Cham($\{6,3\}_{\backslash m,n\backslash}$) = $\{6,3\}_{\backslash 2m,2n\backslash}$ have $48mn$ flags and their respective automorphism group have $8m$ elements. Therefore, $\{6,3\}_{|2m,2n|}$ and $\{6,3\}_{\backslash 2m,2n\backslash}$ are $6n$-orbit maps. In Figures 6.10 and 6.11 are depicted examples of maps of type $\{6,3\}_{|m,1|}$ and $\{6,3\}_{\backslash m,1\backslash}$, with m even and odd, and its chamfering maps. Note that both maps of type $\{6,3\}_{|m,1|}$ and $\{6,3\}_{\backslash m,1\backslash}$ have symmetry type 3^{02}, while their chamfering maps $\{6,3\}_{|2m,2|}$ and $\{6,3\}_{\backslash 2m,2\backslash}$ have symmetry type 6_{H_p}.
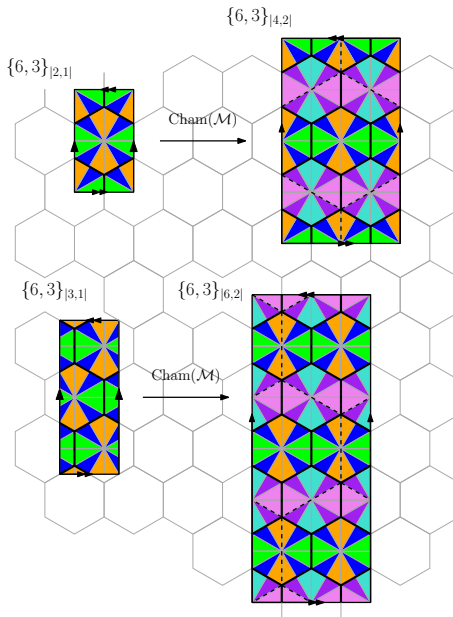

Figure 6.10: Chamfering of a 3-orbit map of type $\{6,3\}_{|m,1|}$ in the Klein bottle.

Corollary 6.1. *If $\mathcal{M}$ is a k-orbit equivelar toroidal map of type $\{6,3\}$, then Cham($\mathcal{M}$) is a k-orbit map, with $k = 1, 2, 3, 6$. If $\mathcal{M}$ is a k-orbit equivelar map of type $\{6,3\}$ in the Klein bottle, then $3|k$ and Cham($\mathcal{M}$) is a $2k$-orbit map.*
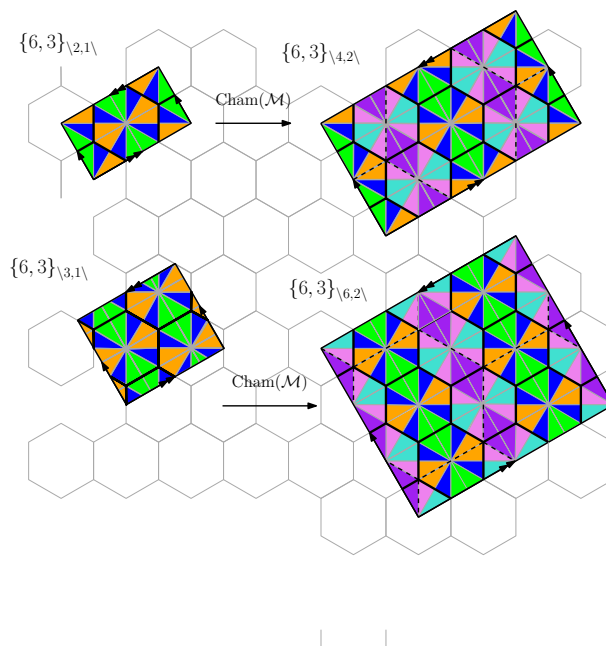
Figure 6.11: Chamfering of a 3-orbit map of type $\{6,3\}_{\backslash m,1\backslash}$ in the Klein bottle.

6.2   Chamfering map of k-orbit maps

Putting our results together we see that lemma 6.1 implies that if $\mathcal{M}$ is a k-orbit map such that $\mathrm{Cham}(\mathcal{M})$ is not a $4k$-orbit map, then it is of type $\{6,3\}$. Hence, Corollary 6.1 implies the following theorem.

Theorem 6.1. *Let $\mathcal{M}$ be a k-orbit map. Then, $\mathrm{Cham}(\mathcal{M})$ has either k, $2k$ or $4k$ flag-orbits.*

We denote as $T(\mathrm{Cham}(T'))$ the chamfering symmetry type graph with $4k$ vertices that results from applying the algorithm in Figure 6.4 to the symmetry type graph T' of a k-orbit map. (See for instance Figure 6.12). As a consequence of the above discussion we have the following corollary.

Corollary 6.2. *Let $\mathcal{M}$ be a k-orbit map with symmetry type either 1, 2, 3^{02} or 6_{H_p}, and $\mathrm{Cham}(\mathcal{M})$ its chamfering map. Then the following holds.*

  (1) If $\mathcal{M}$ is a regular map, then $\mathrm{Cham}(\mathcal{M})$ is either regular of type $\{6,3\}$ (and hence toroidal), or has symmetry type 4_{D_p}.

  (2) If $\mathcal{M}$ is a chiral map, then $\mathrm{Cham}(\mathcal{M})$ is either chiral of type $\{6,3\}$ (and hence toroidal), or has symmetry type graph $T(\mathrm{Cham}(2))$ with 8 vertices. (See Figure 6.12.)

(3) *If $\mathcal{M}$ has symmetry type 3^{02}, then $\mathrm{Cham}(\mathcal{M})$ is either a toroidal map of type $\{6,3\}$ with symmetry type graph 3^{02}, or $\mathrm{Cham}(\mathcal{M})$ is a 6-orbit map in the Klein bottle and has symmetry type graph 6_{H_p}, or it has symmetry type graph $T(\mathrm{Cham}(3^{02}))$ with 12 vertices. (See Figure 6.12.)*

(4) *If $\mathcal{M}$ has symmetry type 6_{H_p}, then $\mathrm{Cham}(\mathcal{M})$ is either a toroidal map of type $\{6,3\}$ and has symmetry type graph 6_{H_p}, or $\mathrm{Cham}(\mathcal{M})$ is a 12-orbit map in the Klein bottle, or it has symmetry type graph $T(\mathrm{Cham}(6_{H_p}))$ with 24 vertices. (See Figure 6.12.)*
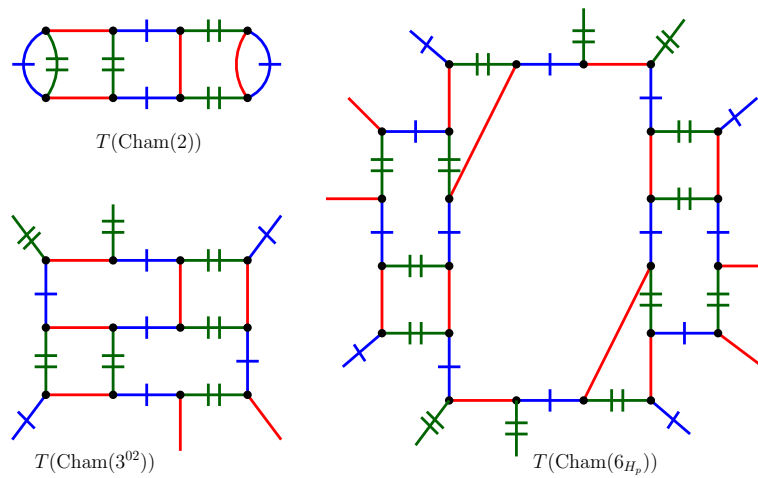
Figure 6.12: Symmetry type graphs of $\mathrm{Cham}(\mathcal{M})$, with $\mathcal{M}$ of type 2, 3^{02} and 6_{H_p}.

In [15] A. Deza, M. Deza and V. Grishukhin denote by $\mathrm{Cham}_t(\mathcal{M})$ the t-times chamfering of $\mathcal{M}$. It is straightforward to see that $\mathrm{Cham}_t(\mathcal{M})$ of a k-orbit equivelar map $\mathcal{M}$ on the torus is a k-orbit map described as $\{6,3\}_{2^t v_1, 2^t v_2}$. Similarly, $\mathrm{Cham}_t(\mathcal{M})$ of a k-orbit equivelar map $\mathcal{M}$ on the Klein bottle is a $2k$-orbit map denoted either $\{6,3\}_{|2^t m, 2^t n|}$ or $\{6,3\}_{\backslash 2^t m, 2^t n \backslash}$.

Finally, based on the results obtained in the previous section, we conclude with the following theorem.

Theorem 6.2. *Let $\mathcal{M}$ be a k-orbit map and $\mathrm{Cham}_t(\mathcal{M})$ the t-times chamfering map of $\mathcal{M}$ having s flag-orbits. Then one of the following holds.*

1. *$s = 4^t k, 2^t k$ or k.*

2. *If $s \neq 4^t k$, then $\chi(\mathcal{M}) = 0$ ($\mathcal{M}$ is on the torus or on the Klein bottle) and $\mathcal{M}$ is of type $\{6,3\}$.*

3. *If $\mathcal{M}$ is a toroidal map of type $\{6,3\}$ then $s = k$ and $k = 1, 2, 3, 6$.*

4. If $\mathcal{M}$ is on the Klein bottle of type $\{6,3\}$ then $s = 2^t k$ and $3|k$.

6.3   Dual of chamfering map

Regarding to the dual of the chamfering of a map $\mathcal{M}$, since the vertices of $\text{Cham}(\mathcal{M})$ are divided on those that have valency 3 and those with the same valency as those in $V(\mathcal{M})$, the faces of $(\text{Cham}(\mathcal{M}))^*$ are triangles and n-gons, where n is the corresponding valency of each vertex in $V(\mathcal{M})$. The faces, corresponding to the elements of $V(\mathcal{M})$ in $(\text{Cham}(\mathcal{M}))^*$ are surrounded by triangles, Moreover, as the vertices of $(\text{Cham}(\mathcal{M}))^*$ correspond to the faces of $\text{Cham}(\mathcal{M})$, then there are vertices in $(\text{Cham}(\mathcal{M}))^*$ of valency 6, those corresponding to the elements in $E(\mathcal{M})$, and others of valency equal to the length of the elements in $F(\mathcal{M})$. In Figure 6.13 is depicted the dual of the chamfering of the dodecahedron.
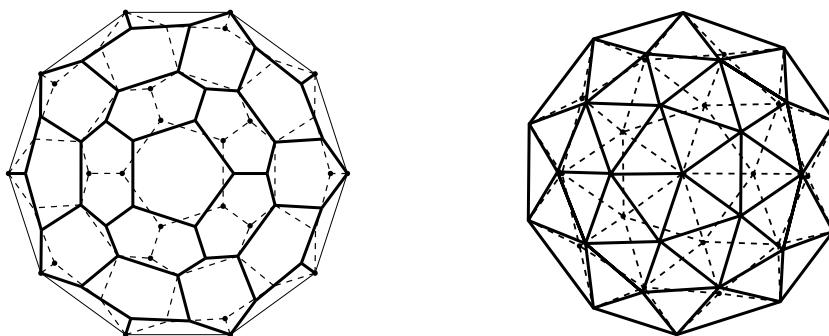
Figure 6.13: Chamfering of the dodecahedron (left) and its dual (right).

Once more, recall that the bijection $\delta : \text{Mon}(\mathcal{M}) \to \text{Mon}(\mathcal{M}^*)$ induces a permutation on the edges of $\mathcal{G}_\mathcal{M}$ sending edges of colour $i = 0, 1, 2$ to edges of colour $2 - i$. Then, the following proposition is a consequence from Proposition 6.1.

Proposition 6.2. *The flag graph $\mathcal{G}_{(\text{Cham}(\mathcal{M}))^*}$, of the dual of the chamfering map $(\text{Cham}(\mathcal{M}))^*$ of a map $\mathcal{M}$, can be quotient into a graph isomorphic to the self-dual symmetry type graph 4_{D_p}.*

Chapter 7

Truncation operation on maps

Another interesting operation is the *truncation* of a map (see [45, 49]). The medial operation can be understood as the truncation of a map up to the midpoint of its edges. Moreover, when the truncation goes further than the midpoint on the edges of the map $\mathcal{M}$, then the obtained map is known as the *leapfrog* map of $\mathcal{M}$, [18]. If the vertices of $\mathcal{M}$ become the faces of the truncated map, then the resulting map is the dual map of $\mathcal{M}$. For instance, by truncating regular polyhedra, we can obtain some of the 13 Archimedean solids as is discussed in [7] and [52].

The truncation operation consist on replace the vertices of a map by faces, leaving the faces with twice the number of vertices than the original ones. An example is the truncated icosahedron, shown in Figure 7.1, it has twelve pentagonal faces and twenty

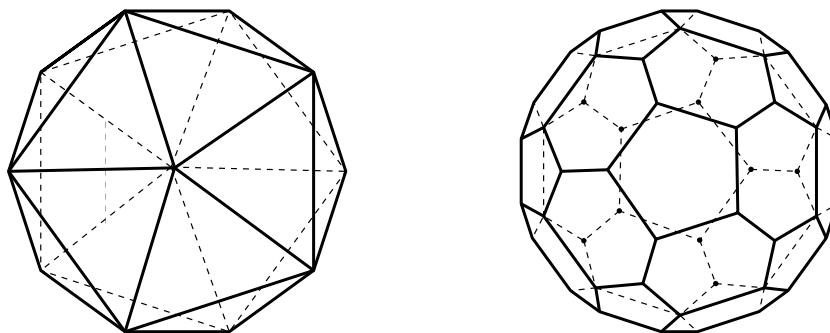Figure 7.1: Icosahedron (left) and truncated icosahedron (right).

hexagonal faces that correspond to the vertices and faces of the icosahedron, respectively. Hence, there is a correspondence between the set of faces of the truncated map $\mathrm{Tr}(\mathcal{M})$ of $\mathcal{M}$ with the set of vertices and faces of $\mathcal{M}$, i.e

$$F(\mathrm{Tr}(\mathcal{M})) = V(\mathcal{M}) \cup F(\mathcal{M}).$$

Furthermore, for each edge of $\mathcal{M}$ there are exactly two vertices of $\mathrm{Tr}(\mathcal{M})$, two of these vertices have an edge joining them if either both belong to a common edge of $\mathcal{M}$ or if the corresponding edges in $\mathcal{M}$ share a vertex and belong to the same face. Then, the sets of edges and vertices of $\mathrm{Tr}(\mathcal{M})$ are

$$E(\mathrm{Tr}(\mathcal{M})) = E(\mathcal{M}) \cup \{\{\Phi_0, \Phi_2\} | \Phi \in \mathcal{F}(\mathcal{M})\} \quad \text{and}$$

$$V(\mathrm{Tr}(\mathcal{M})) = \{\{\Phi_0, \Phi_1\} | \Phi \in \mathcal{F}(\mathcal{M})\},$$

respectively. Each vertex of $\mathrm{Tr}(\mathcal{M})$ has valency 3 and therefore, the truncated map $\mathrm{Tr}(\mathcal{M})$ contains $2|E(\mathcal{M})|$ vertices and $3|E(\mathcal{M})|$ edges.

In Figure 7.2 is depicted how every flag in $\mathcal{F}(\mathcal{M})$ is divided into three different flags of the truncated map $\mathrm{Tr}(\mathcal{M})$. This is, for each flag
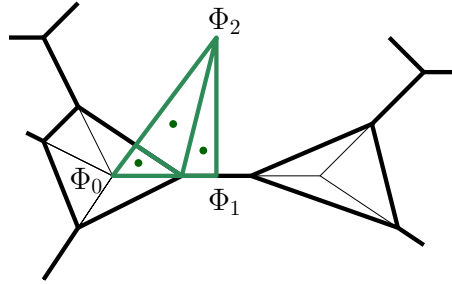
Figure 7.2: The three flags of $\mathcal{F}(\mathrm{Tr}(\mathcal{M}))$ corresponding to the flag $\Phi = (\Phi_0, \Phi_1, \Phi_2) \in \mathcal{F}(\mathcal{M})$.

$\Phi = (\Phi_0, \Phi_1, \Phi_2) \in \mathcal{F}(\mathcal{M})$, there are three flags: $(\Phi, 0) := (\{\Phi_0, \Phi_1\}, \{\Phi_0, \Phi_2\}, \Phi_0)$,

$$(\Phi, 1) := (\{\Phi_0, \Phi_1\}, \Phi_1, \Phi_2) \quad \text{and} \quad (\Phi, 2) := (\{\Phi_0, \Phi_1\}, \{\Phi_0, \Phi_2\}, \Phi_2),$$

corresponding to Φ in $\mathcal{F}(\mathrm{Tr}(\mathcal{M}))$. The adjacencies between the flags in $\mathcal{F}(\mathrm{Tr}(\mathcal{M}))$ are given as follows.

$$
\begin{array}{lll}
(\Phi, 0)^0 = (\Phi^{s_1}, 0), & (\Phi, 0)^1 = (\Phi^{s_2}, 0), & (\Phi, 0)^2 = (\Phi, 2); \\
(\Phi, 1)^0 = (\Phi^{s_0}, 1), & (\Phi, 1)^1 = (\Phi, 2), & (\Phi, 1)^2 = (\Phi^{s_2}, 1); \\
(\Phi, 2)^0 = (\Phi^{s_1}, 2), & (\Phi, 2)^1 = (\Phi, 1), & (\Phi, 2)^2 = (\Phi, 0),
\end{array}
$$

where s_0, s_1 and s_2 are the distinguished generators of $\mathrm{Mon}(\mathcal{M})$. Let t_0, t_1 and t_2 be the distinguished generators of $\mathrm{Mon}(\mathrm{Tr}(\mathcal{M}))$, since all the vertices of $\mathrm{Tr}(\mathcal{M})$ have valency 3, then $(t_1 t_2)^3 = id$. Consequently, in Figure 7.3 is presented an algorithm to construct the flag graph of $\mathrm{Tr}(\mathcal{M})$ from $\mathcal{G}_{\mathcal{M}}$. Such algorithm induces a partition $(\mathcal{A}_0, \mathcal{A}_1, \mathcal{A}_2)$ on the vertices of $\mathcal{G}_{\mathrm{Tr}(\mathcal{M})}$, where $\mathcal{A}_i := \{(\Phi, i) | \Phi \in \mathcal{F}(\mathcal{M})\}$ with $i = 0, 1, 2$, and therefore we have Proposition 7.1.

Figure 7.3: Any local representation of a flag, in the left. The result under the medial operation, locally obtained, in the right.
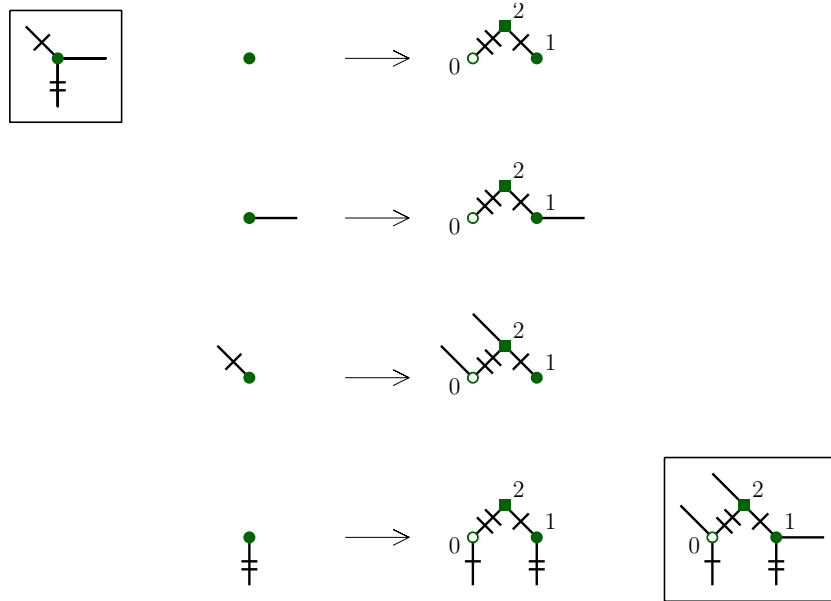
Proposition 7.1. *The flag graph $\mathcal{G}_{\mathrm{Tr}(\mathcal{M})}$, of the truncation map $\mathrm{Tr}(\mathcal{M})$ of a map $\mathcal{M}$, can be quotient into a graph isomorphic to the symmetry type graph 3^0.*

Proof. Let $\mathcal{A}_i = \{(\Phi, i) | \Phi \in \mathcal{F}(\mathcal{M})\}$, with $i = 0, 1, 2$. Then, $\mathcal{F}(\mathrm{Tr}(\mathcal{M})) = \mathcal{A}_0 \cup \mathcal{A}_1 \cup \mathcal{A}_2$ and $\mathcal{A}_i \cap \mathcal{A}_j = \emptyset$, with $i \neq j$ and $i, j \in \{0, 1, 2\}$. Hence, $(\mathcal{A}_0, \mathcal{A}_1, \mathcal{A}_2)$ is a partition of the set of flags $\mathcal{F}(\mathrm{Tr}(\mathcal{M}))$. Based on Figure 7.3, it is straightforward to see that the quotient of $\mathcal{G}_{\mathrm{Tr}(\mathcal{M})}$ over such partition, is isomorphic to the symmetry type graph of a map with symmetry type 3^0 (see Figure 3.3). ∎

7.1   Truncation of k-orbit maps

In [45], in order to characterize the symmetry types of all truncated maps of k-orbit maps up to $k \leq 3$, using coset enumeration ([9, Chapter 2]), Orbanić, Pellicer and Weiss showed that the truncated map $\mathrm{Tr}(\mathcal{M})$ of a k-orbit map $\mathcal{M}$ is either a k-orbit, a $\frac{3k}{2}$-orbit (with k even) or a $3k$-orbit map. The authors also presented examples of when any of this cases is possible, some of these examples are depicted in Figures 7.4–7.6.

With regard to this result, using once more the coset enumeration, the authors in [45] show that in particular if a k-orbit map $\mathcal{M}$ which truncation map $\mathrm{Tr}(\mathcal{M})$ is either a $\frac{3k}{2}$-orbit or a k-orbit map, then there is a bi-partition on the vertices of $\mathcal{G}_{\mathcal{M}}$ in such way that $\mathcal{G}_{\mathcal{M}}$ can be quotient into a graph isomorphic to the symmetry type graph 2_{01}.
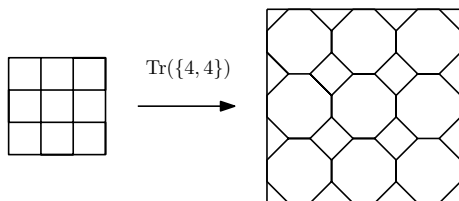
Figure 7.4: A 3-orbit map (right), obtained by truncation of a regular map of type $\{4, 4\}$ (left).

$\{3, 6\}_{(2,0),(0,2)}$ $\{6, 3\}_{(2,2),(4,-2)}$

$\{3, 6\}_{(2,2),(4,-2)}$

$\{6, 3\}_{(6,0),(0,6)}$
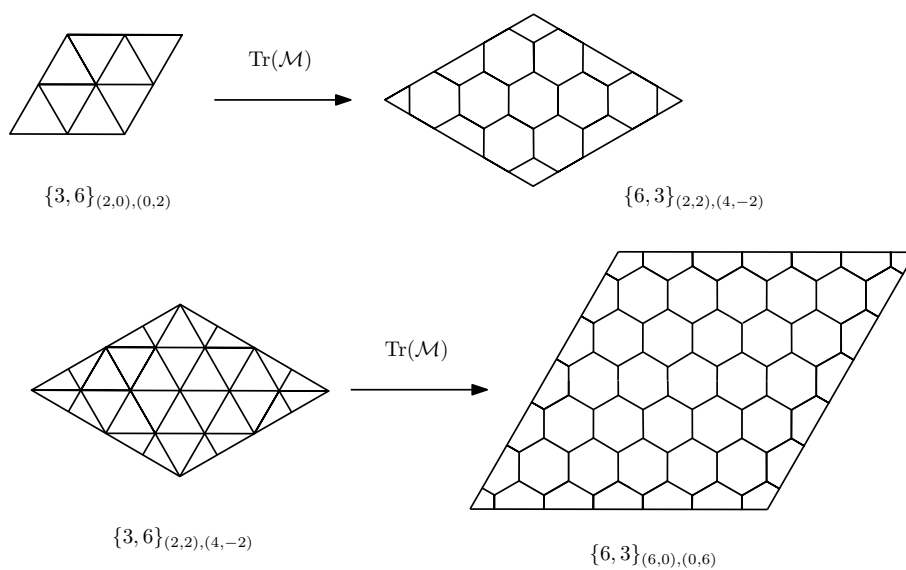
Figure 7.5: Regular maps of type $\{6, 3\}$ (right), obtained by truncation of regular maps of type $\{3, 6\}$ (left).
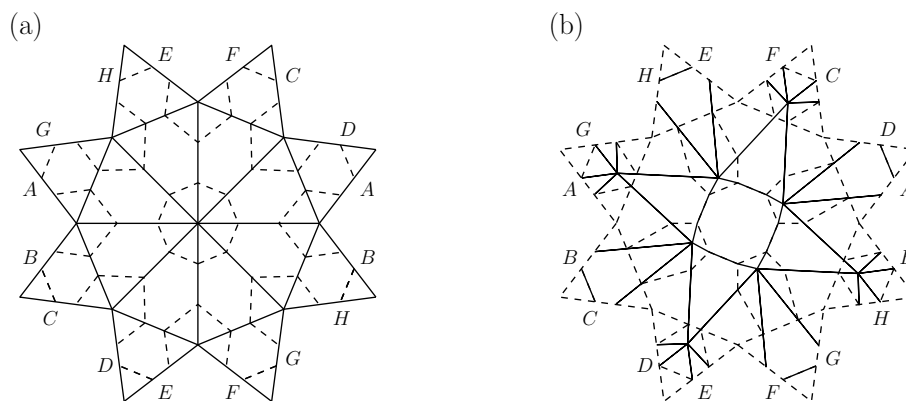
Figure 7.6: A map (in dotted lines), with symmetry type 3^0, obtained by truncation of a regular map (a) or of a 2-orbit map (b), [45].

Recall that if $\mathcal{M}$ is a regular map, the distinguished generators of $\mathrm{Aut}(\mathcal{M})$ with respect to a base flag $\Phi \in \mathcal{F}(\mathcal{M})$ are involutions ρ_0, ρ_1, ρ_2 such that $\Phi\rho_i = \Phi^i$ (Section 3.2). In [45], it was shown that for a regular map $\mathcal{M}$ and the subgroup $G = \langle \rho_0, \rho_1, \rho_2\rho_1\rho_2 \rangle$ of the automorphism group $\mathrm{Aut}(\mathcal{M})$, the truncation map $\mathrm{Tr}(\mathcal{M})$ is regular if and only if $[\mathrm{Aut}(\mathcal{M}) : G] = 2$ and there exist an automorphism $\tau \in \mathrm{Aut}(G)$ interchanging ρ_0 and ρ_1 and fixing $\rho_2\rho_1\rho_2$.

By Proposition 7.1, we have that there exists a partition $(\mathcal{A}_0, \mathcal{A}_1, \mathcal{A}_2)$ of the vertices of the flag graph $\mathcal{G}_{\mathrm{Tr}(\mathcal{M})}$ of the truncation map $\mathrm{Tr}(\mathcal{M})$ in such way that for each $\Upsilon \in \mathcal{A}_0$, the vertices Υ^2 and $\Upsilon^{2,1}$ are elements in $\mathcal{A}_2$ and $\mathcal{A}_1$, respectively. Then, the flags $\Upsilon, \Upsilon^2, \Upsilon^{2,1} \in \mathcal{F}(\mathrm{Tr}(\mathcal{M}))$ correspond to a flag $\Phi_\Upsilon \in \mathcal{F}(\mathcal{M})$ where the face Υ_2 is an element of $V(\mathcal{M})$, [45].

Finally the authors, in [45], conclude that the flag graph $\mathcal{G}_{\mathrm{Tr}(\mathcal{M})}$ can be quotient in to a graph isomorphic to the symmetry type graph 3^0 under the action of a subgroup $H \leq \mathrm{Aut}(\mathrm{Tr}(\mathcal{M}))$, of the automorphism group of $\mathrm{Tr}(\mathcal{M})$, if and only if $\mathcal{M}$ is a regular map.

In what follows, supported by Proposition 7.1 and defining the flags in $\mathcal{F}(\mathcal{M})$ as flags $\Phi_\Upsilon := \{\Upsilon, \Upsilon^2, \Upsilon^{2,1}\}$ where $\Upsilon_2 \in V(\mathcal{M})$ and $\Upsilon, \Upsilon^2, \Upsilon^{2,1} \in \mathcal{F}(\mathrm{Tr}(\mathcal{M}))$, as it was described above, we discuss the results of Orbanić, Pellicer and Weiss on truncation of regular, 2-orbit and 3-orbits maps. Moreover, we show results on the truncation of k-orbit maps, with $k = 4, \ldots, 7, 9$. Due to the large number of cases for $k = 8$, the truncation of 8-orbit maps is left on aside.

7.1.1 Truncation symmetry type graphs

As the vertices of the map $\mathrm{Tr}(\mathcal{M})$ have valency three, there are exactly six flags of $\mathcal{F}(\mathrm{Tr}(\mathcal{M}))$ around each vertex in $\mathrm{Tr}(\mathcal{M})$. Recall that the vertices of the map $\mathrm{Tr}(\mathcal{M})$ are identified with the orbits of the subgroup $\langle t_1, t_2 \rangle$ on $\mathcal{F}(\mathrm{Tr}(\mathcal{M}))$. Since the automorphism group of a map partitions its set of flags into orbits of the same size, then Lemma 3.2 implies that the 2-factors coloured by 1 and 2 in the symmetry type graph $T(\mathrm{Tr}(\mathcal{M}))$ must be as those in Figure 7.7.

Truncation of regular, 2-orbit and 3-orbit maps.

As it was said previously, if $\mathcal{M}$ is a regular map, then $\mathrm{Tr}(\mathcal{M})$ is either regular or a 3-orbit map, which has symmetry type graph 3^0. On another hand, if $\mathcal{M}$ is a 2-orbit or a 3-orbit map, Orbanić, Pellicer and Weiss conclude with the following results on the truncation map of $\mathcal{M}$, [45].
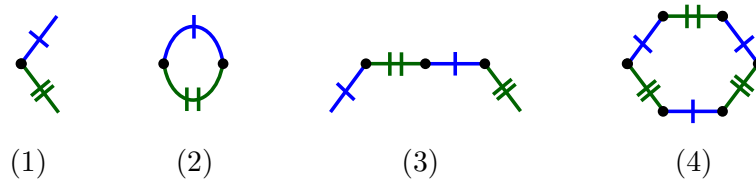
Figure 7.7: Possible quotients of 1-2 coloured 6-cycles of $\mathcal{G}_{\mathrm{Tr}(\mathcal{M})}$.

Proposition 7.2. *[45] If the truncation* $\mathrm{Tr}(\mathcal{M})$ *of a 2-orbit map* $\mathcal{M}$ *is a 2-orbit map, then one of the following holds*

(i) $\mathcal{M}$ *and* $\mathrm{Tr}(\mathcal{M})$ *are of type 2,*

(ii) $\mathcal{M}$ *is of type* 2_{01} *and* $\mathrm{Tr}(\mathcal{M})$ *is of type* 2_0*, or*

(iii) $\mathcal{M}$ *is of type* 2_2 *and* $\mathrm{Tr}(\mathcal{M})$ *is of type* 2_{12}*.*

Proposition 7.3. *[45] If the truncation* $\mathrm{Tr}(\mathcal{M})$ *of a 2-orbit map is a 3-orbit map, then* $\mathcal{M}$ *is of type* 2_{01} *and* $\mathrm{Tr}(\mathcal{M})$ *is of type* 3^0*.*

Proposition 7.4. *[45] If the truncation* $\mathrm{Tr}(\mathcal{M})$ *of a 3-orbit map is a 3-orbit map, then* $\mathcal{M}$ *and* $\mathrm{Tr}(\mathcal{M})$ *are of type* 3^{02}*.*

In other words, if $\mathcal{M}$ is a regular, a 2-orbit or a 3-orbit map, and $\mathrm{Tr}(\mathcal{M})$ has either 1, 2 or 3 flag-orbits, then the symmetry type of $\mathrm{Tr}(\mathcal{M})$ is either 1, 2, 2_0, 2_{12}, 3^0 or 3^{02}. These are in fact, the only possible symmetry type graphs with 1, 2 and 3 vertices, consistent with the (1,2) 2-factors in Figure 7.7.
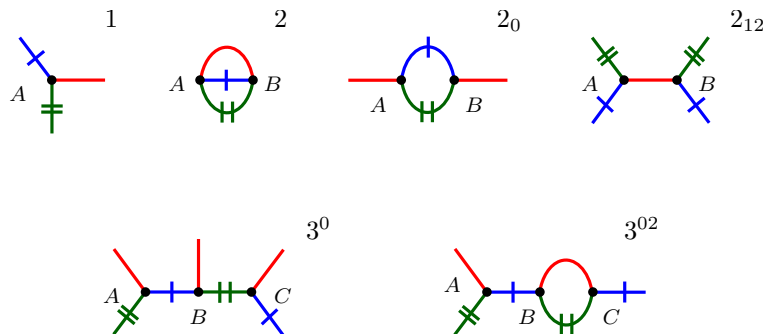
Figure 7.8: Symmetry type graphs with at most 3 vertices and (1,2) 2-factors as in Figure 7.7.

Orbanić, Pellicer and Weiss prove Propositions 7.2, 7.3 and 7.4 based on the following facts.

(i) All the vertices of the map $\mathrm{Tr}(\mathcal{M})$ have valency 3.

(ii) The vertex set of $\mathcal{M}$ is a proper subset of the set of faces of $\mathrm{Tr}(\mathcal{M})$.

(iii) Each flag $\Phi_\Upsilon \in \mathcal{F}(\mathcal{M})$ of $\mathcal{M}$ is divided in exactly three flags $(\Phi_\Upsilon, 0) =: \Upsilon$, $(\Phi_\Upsilon, 2) =: \Upsilon^2$, $(\Phi_\Upsilon, 1) =: \Upsilon^{2,1} \in \mathcal{F}(\mathrm{Tr}(\mathcal{M}))$ of $\mathrm{Tr}(\mathcal{M})$, where $\Upsilon_2 \in V(\mathcal{M})$. (Figures 7.2 and 7.3).

Then, to prove each proposition above they proceed by using local arrangements to the flags in the truncated map $\mathrm{Tr}(\mathcal{M})$, by assembling flags $\Upsilon, \Upsilon^2, \Upsilon^{2,1}, \in \mathcal{F}(\mathrm{Tr}(\mathcal{M}))$ into a new flag $\Phi_\Upsilon \in \mathcal{F}(\mathcal{M})$, where the face Υ_2 shall represent an element in $V(\mathcal{M})$. Based on such local flag-arrangements of $\mathcal{F}(\mathrm{Tr}(\mathcal{M}))$, used in [45], we proof Propositions 7.2–7.4 with a similar method that follows the notation on this work, as is presented next.

Suppose that the truncation map $\mathrm{Tr}(\mathcal{M})$, of a k-orbit map $\mathcal{M}$, has either k or $\frac{3k}{2}$ orbits in $\mathcal{F}(\mathrm{Tr}(\mathcal{M}))$, with $k = 2, 3$. Then, the symmetry type graph $T(\mathrm{Tr}(\mathcal{M}))$ must be one of the shown in Figure 7.8 (as are the only ones with the (1,2) 2-factors as in Figure 7.7). Consider the partition $(\mathcal{A}_0, \mathcal{A}_1, \mathcal{A}_2)$ of the set $\mathcal{F}(\mathrm{Tr}(\mathcal{M}))$ and let $\Upsilon \in \mathcal{A}_0$, $\Upsilon^2 \in \mathcal{A}_2$ and $\Upsilon^{2,1} \in \mathcal{A}_1$, be such that $\Upsilon_2 \in V(\mathcal{M})$. Assume that the flag $\Upsilon \in \mathcal{A}_0$ represents a particular orbit of the flags of $\mathrm{Tr}(\mathcal{M})$, A say. Let $i_0, i_1, \ldots, i_n$ be an edge-coloured walk between the vertex A and any other vertex, B say, in the corresponding symmetry type graph $T(\mathrm{Tr}(\mathcal{M}))$. Thus, we shall choose the flag $\Upsilon^{i_0, i_1, \ldots, i_n}$ as the representative of the orbit B of $\mathcal{F}(\mathrm{Tr}(\mathcal{M}))$. Proceeding in a similar fashion, we can determine to which orbit of $\mathcal{F}(\mathrm{Tr}(\mathcal{M}))$ belong the other flags in each of the partitions $\mathcal{A}_0$, $\mathcal{A}_1$ and $\mathcal{A}_2$. Finally, we proceed to determine the symmetry type of $\mathcal{M}$ as follows. Consider the flag $\Phi_\Upsilon := \{\Upsilon, \Upsilon^2, \Upsilon^{2,1}\} \in \mathcal{F}(\mathcal{M})$ as the base flag of $\mathcal{M}$ representing one of the k flag-orbits of $\mathcal{M}$. The number of orbits of the map $\mathcal{M}$ is determined by the different types of flags obtained in the process. Observe if any of its adjacent flags $(\Phi_\Upsilon)^0 := \Phi_{\Upsilon^{2,1,0,1,2}}$, $(\Phi_\Upsilon)^1 := \Phi_{\Upsilon^1}$, $(\Phi_\Upsilon)^2 := \Phi_{\Upsilon^0} \in \mathcal{F}(\mathcal{M})$ belong or not to the same orbit of $\mathcal{F}(\mathcal{M})$ than Φ_Υ, so we can identify which particular flag-orbit of $\mathcal{M}$ is represented by Φ_Υ. Later, find which other flags in $\mathcal{F}(\mathcal{M})$ belong to different flag-orbits than Φ_Υ, and display how the corresponding orbits of these flags are related to each other. We shall refer to this method as the *"untruncation" method*.

To verify Proposition 7.2 we first note that if $\mathcal{M}'$ is a 2-orbit map with all its vertices with valency 3, since maps in classes 2_1, 2_2, 2_{02} and 2_{01} have even vertex-valency, the symmetry type graph $T(\mathcal{M}')$ of $\mathcal{M}'$ is of type 2, 2_0 or 2_{12} (Figure 7.8). Let $\mathcal{M}' := \mathrm{Tr}(\mathcal{M})$ be the truncation of another map $\mathcal{M}$, and consider the partition $(\mathcal{A}_0, \mathcal{A}_1, \mathcal{A}_2)$ of the flags of $\mathrm{Tr}(\mathcal{M})$ as was said previously. Then, we will apply the "untruncation" method, in order

to construct the map $\mathcal{M}$ and find out its symmetry type. Let $\Upsilon \in \mathcal{A}_0$ be a flag in the map $\mathrm{Tr}(\mathcal{M})$. Note that the maps of types 2, 2_0 and 2_{12} are transitive on their faces; that is, every face of such maps contains flags on the two orbits of $\mathcal{F}(\mathrm{Tr}(\mathcal{M}))$. Hence, we can assume that the face Υ_2 of any flag $\Upsilon \in \mathcal{A}_0$ is an element in the set $V(\mathcal{M})$. In particular, suppose that the flag $\Upsilon \in \mathcal{A}_0$ is in the orbit A and consider the i-adjacent flag Υ^i which is in the orbit B, where $i \in \{0, 1\}$. In such way, we obtain a pair of representative flags of $\mathcal{M}$, as those depicted in the Figure 7.9, as is explained in the next two cases.
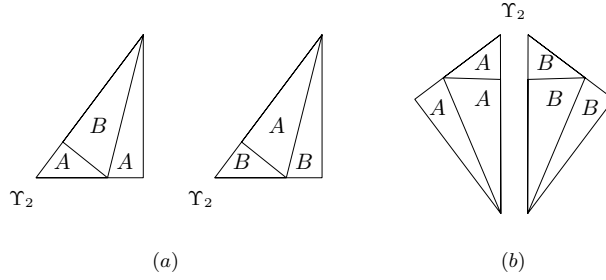

Figure 7.9: Representative flags of a 2-orbit map $\mathcal{M}$, as assembled flags from the truncation map $\mathrm{Tr}(\mathcal{M})$, where in (a) $\mathrm{Tr}(\mathcal{M})$ has symmetry type 2 or 2_0, and in (b) $\mathrm{Tr}(\mathcal{M})$ has symmetry type 2_{12}. The element $\Upsilon_2 \in V(\mathcal{M})$ corresponds to the face of the base flag $\Upsilon \in \mathcal{F}(\mathrm{Tr}(\mathcal{M}))$.

(a) If a map $\mathrm{Tr}(\mathcal{M})$ has symmetry type 2 or 2_0, with flag-orbits A and B, then the two flags $\Upsilon \in \mathcal{A}_0$ and $\Upsilon^{2,1} \in \mathcal{A}_1$ belong to the orbit A, while the flag $\Upsilon^2 \in \mathcal{A}_2$ belongs to the orbit B. Thus, when we construct the map $\mathcal{M}$, the flags $\Phi_{\bar{\Upsilon}} \in \mathcal{F}(\mathcal{M})$ in the same orbit as $\Phi_{\Upsilon} \in \mathcal{F}(\mathcal{M})$ must have two flags $\bar{\Upsilon} \in \mathcal{A}_0$ and $\bar{\Upsilon}^{2,1} \in A_1$ in the orbit A, and the flag $\bar{\Upsilon}^2 \in \mathcal{A}_2$ in the orbit B. Moreover, in both symmetry type maps, the flags $\Upsilon^1 \in \mathcal{A}_0$ and $\Upsilon^{1,2,1} \in \mathcal{A}_2$ are flags in the flag-orbit B in $\mathrm{Tr}(\mathcal{M})$, and the flag $\Upsilon^{0,2} \in \mathcal{A}_2$ is in the flag-orbit A. Hence, the flag $\Phi_{\Upsilon^1} \in \mathcal{F}(\mathcal{M})$ represents a different orbit of the flags in $\mathcal{F}(\mathcal{M})$ than Φ_{Υ}. Therefore, it follows that the map $\mathcal{M}$ is a 2-orbit map with symmetry type graph either 2 or 2_{01}. Inducing (i) and (ii) in Proposition 7.2, respectively.

(b) On another hand, if $\mathrm{Tr}(\mathcal{M})$ is of type 2_{12}, with flag-orbits A and B, the flags $\Phi_{\bar{\Upsilon}} \in \mathcal{F}(\mathcal{M})$ in the same orbit as the representative flag $\Phi_{\Upsilon} \in \mathcal{F}(\mathcal{M})$ have all flags $\bar{\Upsilon} \in \mathcal{A}_0$, $\bar{\Upsilon}^2 \in \mathcal{A}_2$ and $\bar{\Upsilon}^{2,1} \in \mathcal{A}_1$ in the orbit A. While other flags in $\mathcal{F}(\mathcal{M})$ as Φ_{Υ^0}, correspond to the other orbit of the flags in $\mathcal{F}(\mathcal{M})$, with all the flags $\Upsilon^0 \in \mathcal{A}_0$, $\Upsilon^{0,2} \in \mathcal{A}_2$ and $\Upsilon^{0,2,1} \in \mathcal{A}_1$ in the flag-orbit B. Inducing that $\mathcal{M}$ is a 2-orbit map of symmetry type 2_2. Therefore, we obtain (iii) in Proposition 7.2.

Similarly, if $\mathrm{Tr}(\mathcal{M})$ is a 3-orbit map. Then, $\mathrm{Tr}(\mathcal{M})$ has symmetry type either 3^0 or 3^{02}. Observe that the maps of type 3^{02} are face-transitive, while the maps of type 3^0

are not face transitive. Hence, if $\mathrm{Tr}(\mathcal{M})$ is of type 3^0, the faces corresponding to the set $V(\mathcal{M})$ might contain all flags in one orbit (C say), or flags in two orbits (A and B say); depending on which of both type of faces are the elements of $V(\mathcal{M})$ in $\mathrm{Tr}(\mathcal{M})$. Only one choice of these two later will produce a 2-orbit map, as we see next, and show Proposition 7.3.

Let $\mathrm{Tr}(\mathcal{M})$ be the truncation map of a map $\mathcal{M}$. Suppose that $\mathrm{Tr}(\mathcal{M})$ has symmetry type 3^0, and consider the partition $(\mathcal{A}_0, \mathcal{A}_1, \mathcal{A}_2)$ of the set $\mathcal{F}(\mathrm{Tr}(\mathcal{M}))$. Let C be the orbit of $\mathcal{F}(\mathrm{Tr}(\mathcal{M}))$ with all its flags in the same face-orbit. If a flag $\Upsilon \in \mathcal{F}(\mathrm{Tr}(\mathcal{M}))$ of the partition $\mathcal{A}_0$ belongs to the orbit C, then it follows that the flags $\Upsilon^2 \in \mathcal{A}_2$ and $\Upsilon^{2,1}$ are in orbits B and A, respectively. Then, if we assume that the face Υ_2 is an element in $V(\mathcal{M})$, following the "untruncation" method we obtain that the flag $\Phi_\Upsilon \in \mathcal{F}(\mathcal{M})$ represents a unique type of flags in $\mathcal{M}$. That is, the map $\mathcal{M}$ is a regular map. On another hand, if the flag $\Upsilon \in \mathcal{A}_0$ belongs to any of the other two flag-orbits, distinct than C, then the face Υ_2 contains flags in both orbits A and B. Hence, we obtain two different types of flags, represented by Φ_Υ and $\Phi_{\Upsilon^1} := (\Phi_\Upsilon)^2$. That is, for each flag $\Upsilon \in \mathcal{A}_0$ that belongs to the orbit A, say, the flags $\Upsilon^2 \in \mathcal{A}_2$ and $\Upsilon^{2,1} \in \mathcal{A}_1$ are in the orbits A and B, respectively. Consequently, $\Upsilon^1 \in \mathcal{A}_0$ belongs to the orbit B, and the flags $\Upsilon^{1,2} \in \mathcal{A}_2$ and $\Upsilon^{1,2,1} \in \mathcal{A}_1$ are both in the orbit C (see Figure 7.10 (a)). Therefore, the map $\mathcal{M}$ is
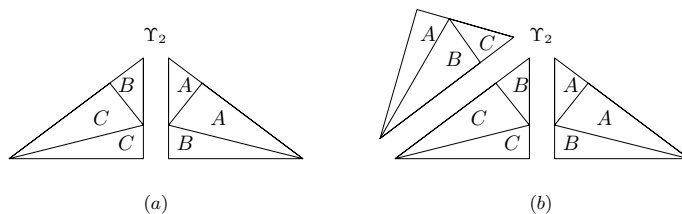
Figure 7.10: Representative flags of a (a) 2-orbit map and (b) 3-orbit map $\mathcal{M}$, as assembled flags from $\mathrm{Tr}(\mathcal{M})$, where in (a) $\mathrm{Tr}(\mathcal{M})$ has symmetry type 3^0, and in (b) $\mathrm{Tr}(\mathcal{M})$ has symmetry type 3^{02}. The element $\Upsilon_2 \in V(\mathcal{M})$ corresponds to the face of the base flag $\Upsilon \in \mathcal{F}(\mathrm{Tr}(\mathcal{M}))$.

a 2-orbit map with symmetry type 2_{01}, implying Proposition 7.3. Furthermore, we can proceed similarly as when we verified Proposition 7.2, with the flags of a 3-orbit face-transitive map $\mathrm{Tr}(\mathcal{M})$ with symmetry type 3^{02} and obtain three different flags as those in Figure 7.10 (b), following Proposition 7.4.

If $\mathrm{Tr}(\mathcal{M})$ is a $3k$-orbit map, applying the algorithm presented in the Figure 7.3 to the symmetry type graph $T(\mathcal{M})$ with k vertices, we obtain straightforward the symmetry type graph of $\mathrm{Tr}(\mathcal{M})$ with $3k$ vertices, and we will refer to this as the *truncated symmetry type graph* of $T(\mathcal{M})$. For instance, the truncated symmetry type graphs with 6 vertices, that correspond to the seven symmetry type graphs of maps with 2 vertices are depicted in Figure 7.11.
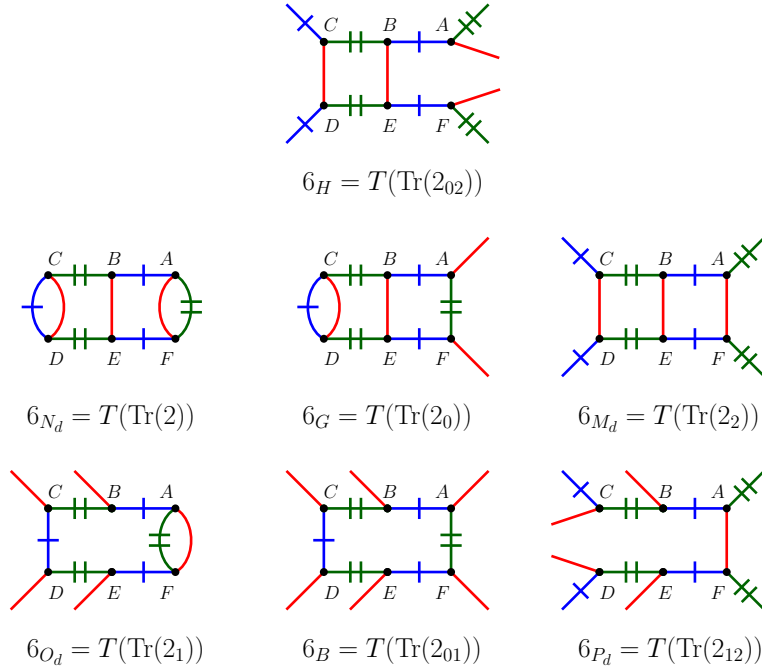
Figure 7.11: Truncation symmetry type graphs with 6 vertices, of the seven 2-orbit symmetry type graphs.

Now we proceed to our first goal: to find the possible symmetry type graphs with k and $\frac{3k}{2}$ vertices, of maps that correspond to truncation of a k-orbit map $\mathcal{M}$, with $k = 4, 5, 6, 7, 9$. Extending the results of [45], for the truncation of these k-orbit maps. To find the corresponding symmetry type of the map $\mathcal{M}$, we use the same "untruncation" method used previously on the flags of $\mathrm{Tr}(\mathcal{M})$, assembling the flags $\Upsilon, \Upsilon^2, \Upsilon^{2,1} \in \mathcal{F}(\mathrm{Tr}(\mathcal{M}))$ defining a new flag $\Phi_\Upsilon \in \mathcal{F}(\mathcal{M})$, under the appropriate partition $(\mathcal{A}_0, \mathcal{A}_1, \mathcal{A}_2)$ of the flags in $\mathcal{F}(\mathrm{Tr}(\mathcal{M}))$ according to the Proposition 7.1.

Truncation of 4-orbit maps.

The truncation map $\mathrm{Tr}(\mathcal{M})$ of a 4-orbit map $\mathcal{M}$ has either 4, 6 or 12 orbits on its flags. Consider a 4-orbit map $\mathcal{M}$ and suppose that the map $\mathrm{Tr}(\mathcal{M})$ also has 4 orbits on its flags. Then, by a proper combination of the $(1,2)$ 2-factors shown in Figure 7.7, into a symmetry type graph with 4 vertices (and looking at the twenty two symmetry type graphs with 4 vertices, in Figures 3.5 and 3.6), it can be seen that $\mathrm{Tr}(\mathcal{M})$ has either symmetry type 4_{D_p}, 4_D or 4_{G_d} (see Figure 7.12). First we study the possible case when the truncation map $\mathrm{Tr}(\mathcal{M})$ has symmetry type 4_{D_p}. Later, we describe the case when the map 4-orbit $\mathrm{Tr}(\mathcal{M})$ is face-transitive with symmetry type either 4_D or 4_{G_d}.

Figure 7.12: Possible symmetry type graphs of the 4-orbit maps that correspond to the truncation of another map.

Let $(\mathcal{A}_0, \mathcal{A}_1, \mathcal{A}_2)$ be the partition of the set of flags of the map $\mathrm{Tr}(\mathcal{M})$ with symmetry type graph 4_{D_p}. Even thought that the maps with the symmetry type 4_{D_p} have two o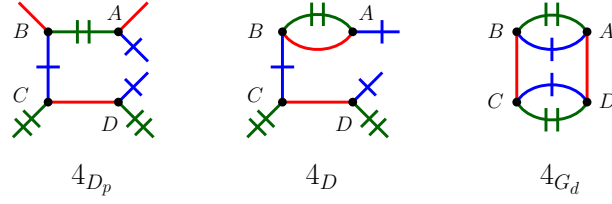rbits on their faces, where one type of faces contains flags in three orbits of flags and the other type contains all its flags in the fourth flag-orbit, we find exactly four types of flags representing flags of the map $\mathcal{M}$, as those shown in Figure 7.13, in the following way. Let
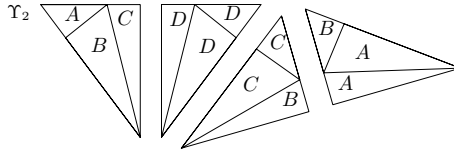
Figure 7.13: Representative flags $\Phi_\Upsilon, \Phi_{\Upsilon^{2,1,0,1,2}}, \Phi_{\Upsilon^{2,1,0,1,2,0}}$ and $\Phi_{\Upsilon^{2,1,0,1,2,0,1}}$ in $\mathcal{F}(\mathcal{M})$, as assembled flags from the truncation map $\mathrm{Tr}(\mathcal{M})$ with symmetry type 4_{D_p}. The element $\Upsilon_2 \in V(\mathcal{M})$ corresponds to the face of the base flag $\Upsilon \in \mathcal{F}(\mathrm{Tr}(\mathcal{M}))$.

A be the orbit of $\mathcal{F}(\mathrm{Tr}(\mathcal{M}))$ such that all its flags correspond to the same type of face in $\mathrm{Tr}(\mathcal{M})$ (Figure 7.12). If a flag $\Upsilon \in \mathcal{A}_0$ belongs to the flag-orbit A, then the flags $\Upsilon^2 \in \mathcal{A}_2$ and $\Upsilon^{2,1} \in \mathcal{A}_1$ are in the orbits B and C, respectively. Suppose that the face Υ_2 is an element in $V(\mathcal{M})$, and consider the base flag $\Phi_\Upsilon \in \mathcal{F}(\mathcal{M})$ in the map $\mathcal{M}$. On one hand, observe that the flags $(\Phi_\Upsilon)^1 =: \Phi_{\Upsilon^0}$ and $(\Phi_\Upsilon)^2 =: \Phi_{\Upsilon^1}$ are flags of the same type as Φ_Υ in $\mathcal{M}$. While, on the other hand, the flag

$$(\Phi_\Upsilon)^0 =: \Phi_{\Upsilon^{2,1,0,1,2}} = \{\Upsilon^{2,1,0,1,2}, \Upsilon^{2,1,0,1}, \Upsilon^{2,1,0}\}$$

is a different type of flag than Φ_Υ, where the flags $\Upsilon^{2,1,0,1,2} \in \mathcal{A}_0$, $\Upsilon^{2,1,0,1} \in \mathcal{A}_2$ and $\Upsilon^{2,1,0} \in \mathcal{A}_1$ are all in the orbit D. Moreover, the face $(\Upsilon^{2,1,0,1,2})_2$ is an element in $V(\mathcal{M})$. Furthermore, the flag $(\Phi_\Upsilon)^{0,2}$ is of the same type as $(\Phi_\Upsilon)^0$, but the flag

$$(\Phi_\Upsilon)^{0,1} =: \Phi_{\Upsilon^{2,1,0,1,2,0}} = \{\Upsilon^{2,1,0,1,2,0}, \Upsilon^{2,1,0,1,0}, \Upsilon^{2,1,0,1,0,1}\}$$

is a different type of flag than Φ_Υ and $(\Phi_\Upsilon)^0$ in the map $\mathcal{M}$. Obtaining a the third type of flag in $\mathcal{M}$, composed with two flags $\Upsilon^{2,1,0,1,2,0}, \Upsilon^{2,1,0,1,0} \in \mathcal{F}(\mathrm{Tr}(\mathcal{M}))$ in the flag-orbit C and one flag $\Upsilon^{2,1,0,1,0,1} \in \mathcal{F}(\mathrm{Tr}(\mathcal{M}))$ in the orbit B in $\mathrm{Tr}(\mathcal{M})$. Thus, we proceed in a

similar fashion, and find that the fourth type of flags in $\mathcal{M}$, represented by the flag

$$(\Phi_\Upsilon)^{0,1,2} =: \Phi_{\Upsilon^{2,1,0,1,2,0,1}} = \{\Upsilon^{2,1,0,1,2,0,1}, \Upsilon^{2,1,0,1,2,0,1,2}, \Upsilon^{2,1,0,1,2,0,1,2,1}\},$$

with the flag $\Upsilon^{2,1,0,1,2,0,1}$ in the flag-orbit B and the flags $\Upsilon^{2,1,0,1,2,0,1,2}$ and $\Upsilon^{2,1,0,1,2,0,1,2,1}$ in the flag-orbit A in $\mathrm{Tr}(\mathcal{M})$. Also, we note that the face $(\Upsilon^{2,1,0,1,2})_2 \in V(\mathcal{M})$ has all its flags in the three orbits B, C and D in $\mathrm{Tr}(\mathcal{M})$. This later implies that for any flag $\Upsilon \in \mathcal{A}_0$ in $\mathcal{F}(\mathrm{Tr}(\mathcal{M}))$, we can define the face Υ_2 as an element in $V(\mathcal{M})$, no matter in which flag-orbit of $\mathrm{Tr}(\mathcal{M})$ is contained the flag Υ. Finally, we conclude that $\mathcal{M}$ is a 4-orbit map also with symmetry type 4_{D_p}.

In case that the map $\mathrm{Tr}(\mathcal{M})$ has symmetry type 4_D or 4_{G_d}, we observe that $\mathrm{Tr}(\mathcal{M})$ is a face-transitive map. That is, every face in $\mathrm{Tr}(\mathcal{M})$ contains flags in the four orbits in $\mathcal{F}(\mathrm{Tr}(\mathcal{M}))$. Let $(\mathcal{A}_0, \mathcal{A}_1, \mathcal{A}_2)$ be a proper partition on the set $\mathcal{F}(\mathrm{Tr}(\mathcal{M}))$, where for any $\Upsilon \in \mathcal{A}_0$, $\Upsilon^2 \in \mathcal{A}_2$ and $\Upsilon^{2,1} \in \mathcal{A}_1$. Recall that, in previous cases, where the map $\mathrm{Tr}(\mathcal{M})$ is face-transitive, given any flag $\Upsilon \in \mathcal{A}_0$ we can define the face Υ_2 as an element in $V(\mathcal{M})$. Hence, following the "untruncation" method, we find the corresponding symmetry type of the map $\mathcal{M}$, whenever $\mathrm{Tr}(\mathcal{M})$ has symmetry type either 4_D or 4_{G_d}, as follows.

Suppose that $\mathrm{Tr}(\mathcal{M})$ is a face-transitive map of type 4_D. Let $\Upsilon \in \mathcal{A}_0$ be a flag in the flag-orbit A (Figure 7.12), where $\Upsilon_2 \in V(\mathcal{M})$. Then, the flags $\Upsilon^2 \in \mathcal{A}_2$ and $\Upsilon^{2,1} \in \mathcal{A}_1$ belong to the orbits B and C in $\mathcal{F}(\mathrm{Tr}(\mathcal{M}))$. Inducing the representative flag $\Phi_\Upsilon \in \mathcal{F}(\mathcal{M})$ as that in the very left of Figure 7.14 (a). Where the other three different types of flags,

(a) (b)
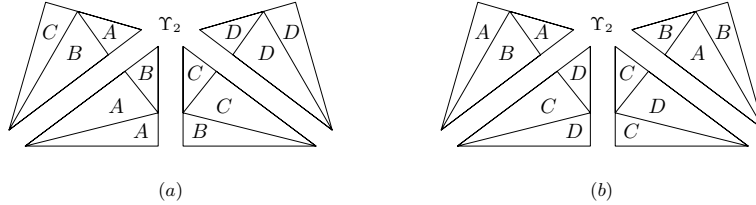
Figure 7.14: Representative flags of a 4-orbit map $\mathcal{M}$, as assembled flags from the map $\mathrm{Tr}(\mathcal{M})$, where in (a) $\mathrm{Tr}(\mathcal{M})$ has symmetry type 4_D, and in (b) $\mathrm{Tr}(\mathcal{M})$ has symmetry type 4_{G_d}. The element $\Upsilon_2 \in V(\mathcal{M})$ corresponds to the face of the base flag $\Upsilon \in \mathcal{F}(\mathrm{Tr}(\mathcal{M}))$.

representing the other the orbits in $\mathcal{F}(\mathcal{M})$ are described as

- Φ_{Υ^0}, with the flag $\Upsilon^0 \in \mathcal{A}_0$ in the orbit B and the flags $\Upsilon^{0,2} \in \mathcal{A}_2$ and $\Upsilon^{0,2,1} \in \mathcal{A}_1$ in the orbit A;

- $\Phi_{\Upsilon^{0,1}}$, with the flags $\Upsilon^{0,1} \in \mathcal{A}_0$ and $\Upsilon^{0,1,2} \in \mathcal{A}_2$ in the orbit C and the flag $\Upsilon^{0,1,2,1} \in \mathcal{A}_1$ in the orbit B; and

- $\Phi_{\Upsilon^{0,1,0}}$, with the flags $\Upsilon^{0,1,0} \in \mathcal{A}_0$, $\Upsilon^{0,1,0,2} \in \mathcal{A}_2$ and the flag $\Upsilon^{0,1,0,2,1} \in \mathcal{A}_1$ in the orbit D.

Proceed in similar way with the flags of a face-transitive map $\mathrm{Tr}(\mathcal{M})$ of type 4_{G_d}. Suppose that for any flag $\Upsilon \in \mathcal{A}_0$ that belong to the flag-orbit A, the face $\Upsilon_2 \in V(\mathcal{M})$. Then, the flags $\Upsilon^{2,1} \in \mathcal{A}_1$ and $\Upsilon^2 \in \mathcal{A}_2$ belong to the flag-orbits A and B, respectively (Figure 7.12). Similarly as in the previous case, we can find four different types of flags produced by the "untruncation" method on the flags of $\mathrm{Tr}(\mathcal{M})$. These latter are as those in Figure 7.14 (b). Where the representative flags of the orbits in $\mathcal{F}(\mathcal{M})$ are Φ_Υ;

- Φ_{Υ^0}, with the flags $\Upsilon^0 \in \mathcal{A}_0$ and $\Upsilon^{0,2,1} \in \mathcal{A}_1$ are in the orbit D and the flag $\Upsilon^{0,2} \in \mathcal{A}_2$ in the orbit C;

- $\Phi_{\Upsilon^{0,1}}$, with the flags $\Upsilon^{0,1} \in \mathcal{A}_0$ and $\Upsilon^{0,1,2,1} \in \mathcal{A}_1$ in the orbit C and the flag $\Upsilon^{0,1,2} \in \mathcal{A}_2$ in the orbit D; and

- $\Phi_{\Upsilon^{0,1,0}}$, with the flags $\Upsilon^{0,1,0} \in \mathcal{A}_0$ and $\Upsilon^{0,1,0,2,1} \in \mathcal{A}_1$ in the orbit B and the flag $\Upsilon^{0,1,0,2} \in \mathcal{A}_2$ in the orbit A.

Therefore, if we assume that $\mathrm{Tr}(\mathcal{M})$ and $\mathcal{M}$ are 4-orbit maps, then we obtain the following proposition.

Proposition 7.5. *If the truncation $\mathrm{Tr}(\mathcal{M})$ of a 4-orbit map $\mathcal{M}$ is a 4-orbit map, then exactly one of the following holds.*

(i) $\mathcal{M}$ and $\mathrm{Tr}(\mathcal{M})$ are of type 4_{D_p},

(ii) $\mathcal{M}$ is of type 4_E and $\mathrm{Tr}(\mathcal{M})$ is of type 4_D, or

(iii) $\mathcal{M}$ is of type 4_G and $\mathrm{Tr}(\mathcal{M})$ is of type 4_{G_d}.

Given a 4-orbit map $\mathcal{M}$, its truncated map $\mathrm{Tr}(\mathcal{M})$ might be a 6-orbit map. To find the possible symmetry types of maps with six orbits on its flags that would correspond to the symmetry type of a map $\mathrm{Tr}(\mathcal{M})$, when $\mathcal{M}$ is a 4-orbit map, it is necessary to observe the following.

The symmetry type graph of a 6-orbit map $\mathrm{Tr}(\mathcal{M})$, constructed by a proper combination of the $(1,2)$ 2-factors shown in Figure 7.7, contains either exactly one copy of the 2-factor (4), two copies of the 2-factor (3), or exactly one copy of the 2-factors (1), (2) and (3); joined consistently with the $(0,2)$ 2-factors in Figure 3.1. In fact, there are sixteen symmetry type graphs with six vertices that satisfy any of the three later conditions, depicted in Figures 7.11, 7.15 and 7.16. Furthermore. looking at the symmetry type graphs with 6 vertices in Figures 7.11, 7.15 and 7.16, we deduce the following observations on the sixteen symmetry types, that follow the latter paragraph.
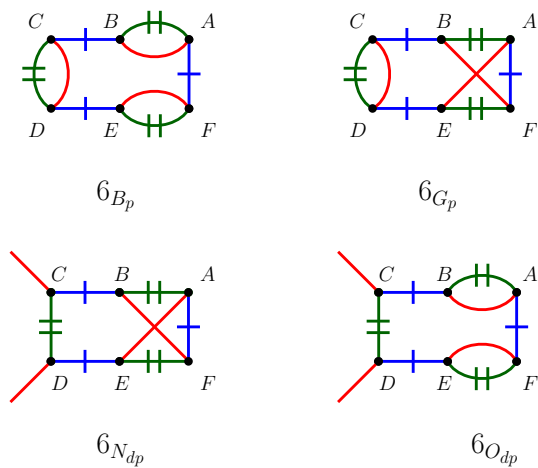
Figure 7.15: Possible symmetry type graphs of 6-orbit vertex-transitive maps $\mathrm{Tr}(\mathcal{M})$, where $\mathcal{M}$ is a 6-orbit map.
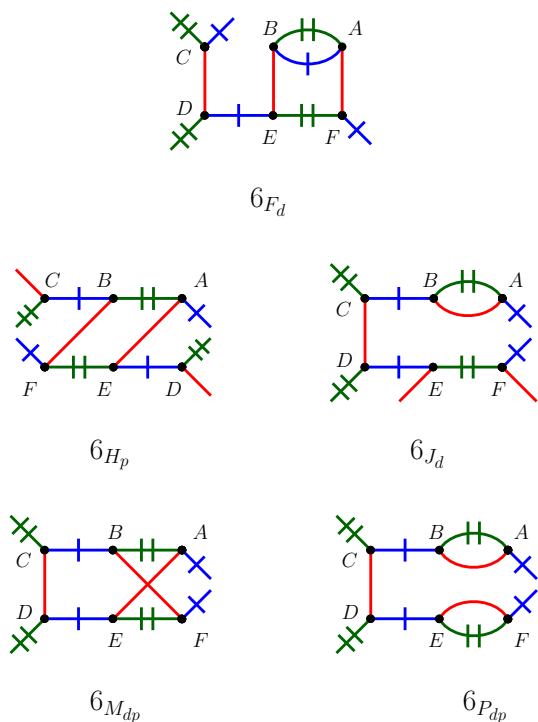

Figure 7.16: Possible symmetry type graphs of 6-orbit maps $\mathrm{Tr}(\mathcal{M})$ which are not vertex-transitive, derived from 6-orbit maps $\mathcal{M}$.

i) 6_B, has three face-orbits, each containing 2 flag-orbits (this corresponds to the truncation symmetry type graph of 2_{01});

ii) 6_{P_d}, has three face-orbits, one with 4 flag-orbits and the others with one flag-orbit each;

iii) 6_G, 6_H, 6_{M_d}, 6_{N_d}, 6_{O_d}, have two face-orbits, one with 4 flag-orbits and the other with 2 flag-orbits;

iv) 6_{H_p}, has two face-orbits, both with 3 flag-orbits;

v) 6_{J_d}, has two face-orbits, one with 5 flag-orbits and the other with one flag-orbit; and

vi) 6_{B_p} 6_{F_d}, 6_{G_p}, $6_{M_{dp}}$, $6_{N_{dp}}$, $6_{O_{dp}}$, $6_{P_{dp}}$, that are transitive on their faces.

As we will see next, the cases *ii)* and *iii)* above, are the only possible cases to be consider in manner to find when is that from a 4-orbit map $\mathcal{M}$ the truncation map $\mathrm{Tr}(\mathcal{M})$ is a 6-orbit map. The other cases will be considered when we study the truncation of 6-orbit maps. That is, suppose now that the map $\mathrm{Tr}(\mathcal{M})$ has symmetry type either 6_G, 6_H, 6_{M_d}, 6_{N_d}, 6_{O_d}, or 6_{P_d} (Figure 7.11). Then, consider the face-orbit in $\mathrm{Tr}(\mathcal{M})$ containing four flag-orbits, A, B, E and F (Figure 7.11), and continue as follows.

(a) Let $\mathrm{Tr}(\mathcal{M})$ be a 6-orbit map with symmetry type graph 6_G, 6_{N_d} or 6_{O_d}, and $(\mathcal{A}_0, \mathcal{A}_1, \mathcal{A}_2)$ a partition of its set of flags $\mathcal{F}(\mathrm{Tr}(\mathcal{M}))$. If we suppose that there is a flag $\Upsilon \in \mathcal{A}_0$ in the orbit A of $\mathcal{F}(\mathrm{Tr}(\mathcal{M}))$, then the flags $\Upsilon^2 \in \mathcal{A}_2$, and $\Upsilon^{2,1} \in \mathcal{A}_1$ belong to the orbits F and E, respectively. These three later flags induce a flag $\Phi_\Upsilon \in \mathcal{F}(\mathcal{M})$, with $\Upsilon_2 \in V(\mathcal{M})$. Consequently, it can be seen that the flag $(\Phi_\Upsilon)^2 =: \Phi_{\Upsilon^1}$ represent a distinct type of flags than Φ_Υ, since $\Upsilon^1 \in \mathcal{A}_0$, $\Upsilon^{1,2} \in \mathcal{A}_2$ and $\Upsilon^{1,2,1} \in \mathcal{A}_1$ belong to the flag-orbits B, C and D in $\mathrm{Tr}(\mathcal{M})$, respectively. These two flags, Φ_Υ and Φ_{Υ^1}, are as the first two flags shown in Figure 7.17 (*a*). Similarly, we can obtain the other two types of flags in $\mathcal{M}$, represented by the flags $(\Phi_\Upsilon)^{2,1}$ and $(\Phi_\Upsilon)^{2,1,2}$. Thus, we deduce the corresponding symmetry type of the 4-orbit map $\mathcal{M}$.

(b) Similarly, for a 6-orbit map $\mathrm{Tr}(\mathcal{M})$ with symmetry type graph 6_H, 6_{M_d} or 6_{P_d}, and a partition $(\mathcal{A}_0, \mathcal{A}_1, \mathcal{A}_2)$ of its set of flags $\mathcal{F}(\mathrm{Tr}(\mathcal{M}))$. If there is a flag $\Upsilon \in \mathcal{A}_0$ that belongs to the orbit A of $\mathcal{F}(\mathrm{Tr}(\mathcal{M}))$, then the flags $\Upsilon^2 \in \mathcal{A}_2$, and $\Upsilon^{2,1} \in \mathcal{A}_1$ are flags in the orbits A and B, respectively. Hence, the induced flag $\Phi_\Upsilon \in \mathcal{F}(\mathcal{M})$ corresponds to the first type of flags shown in Figure 7.17 (*b*), with $\Upsilon_2 \in V(\mathcal{M})$. Moreover, the flag $(\Phi_\Upsilon)^2 =: \Phi_{\Upsilon^1}$ is composed by a flag $\Upsilon^1 \in \mathcal{A}_0$ in the flag orbit B and two flags $\Upsilon^{1,2} \in \mathcal{A}_2$ and $\Upsilon^{1,2,1} \in \mathcal{A}_1$ in the orbit C in $\mathrm{Tr}(\mathcal{M})$ is of different type than $\Phi_\Upsilon \in \mathcal{F}(\mathcal{M})$. Furthermore, the flags $(\Phi_\Upsilon)^{2,1}$ and $(\Phi_\Upsilon)^{2,1,2}$ represent other two different types of flags in $\mathcal{M}$. In such way, we complete the list of different types of flag in $\mathcal{M}$, deducing that $\mathcal{M}$ is a 4-orbit map.
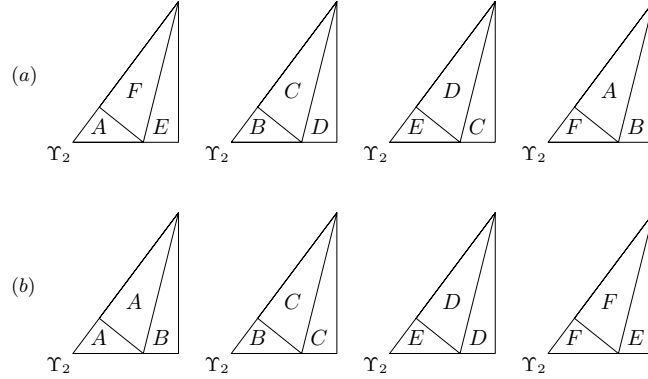
Figure 7.17: Representative flags of 4-orbit maps, as assembled flags in a 6-orbit map $\mathrm{Tr}(\mathcal{M})$, where in (a) $\mathrm{Tr}(\mathcal{M})$ has symmetry type graph 6_G, 6_{N_d} or 6_{O_d}, and in (b) $\mathrm{Tr}(\mathcal{M})$ has symmetry type graph 6_H, 6_{M_d} or 6_{P_d}. The element $\Upsilon_2 \in V(\mathcal{M})$ corresponds to face of the base flag $\Upsilon \in \mathcal{F}(\mathrm{Tr}(\mathcal{M}))$.

Consequently, we obtain the following proposition.

Proposition 7.6. *If the truncation* $\mathrm{Tr}(\mathcal{M})$ *of a 4-orbit map* $\mathcal{M}$ *is a 6-orbit map, then exactly one of the following holds.*

(i) $\mathcal{M}$ *is of type* 4_B *and* $\mathrm{Tr}(\mathcal{M})$ *are of type* 6_{P_d},

(ii) $\mathcal{M}$ *is of type* 4_C *and* $\mathrm{Tr}(\mathcal{M})$ *is of type* 6_{O_d},

(iii) $\mathcal{M}$ *is of type* 4_G *and* $\mathrm{Tr}(\mathcal{M})$ *is either of type* 6_{N_d} *or of type* 6_{M_d}, *or*

(iv) $\mathcal{M}$ *is of type* 4_H *and* $\mathrm{Tr}(\mathcal{M})$ *is either of type* 6_G *or of type* 6_H.

To conclude with the truncation of 4-orbit maps, we shall point out that there are twenty two truncated symmetry type graphs with 12 vertices, corresponding to the twenty two symmetry type graphs with four vertices, determined by applying the algorithm in Figure 7.3 to each.

Truncation of 5-orbit maps.

Similarly to the previous section, if $\mathcal{M}$ is a 5-orbit map, its truncation map $\mathrm{Tr}(\mathcal{M})$ is either a 5-orbit or a 15-orbit map.

Notice that out of the thirteen different symmetry type graphs of 5-orbit maps, (see Figure 3.7), the only possible combination of the (1,2) 2-factors with 2 and 3 vertices in Figure 7.7 is the symmetry type 5_{B_d} (Figure 7.18). This is, a 5-orbit map $\mathrm{Tr}(\mathcal{M})$ is the truncation of a 5-orbit map $\mathcal{M}$, if $\mathrm{Tr}(\mathcal{M})$ is of type 5_{B_d}.

$$5_{B_d}$$
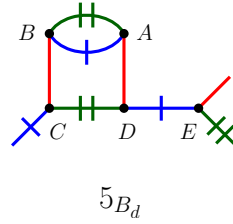
Figure 7.18: Only possible symmetry type graph of a 5-orbit map, corresponding to the trunca-
tion of another 5-orbit map.

Let $(\mathcal{A}_0, \mathcal{A}_1, \mathcal{A}_2)$ be the partition on the flags of a map $\mathrm{Tr}(\mathcal{M})$ with symmetry type graph 5_{B_d}, such that the flags $\Upsilon \in \mathcal{A}_0$, $\Upsilon^2 \in \mathcal{A}_2$ and $\Upsilon^{2,1} \in \mathcal{A}_1$ induce the flag $\Phi_\Upsilon \in \mathcal{F}(\mathcal{M})$. Clearly, the maps of type 5_{B_d} are face-transitive. Then, without lost of generality we can assume that the flag $\Upsilon \in \mathcal{A}_0$ belongs to the flag-orbit A of $\mathrm{Tr}(\mathcal{M})$, and define the face Υ_2 as an element in $V(\mathcal{M})$. Observe that the flags $\Upsilon^2 \in \mathcal{A}_2$ and $\Upsilon^{2,1} \in \mathcal{A}_1$ are flags in the orbits B and A, respectively. Hence, $\Phi_\Upsilon \in \mathcal{F}(\mathcal{M})$ represents one type of the flags of $\mathcal{M}$. Moreover, the flags $\Phi_{\Upsilon^1}, \Phi_{\Upsilon^{1,0}}, \Phi_{\Upsilon^0}, \Phi_{\Upsilon^{0,1}} \in \mathcal{F}(\mathcal{M})$, represent the other four types of flags in $\mathcal{F}(\mathcal{M})$, with Υ^1, $\Upsilon^{1,0}$, Υ^0 and $\Upsilon^{0,1}$ flags in the orbits B, C, D and E of $\mathcal{F}(\mathrm{Tr}(\mathcal{M}))$, respectively, see Figure 7.19. Obtaining the following Proposition.
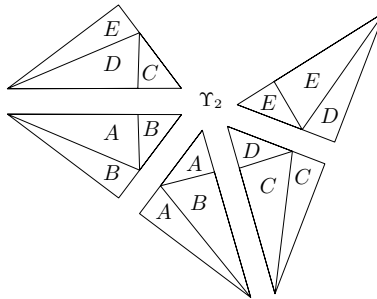
Figure 7.19: Representative flags of a 5-orbit map $\mathcal{M}$ as assembled flags from the truncation map $\mathrm{Tr}(\mathcal{M})$, where $\Upsilon_2 \in V(\mathcal{M})$ is the corresponding face in $\mathrm{Tr}(\mathcal{M})$ in a base flag $\Upsilon \in \mathcal{F}(\mathrm{Tr}(\mathcal{M}))$.

Proposition 7.7. *If the truncation* $\mathrm{Tr}(\mathcal{M})$ *of a 5-orbit map is a 5-orbit map, then* $\mathcal{M}$ *is of type* 5_{B_p} *and* $\mathrm{Tr}(\mathcal{M})$ *is of type* 5_{B_d}.

With regards to the truncated symmetry type graphs with 15 vertices that correspond to the all thirteen symmetry type graphs with five vertices we can apply the algorithm in Figure 7.3 to the symmetry type graphs shown in Figure 3.7.

Truncation of 6-orbit maps.

Given a 6-orbit map $\mathcal{M}$, we know that its truncation map $\mathrm{Tr}(\mathcal{M})$ has either 6, 9 or 18 orbits on its flags. In this part of the section we go through the remaining nine possible symmetry type of 6-orbit maps: 6_{H_p}, 6_{J_d}, 6_{B_p}, 6_{F_d}, 6_{G_p}, $6_{M_{dp}}$, $6_{N_{dp}}$, $6_{O_{dp}}$ and $6_{P_{dp}}$. As it was mentioned while we studied the truncation of 4-orbit maps, these later symmetry type of 6-orbit maps might correspond to the truncation map $\mathrm{Tr}(\mathcal{M})$ of some map $\mathcal{M}$. Further on, we find the possible symmetry type graphs with 9 vertices that correspond to the truncation $\mathrm{Tr}(\mathcal{M})$ of a map $\mathcal{M}$ and determine which of them are related to the truncation of a 6-orbit or 9-orbit map.

Observe that a map $\mathrm{Tr}(\mathcal{M})$ with symmetry type graph 6_{B_p}, 6_{G_p}, $6_{N_{dp}}$, or $6_{O_{dp}}$ is transitive on its sets of faces and vertices, under the action of its automorphism group, see Figure 7.15. Consider, the partition $(\mathcal{A}_0, \mathcal{A}_1, \mathcal{A}_2)$ on the flags of a map $\mathrm{Tr}(\mathcal{M})$, such that the flags $\Upsilon \in \mathcal{A}_0$, $\Upsilon^2 \in \mathcal{A}_2$ and $\Upsilon^{2,1} \in \mathcal{A}_1$ induce a flag $\Phi_\Upsilon \in \mathcal{F}(\mathcal{M})$. Then, every face in $\mathrm{Tr}(\mathcal{M})$ contains flags of the six flag-orbits of $\mathcal{F}(\mathrm{Tr}(\mathcal{M}))$. Hence, for any flag $\Upsilon \in \mathcal{A}_0$ we can define a face Υ_2 in $\mathrm{Tr}(\mathcal{M})$ as an element in $V(\mathcal{M})$. Moreover, as we saw previously in similar cases, the choice of orbit of $\mathcal{F}(\mathrm{Tr}(\mathcal{M}))$ is independent for the flag $\Upsilon \in \mathcal{A}_0$ because the face $\Upsilon_2 \in V(\mathcal{M})$ contains flags in all six orbits, and the connectivity of the graph $T(\mathrm{Tr}(\mathcal{M}))$ infers the same graph (up to isomorphisms) $T(\mathcal{M})$, defined by the same type of flags for $\mathcal{F}(\mathcal{M})$ after we apply the "untruncation" method. Therefore, we proceed with our construction as follows. If there is a flag $\Upsilon \in \mathcal{A}_0$ that belongs to the flag-orbit A of $\mathcal{F}(\mathrm{Tr}(\mathcal{M}))$, say, it follows that the flags $\Upsilon^2 \in \mathcal{A}_2$ and $\Upsilon^{2,1} \in \mathcal{A}_1$ are in the flag-orbits B and C of $\mathcal{F}(\mathrm{Tr}(\mathcal{M}))$, respectively. Hence, the induced flag $\Phi_\Upsilon \in \mathcal{F}(\mathcal{M})$ is described as the very left flag in Figure 7.20. Consequently, the flag $(\Phi_\Upsilon)^2 =: \Phi_{\Upsilon^1}$ is induced by the

Figure 7.20: Representative flags of a 6-orbit map $\mathcal{M}$, as assembled flags of a vertex- and face-transitive 6-orbit map $\mathrm{Tr}(\mathcal{M})$, where $\Upsilon_2 \in V(\mathcal{M})$ is the corresponding face in $\mathrm{Tr}(\mathcal{M})$ in a base flag $\Upsilon \in \mathcal{F}(\mathrm{Tr}(\mathcal{M}))$.

flags $\Upsilon^1 \in \mathcal{A}_0$, $\Upsilon^{1,2} \in \mathcal{A}_2$ and $\Upsilon^{1,2,1} \in \mathcal{A}_1$ in the orbits F, E and D, respectively. This later is shown in the very right side in Figure 7.20. Following with this procedure, we can find that there are exactly six types of flags for the map $\mathcal{M}$, all in the same vertex orbit that $\Upsilon_2 \in V(\mathcal{M})$. Therefore, $\mathcal{M}$ is a 6-orbit vertex-transitive map with symmetry type either 6_{B_p}, 6_{G_p}, $6_{M_{opp}}$, or $6_{P_{opp}}$ whose truncation 6-orbit map has symmetry type graph

either 6_{B_p}, 6_{G_p}, $6_{N_{dp}}$ or $6_{O_{dp}}$, respectively.

Concerning the possible symmetry type graphs of maps, depicted in Figure 7.16, that the 6-orbit map $\mathrm{Tr}(\mathcal{M})$ might have, we recall the following observations.

iv) A map with symmetry type 6_{H_p} has two face-orbits, both with 3 flag-orbits.

v) A map with symmetry type 6_{J_d} has two face-orbits, one with 5 flag-orbits and the other with one flag-orbit.

vi) A map with symmetry type 6_{F_d}, $6_{M_{dp}}$ or $6_{P_{dp}}$ is face-transitive.

This latter observations infer that unlike to the previous analysis, the construction of the map $\mathcal{M}$ from a 6-orbit map $\mathrm{Tr}(\mathcal{M})$ is not that straight-forward. Nevertheless, it can be seen that for each map $\mathrm{Tr}(\mathcal{M})$ with symmetry type graph as those in Figure 7.16, the resulting symmetry type of the corresponding map $\mathcal{M}$ after we apply the "untruncation" method has the same type of vertex-orbits in $\mathcal{M}$ than face-orbits in $\mathrm{Tr}(\mathcal{M})$. Hence, the construction of the map $\mathcal{M}$ is independent of the choice of flag and of orbit that we consider in $\mathcal{F}(\mathrm{Tr}(\mathcal{M}))$. Therefore, we can always choose a flag $\Upsilon \in \mathcal{F}(\mathrm{Tr}(\mathcal{M}))$ in any flag-orbit of $\mathrm{Tr}(\mathcal{M})$ and define its face Υ_2 in $\mathrm{Tr}(\mathcal{M})$ as an element in $V(\mathcal{M})$. That is, any choice of flag and of orbit in $\mathcal{F}(\mathrm{Tr}(\mathcal{M}))$ will yield the same result on the symmetry type of $\mathcal{M}$.

Given the partition $(\mathcal{A}_0, \mathcal{A}_1, \mathcal{A}_2)$ of the flags of $\mathrm{Tr}(\mathcal{M})$. Suppose that the flag $\Upsilon \in \mathcal{A}_0$ is a flag in the flag-orbit F in $\mathrm{Tr}(\mathcal{M})$. Then, the flags $\Upsilon^2 \in \mathcal{A}_2$ and $\Upsilon^{2,1} \in \mathcal{A}_1$ are in the flag-orbits E and D of $\mathcal{F}(\mathrm{Tr}(\mathcal{M}))$, respectively. Inducing a flag $\Phi_\Upsilon \in \mathcal{F}(\mathcal{M})$ (as the very right one of the Figure 7.21 (a) and (b)), that represents one type of flags of $\mathcal{F}(\mathcal{M})$. Suppose that the face Υ_2 is an element in $V(\mathcal{M})$ and $\mathrm{Tr}(\mathcal{M})$ has symmetry type graph either

(a) 6_{F_d}. Then, it follows that the flags $\Phi_{\Upsilon^0} := (\Phi_\Upsilon)^1$, $\Phi_{\Upsilon^{0,1}} := (\Phi_\Upsilon)^{1,2}$, $\Phi_{\Upsilon^{0,1,0}} := (\Phi_\Upsilon)^{1,2,1}$, $\Phi_{\Upsilon^{0,1,0,1}} := (\Phi_\Upsilon)^{1,2,1,2}$, and $\Phi_{\Upsilon^{0,1,0,1,0}} := (\Phi_\Upsilon)^{1,2,1,2,1}$ in $\mathcal{F}(\mathcal{M})$ describe other five types of flags in $\mathcal{M}$, distinct than Φ_Υ, with $\Upsilon, \Upsilon^0, \Upsilon^{0,1}, \Upsilon^{0,1,0}, \Upsilon^{0,1,0,1}, \Upsilon^{0,1,0,1,0} \in \mathcal{A}_0$,; or

(b) 6_{H_p}, 6_{J_d}, $6_{M_{dp}}$ or $6_{P_{dp}}$. Following the adjacency on the flags in $\mathrm{Tr}(\mathcal{M})$ and arranging the flag $(\Phi_\Upsilon)^2 \in \mathcal{F}(\mathcal{M})$, we obtain that this is of the same type as Φ_Υ, in all four cases. However, the corresponding flags to $(\Phi_\Upsilon)^0$ and $(\Phi_\Upsilon)^1$ in $\mathcal{F}(\mathcal{M})$, determine other three types of flags in $\mathcal{F}(\mathcal{M})$. These latter are described by flags of $\mathcal{A}_0$ in the orbits A, B or E, inducing that their corresponding 2-adjacent flags in $\mathcal{A}_2$ and $(2,1)$-adjacent flags in $\mathcal{A}_1$ belong to the flag-orbits B, A, or F and C, A and F, respectively. These three types of flags, in $\mathcal{F}(\mathcal{M})$, are the first, second and fifth flags depicted in Figure 7.21, from left to right, respectively. By the connectivity of
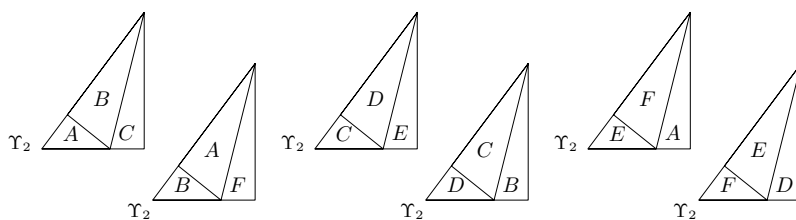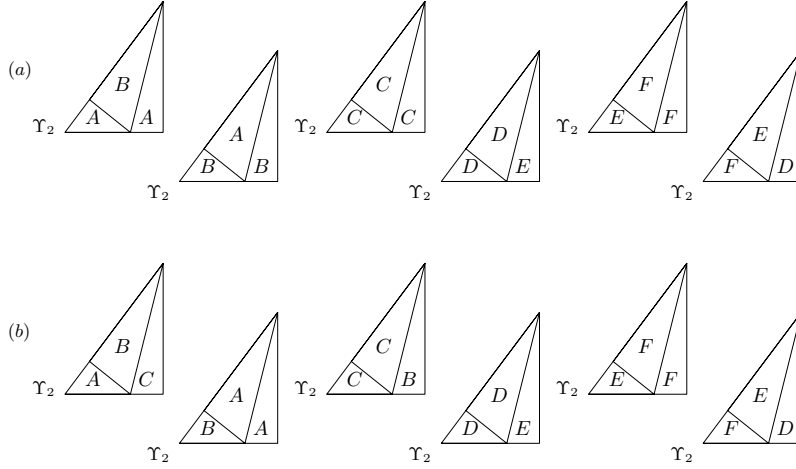
Figure 7.21: Reresentative flags of a 6-orbit maps, as assembled flags of the no vertex-transitive 6-orbit map $\mathrm{Tr}(\mathcal{M})$ with (a) symmetry type 6_{F_d}, and (b) symmetry type 6_{H_p}, 6_{J_d}, $6_{M_{dp}}$ or $6_{P_{dp}}$, where $\Upsilon_2 \in V(\mathcal{M})$ is the corresponding face in $\mathrm{Tr}(\mathcal{M})$ in a base flag $\Upsilon \in \mathcal{F}(\mathrm{Tr}(\mathcal{M}))$.

$\mathcal{G}_{\mathrm{Tr}(\mathcal{M})}$ we can proceed in a similar fashion and find the remaining two other types of flags in $\mathcal{F}(\mathcal{M})$ and determine the cubic 3-edge-coloured connected graph $T(\mathcal{M})$.

We conclude with the following proposition.

Proposition 7.8. *If the truncation* $\mathrm{Tr}(\mathcal{M})$ *of a 6-orbit map is a 6-orbit map, then one of the following holds.*

(i) $\mathcal{M}$ *and* $\mathrm{Tr}(\mathcal{M})$ *are of type* 6_{B_p},

(ii) $\mathcal{M}$ *and* $\mathrm{Tr}(\mathcal{M})$ *are of type* 6_{G_p},

(iii) $\mathcal{M}$ *and* $\mathrm{Tr}(\mathcal{M})$ *are of type* 6_{H_p},

(iv) $\mathcal{M}$ *is of type* 6_{J_p} *and* $\mathrm{Tr}(\mathcal{M})$ *is of type* 6_{J_d},

(v) $\mathcal{M}$ *is of type* $6_{M_{opp}}$ *and* $\mathrm{Tr}(\mathcal{M})$ *is of type* $6_{N_{dp}}$,

(vi) $\mathcal{M}$ *is of type* $6_{N_{opp}}$ *and* $\mathrm{Tr}(\mathcal{M})$ *is of type* 6_{F_d} *or of type* $6_{M_{dp}}$,

(vii) $\mathcal{M}$ *is of type* $6_{O_{opp}}$ *and* $\mathrm{Tr}(\mathcal{M})$ *is of type* $6_{P_{dp}}$, *or*

(viii) $\mathcal{M}$ *is of type* $6_{P_{opp}}$ *and* $\mathrm{Tr}(\mathcal{M})$ *is of type* $6_{O_{dp}}$.

The truncation of a 6-orbit map $\mathcal{M}$ can be a 9-orbit or a 18-orbit map. We shall say that there are seventy possible symmetry type graphs with 18 vertices, obtained by

applying once more the so called algorithm in Figure 7.3 to each symmetry type graph $T(\mathcal{M})$ with 6 vertices. (Forty-two of the symmetry type of maps with 6 vertices are mentioned together in this chapter and in Chapter 4, the other twenty-two can easily be founded by applying the dual and Petrie operators.)

Finally, to determine which of the many symmetry types of 9-orbit maps correspond to be the symmetry type of the truncation $\mathrm{Tr}(\mathcal{M})$ of a 6-orbit map $\mathcal{M}$, we recall the necessary $(0,2)$ and $(1,2)$ 2-factors in Figures 3.1 and 7.7, respectively, that the symmetry type graph of the truncation of a map must contain. There are exactly ten possible symmetry type graphs with 9 vertices that satisfy the conditions to correspond to the symmetry type of a 9-orbit map $\mathrm{Tr}(\mathcal{M})$, as the truncation on either a 3-orbit, a 6-orbit or a 9-orbit map $\mathcal{M}$, see Figure 7.22.

In fact, applying the algorithm in Figure 7.3 to the three symmetry type graphs of 3-orbit maps, it can be seen that the three graphs labelled by 9_A, 9_B and 9_{C_d} in Figure 7.22 are isomorphic to the truncated symmetry type graphs of the symmetry type graphs 3^0, 3^2 and 3^{02}, respectively. Moreover, applying the "untruncation" method to a 9-orbit map $\mathrm{Tr}(\mathcal{M})$ with symmetry type either 9_A, 9_B or 9_{C_d} in such way that if we suppose that each flag $\Upsilon \in \mathcal{A}_0$ belongs either to the flag-orbit C, D or I (Figure 7.22), then the flags $\Upsilon^2 \in \mathcal{A}_2$ and $\Upsilon^{2,1}$ are in the flag orbits B, E or H and A, F or G, respectively. Where $(\mathcal{A}_0, \mathcal{A}_1, \mathcal{A}_2)$ is the proper partition of the set $\mathcal{F}(\mathrm{Tr}(\mathcal{M}))$, induced by Proposition 7.1.

Furthermore, suppose that a map $\mathrm{Tr}(\mathcal{M})$ of type 9_A, 9_B or 9_{C_d} with the corresponding partition $(\mathcal{A}_0, \mathcal{A}_1, \mathcal{A}_2)$ of the set $\mathcal{F}(\mathrm{Tr}(\mathcal{M}))$ such that a flag $\Upsilon \in \mathcal{A}_0$, does not belong to the flag-orbits C, D nor I, unlike in the above paragraph. Then, applying the "untruncation" method, it can be seen the we can obtain six the different flags that represent the flag-orbits of $\mathcal{M}$, as those shown in Figure 7.23 (a) or (b), respectively. Inducing the results in Proposition 7.9.

Proposition 7.9. *If the truncation $\mathrm{Tr}(\mathcal{M})$ of a 6-orbit map is a 9-orbit map, then one of the following holds.*

(i) *$\mathcal{M}$ is of type 6_D and $\mathrm{Tr}(\mathcal{M})$ is of type 9_A,*

(ii) *$\mathcal{M}$ is of type 6_F and $\mathrm{Tr}(\mathcal{M})$ is of type 9_B, or*

(iii) *$\mathcal{M}$ is of type $6_{M_{opp}}$ and $\mathrm{Tr}(\mathcal{M})$ is of type 9_{C_d}.*

The remaining symmetry type graphs in Figure 7.22 of 9-orbit maps, different from 9_A, 9_B and 9_{C_d} will be study next, on the analysis of the truncation of 9-orbit maps.
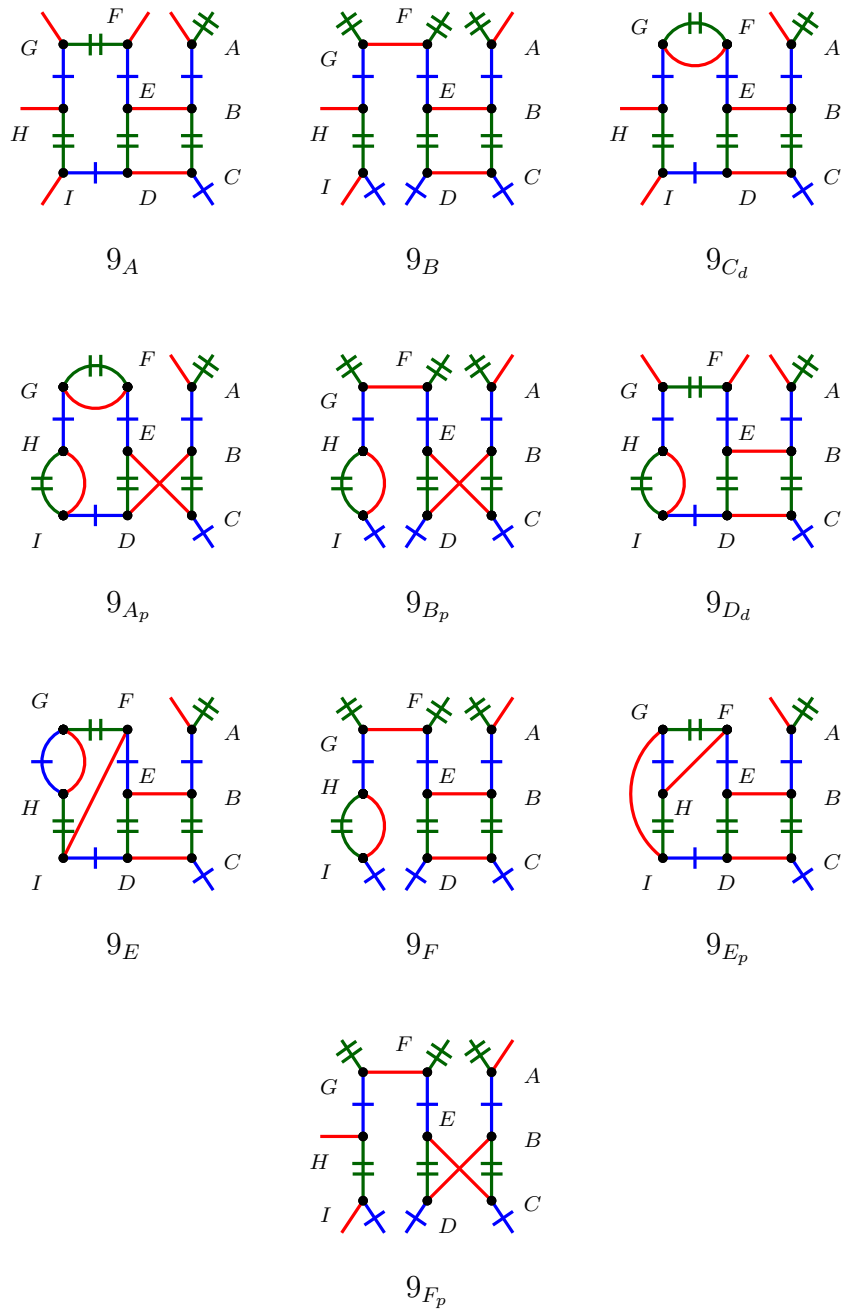
Figure 7.22: Symmetry type graphs with 9 vertices of truncated 3-orbit, 6-orbit or 9-orbit maps.
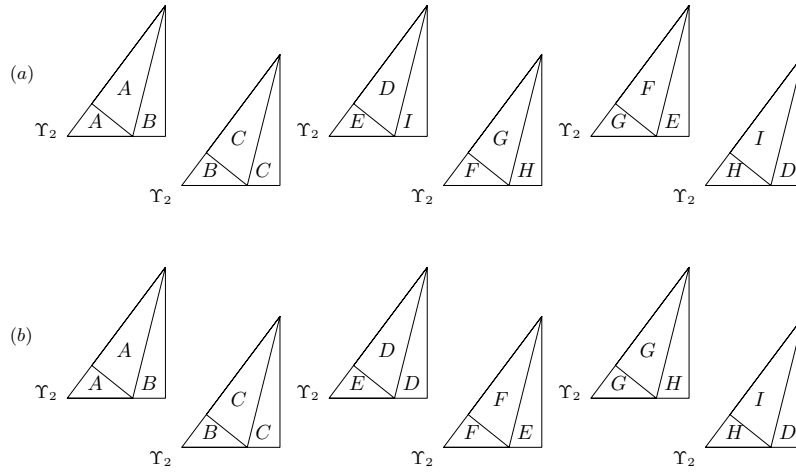
Figure 7.23: Representative flags of 6-orbit maps, as assembled flags of the 9-orbit map $\mathrm{Tr}(\mathcal{M})$, where in (a) $\mathrm{Tr}(\mathcal{M})$ has symmetry type graph 9_A or 9_{C_d}, and in (b) $\mathrm{Tr}(\mathcal{M})$ has symmetry type graph 9_B. The element $\Upsilon_2 \in V(\mathcal{M})$ correspond to a face in $\mathrm{Tr}(\mathcal{M})$ in a base flag $\Upsilon \in \mathcal{F}(\mathrm{Tr}(\mathcal{M}))$.

Truncation of 7-orbit and 9-orbit maps.

In this part we complete the study on truncation of k-orbit maps with $k \leq 7$ and $k = 9$. Once again, one can find all truncated symmetry type graphs with 21 and with 27 vertices, associated to each symmetry type graphs with 7 and 9 vertices, respectively, by applying the algorithm in Figure 7.3, once that is known the symmetry type graph $T(\mathcal{M})$ with 7 or with 9 vertices.

By a proper combination of the (1,2) 2-factors in Figure 7.7, it can be seen that there are exactly two different symmetry type graphs with 7 vertices: 7_J and 7_{J_p}, that correspond to the symmetry type of the truncation of a 7-orbit map, depicted in the Figure 7.24. Let $\mathrm{Tr}(\mathcal{M})$ be a map with symmetry type either 7_J or 7_{J_p}, and $(\mathcal{A}_0, \mathcal{A}_1, \mathcal{A}_2)$
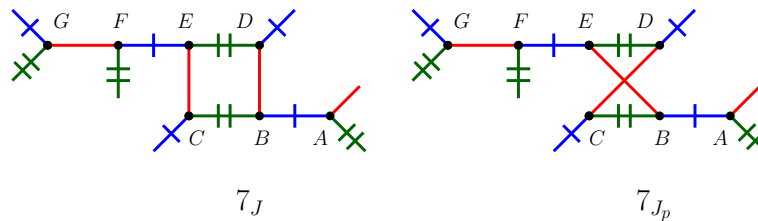
Figure 7.24: Symmetry type graphs with 7 vertices of truncated 7-orbit maps.

the partition on the flags of $\mathrm{Tr}(\mathcal{M})$. The analysis of these 7-orbit maps $\mathrm{Tr}(\mathcal{M})$ results similar to that for the 4-orbit truncated map with symmetry type graph 4_{D_p}. Observe that a map $\mathrm{Tr}(\mathcal{M})$ with symmetry type 7_J has two face-orbits, one with four flag-orbits

and the other with three flag-orbits in $\mathrm{Tr}(\mathcal{M})$. While, a map $\mathrm{Tr}(\mathcal{M})$ with symmetry type 7_{J_p} also has two face-orbits, but one has five flag-orbits and the other has two flag-orbits in $\mathrm{Tr}(\mathcal{M})$. In fact, for both cases when $\mathrm{Tr}(\mathcal{M})$ has symmetry type either 7_J or 7_{J_p}, the construction of the map $\mathcal{M}$ is independent of the choice of flag $\Upsilon \in \mathcal{A}_0$ and of flag orbit in $\mathcal{F}(\mathrm{Tr}(\mathcal{M}))$ as we find out next.

Supposing that the flag $\Upsilon \in \mathcal{A}_0$ is a flag in the orbit A, then the flags $\Upsilon^2 \in \mathcal{A}_2$ and $\Upsilon^{2,1} \in \mathcal{A}_1$ are in the orbits A and B, respectively. Thus, the induced flag $\Phi_\Upsilon \in \mathcal{F}(\mathcal{M})$ represents the very left type of flag of the 7 different flags in Figure 7.25, in $\mathcal{M}$. Moreover,


Figure 7.25: Representative flags of 7-orbit maps, as assembled flags of the corresponding truncated 7-orbit map $\mathrm{Tr}(\mathcal{M})$, where $\Upsilon_2 \in V(\mathcal{M})$ is the corresponding face in $\mathrm{Tr}(\mathcal{M})$ in a base flag $\Upsilon \in \mathcal{F}(\mathrm{Tr}(\mathcal{M}))$.

the flag $(\Phi_\Upsilon)^1 =: \Phi_{\Upsilon^0}$ is of the same type as Φ_Υ in $\mathcal{M}$. However, the flags $(\Phi_\Upsilon)^0$ and $(\Phi_\Upsilon)^2$ represent two different different types of flags in $\mathcal{M}$, also depicted in Figure 7.25. Following the adjacencies of the flags in $\mathcal{G}_{\mathrm{Tr}(\mathcal{M})}$ and arranging flags in $\mathcal{M}$, we can easily find the remaining types of flags in $\mathcal{M}$, as those in Figure 7.25. Consequently, it follows Proposition 7.10.

Proposition 7.10. *If the truncation $\mathrm{Tr}(\mathcal{M})$ of a 7-orbit map is again a 7-orbit map, then one of the following holds.*

(i) $\mathcal{M}$ is of type 7_K and $\mathrm{Tr}(\mathcal{M})$ is of type 7_J, or

(ii) $\mathcal{M}$ is of type 7_L and $\mathrm{Tr}(\mathcal{M})$ is of type 7_{J_p}.

Regarding to the truncation map $\mathrm{Tr}(\mathcal{M})$ of a 9-orbit map $\mathcal{M}$. Recall the symmetry type graphs of 9-orbit maps, different of 9_A, 9_B and 9_{C_d}, in Figure 7.22. Let $\mathrm{Tr}(\mathcal{M})$ be a map with symmetry type 9_{A_p}, 9_{B_p}, 9_{D_d}, 9_E, 9_{E_p}, 9_F, or 9_{F_p}, and consider the partition $(\mathcal{A}_0, \mathcal{A}_1, \mathcal{A}_2)$ of the set $\mathcal{F}(\mathrm{Tr}(\mathcal{M}))$. Observe that the maps with symmetry type

- 9_{A_p} or 9_{E_p} are face-transitive.

- 9_{B_p} have two face-orbits, one with three flag-orbits and the other with six flags-orbits.

- 9_{D_d} have two face-orbits, one with four flag-orbits and the other with five flags-orbits.

- 9_E or 9_F have two face-orbits, one with two flag-orbits and the other with seven flags-orbits.

- 9_{F_p} have three face-orbits, one with all flags in the same flag-orbit, other with three flag-orbits and the third one with five flags-orbits.

Hence, we follow in a similar fashion and choose any flag in the partition $\mathcal{A}_0$ and suppose this is in a particular flag-orbit, say A, in $\mathrm{Tr}(\mathcal{M})$. Then, we apply the "untruncation" method and construct the map $\mathcal{M}$ and obtain two sets of 9 different flags of the truncation map $\mathrm{Tr}(\mathcal{M})$ as those in Figure 7.26. Where the set (a) correspond to maps $\mathrm{Tr}(\mathcal{M})$ with
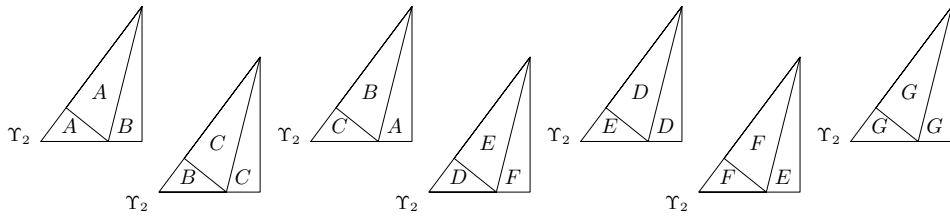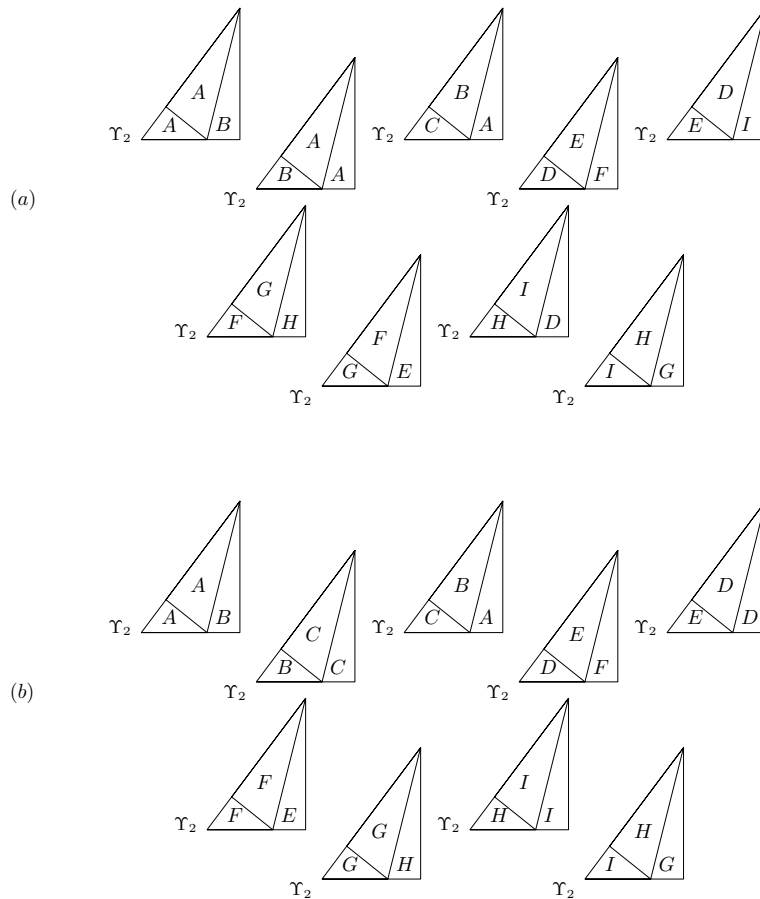

Figure 7.26: Representative flags of maps 9-orbit maps, as assembled flags of the truncated 9-orbit map $\mathrm{Tr}(\mathcal{M})$, where in (a) $\mathrm{Tr}(\mathcal{M})$ has symmetry type graph 9_{A_p}, 9_{D_d}, 9_E, or 9_{E_p}, and in (b) $\mathrm{Tr}(\mathcal{M})$ has symmetry type graph 9_{B_p}, 9_F, or 9_{F_p}. The element $\Upsilon_2 \in V(\mathcal{M})$ corresponds to the face in $\mathrm{Tr}(\mathcal{M})$ in a base flag $\Upsilon \in \mathcal{F}(\mathrm{Tr}(\mathcal{M}))$.

symmetry type 9_{A_p}, 9_{D_d}, 9_E, or 9_{E_p} and the set (b) to maps $\mathrm{Tr}(\mathcal{M})$ with symmetry type 9_{B_p}, 9_F, or 9_{F_p}. Inducing the following Proposition.

Proposition 7.11. *If the truncation* $\mathrm{Tr}(\mathcal{M})$ *of a 9-orbit map is again a 9-orbit map, then one of the following holds.*

(i) $\mathcal{M}$ *is of type* 9_C *and* $\mathrm{Tr}(\mathcal{M})$ *is of type* 9_{B_p},

(ii) $\mathcal{M}$ *is of type* 9_{G_p} *and* $\mathrm{Tr}(\mathcal{M})$ *is of type* 9_{E_p},

(iii) $\mathcal{M}$ *is of type* 9_{H_p} *and* $\mathrm{Tr}(\mathcal{M})$ *is of type* 9_{A_p}.

(iv) $\mathcal{M}$ *is of type* 9_I *and* $\mathrm{Tr}(\mathcal{M})$ *is of type* 9_{D_d},

(v) $\mathcal{M}$ *is of type* 9_J *and* $\mathrm{Tr}(\mathcal{M})$ *is of type* 9_E,

(vi) $\mathcal{M}$ *is of type* 9_K *and* $\mathrm{Tr}(\mathcal{M})$ *is of type* 9_F, *or*

(vii) $\mathcal{M}$ *is of type* 9_L *and* $\mathrm{Tr}(\mathcal{M})$ *is of type* 9_{F_p}.

In this way, we conclude with the results obtained so far on truncation of k-orbit maps, with $k = 1, \ldots, 6, 7, 9$. Such results are listed in the Tables 7.1 and 7.2.

Sym type of $\mathcal{M}$	Sym type of $\mathrm{Tr}(\mathcal{M})$ with		
	k orbits	$\frac{3k}{2}$ orbits	$3k$-orbits
1	1	—	3^0
2	2	—	6_{N_d}
2_0	—	—	6_G
2_2	2_{12}	—	6_{M_d}
2_1	—	—	6_{O_d}
2_{01}	2_0	3^0	6_B
2_{12}	—	—	6_{P_d}
2_{02}	—	—	6_H
3^0	—	—	9_A
3^2	—	—	9_B
3^{02}	3^{02}	—	9_{C_d}
4_B	—	6_{P_d}	12_B
4_C	—	6_{O_d}	12_C
4_{D_p}	4_{D_p}	—	12_D
4_E	4_D	—	12_E
4_G	—	$6_{N_d}, 6_{M_d}$	12_G
4_{G_d}	4_G	—	12_H
4_H	—	$6_G, 6_H$	12_C
5_{B_p}	5_{B_d}	—	15_A

Table 7.1: Truncation symmetry types of k-orbit maps, with $1 \leq k \leq 5$.

Sym type of $\mathcal{M}$	Sym type of $\text{Le}(\mathcal{M})$ with		
	k orbits	$\frac{3k}{2}$ orbits	$3k$-orbits
6_{B_p}	6_{B_p}	—	18_B
6_D	—	9_A	18_D
6_F	—	9_B	18_F
6_{G_p}	6_{G_p}	—	18_G
6_{H_p}	6_{H_p}	—	18_H
6_{J_p}	6_{J_d}	—	18_J
$6_{M_{opp}}$	$6_{N_{dp}}$	9_{C_d}	18_M
$6_{N_{opp}}$	$6_{F_d}, 6_{M_{dp}}$	—	18_N
$6_{O_{opp}}$	$6_{P_{dp}}$	—	18_O
$6_{P_{opp}}$	$6_{O_{dp}}$	—	18_P
7_K	7_J	—	21_K
7_L	7_{J_p}	—	21_L
9_C	9_{B_p}	—	27_C
9_{G_p}	9_{E_p}	—	27_G
9_{H_p}	9_{A_p}	—	27_H
9_I	9_{D_d}	—	27_I
9_J	9_E	—	27_J
9_K	9_F	—	27_K
9_L	9_{F_p}	—	27_L

Table 7.2: Truncation symmetry types of k-orbit maps, with $k = 6, 7, 9$.

7.2 Composition of dual and truncation

For a given map $\mathcal{M}$, the vertices of its truncation map $\text{Tr}(\mathcal{M})$ have valency 3. Then, the dual map of $\text{Tr}(\mathcal{M})$ is a map with triangular faces. Hence, there is a correspondence between the sets of vertices and faces of $\mathcal{M}$ with the vertex set of the dual map $(\text{Tr}(\mathcal{M}))^*$, also known as the *two-dimensional subdivision* of $\mathcal{M}$, [49]. In Figure 7.27 is depicted the two-dimensional subdivision of the icosahedron or dual map of the truncated icosahedron. Its flag graph can easily be founded by exchanging the colours i and $2-i$, with $i \in \{0, 1, 2\}$, on the edges of the graphs $\mathcal{G}_{\text{Tr}(\mathcal{M})}$ and $\mathcal{G}_{(\text{Tr}(\mathcal{M}))^*}$ as it was mentioned in section 4.1. Thus, the following proposition is a consequence from Proposition 7.1.

Proposition 7.12. *The flag graph* $\mathcal{G}_{(\text{Tr}(\mathcal{M}))^*}$, *of the two-dimensional subdivision map* $(\text{Tr}(\mathcal{M}))^*$ *of any map* $\mathcal{M}$, *can be quotient into a graph as the symmetry type graph* 3^2.
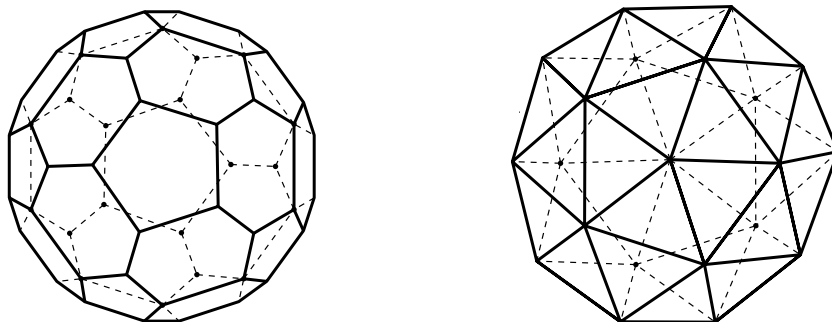
Figure 7.27: Trunated icosahedron (left) and the two-dimensional subdivision of the icosahedron (right).

However, if we consider the truncation of the dual of a map $\mathcal{M}^*$, then we produce a map isomorphic to the map known as the *leapfrog* map $\text{Le}(\mathcal{M})$ of a map $\mathcal{M}$, [49, 24, 18]. In other words, $\text{Le}(\mathcal{M}) \cong \text{Tr}(\mathcal{M}^*)$. And this gives a completely different result than the map $(\text{Tr}(\mathcal{M}))^*$ as one can see below.

7.2.1   Leapfrog: trucation of dual map.

As we said before, the leapfrog map $\text{Le}(\mathcal{M})$ of $\mathcal{M}$ is isomorphic to the truncation of the dual map $\mathcal{M}^*$ of $\mathcal{M}$. One way to construct the leapfrog map $\text{Le}(\mathcal{M})$ of the map $\mathcal{M}$ is by drawing, on the surface, a perpendicular edge to each edge of $\mathcal{M}$ and joining by an edge the two end points of two edges if the corresponding edges in $\mathcal{M}$ share a vertex and belong to the same face. In this way, we obtain a one-to-one correspondence between the faces of $\text{Le}(\mathcal{M})$ and the set of faces and vertices of $\mathcal{M}$. In Figure 7.28 is shown the image of the icosahedron after apply the leapfrog operation.
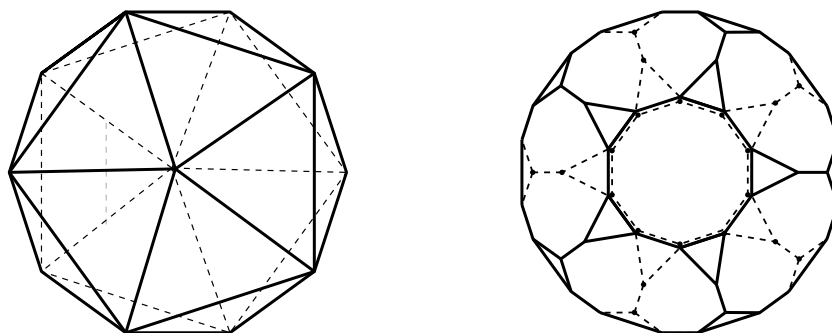
Figure 7.28: Icosahedron (left) and its leapfrog image (right), isomorphic to the truncated dodecahedron.

Notice that all the vertices of the map $\mathrm{Le}(\mathcal{M})$ have valence three. The faces of $\mathrm{Le}(\mathcal{M})$ that are in correspondence with the faces of $\mathcal{M}$ remain of the same length, while the faces of $\mathrm{Le}(\mathcal{M})$ that correspond to the vertices of $\mathcal{M}$ are of length two times the valence of its corresponding vertex. It is not hard to see that if $\mathcal{M}$ contains $|E|$ edges, then the map $\mathrm{Le}(\mathcal{M})$ contains $3|E|$ edges.

As is depicted in the Figure 7.29, every flag in $\mathcal{F}(\mathcal{M})$ is divided into three different flags of the leapfrog map $\mathrm{Le}(\mathcal{M})$. Let $\Phi = (\Phi_0, \Phi_1, \Phi_2) \in \mathcal{F}(\mathcal{M})$ be a flag in
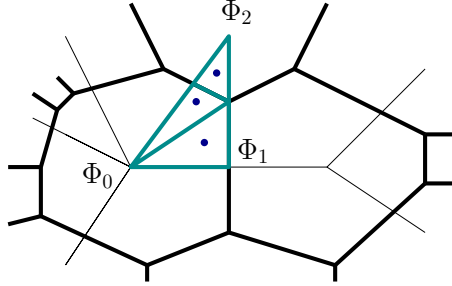

Figure 7.29: The three respective flags of $\mathcal{F}(\mathrm{Le}(\mathcal{M}))$ to the flag $\Phi = (\Phi_0, \Phi_1, \Phi_2) \in \mathcal{F}(\mathcal{M})$.

$\mathcal{F}(\mathcal{M})$, then $(\Phi, 0) := (\{\Phi_1, \Phi_2\}, \Phi_1, \Phi_0\})$, $(\Phi, 1) := (\{\Phi_1, \Phi_2\}, \{\Phi_0, \Phi_2\}, \Phi_0)$ and $(\Phi, 2) := (\{\Phi_1, \Phi_2\}, \{\Phi_0, \Phi_2\}, \Phi_2)$, denote the three corresponding flags of Φ in $\mathcal{F}(\mathrm{Le}(\mathcal{M}))$. The adjacency between these is given as follows.

$$(\Phi, 0)^0 = (\Phi^{s_2}, 0), \qquad (\Phi, 0)^1 = (\Phi, 1), \qquad (\Phi, 0)^2 = (\Phi^{s_0}, 0);$$
$$(\Phi, 1)^0 = (\Phi^{s_1}, 1), \qquad (\Phi, 1)^1 = (\Phi, 0), \qquad (\Phi, 1)^2 = (\Phi, 2);$$
$$(\Phi, 2)^0 = (\Phi^{s_1}, 2), \qquad (\Phi, 2)^1 = (\Phi^{s_0}, 2), \qquad (\Phi, 2)^2 = (\Phi, 1).$$

Let l_0, l_1 and l_2 be the distinguished generators of the monodromy group $\mathrm{Mon}(\mathrm{Le}(\mathcal{M}))$, with $(l_1 l_2)^3 = id$. Thus, we also present the algorithm shown in Figure 7.30 to construct, from $\mathcal{G}_{\mathcal{M}}$, the flag graph of $\mathrm{Le}(\mathcal{M})$.

Recall that a k-orbit map $\mathcal{M}$ which truncation map $\mathrm{Tr}(\mathcal{M})$ is a k-orbit or a $\frac{3k}{2}$-orbit map, can be quotient into a graph isomorphic to the symmetry type graph 2_{01}, [45]. Meaning that there exist a bipartition (A, B) on the vertices of $\mathcal{G}_{\mathcal{M}}$ such that each vertex in the partition A is adjacent to a vertex in the partition B by and edge of colour 2. In addition, recall that there is a bijection $\delta : \mathcal{F}(\mathcal{M}) \to \mathcal{F}(\mathcal{M}^*)$ such that for each $\Phi \in \mathcal{F}(\mathcal{M})$ and each $i \in \{0, 1, 2\}$, $\Phi^i \delta = (\Phi\delta)^{2-i}$. Since $\mathrm{Le}(\mathcal{M}) \cong \mathrm{Tr}(\mathcal{M}^*)$, we shall say that a k-orbit map $\mathcal{M}$ such that its leapfrog map is a k-orbit or a $\frac{3k}{2}$-orbit map, can be quotient into a graph as the symmetry type graph 2_{12}.

However, based on the algorithm in Figure 7.30, observe that we can give the partition $(\mathcal{A}_0, \mathcal{A}_1, \mathcal{A}_2)$ of the vertices of the flag graph $\mathcal{G}_{\mathrm{Le}(\mathcal{M})}$ of the leapfrog map $\mathrm{Le}(\mathcal{M})$ in such way that for each vertex $\Upsilon \in \mathcal{F}(\mathrm{Le}(\mathcal{M}))$ in the partition $\mathcal{A}_2$, the vertices Υ^2 and $\Upsilon^{2,1}$
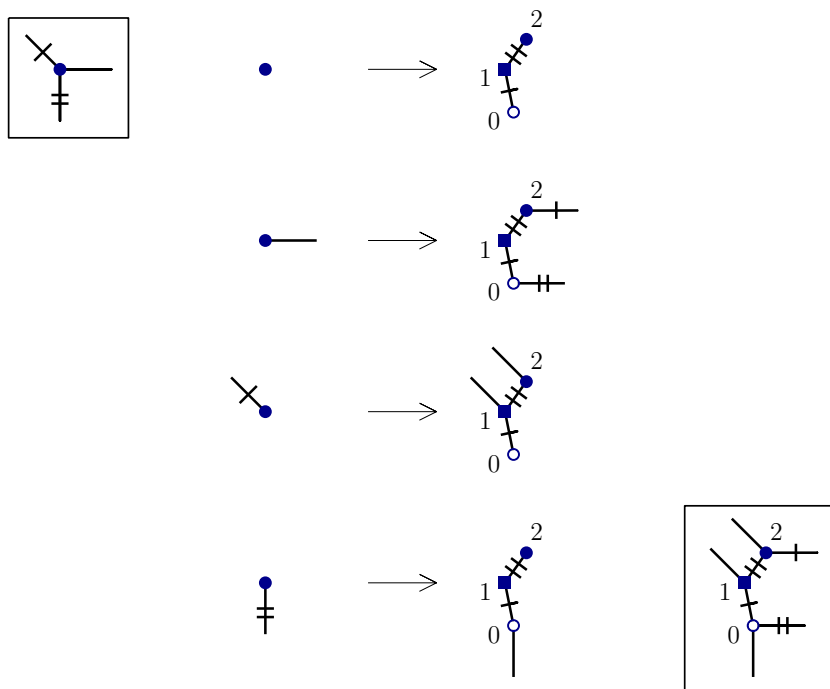
Figure 7.30: Any local representation of a flag, in the left. The result under the medial operation, locally obtained, in the right.

correspond to the partitions $\mathcal{A}_1$ and $\mathcal{A}_2$, respectively. Thus, the assembling these flags we obtain a new flag $\Phi_\Upsilon := \{\Upsilon, \Upsilon^2, \Upsilon^{2,1}\} \in \mathcal{F}(\mathcal{M})$, where the face Υ_2 will be considered as an element of $F(\mathcal{M})$. Hence, we obtain the following proposition.

Proposition 7.13. *The flag graph $\mathcal{G}_{\mathrm{Le}(\mathcal{M})}$, of the leapfrog map $\mathrm{Le}(\mathcal{M})$ of any map $\mathcal{M}$, can be quotient into a graph as the symmetry type graph 3^0.*

Therefore, by the results on truncation, shown in the Tables 7.1 and 7.2, we can obtain the classification given in the Table 7.3 where are listed the symmetry types that the map $\mathrm{Le}(\mathcal{M})$ can have.

Sym type of $\mathcal{M}$	Sym type of $\mathrm{Le}(\mathcal{M})$ with		
	k orbits	$\frac{3k}{2}$ orbits	$3k$-orbits
1	1	—	3^0
2	2	—	6_{N_d}
2_0	2_{12}	—	6_{M_d}
2_2	—	—	6_G
2_1	—	—	6_{O_d}
2_{01}	—	—	6_{P_d}
2_{12}	2_0	3^0	6_B
2_{02}	—	—	6_H
3^0	—	—	9_B
3^2	—	—	9_A
3^{02}	3^{02}	—	9_{C_d}
4_{B_d}	—	6_{P_d}	12_B
4_{C_d}	—	6_{O_d}	12_C
4_{D_p}	4_{D_p}	—	12_D
4_{E_d}	4_D	—	12_E
4_G	4_G	—	12_H
4_{G_d}	—	$6_{N_d}, 6_{M_d}$	12_G
4_{H_d}	—	$6_G, 6_H$	12_C
5_{B_p}	5_{B_d}	—	15_A
6_{B_p}	6_{B_p}	—	18_B
6_{D_d}	—	9_A	18_D
6_{F_d}	—	9_B	18_F
6_{G_p}	6_{G_p}	—	18_G
6_{H_p}	6_{H_p}	—	18_H
6_{J_p}	6_{J_d}	—	18_J
$6_{M_{dp}}$	$6_{N_{dp}}$	9_{C_d}	18_M
$6_{N_{dp}}$	$6_{F_d}, 6_{M_{dp}}$	—	18_N
$6_{O_{dp}}$	$6_{P_{dp}}$	—	18_O
$6_{P_{dp}}$	$6_{O_{dp}}$	—	18_P
7_{K_d}	7_J	—	21_K
7_{L_d}	7_{J_p}	—	21_L
9_{C_d}	9_{B_p}	—	27_C
$9_{G_{pd}}$	9_{E_p}	—	27_G
$9_{H_{pd}}$	9_{A_p}	—	27_H
9_{I_d}	9_{D_d}	—	27_I
9_{J_d}	9_E	—	27_J
9_{K_d}	9_F	—	27_K
9_{L_d}	9_{F_p}	—	27_L

Table 7.3: Leapfrog symmetry types k-orbit maps, with $1 \leq k \leq 7$ and $k = 9$.

Conclusions

Symmetry type graphs have numerous applications and admit powerful generalizations. For instance, in [44] Orbanić, Pellicer, Pisanski and Tucker (2011), show the edge-transitive maps fall into 14 types, obtained in [26, 53], each of them described by its symmetry type graph. In this thesis, with the symmetry type graph, we have presented a method that helps in enumerate the possible symmetry types of maniplexes, from the action of the automorphism group of the maniplex on its set of flags.

The main results of the first part of the thesis were presented in Chapter 3, where we also present all possible symmetry type graphs of 2-maniplexes of up to 5 vertices, classify 3-orbit maniplexes and give generators of their automorphism groups. In particular, we show that 3-orbit maniplexes are never fully-transitive, but they are i-face-transitive for all but one or two values of i, depending on the symmetry type. We extend further the study of symmetry type graphs to show that if a 4-orbit maniplex is not fully-transitive, then it is i-face-transitive for all i but at most three ranks. Moreover, we show that a fully-transitive 3-maniplex that is not regular cannot have an odd number of orbits of flags, under the action of the automorphism group. Also, given the symmetry type graph of a maniplex we give generators for the automorphism group of a k-orbit maniplex with respect to some base flag, Theorem 3.5.

In the second part of the thesis, we saw how symmetry type graphs can also be applied to operations on maps, such as medial, chamfering and truncation. Medial operation helped us to find the possible symmetry types of the medial k-orbit map, with $k \leq 5$. With truncation operation we completed a classification of possible symmetry types for the truncation and leapfrog of k-orbit maps for $k \leq 7$ and $k = 9$.

Furthermore, joining the results obtained for the medial and truncation operations on k-orbit maps, together with the results obtained for the chamfering operation on k-orbit maps, we obtain the following table, where are listed all possible number of flag-orbits of a map $\mathcal{M}'$ with regards to $k = |\mathrm{Orb}(\mathcal{M})|$, where $\mathcal{M}'$ is the medial, truncation or chamfering map of $\mathcal{M}$.

$\mathcal{M}'$	$\text{Me}(\mathcal{M})$	$\text{Tr}(\mathcal{M})$	$\text{Cham}(\mathcal{M})$		
$|\text{Orb}(\mathcal{M}')|$	$2k$ or k	$3k$, $\frac{3k}{2}$ or k	$4k$,	$2k$	or k
				$k|3$	$k = 1, 2, 3, 6$

Table 7.4: Possible number of flag-orbits of a map $\mathcal{M}'$ with regard to $k = |\text{Orb}(\mathcal{M})|$, where $\mathcal{M}'$ is the medial, truncation or chamfering map of $\mathcal{M}$.

Regarding the symmetry types of maniplexes, in order to characterize the symmetry types of k-orbit maniplexes, as well it was done in this thesis for 2-maniplexes, we lead to the open problems of study different operations on maniplexes and the symmetry types of maniplexes that are obtained from applying such operations on a maniplex.

Bibliography

[1] G. Araujo-Pardo, I. Hubard, D. Oliveros and E. Schulte, Colorful polytopes and graphs. Isr. J. Math. **xxx** (2012).

[2] A. T. Balaban and T. Pisanski, Flag graphs and their applications in mathematical chemistry for benzenoids. *J. Math. Chem.* **50 (4)** (2012) 893–903.

[3] A. Bondy and U. S. R. Murty, *Graph theory.* Graduate Texts in Mathematics, Springer **244** (2008).

[4] G. Brinkmann, N. Van Cleemput and T. Pisanski, Generation of various classes of trivalent graphs. *Theor. Comp. Sci.* **502** (2013) 16–29.

[5] P. J. Cameron, *Permutation groups.* London Mathematical Society Student Texts **45**. (1999).

[6] H. S. M. Coxeter, The densities of the regular polytopes. Proc. Camb. Phil. Soc., **27** (1931) 201–211.

[7] H. S. M. Coxeter, *Regular polytopes.* Third edition. Dover Publications, Inc., New York (1973).

[8] H. S. M. Coxeter, *Regular Complex Polytopes (2nd edition).* Cambridge University Press, Cambridge (1991).

[9] H. S. M. Coxeter and W. O. J. Moser, *Generators and relations for discrete groups.* Springer-Verlag. Berlin, Göttigen, Heidelberg (1957).

[10] G. Cunningham, M. del Río-Francos, I. Hubard and M. Toledo, Symmetry type graphs of polytopes and maniplexes, Annals of Combinatorics, in press.

[11] M. del Río Francos, Truncated symmetry type graphs. Ars Combinatoria, in press.

[12] M. del Río Francos, Chamfering operation on k-orbit maps. submitted.

[13] M. del Río-Francos, I. Hubard, A. Orbanić and T. Pisanski, Medial Symmetry type graphs, Electronic J. of Comb. **20 (3)** (2013) P29.

[14] O. Delgado Friedrichs and D. H. Huson, Tiling space by Platonic solids. I. Discrete Comput. Geom. **21 (2)** (1999) 299–315.

[15] A. Deza, M. Deza and V. P. Grishukhim, Fullerenes and coodination polyhedra versus half-cube embeddings *Disc. Math.* **192** (1998) 41-80.

[16] R. Diestel, *Graph theory* Graduate Texts in Mathematics, Springer **173** (2000).

[17] M. V. Diudea and R. B. King, The chirality of icosahedral fullerenes: a comparison of tripling (leapfrog), quadrupling (chamfering), and septupling (capra) transformations. *J. Math. Chem.* **39 (314)** (2006) 597-604.

[18] M. V. Diudea, P. E. John, A. Graovac, M. Primorac and T. Pisanski, Leapfrog and Related Operations on Toroidal Fullerenes. Croat. Chem. Acta, **76 (2)** (2003), 153-159.

[19] J. D. Dixon and B. Mortimer, *Permutation Groups.* Graduate texts in mathematics, Springer **163** (1996).

[20] A. W. M. Dress, Presentations of discrete groups, acting on simply connected manifolds, in terms of parametrized systems of Coxeter matrices. Adv. in Math. **63 (2)** (1987) 196–212.

[21] A. W. M. Dress and D. H. Huson, On Tilings of the Plane. Geometriae Dedicata, **24** (1987) 295–310.

[22] A. W. M. Dress and G. Brinkmann, Phantasmagorical Fulleroids. MATCH Commun. Math. Comput. Chem., **33** (1996) 87–100.

[23] R. Duarte, *2-Restrictedly-regular hypermaps of small genus.* PhD thesis, University of Aveiro, Aveiro, Portugal (2007).

[24] P. Fowler and T. Pisanski, Leapfrog Transformations and Polyhedra of Clar Type. J. Chem.Soc.Faraday Trans., **90 (19)** (1994), 2865-2871.

[25] C. Godsil and G. F. Royle, *Algebraic graph theory.* Graduate Texts in Mathematics, 207, Springer-Verlag, New York, (2001).

[26] J. E. Graver and M. E. Watkins, Locally finite, planar, edge-transitive graphs. Mem. Amer. Math. Soc., **126 (601)** (1997) 75 p.

[27] J. L. Gross and T. W. Tucker, *Topological Graph Theory.* Wiley Interscience Series in Discrete Mathematics and Optimization (1987).

[28] M. I. Hartley, I. Hubard and D. Leemans, Two atlases of abstract chiral polytopes for small groups. *Ars Math. Contemp.* **5** (2012) 371–382.

[29] I Hubard, Two-orbit polyhedra from groups. European J. Combin., **31 (3)** (2010) 943–960.

[30] I. Hubard, *From geometry to groups and back: The study of highly symmetric polytopes*, ProQuest LLC, Ann Arbor, MI, 2007, Thesis (Ph.D.)ï¿$\frac{1}{2}$York University (Canada). MR 2712832

[31] I. Hubard, A. Orbanić, D. Pellicer and A. I. Weiss, Symmetries of equivelar 4-toroids. Disc. Comp. Geom. **48** (2012) 1110–1136.

[32] I. Hubard, A. Orbanić and A. I. Weiss, Monodromy groups and self-invariance. Canad. J. Math., **61 (6)** (2009) 1300–1324.

[33] I. Hubard and A. I. Weiss, Self-duality of chiral polytopes. J. Combin. Theory Ser. A **111 (1)** (2005) 128–136.

[34] D. H. Huson, The generation and classification of tile-k-transitive tilings of Euclidean plane, the sphere and the hyperbolic plane Geom. Dedicata **47 (3)** (1993) 269–296.

[35] G. A. Jones and J. S. Thornton, Operations on Maps, and Outer Automorphisms. J. Combin. Theory, Ser. B **35 (2)** (1983) 93–103.

[36] J. Kocič, Symmetry-type graphs of Platonic and Archimedean solids, Mathematical Communications **16** (2011), 491–507.

[37] S. Lins, Graph-Encoded Maps. J. Comb. Theory, Ser. B **32 (2)** (1982) 171–181.

[38] A. Malnič, Action graphs and coverings. Discrete Mathematics. **244 (1-3)** (2002) 299-322.

[39] P. McMullen, Regular polytopes of nearly full rank: Addendum Discrete Comput. Geom. **49 (3)** (2013) 703–705.

[40] P. McMullen and E. Schulte, *Abstract Regular Polytopes*. Encyclopedia of Mathematics and its Applictions, Volume 92, Cambridge University Press (Cambridge - New York, 2002), 566 pp.

[41] P. McMullen, Ch. Schulz and J. M. Wills, Equivelar polyhedral manifolds in E^3. Israel J. Math. **41 (4)** (1982), 331–346.

[42] A. Orbanić, Database of small non-degenerate edge-transitive maps. `http://www.ijp.si/RegularMaps`

[43] A. Orbanić, *Edge-transitive maps* PhD thesis, Unniversity of Ljubljana, Ljubljana, Slovenia (2006).

[44] A. Orbanić, D. Pellicer, T. Pisanski and T. W. Tucker, Edge-transitive maps of low genus. *Ars Math. Contemp.* **4 (2)** (2011) 385–402.

[45] A. Orbanić, D. Pellicer and A. I. Weiss, Map operation and k-orbit maps. J. Combin. Theory, Ser. A **117 (4)** (2009) 411–429.

[46] D. Pellicer, Developments and open problems on chiral polytopes. *Ars Math. Contemp.* **5** (2012) 333–354.

[47] D. Pinto, Duality of hypermaps with symmetric or alternating monodromy group, *Ars Math. Contemp.* **5** (2012) 259–354.

[48] T. Pisanski, A classification of cubic bicirculants. *Disc. Math.* **307 (3–5)** (2007) 567–578.

[49] T. Pisanski and M. Randić, Bridges between geometry and graph theory. Geometry at work, MAA Notes, 53, Math. Assoc. America, Washington, DC, (2000) 174–194.

[50] T. Pisanski and A. Žitnik, Representing graphs and maps. In *Topics in topological graph theory.* Edited by Lowell W. Beineke and Robin J. Wilson. Encyclopedia of Mathematics and its Applications, 128. Cambridge University Press, Cambridge, (2009) 151–180.

[51] O. Schreier, Die Untergruppen der frein Gruppen. Abh. Math. Sem. Univ. Hamburg **5**, (1927) 161–183.

[52] J. Suárez, E. Gancedo, J. M. Álvarez and A. Morán, Truncating and chamfering diagrams of regular polyhedra Journal of Mathematical Chemistry, **46**, 1, 155-163 (2009).

[53] J. Širáň, T. W. Tucker and M. E. Watkins, Realizing finite edge-transitive orientable maps. J. Graph Theory, **37 (1)** (2001) 1–34.

[54] A. Vince, Combinatorial Maps J. Combin. Theory, Ser. B **34** (1983) 1-21.

[55] A. T. White. *Graphs of groups surfaces* North Holland Mathematics Studies **188** Elsevier (2001).

[56] S. E. Wilson, Maniplexes: Part 1: Maps, Polytopes, Symmetry and Operators, Symmetry, **4** (2012), 265–275.

[57] S. E. Wilson, Operators over regular maps. Pacific J. Math., **81 (2)** (1979) 559–568.

[58] S. E. Wilson, Uniform Maps on the Klein Bottle. J. Geom. Graph., **10 (2)** (2006) 161–171.

Razširjeni povzetek

Uvod

Matematiki že od nekdaj z zanimanjem preučujejo simetrične objekte; tako se je npr. raziskovanje "najpravilnejših", t.i. platonskih in arhimedskih teles, začelo že v antiki. Ideja "najbolj simetričnega", t.j. regularnega ali platonskega poliedra, je kasneje navdihnila več pomembnih posplošitev: od regularnih zemljevidov do regularnih abstraktnih politopov.

Predmet naše raziskave so t.i. zemljevidi in manipleksi ranga n, katerih kombinatorična struktura je popolnoma določena z n-valentnim grafom s pobarvanimi (oz. z $0, 1, ..., n-1$ oštevilčenimi) povezavami, ki mu pogosto pravijo tudi praporni graf (ali graf praporov). Tak graf lahko razumemo tudi kot Schreierjev odsekovni graf ([9, 51]). Tako je npr. praporni graf zemljevida kubičen (trivalenten) graf. Abstraktni politopi so kombinatorične posplošitve klasičnih poliedrov in politopov ([40]), manipleksi pa so posplošitve zemljevidov na ploskvah in (prapornih grafov) abstraktnih politopov; tako lahko zemljevide obravnavamo kot maniplekse ranga 2 (ali 2-maniplekse). Nekaj drugih zanimivih lastnosti prapornih grafov je opisanih v [1].

Cilj disertacije je klasificirati simetrijske tipe manipleksov. V ta namen vpeljemo t.i. simetrijski graf manipleksa. Iz njega lahko razberemo različne lastnosti in informacije o simetrijah manipleksa ranga $n-1$, npr. njegovo morebitno regularnost, tranzitivnost po vozliščih, povezavah, licih ali katerihkoli drugih licih ranga $\leq n-1$. S pomočjo simetrijskih grafov lahko definiramo tudi simetrijske razrede manipleksov, in sicer tako, da vse maniplekse, katerih simetrijski grafi so izomorfni, uvrstimo v isti simetrijski razred, ki mu priredimo ustrezni simetrijski graf. Strategija za njihovo generiranje je razložena v [4]. Dress in Huson (1987) obravnavata takšne grafe kot Delaney-Dressove simbole, [21]. Dress in Brinkmann (1996) ter Balaban in Pisanski (2012) so jih uporabili v matematični kemiji, [22] in [2]. Simetrijski grafi platonskih in arhimedskih teles so določeni v [36].

Orbanić, Pellicer in Weiss so klasificirali k-orbitne zemljevide za $k \leq 4$ s pomočjo operacij na zemljevidih, npr. z operacijama sredinjenja (angl. medial) in prisekanja (angl. truncation) [45]. V tej disertaciji, ki jo je motiviralo njihovo delo, nadgradimo

njihove rezultate in podamo (z uporabo istih operacij na zemljevidih) klasifikacijo vseh k-orbitnih zemljevidov s $k \leq 6$ orbitami. Vse simetrijske tipe zemljevidov za $k \leq 10$ tudi oštevilčimo v strnjeni obliki (tabela 3.5). Poleg tega smo raziskali tudi nekatere druge operacije na zemljevidih, npr. operaciji brušenja (angl. chamfering) in preskoka (angl. leapfrog), kar je odprlo naslednje vprašanje: Koliko prapornih orbit ima zemljevid, ki ga dobimo iz k-orbitnega zemljevida, če na njem uporabimo katerokoli od (omenjenih) operacij na zemljevidih?

Vsebina disertacije je razdeljena na tri dele. V prvem delu predstavimo osnovne pojme teorije permutacijskih grup in teorije grafov ([5, 19], [3, 16]). Podobno, v poglavjih 2 in 3 najprej definiramo osnovne pojme in pregledno predstavimo osnovno teorijo zemljevidov, manipleksov in simetrijskih grafov, nato pa poiščemo vse možne simetrijske tipe k-orbitnih zemljevidov za vrednosti $k \leq 5$. Na koncu tega dela predstavimo tri dobro znane operatorje na zemljevidih in manipleksih: dual, petrial in nasprotni operator, ter analiziramo, kako morebitna dualnost zemljevida vpliva na njegov simetrijski graf oz. kako lahko definiramo razširjeni simetrijski graf sebi-dualnega (ali samodualnega) zemljevida.

V drugem delu predstavimo razširitev rezultatov iz [45] za operaciji sredinjenja in prisekanja k-orbitnih zemljevidov in raziščemo operaciji brušenja in preskoka. Vse štiri operacije lahko opišemo kot razdelitev trikotnikov, ki ustrezajo praporom prvotnega zemljevida, na manjše (glej npr. [32, 50]). Te operacije lahko opišemo tudi kot pravila za transformacijo praporega grafa prvotnega zemljevida v praporni graf njegovega sredinjenega, brušenega, prisekanega ali preskočenega zemljevida, in raziskujemo ustrezne simetrijske grafe. Odgovorimo tudi na vprašanje, kako operaciji prisekanja in preskoka vplivata na število praporih orbit zemljevida.

Nazadnje, v tretjem delu disertacije, predstavimo povzetek naših rezultatov in nakažemo možne nadaljnje smeri raziskovanja.

I. del

Zemljevidi in manipleksi

Topološko gledano lahko *zemljevid* $\mathcal{M}$ definiramo kot celično vložitev povezanega grafa v sklenjeno kompaktno ploskev. Vozlišča, povezave in lica v $\mathcal{M}$ imenujemo tudi 0-, 1- in 2-lica v $\mathcal{M}$. V letih 1982-83 sta Lins in Vince razvila koncept kombinatoričnih zemljevidov v [37] in [54]. V tej disertaciji uporabljamo prav takšno kombinatorično definicijo zemljevida. Torej, zemljevid $\mathcal{M}$ razumemo kot kubični graf $\mathcal{G}_{\mathcal{M}}$ z oštevilčenimi (pobarvanimi) povezavami, ki ga pogosto imenujejo *praporni graf* zemljevida.

Leta 2012 je Wilson, v želji da poenoti pojma zemljevidov in abstraktnih politopov, vpeljal koncept manipleksov [56]; bralcu priporočamo [40] za spoznavanje z osnovno teorijo

abstraktnih politopov. Čeprav abstraktnih politopov v tej disertaciji ne definiramo, ni težko preveriti, da lahko vse, kar pokažemo za maniplekse, prevedemo v ustrezne trditve o abstraktnih politopih (oz. o njihovih prapornih grafih), kakor je prikazano v [10]. Kombinatorična struktura *manipleksa* $\mathcal{M}$ ranga $n-1$ (ali $(n-1)$-*manipleksa*) je popolnoma določena s po povezavah pobarvanim n-valentnim grafom $\mathcal{G}_{\mathcal{M}}$ s kromatičnim številom n, ki ga pogosto imenujejo praporni graf. Tako npr. nedegenerirani zemljevidi ustrezajo 2-manipleksom.

Vsakemu manipleksu $\mathcal{M}$ ranga $n-1$ lahko priredimo podgrupo $\mathrm{Mon}(\mathcal{M})$ permutacijske grupe $Sym(\mathcal{F}(\mathcal{M}))$ njegove množice praporov $\mathcal{F}(\mathcal{M})$, t.i. *monodromijsko grupo* manipleksa $\mathcal{M}$. Monodromijska grupa $\mathrm{Mon}(\mathcal{M})$ $(n-1)$-manipleksa $\mathcal{M}$ je generirana z zaporedjem n involucij $(s_0, s_1, \ldots, s_{n-1})$; vsaka od involucij $s_i \in \mathrm{Mon}(\mathcal{M})$ preslika vsak prapor $\Phi \in \mathcal{F}(\mathcal{M})$ v njegov i-sosedni prapor. Poleg tega so vsi generatorji s_i in permutacije $s_i s_j$ za $|i-j| \geq 2$ brez fiksnih točk, grupa $\mathrm{Mon}(\mathcal{M})$ pa deluje tranzitivno na $\mathcal{F}(\mathcal{M})$.

Množica i-*lic* $(n-1)$-manipleksa ustreza prapornim orbitam v $\mathcal{F}(\mathcal{M})$, doloèenim z delovanjem grupe, generirane z množico $S_i := \{s_j | i \neq j\}$ za $i \in \{0, 1, \ldots, n\}$. Grupa $\mathrm{Mon}(\mathcal{M})$ na vsaki od množic i-lic deluje tranzitivno.

Avtomorfizem α n-manipleksa $\mathcal{M}$ je tak avtomorfizem grafa $\mathcal{G}_{\mathcal{M}}$, ki ohranja barve njegovih povezav. Torej lahko na α gledamo kot na permutacijo praporov v $\mathcal{F}$, ki komutira z vsako permutacijo iz monodromijske grupe. Ker je graf $\mathcal{G}_{\mathcal{M}}$ povezan, je delovanje grupe avtomorfizmov $\mathrm{Aut}(\mathcal{M})$ manipleksa $\mathcal{M}$ semiregularno na vozliščih grafa $\mathcal{G}_{\mathcal{M}}$. Pravimo, da je manipleks $\mathcal{M}$ i-*lično (ali po licih) tranzitiven*, če je grupa $\mathrm{Aut}(\mathcal{M})$ tranzitivna na licih ranga i. Manipleks $\mathcal{M}$ je *polno tranzitiven*, če je i-lično tranzitiven za vsak $i = 0, \ldots, n-1$.

Če ima $\mathrm{Aut}(\mathcal{M})$ k prapornih orbit v $\mathcal{M}$, pravimo, da je $\mathcal{M}$ k-*orbitni* manipleks. 1-orbitni manipleks imenujemo tudi regularen ali *refleksibilen* manipleks. 2-orbitni manipleks, v katerem sosedni prapori pripadajo različnim orbitam, je *kiralen* manipleks. Ta dva tipa zemljevidov in politopov sta bila po dolgem in počez raziskana ([40, 57] in [28, 33, 46]), zelo malo pa je znanega o takšnih, ki niso ne regularni ne kiralni.

Hubard v [30] karakterizira grupe avtomorfizmov 2-orbitnih in polno tranzitivnih poliedrov (t.j. vozliščno, povezavno in lično tranzitivnih poliedrov) s pomočjo različnih generatorjev (in relacij med njimi). Našla je tudi generatorje grupe avtomorfizmov 2-orbitnega politopa kateregakoli ranga. Duarte in Hubard sta v [23] in [29] raziskala vseh sedem tipov 2-orbitnih zemljevidov v različnih kontekstih.

Simetrijski grafi

V tem razdelku definiramo in podamo lastnosti n-valentnega grafa s pobarvanimi povezavami, ki ga imenujemo *simetrijski graf* $(n-1)$-manipleksa, $n \leq 3$. Simetrijski

graf $T(\mathcal{M})$ danega manipleksa $\mathcal{M}$ uporabimo kot orodje za določanje lastnosti $\mathcal{M}$ in za pridobitev informacij o njegovih simetrijah. Graf $T(\mathcal{M})$ je pravzaprav kvocientni graf prapornega grafa manipleksa $\mathcal{M}$, določen z delovanjem grupe avtomorfizmov $\mathcal{M}$ na praporih. Zato za opis strukture $T(\mathcal{M})$ v splošnem potrebujemo t.i. predgrafe, t.j. grafe, v katerih so dovoljene večkratne povezave in polpovezave (povezave z enim samim krajiščem). Notacija simetrijskega grafa je ekvivalentna Delaney-Dressovemu simbolu, opisanem v [21].

Očitno velja: če je $\mathcal{M}$ k-orbitni $(n-1)$-mapleks, potem ima $T(\mathcal{M})$ natanko k vozlišč. Torej je število tipov (oz. ekvivalenčnih razredov) k-orbitnih manipleksov odvisno od števila n-valentnih predgrafov na k točkah, ki so lahko pravilno pobarvani po povezavah s tremi barvami in katerih povezane komponente 2-faktorja z barvama i in j so vedno takšne kot na sliki 3.1 za $|i - j| \geq 2$. Obstaja natanko sedem tipov 2-orbitnih 2-manipleksov (slika 3.2) in le trije tipi 3-orbitnih 2-manipleksov (slika 3.3). Orbanić, Pellicer in Weiss v [45] študirajo vse tipe k-orbitnih 2-manipleksov v kontekstu zemljevidov za $k \leq 4$. Za simetrijske grafe 2-manipleksov s tremi ali štirimi orbitami v tej disertaciji uporabljamo notacijo iz [45].

Kot smo že poudarili, so simetrijski grafi refleksibilnega $(n-1)$-manipleksa sestavljeni iz enega vozlišča in n polpovezav. Klasifikacija dvo-orbitnih manipleksov v kontekstu lokalne konfiguracije njihovih praporov neposredno sledi iz nabora možnih simetrijskih grafov. Dejansko za vsak n obstaja $2^n - 1$ možnih simetrijskih grafov z dvema vozliščema in n (pol)povezavami, saj za vsako pravo podmnožico I barv $\{0, 1, \ldots, n-1\}$ obstaja simetrijski graf z dvema vozliščema in $|I|$ polpovezavami, ki ustrezajo barvam I povezav, incidentnih vsakemu od obeh vozlišč, in ker so vse povezave med dvema vozliščema pobarvane z barvami, ki niso v I (slika 3.4). Iz [29] in razmišljanja o n-politopu kot o $(n-1)$-manipleksu lahko sklepamo, da ta simetrijski graf natanko ustreza manipleksom razreda 2_I.

"Visoko simetrični" manipleksi (t.j. manipleksi z bogato grupo simetrij) so praviloma tisti z manj prapori in tisti z "visoko tranzitivnostjo" lic. Iz simetrijskega grafa n-manipleksa, oz. iz njegovih primerno pobarvanih podgrafov, lahko razberemo različne vrste tranzitivnosti lic danega manipleksa.

Izrek 1. *Naj bo $\mathcal{M}$ $(n-1)$-manipleks s simetrijskim grafom $T(\mathcal{M})$. Potem število povezanih komponent v $(n-1)$-faktorju grafa $T(\mathcal{M})$, pobarvanih z barvami $\{0, 1, \ldots, n-1\} \setminus \{i\}$, določa število orbit i-lic v $\mathcal{M}$ za $i \in \{0, 1, \ldots, n-1\}$.*

Tako npr. iz izreka 1 sledi, da ima povezavno-tranzitiven 2-manipleks $\mathcal{M}$ simetrijski graf $T(\mathcal{M})$ z eno samo povezano komponento 2-faktorja barv 0 in 2, kot grafi na sliki 3.1 za $i, j \in \{0, 2\}$. Torej ima $T(\mathcal{M})$ 1, 2 ali 4 vozlišča. Tako vidimo, da je povezavno-tranzitiven 2-manipleks 1-, 2- ali 4-orbitni 2-manipleks ([26]). Povezavno-tranzitivne zemljevide so študirali Širan, Tucker in Watkins [53]. Kot je poudarjeno v [45], obstaja 22 tipov 4-

orbitnih 2-manipleksov. Sedem povezavno-tranzitivnih je prikazanih na sliki 3.5, petnajst povezavno-netranzitivnih pa na sliki 3.6.

Za simetrijske grafe 3-orbitnih manipleksov lahko pokažemo, da obstaja natanko $2n-3$ različnih simetrijskih grafov 3-orbitnih manipleksov ranga $n-1$. Poleg tega, 3-orbitni manipleksi nikoli niso polno tranzitivni, so pa po i-lično tranzitivni za vse razen za eno ali dve vrednosti i, odvisno od simetrijskega tipa. Hitro ugotovimo, da je štetje oz. določanje vseh možnih simetrijskih grafov s $k \geq 4$ vozlišči in njihova morebitna klasifikacija po zgledu tistih za 2 ali 3 vozlišča, veliko zahtevnejši izziv. Kljub temu v tej disertaciji razširimo področje raziskovanja simetrijskih grafov in pokažemo, da če 4-orbitni manipleks ni polno tranzitiven, potem je i-lično tranzitiven za vse i, razen za največ tri range.

Analiza polno tranzitivnih n-manipleksov za $n \geq 3$ postane še veliko bolj zapletena. Hubard v [29] pokaže, da obstaja $2^{n+1} - n - 2$ razredov polno tranzitivnih dvo-orbitnih n-manipleksov. Po izreku 3.2 ne obstaja 3-orbitni polno tranzitiven n-manipleks. Razširimo 22 možnih grafov simetrijskih tipov 4-orbitnih 2-manipleksov z dodajanjem (semi)povezav barve 3 tako, da sta $(0,3)$ in $(1,3)$ 2-faktorja kot na sliki 3.1. Izkaže se, da obstaja 20 možnih grafov simetrijskih tipov 4-orbitnih 3-manipleksov, ki so polno tranzitivni (slika 3.14). Nadalje v tej disertaciji pokažemo, da polno tranzitivni 3-manipleks, če ni regularen, ne more imeti lihega števila prapornih orbit (glede na delovanje grupe avtomorfizmov).

Iz danega simetrijskega grafa manipleksa zlahka razberemo generatorje grupe avtomorfizmov k-orbitnega manipleksa glede na nek bazni prapor(izrek 2).

Izrek 2. *Naj bo $\mathcal{M}$ k-orbitni n-manipleks in naj bo $T(\mathcal{M})$ njegov simetrijski graf. Predpostavimo, da je $v_1, e_1, v_2, e_2 \ldots, e_{q-1}, v_q$ sprehod, ki obišče vsako vozlišče v $T(\mathcal{M})$, povezava e_i pa ima barvo a_i za vsak $i = 1, \ldots q-1$. Naj bo $S_i \subset \{0, \ldots, n-1\}$ takšen, da ima v_i polpovezavo barve s natanko takrat, ko je $s \in S_i$. Naj bo $B_{i,j} \subset \{0, \ldots, n-1\}$ množica barv povezav med vozliščema v_i in v_j (za $i < j$), ki nista v sprehodu, in naj bo $\Phi \in \mathcal{F}(\mathcal{M})$ bazni prapor v $\mathcal{M}$, katerega projekcija v $T(\mathcal{M})$ je v_1. Potem je grupa avtomorfizmov manipleksa $\mathcal{M}$ generirana z unijo množic*

$$\{\alpha_{a_1, a_2, \ldots, a_i, s, a_i, a_{i-1}, \ldots, a_1} \mid i = 1, \ldots, k-1, s \in S_i\},$$

in

$$\{\alpha_{a_1, a_2, \ldots, a_i, b, a_j, a_{j-1}, \ldots, a_1} \mid i, j \in \{1, \ldots, k-1\}, i < j, b \in B_{i,j}\}.$$

Naslednji dve posledici podajata množici generatorjev 2-orbitnih in 3-orbitnih politopov danega razreda. Notacija sledi tisti v izreku 2; če indeksi nekega α ne ustrezajo parametrom množice, se razume, da je tak avtomorfizem identiteta.

Posledica 1. *[30] Naj bo $\mathcal{M}$ 2-orbitni $(n-1)$-manipleks v razredu 2_I za nek $I \subset \{0, \ldots, n-1\}$ in naj bo $j_0 \notin I$. Potem je*

$$\{\alpha_i, \alpha_{j_0, i, j_0}, \alpha_{k, j_0} \mid i \in I, \ k \notin I\}$$

množica generatorjev grupe $\mathrm{Aut}(\mathcal{M})$.

Posledica 2. *Naj bo* $\mathcal{M}$ *3-orbitni* $(n-1)$-*manipleks.*

1. *Če je* $\mathcal{M}$ *v razredu* 3^i *za nek* $i \in \{1, \ldots, n-2\}$, *potem je*

$$\left\{\alpha_j, \alpha_{i,i-1,i+1,i}, \alpha_{i,i+1,i+2,i+1,i}, \alpha_{i,i+1,i,i+1,i} \mid j \in \{0, \ldots, n-1\} \setminus \{i\}\right\}$$

   množica generatorjev za $\mathrm{Aut}(\mathcal{M})$.

2. *Če je* $\mathcal{M}$ *v razredu* $3^{i,i+1}$ *za nek* $i \in \{0, \ldots, n-2\}$, *potem je*

$$\left\{\alpha_j, \alpha_{i,i-1,i}, \alpha_{i,i+1,i+2,i+1,i}, \alpha_{i,i+1,i,i+1,i} \mid j \in \{0, \ldots, n-1\} \setminus \{i\}\right\}$$

   množica generatorjev grupe $\mathrm{Aut}(\mathcal{M})$.

Operacije na zemljevidih in manipleksih

Leta 1979 je Wilson "sestavil" (obravnaval hkrati) tri različne operatorje na zemljevidih: *dual, petrial* in *nasprotni operator*; to je naredil z namenom, da bi regularen zemljevid transformiral v drug regularen zemljevid [57]. Kasneje, 1982, je Lins prikazal lastnosti teh operatorjev na prapornih grafih zemljevida; imel jih je za dualnosti zemljevida in jih imenoval *dual, phial* in *skew*, [37]. Tako Wilson kot Lins sta pokazala, da dual in petrial generirata kopijo grupe S_3 z nasprotnim operatorjem kot tretjo involucijo grupe.

Hubard, Orbanić in Weiss so leta 2009 posplošili koncept dualnosti in razširili koncept petriala na višje range v kontekstu abstraktnih politopov [32]. Kasneje, leta 2012, je Wilson definiral dual, petrial in nasprotni operator za maniplekse. Ni težko videti, da za $n \geq 3$ dual in petrial na n-manipleksih generirata podgrupo grupe $Sym(\mathcal{F}(\mathcal{M}))$, izomorfno diedrski grupi $D_4 = \langle \delta, \pi | \delta^2, \pi^2, (\delta\pi)^4 \rangle$. V tem poglavju definiramo in prikažemo nekaj lastnosti teh treh operatorjev na zemljevidih in manipleksih.

Imejmo dan praporni graf $\mathcal{G}_\mathcal{M}$, prirejen zemljevidu ali manipleksu $\mathcal{M}$. Lastnost teh operatorjev na $\mathcal{M}$ je, da imajo vsi trije grafi $\mathcal{G}_{\mathcal{M}^*}$, $\mathcal{G}_{\mathcal{M}^P}$ in $\mathcal{G}_{\mathcal{M}^{opp}}$, ki ustrezajo dualu $\mathcal{M}^*$, petrialu $\mathcal{M}^P$ in nasprotnemu zemljevidu ali manipleksu $\mathcal{M}^{opp}$, isto množico vozlišč $\mathcal{F}(\mathcal{M})$ kot $\mathcal{G}_\mathcal{M}$. Velja tudi, da vsaka bijekcija δ, π in *opp* med generatorji monodromijske grupe $\mathrm{Mon}(\mathcal{M})$ in generatorji pripadajočih monodromijskih grup $\mathrm{Mon}(\mathcal{M}^*)$, $\mathrm{Mon}(\mathcal{M}^P)$ ali $\mathrm{Mon}(\mathcal{M}^{opp})$ inducira permutacijo na povezavah grafa $\mathcal{G}_\mathcal{M}$, ki opisuje praporne grafe $\mathcal{G}_{\mathcal{M}^*}$, $\mathcal{G}_{\mathcal{M}^P}$ in $\mathcal{G}_{\mathcal{M}^{opp}}$ duala, petriala in nasprotnega zemljevida ali manipleksa prvotnega zemljevida ali manipleksa $\mathcal{M}$. Kasneje lahko z uporabo iste permutacije na povezavah v $\mathcal{G}_\mathcal{M}$ (zato da dobimo grafe $\mathcal{G}_{\mathcal{M}^*}$, $\mathcal{G}_{\mathcal{M}^P}$ in $\mathcal{G}_{\mathcal{M}^{opp}}$ iz $\mathcal{G}_\mathcal{M}$), izpeljemo iz $T(\mathcal{M})$ možne simetrijske grafe $T(\mathcal{M}^*)$, $T(\mathcal{M}^P)$ in $T(\mathcal{M}^{opp})$.

Za dani sebi-dualni (oz. samodualni) manipleks $\mathcal{M}$ bijekcija δ inducira permutacijo d vozlišč v $T(\mathcal{M})$ tako, da se barvi povezav i in $n-i$ zamenjata za $i = 0, 1, \ldots, n$.

Takšno permutacijo d bomo imenovali dualnost sebi-dualnega simetrijskega grafa $T(\mathcal{M})$ sebi-dualnega manipleksa $\mathcal{M}$. Simetrijski graf pravega sebi-dualnega manipleksa ima dualnost, ki fiksira vsa vozlišča, simetrijski graf nepravega samodualnega manipleksa pa ima dualnost, ki prestavi vsaj dve vozlišči. Vendar za dani sebi-dualni manipleks $\mathcal{M}$ njegov simetrijski graf $T(\mathcal{M})$ morda ne nudi dovolj informacij o tem, ali je $\mathcal{M}$ pravi ali nepravi samodual. Primer tega je dejstvo, da je kiralni manipleks lahko pravi ali nepravi samodual ([33]), tako da graf simetrijskih tipov kiralnega manipleksa dopušèa dualnosti, ki vozlišča tako fiksirajo kot tudi izmenjajo. To nas spodbudi, da vsakemu vozlišču samodualnega simetrijskega grafa $T(\mathcal{M})$ dodamo še eno povezavo (ali polpovezavo) barve D, ki predstavlja delovanje dualnosti manipleksa $\mathcal{M}$ na prapornih orbitah. Nov predgraf imenujemo *razširjeni simetrijski graf* sebi-dualnega manipleksa $\mathcal{M}$ in ga označimo s $\overline{T(\mathcal{M})}$.

Gledano do 7 orbit, tipi, ki pravilno določijo samodualnost, so 1, 2, 2_1, 2_{02}, 3^{02}, 4_{Ap}, 4_{B_p}, 4_{C_p}, 5_{C_p}, 6_{A_p}, 6_{B_p}, 6_{C_p} in 7_{A_p} (slike 3.2, 3.3, 3.6 in 3.7).

II. del

V drugem delu disertacije geometrijsko in kombinatorično definiramo operacije sredinjenja (angl. medial), brušenja (angl. chamfering), prisekanja (angl. truncation) in preskoka (angl. leapfrog). Natančneje, raziskujemo možne simetrijske grafe zemljevidov, ki jih dobimo s temi operacijami. Za razliko od dualov, petrialov in nasprotnih zemljevidov, pri katerih imajo praporni grafi $\mathcal{G}_{\mathcal{M}}$, $\mathcal{G}_{\mathcal{M}^*}$, $\mathcal{G}_{\mathcal{M}^P}$ in $\mathcal{G}_{\mathcal{M}^{opp}}$ isto število vozlišč (kot prvotni zemljevid), je pri sredinjenju, brušenju, prisekanju ali preskoku zemljevida $\mathcal{M}$ množica praporov novega zemljevida $\widetilde{\mathcal{M}}$ celoštevilski večkratnik $|\mathcal{F}(\mathcal{M})|$.

Pravzaprav lahko vsako od teh operacij opišemo z delitvijo fundamentalnih trikotnikov (baricentrične subdivizije $\mathcal{BS}(\mathcal{M})$), ki inducira algoritem za izpeljavo $\mathcal{G}_{\widetilde{\mathcal{M}}}$ iz $\mathcal{G}_{\mathcal{M}}$. Tak algoritem nam omogoča najti ustrezne particije $(\mathcal{A}_0, \ldots, \mathcal{A}_r)$ množice vozlišč prapornega grafa $\mathcal{G}_{\widetilde{\mathcal{M}}}$ sredinjenega, brušenega, prisekanega ali preskočenega zemljevida $\widetilde{\mathcal{M}}$, tako da velja $\mathcal{F}(\widetilde{\mathcal{M}}) = \mathcal{A}_0 \cup \cdots \cup \mathcal{A}_r$ za vsak $\mathcal{A}_j$ blok monodromijske grupe $\text{Mon}(\widetilde{\mathcal{M}})$ za $j = 0, \ldots, r$.

Ni težko opaziti, da grupa avtomorfizmov $\text{Aut}(\mathcal{M})$ za $\mathcal{M}$ inducira podgrupo $H \leq \text{Aut}(\widetilde{\mathcal{M}})$ grupe avtomorfizmov zemljevida $\widetilde{\mathcal{M}}$. Intuitivno pomislimo, da če velja $|\mathcal{F}(\widetilde{\mathcal{M}})| = r|\mathcal{F}(\mathcal{M})|$, potem je zemljevid $\widetilde{\mathcal{M}}$ rk-orbitni zemljevid, saj grupa avtomorfizmov zemljevida $\mathcal{M}$ razdeli njegovo množico praporjev na k orbit. Vendar se lahko zgodi, da ima $\widetilde{\mathcal{M}}$ manj kot rk prapornih orbit. V tem delu disertacije se posvetimo tudi temu fenomenu.

Operacija sredinjenja (medial) na zemljevidih

Znano je, da je sredinjenje (medial) tetrahedra oktaeder, njegov medial pa kuboktaeder (slika 5.1). Medtem ko je prvi polieder regularen, je drugi le 2-orbiten in povezavno-

tranzitiven kot zemljevid.

Za poljuben zemljevid $\mathcal{M}$ definiramo *medial* za $\mathcal{M}$, $\mathrm{Me}(\mathcal{M})$ takole. Množica oglišč mediala $\mathrm{Me}(\mathcal{M})$ je množica povezav prvotnega zemljevida $\mathcal{M}$, $E(\mathcal{M})$. Dve oglišči v $\mathrm{Me}(\mathcal{M})$ sta povezani, če si ustrezni povezavi v $\mathcal{M}$ delita oglišče in pripadata istemu licu. Tako dobimo graf, vložen na isto ploskev kot $\mathcal{M}$. Torej lica $\mathrm{Me}(\mathcal{M})$ natanko ustrezajo povezanim komponentam komplementa grafa (1-skeleta prvotnega zemljevida) na ploskvi. Zato ni težko videti, da je množica lic mediala $\mathrm{Me}(\mathcal{M})$ v bijektivni korespondenci z množico, ki vsebuje vsa lica in oglišča zemljevida $\mathcal{M}$, t.j. $F(\mathrm{Me}(\mathcal{M})) := F(\mathcal{M}) \cup V(\mathcal{M})$. Ni težko videti, da sta medial zemljevida $\mathcal{M}$ in medial njegovega duala $\mathcal{M}^*$ izomorfna.

Opazimo, da je vsak prapor prvotnega zemljevida $\mathcal{M}$ razdeljen na dva prapora medialnega zemljevida $\mathrm{Me}(\mathcal{M})$ (slika 5.2). Torej je $\mathcal{F}(\mathrm{Me}(\mathcal{M})) = \mathcal{F}(\mathcal{M}) \times \{0,2\}$. Sosednost praporjev v $\mathrm{Me}(\mathcal{M})$ je v bližnji relaciji s sosednostjo praporjev v $\mathcal{M}$; ta relacija je naslednja:

$$(\Phi,0)^0 = (\Phi^{s_1},0), \quad (\Phi,0)^1 = (\Phi^{s_2},0), \quad (\Phi,0)^2 = (\Phi,2),$$
$$(\Phi,2)^0 = (\Phi^{s_1},2), \quad (\Phi,2)^1 = (\Phi^{s_0},2), \quad (\Phi,2)^2 = (\Phi,0),$$

kjer so s_0, s_1 in s_2 generatorji $\mathrm{Mon}(\mathcal{M})$ in $\Phi \in \mathcal{F}(\mathcal{M})$. Naj bodo m_0, m_1 in m_2 različni generatorji $\mathrm{Mon}(\mathrm{Me}(\mathcal{M}))$. Potem so m_0, m_1 in m_2 involucije brez negibnih točk za $m_0 m_2 = m_2 m_0$ in $(m_1 m_2)^4 = id$. Zadnja relacija sledi iz dejstva, da ima vsako oglišče medialnega zemljevida $\mathrm{Me}(\mathcal{M})$ valenco 4.

Na sliki 5.3 je prikazan algoritem za konstrukcijo prapornega grafa mediala $\mathrm{Me}(\mathcal{M})$ iz prapornega grafa $\mathcal{M}$. Takšen algoritem inducira dvodelno particijo $(\mathcal{A}_0, \mathcal{A}_2)$ množice oglišč v $\mathcal{G}_{\mathrm{Me}(\mathcal{M})}$, kjer je $\mathcal{A}_0 := \{(\Phi,0) | \Phi \in \mathcal{F}(\mathcal{M})\}$ in $\mathcal{A}_2 := \{(\Phi,2) | \Phi \in \mathcal{F}(\mathcal{M})\}$. Od tod sledi, da praporni graf $\mathcal{G}_{\mathrm{Me}(\mathcal{M})}$ medialnega zemljevida $\mathrm{Me}(\mathcal{M})$ zemljevida $\mathcal{M}$ lahko kvocientno projiciramo v graf, izomorfen simetrijskemu grafu 2_{01}.

Hubard, Orbanić in Weiss v [32] pokažejo, da je grupa avtomorfizmov medialnega zemljevida $\mathrm{Me}(\mathcal{M})$ izomorfna razširjeni grupi $\mathcal{D}(\mathcal{M})$ zemljevida $\mathcal{M}$. Z uporabo pravilnih in nepravilnih samodualnosti zemljevidov so karakterizirali regularne in 2-orbitne medialne zemljevide glede na njihove simetrijske tipe. Pokazali so, da je medialni zemljevid $\mathrm{Me}(\mathcal{M})$ regularen natanko takrat, ko je $\mathcal{M}$ regularen in samodualen. V [32, tabela 4] smo nadalje opazili, da vsak 2-orbiten simetrijski tip nastopa kot medialni zemljevid regularnega ali 2-orbitnega zemljevida. Orbanić, Pellicer in Weiss v [45] razširjajo to v karakterizacijo simetrijskih tipov vseh medialnih zemljevidov 2-orbitnih zemljevidov. Dokazali so tudi, da če je $\mathcal{M}$ k-orbitni zemljevid, potem je $\mathrm{Me}(\mathcal{M})$ k-orbitni ali $2k$-orbitni zemljevid, odvisno od tega, ali je $\mathcal{M}$ samodualni zemljevid ali ne.

Medialni simetrijski graf definiramo kot simetrijski graf medialnega zemljevida in ga označimo $T(\mathrm{Me}(\mathcal{M}))$. V tem poglavju klasificiramo vse možne medialne simetrijske grafe z največ 7 vozlišči. Če zemljevid $\mathcal{M}$ ni sebi-dualen, lahko na oglišča medialnega simetri-

jskega grafa $T(\mathrm{Me}(\mathcal{M}))$ gledamo kot na pridobljena iz dveh kopij vozlišč simetrijskega grafa $T(\mathcal{M})$, in za določitev sosednosti med vozlišči v $T(\mathrm{Me}(\mathcal{M}))$ uporabimo algoritem, prikazan na sliki 5.3. Torej, če k-orbitni zemljevid $\mathcal{M}$ ni samodualen, potem ima medialni simetrijski graf $T(\mathrm{Me}(\mathcal{M}))$ od $\mathrm{Me}(\mathcal{M})$ $2k$ vozlišč. Po drugi strani pa velja, da če je $\mathcal{M}$ samodualen k-orbitni zemljevid, potem lahko njegov medialni simetrijski graf s k vozlišči dobimo iz razširjenega simetrijskega grafa $\overline{T(\mathcal{M})}$. Barve povezav v $T(\mathrm{Me}(\mathcal{M}))$ za samodualni zemljevid $\mathcal{M}$ definiramo z involucijami takole: $m_0 = s_1$, $m_1 = s_0$ (ali s_2) in $m_2 = d$.

Mnogo avtorjev je že opazilo, da je medial kateregakoli regularnega zemljevida povezavno tranzitiven; pravzaprav Hubard, Orbanić in Weiss v [32] pokažejo, da je medial regularnega zemljevida bodisi regularen (če je originalni zemljevid samodualen) bodisi tipa 2_{01} (sicer). V tej disertaciji pokažemo, da je vsak simetrijski tip povezavno tranzitivnega zemljevida medialni simetrijski tip. Orbanić, Pellicer, Pisanski in Tucker (2011) v [44] pokažejo, da so povezavno tranzitivni zemljevidi 14 različnih tipov, vsak od njih je opisan s svojim simetrijskim grafom.

To raziskavo medialnih zemljevidov zaključimo z opažanjem, da ima vsak k-orbitni zemljevid $\mathcal{M}$, za katerega je tudi $\mathrm{Me}(\mathrm{Me}(\mathcal{M}))$ k-orbitni zemljevid, Schläflijev simbol $\{4,4\}$. Zemljevidi tipa $\{4,4\}$ so zemljevidi na torusu ali na Kleinovi steklenici. Hubard, Orbanić, Pellicer in Weiss v [31] raziskujejo simetrijske tipe ekvivelarnih zemljevidov na torusu. Zemljevidi tipa $\{4,4\}$ na torusu imajo simetrijski tip 1, 2, 2_1, 2_{02} ali 4_{C_p} in so vsi samodualni. Medial zemljevida $\{4,4\}$ na torusu tipa 1, 2 ali 4_{C_p} je istega tipa kot original, medtem ko je za tipa 2_1 in 2_{02} medial vedno drugega tipa. Zato ima $\mathrm{Me}(\mathrm{Me}(\mathcal{M}))$ isti simetrijski graf kot $\mathcal{M}$,, kadar je $\mathcal{M}$ zemljevid na torusu s Schläflijevim simbolom $\{4,4\}$. Wilson v [58] pokaže, da obstajata dva tipa zemljevidov tipa $\{4,4\}$ na Kleinovi steklenici, ki ju označuje $\{4,4\}_{\backslash m,n \backslash}$ in $\{4,4\}_{|m,n|}$. Pokazali smo, da je $\mathrm{Me}(\mathrm{Me}(\mathcal{M}))$ k-orbitni zemljevid, če je $\mathcal{M}$ k-orbitni zemljevid na torusu tipa $\{4,4\}$ ali k-orbitni zemljevid na Kleinovi steklenici tipa $\{4,4\}_{|m,n|}$ za lih n.

V tabeli 5.5 so našteti vsi simetrijski tipi samodualov in medialni tipi k-orbitnih zemljevidov za $1 \le k \le 10$.

Operacija brušenja na zemljevidih

Naslednja operacija na zemljevidih, ki je predstavljena v tej disertaciji, je operacija brušenja (angl. chamfering), ki se uporablja v kemiji, kot je predstavljeno v [17].

Brušeni zemljevid $\mathrm{Cham}(\mathcal{M})$ zemljevida $\mathcal{M}$ dobimo, kot to pove njegovo ime, tako, da iz povezav v $\mathcal{M}$ naredimo t.i. bruse. Natančneje, povezave zemljevida $\mathcal{M}$ nadomestimo s šestkotniškimi lici, ki obkrožajo lica zemljevida $\mathcal{M}$ v zemljevidu $\mathrm{Cham}(\mathcal{M})$. Tako je množica lic $\mathrm{Cham}(\mathcal{M})$ v korespondenci z množico lic $F(\mathcal{M})$ in množico povezav $E(\mathcal{M})$ v

$\mathcal{M}$, oziroma, za za množico lic v Cham($\mathcal{M}$) velja $F(\text{Cham}(\mathcal{M})) = F(\mathcal{M}) \cup E(\mathcal{M})$. Zemljevid Cham($\mathcal{M}$) ima dve vrsti povezav: povezave med šestkotniškimi lici in povezave med licem Φ_2 v $F(\mathcal{M})$ in njemu sosednimi šestkotniškimi lici (ki ustrezajo incidentnim povezavam lica Φ_2 v $\mathcal{M}$). Dejansko ima Cham($\mathcal{M}$) natanko $4|E(\mathcal{M})|$ povezav. Množica oglišč $\mathcal{M}$ je prava podmnožica oglišč Cham($\mathcal{M}$), preostalih $2|E(\mathcal{M})|$ oglišč v $V(\text{Cham}(\mathcal{M})) \setminus V(\mathcal{M})$ (vsako od njih je sosednje natanko enemu oglišču v $V(\mathcal{M})$) ima stopnjo 3. Za alternativno definicijo operacije brušenja bralcu priporočamo [15].

V tem poglavju definiramo in uporabimo operacijo brušenja na k-orbitnih zemljevidih in določimo število možnih prapornih orbit brušenja k-orbitnega zemljevida v odvisnoti od k, kakor je prikazano v [12]. Ta operacija razdeli vsak prapor (trojico) prvotnega zemljevida na štiri različne prapore v brušenem zemljevidu, torej velja $\mathcal{F}(\text{Cham}(\mathcal{M})) = \mathcal{F}(\mathcal{M}) \times \{0, 1, 2, 3\}$.

Sosednosti praporov v Cham($\mathcal{M}$) so tesno povezane s sosednostmi praporjev v $\mathcal{M}$. Dejansko velja:

$$
\begin{array}{lll}
(\Phi, 0)^0 = (\Phi, 1), & (\Phi, 0)^1 = (\Phi^{s_2}, 0), & (\Phi, 0)^2 = (\Phi^{s_1}, 0), \\
(\Phi, 1)^0 = (\Phi, 0), & (\Phi, 1)^1 = (\Phi, 2), & (\Phi, 1)^2 = (\Phi^{s_1}, 1), \\
(\Phi, 2)^0 = (\Phi^{s_0}, 2), & (\Phi, 2)^1 = (\Phi, 1), & (\Phi, 2)^2 = (\Phi, 3), \\
(\Phi, 3)^0 = (\Phi^{s_0}, 3), & (\Phi, 3)^1 = (\Phi^{s_1}, 3), & (\Phi, 3)^2 = (\Phi, 2),
\end{array}
$$

pri čemer so s_0, s_1 in s_2 generatorji grupe Mon($\mathcal{M}$) in je $\Phi \in \mathcal{F}(\mathcal{M})$. Na podlagi gornjih relacij smo definirali algoritem, prikazan na sliki 6.4, za konstrukcijo prapornega grafa Cham($\mathcal{M}$) iz $\mathcal{G}_\mathcal{M}$ in posledično pokazali, da je praporni graf $\mathcal{G}_{\text{Cham}(\mathcal{M})}$ brušenega zemljevida Cham($\mathcal{M}$) zemljevida $\mathcal{M}$ s kvocientno projekcijo mogoče preslikati v graf, izomorfen simetrijskemu grafu 4_{D_p}.

Brušeni zemljevid Cham($\mathcal{M}$) k-orbitnega zemljevida $\mathcal{M}$ ima manj kot $4k$ orbite praporov, kadar imata oba zemljevida, $\mathcal{M}$ in Cham($\mathcal{M}$), Schläflijev simbol $\{6, 3\}$. Iz Eulerjeve karakteristike zemljevida sledi, da je ploskev zemljevida s Schläflijevim simbolom $\{6, 3\}$ bodisi torus bodisi Kleinova steklenica. Hubard, Orbanić, Pellicer in Weiss v [31] raziskujejo simetrijske tipe ekvivelarnih zemljevidov na torusu; ti so lahko ali regularni ali kiralni ali pa imajo simetrijski tip 3^{02} ali 6_{H_p}. Wilson v [58] pokaže, da obstajata dve vrsti zemljevidov tipa $\{6, 3\}$ na Kleinovi steklenici in ju označi z $\{6, 3\}_{|m,n|}$ in $\{6, 3\}_{\setminus m,n \setminus}$; ti zemljevidi so $3n$-orbitni. V tej disertaciji pokažemo, da če je $\mathcal{M}$ zemljevid na torusu ali na Kleinovi steklenici (katerekoli od obeh vrst), potem je Cham($\mathcal{M}$) zemljevid na isti ploskvi. Nadalje opazimo tudi, da če je $\mathcal{M}$ k-orbitni torusni zemljevid s Schläflijevim simbolom $\{6, 3\}$, potem je Cham($\mathcal{M}$) k-orbitni zemljevid za $k = 1, 2, 3, 6$. Če je $\mathcal{M}$ k-orbitni zemljevid s Schläflijevim simbolom $\{6, 3\}$ na Kleinovi steklenici, potem velja $3|k$ in Cham($\mathcal{M}$) je $2k$-orbitni zemljevid.

A. Deza, M. Deza in V. Grishukhin v [15] s Cham$_t(\mathcal{M})$ označijo t-kratno uporabo op-

eracije brušenja na zemljevidu $\mathcal{M}$. Razdelek zaključimo z naslednjim izrekom, ki povzame vse rezultate, predstavljene v tem razdelku.

Izrek 3. *Naj bo $\mathcal{M}$ k-orbitni zemljevid in* $\mathrm{Cham}_t(\mathcal{M})$ *zemljevid, ki ga dobimo s t-kratno uporabo operacije posnetja na zemljevidu $\mathcal{M}$, ki ima s prapornih orbit. Potem velja ena izmed naslednjih trditev.*

1. $s = 4^t k, 2^t k$ *ali* k.

2. *Če je* $s \neq 4^t k$, *potem velja* $\chi(\mathcal{M}) = 0$ *($\mathcal{M}$ je na torusu ali na Kleinovi steklenici) in $\mathcal{M}$ je tipa* $\{6, 3\}$.

3. *Če je $\mathcal{M}$ torus tipa* $\{6, 3\}$ *potem velja* $s = k$ *in* $k = 1, 2, 3, 4$.

4. *Če je $\mathcal{M}$ na Kleinovi steklenici tipa* $\{6, 3\}$, *potem velja* $s = 2^t k$ *in* $3 | k$.

Operacija prisekanja in preskoka na zemljevidih

V tem zadnjem poglavju si oglejmo operaciji prisekanja in preskoka ([45, 49]). Medialno operacijo (sredinjenje) lahko razumemo kot prisekanje zemljevida na sredinskih točkah njegovih povezav. Kadar pa sredinske točke na povezavah zemljevida $\mathcal{M}$ preskočimo in zemljevid prisekamo še naprej od njih, tako dobljeni zemljevid imenujemo *preskočeni* zemljevid zemljevida $\mathcal{M}$, [18]. Če oglišča zemljevida $\mathcal{M}$ postanejo lica prisekanega zemljevida, potem je dobljeni zemljevid dual zemljevida $\mathcal{M}$. Tako npr. s prisekanjem regularnega poliedra dobimo nekatera od 13 arhimedskih teles, kakor je razloženo v [7] in [52].

Operacija *prisekanja* sestoji iz zamenjave oglišč zemljevida z lici, pri čemer imajo nova lica dvakrat več oglišč kot prvotna lica. Med množico lic prisekanega zemljevida $\mathrm{Tr}(\mathcal{M})$ zemljevida $\mathcal{M}$ in množico oglišč in lic zemljevida $\mathcal{M}$ obstaja korespondenca: $F(\mathrm{Tr}(\mathcal{M})) = V(\mathcal{M}) \cup F(\mathcal{M})$. Poleg tega za vsako povezavo zemljevida $\mathcal{M}$ obstajata natanko dve oglišči v $\mathrm{Tr}(\mathcal{M})$ tako, da sta ti oglišči povezani z neko povezavo, če bodisi obe oglišči pripadata skupni povezavi v $\mathcal{M}$ ali če si ustrezni povezavi v $\mathcal{M}$ delita oglišče in pripadata istemu licu. Vsako oglišče v $\mathrm{Tr}(\mathcal{M})$ ima valenco 3, torej prisekani zemljevid $\mathrm{Tr}(\mathcal{M})$ vsebuje $2|E(\mathcal{M})|$ oglišč in $3|E(\mathcal{M})|$ povezav.

Vsak prapor $\Phi \in \mathcal{F}(\mathcal{M})$ je razdeljen na tri različne prapore prisekanega zemljevida $\mathrm{Tr}(\mathcal{M})$ (slika 7.2); torej $\mathcal{F}(\mathrm{Tr}(\mathcal{M})) = \mathcal{F}(\mathcal{M}) \times \{0, 1, 2\}$. Sosednost praporov v $\mathcal{F}(\mathrm{Tr}(\mathcal{M}))$ je opisana z naslednjimi relacijami:

$$
\begin{array}{lll}
(\Phi, 0)^0 = (\Phi^{s_1}, 0), & (\Phi, 0)^1 = (\Phi^{s_2}, 0), & (\Phi, 0)^2 = (\Phi, 2); \\
(\Phi, 1)^0 = (\Phi^{s_0}, 1), & (\Phi, 1)^1 = (\Phi, 2), & (\Phi, 1)^2 = (\Phi^{s_2}, 1); \\
(\Phi, 2)^0 = (\Phi^{s_1}, 2), & (\Phi, 2)^1 = (\Phi, 1), & (\Phi, 2)^2 = (\Phi, 0),
\end{array}
$$

140

kjer so s_0, s_1 in s_2 različni generatorji $\mathrm{Mon}(\mathcal{M})$. Naj bodo t_0, t_1 in t_2 različni generatorji $\mathrm{Mon}(\mathrm{Tr}(\mathcal{M}))$, pri čemer je $(t_1 t_2)^3 = id$. Zadnja enakost sledi iz dejstva, da imajo vsa oglišča zemljevida $\mathrm{Tr}(\mathcal{M})$ valenco 3.

Predstavimo še ustrezni algoritem za konstrukcijo prapornega grafa priekanega zemljevida $\mathrm{Tr}(\mathcal{M})$ iz $\mathcal{G}_\mathcal{M}$ (slika 7.3). Takšen algoritem inducira particijo $(\mathcal{A}_0, \mathcal{A}_2, \mathcal{A}_1)$ množice oglišč $\mathcal{G}_{\mathrm{Tr}(\mathcal{M})}$, pri čemer je $\mathcal{A}_i := \{(\Phi, i) | \Phi \in \mathcal{F}(\mathcal{M})\}$ za $i = 0, 1, 2$. Dobimo torej praporni graf $\mathcal{G}_{\mathrm{Tr}(\mathcal{M})}$ prisekanega zemljevida $\mathrm{Tr}(\mathcal{M})$ zemljevida $\mathcal{M}$, ki ga lahko s kvocientno projekcijo preslikamo v graf, izomorfen simetrijskemu grafu 3^0.

Orbanić, Pellicer in Weiss v [45] pokažejo, da je prisekani zemljevid $\mathrm{Tr}(\mathcal{M})$ k-orbitnega zemljevida $\mathcal{M}$ ali k-orbitni ali $\frac{3k}{2}$-orbitni (če je k sod) ali pa $3k$-orbitni zemljevid; na podlagi tega karakterizirajo simetrijske tipe vseh prisekanih zemljevidov k-orbitnega zemljevida za $k \leq 3$, pri čemer so uporabili oštevilčenje odsekov ([9, Poglavje 2]). Avtorji tudi predstavijo primere, ko je katerikoli izmed teh pogojev izpolnjen, nekaj teh primerov je predstavljenih na slikah 7.4–7.6. Avtorji v [45] pokažejo tudi, da s še enkratno uporabo oštevilčenja odsekov na k-orbitnem zemljevidu, katerega prisekani zemljevid $\mathrm{Tr}(\mathcal{M})$ je $\frac{3k}{2}$-orbitni ali k-orbitni zemljevid, dobimo takšno dvodelno particijo oglišč $\mathcal{G}_\mathcal{M}$, da je $\mathcal{G}_\mathcal{M}$ kvocientni graf, izomorfen grafu simetrijskega tipa 2_{01}. Za regularni zemljevid $\mathcal{M}$ in podgrupo $G = \langle \rho_0, \rho_1, \rho_2 \rho_1 \rho_2 \rangle$ grupe avtomorfizmov $\mathrm{Aut}(\mathcal{M})$ je bilo pokazano, da je prisekani zemljevid $\mathrm{Tr}(\mathcal{M})$ regularen natanko takrat, ko je $[\mathrm{Aut}(\mathcal{M}) : G] = 2$ in obstaja avtomorfizem $\tau \in \mathrm{Aut}(G)$, ki izmenja ρ_0 in ρ_1 ter fiksira $\rho_2 \rho_1 \rho_2$.

Na podlagi rezultatov o prisekanju k-orbitnega zemljevida v [45] (predlogi 7.2–7.4) za $k \leq 3$ podamo razširitev teh rezultatov na $k \leq 7$ in $k = 9$. Tako dobimo kar nekaj trditev (7.5–7.11), katerih rezultati so prikazani v tabelah 7.1 in 7.2. Zaradi velikega števila primerov za $k = 8$ je prisekanje 8-orbitnih zemljevidov izpuščeno.

Kasneje definiramo še dvodimenzionalno subdivizijo (dual prisekanega zemljevida) zemljevida in preskočeni zemljevid (prisekanje dualnega zemljevida), in dobimo klasifikacijo vseh možnih simetrijskih grafov preskočenih k-orbitnih zemljevidov za $k \leq 7$ in $k = 9$ (tabeli 7.31 in 7.3).

Opombe

Disertacija odpira nove probleme v zvezi s simetrijskimi tipi manipleksov oziroma v zvezi z uporabo različnih operatorjev na manipleksih. Kar je v tem smislu v tej disertaciji narejeno za 2-maniplekse, je mogoce posplošiti in na podoben način karakterizirati simetrijske tipe k-orbitnih manipleksov.

Izjava

Izjavljam, da je disertacija plod lastnega raziskovalnega dela.

María del Río Francos.